EXPERIMENTAL AND ANALYTICAL STUDY OF TRANSMISSION OF WHOLE BODY VIBRATION TO SEGMENTS OF THE SEATED HUMAN BODY

Anand Madakashira-Pranesh

A Thesis

in

The department

of

Mechanical and Industrial Engineering

Presented in Partial Fulfillment of the Requirements
for the Degree of Doctor of Philosophy at
Concordia University
Montréal, Québec, Canada

March, 2011

CONCORDIA UNIVERSITY

SCHOOL OF GRADUATE STUDIES

This is to certify that the thesis prepared

By: **Anand Madakashira-Pranesh**

Entitled: **Experimental and Analytical Study of Transmission of Whole Body Vibration to Segments of the Seated Human Body**

and submitted in partial fulfillment of the requirements for the degree of

DOCTOR OF PHILOSOPHY (Mechanical Engineering)

complies with the regulations of the University and meets the accepted standards with respect to originality and quality.

Signed by the final examining committee:

_____Chair
Dr. N. Shiri

_____ External Examiner
Dr. D. Wilder

_____ External to Program
Dr. Y. Zeng

_____ Examiner
Dr. R. Sedaghati

_____ Examiner
Dr. C.Y. Su

_____ Thesis Co-Supervisor
Dr. S. Rakheja

_____ Thesis Co-Supervisor
Dr. R.G. DeMont

Approved by
            Dr. W-F. Xie, Graduate Program Director

April 8, 2011   _____
                Dr. Robin A.L. Drew, Dean
                Faculty of Engineering & Computer Science

ABSTRACT

"Experimental and analytical study of transmission of whole body vibration to segments of the seated human body"

Anand Madakashira-Pranesh, Ph. D.
Concordia University, 2011

Prolonged exposure to whole body vibration (WBV) has been associated with prevalence of spinal disorders among operators of vibrating mobile machinery. The study of biodynamic responses of body segments is thus pertinent for our understanding of potential injury mechanisms and designs of interventions. This study concerns seated body biodynamic responses to vertical vibration through measurements at the driving-point and at body segments, and development of an analytical model for prediction of global and localised responses. Experiments were undertaken to simultaneously measure driving-point apparent mass (APMS) and body segment acceleration transmissibility of 12 adult subjects under random vertical vibration in the 0.5-20 Hz frequency range. Measurements were taken at the C7, T5, T12, L3 and L5 vertebral locations along the fore-aft and vertical axes using skin-mounted micro-accelerometers, and at the scalp using a light-weight head strap with a micro-accelerometer. The study involved four sitting postures realised with different combinations of hands position (on the lap or on the steering wheel) and back support (none or a vertical support), and three excitation magnitudes (0.25, 0.5 and 1 m/s^2 RMS). Mathematical correction methods were employed to account for skin effects, sensor misalignments, and seat inertia effects. The corrected body-segment responses of the twelve subjects depicted a clear dependence on the back support condition ($p<0.01$), while the influences of hand position and vibration magnitude were also significant but relatively weaker.

Owing to the significant influences of the postural parameters, it was concluded that different support-specific datasets would be necessary to describe the WBV responses and identification of biodynamic models. A 19 degrees-of-freedom anthropometric multi-body biodynamic (MBD) model of the 50th percentile male subjects was formulated on the basis of the known anthropometric inertial and joint properties to simulate sagittal plane motions of the body under vertical WBV. The visco-elastic parameters of various joints were identified through minimisation of a set of error functions derived from different combinations of target responses using the Genetic Algorithm. The minimisation of an error function based on measured vertical head, and fore-aft head and C7 vibration provided an acceptable convergence in primary resonance peaks in both the APMS and the segmental vibration responses. Eigen analysis of the resulting model revealed the presence of 4 significant modes at frequencies below 15 Hz, including two modes near the primary resonant frequency of 5 Hz (4.76 Hz and 5.71 Hz), corresponding to vertical movement of the whole body and pelvic rotation. The model was subsequently applied to estimate vibratory power absorbed within different joints and the total body. The total absorbed power of the model agreed reasonably well with the measured total power. The study revealed that a large portion of the power was absorbed at the body-seat interface, primarily by the buttock tissue. However, significant energy dissipation also occurred at the abdominal viscera and the lower lumbar joint (L5). The L5 was the only joint that showed relatively higher energy dissipation in translation as well as pitch rotation, which may be associated with the most widely reported location of pain and spinal injury.

ACKNOWLEDGEMENTS

i dedicate this dissertation to my dearest mother, Indira, and father, Pranesh,

where '*i*' is merely a figment of their imagination.

TABLE OF CONTENTS

APPENDIX

LIST OF FIGURES

XIV

XV

LIST OF TABLES

1. Introduction and Scope

1.1 Motivation

Industrialisation has for the most part been a process of facilitating mankind's physical control over nature primarily for the sake of human comfort and wellness. This activity has motivated man to invent machines, from the smallest to the largest in order to quicken the path towards materialistic growth. With the aid of the machinery, mankind has increased its ability to perform high levels of physical activity with greater ease. Ironically, the interactions of the machines with the human operator have become a reason for concern in many operations. The interactions of man, as an operator, with machines in industrial sectors such as agriculture, forestry, snow removal, material handling, transportation and sports, necessitate the human-body to be exposed to vibrations of both cyclic and random nature from these machines. In most machines, humans generally assume a sitting posture as it provides optimal support conditions in the form of a seat platform and a backrest. However, this very structure causes vibrations from the machines to be transmitted to and through the body from the seat–buttock and upper body–backrest interfaces. The musculoskeletal spine lying directly in the path of vibration transmission is subjected to these "vibration loads." Even with whole-body vibration (WBV) excitations limited to the vertical direction, the spine has been found to undergo movements in different axes (Hinz *et al.*, 1998b). The lower level of the human spine just above the hip section (lumbar) is primarily designed for such flexural activity and is thus the site of the majority of the disorders manifesting in the form of pain; particularly the low back pain (LBP).

The frequency of LBP is increasing so as to be included amongst the most common health problems in the world (Cats-Baril and Frymoyer, 1991). It has been of concern to many industries and governments due to decreased productivity, and increased health and compensation costs attributed to LBP (Seidel, 2005). The motivation for this dissertation research stems primarily from this medico-social view point. The primary focus of the dissertation research is to derive an anthropometric-biodynamic model of the seated human body capable of predicting multi-dimensional motions of different body segments under WBV along the vertical axis. For this purpose, comprehensive experiment programme is undertaken to characterise the seated body responses to WBV, particularly the driving-point responses at the seat and the backrest, and vertical and fore-aft motions at the lumbar, thoracic trunk sections and the head. The response characterisations are undertaken under typical sitting postures, namely, with and without a backrest contact, and hands placed on lap and on a steering wheel, and different magnitudes of vertical vibration. The measured data are systematically analysed in order to derive a minimal number of target datasets that would be vital for identifying the biodynamic models. The target datasets are subsequently applied to identify a multi-body biodynamic model of the body seated without a back and hands support.

In the present chapter, the reported studies on the health effects of WBV, human responses to vibration and biodynamic modelling are reviewed. The reviewed studies are summarised and discussed in the following sections so as to formulate the specific scope of the dissertation research and build the essential background knowledge.

1.2   Low Back Pain and the Spine

Low Back Pain (LBP) has been documented to be one of the most common health problems in the world, being termed a "health hazard" in some countries. The decreased productivity of the workforce diagnosed with LBP and the associated increase in health costs have been of concern to many industrial sectors (Cats-Baril and Frymoyer, 1991). A number of field surveys have reported the prevalence of pain and spinal disorders in operators of vibrating mobile machinery in a variety of work environments including forestry, agriculture, construction, mining, transportation and material handling (*e.g.*, Bovenzi and Betta, 1994; Bovenzi *et al*, 2002; Hoy *et al*, 2005). Vehicles employed in these workplaces are known to transmit high magnitudes of shock and vibration to the operator cab predominantly in the low-frequency range below 10 Hz (Nélisse *et al.*, 2008). Prolonged exposure to such excitations (WBV), coupled with the sitting posture in a confined workstation are believed to be the prime causal factors for the high incidences of LBP and spinal disorders reported in the drivers of many work vehicles (*e.g.*, Magnusson and Pope, 1998; Rehn *et al.*, 2002; Wikström *et al.*, 1994).

The available epidemiological data and clinical studies, however, have met only limited success in establishing an objective vibration dose–effect relationship, primarily due to our limited knowledge of the effects of vibration-induced dynamic loading of the spine and the associated tissue that may undergo damage due to vibration exposure (VIN, 2001a). The study of the spine from a biodynamic stand-point thus becomes pertinent for our understanding of the mechanisms that may be causing LBP. A number of studies in biomechanics have been performed with simplified static and quasi-static assumptions to characterise the forces and motions induced in the sub-structures of the spine due to normal human activity such as lifting, walking, and exercise activities (*e.g.*, Cappozzo,

1981; van Deursen *et al.*, 2005). However, the dynamic behaviour of the musculoskeletal spine in the seated and standing postures under exposure to machine-induced vibration is a far more complex issue that is not well-understood. Thus, the acquisition of biodynamic responses of the human body through appropriate measurements in addition to the application of mathematical modelling techniques that could predict experimentally-inaccessible variables such as forces in the spinal tissue are a necessity to WBV research. Such studies could provide vital information necessary for better design of machine interfaces and seating systems that mitigate the health effects of exposure to vibration. The primary focus of this dissertation is to characterise the vibration behaviour of the seated human body, which would help in the ultimate purpose of realising safe and comfortable operator-machinery interfaces (seats and machine components).

The subsequent sections explore the reported epidemiological studies and the methodologies published in the literature for the objective assessment of the effects of vibration on the human body, primarily the responses at various locations of the spine. However, it is appropriate here to introduce the terminology frequented in the description of human body motion, which would serve for better understanding of the discussions in this dissertation. Furthermore, the construction of the human musculoskeletal spine is briefly discussed in order to emphasise the biomechanical nature of the health risks associated with WBV exposure.

1.2.1 Human coordinate systems for motion measurement

As a general rule for any mechanical measurement, it is required to define physical variables such as force and displacement in terms of magnitude and direction based on a coordinate system. The biomechanical studies of the human body have also

imbibed a similar approach. Figure 1-1 illustrates the three orthogonal planes, namely frontal, horizontal and sagittal planes, commonly used to characterise body motion in studies on human biomechanics, with the point of origin considered at the mid-abdominal level. It is evident that the directional vectors of the measured physical variables are primarily determined by the accuracy with which the origin of the axis system is located on the human body. A similar human-centred approach, termed the "biodynamic coordinate system", was originally considered for denoting the vibration responses measured from human subjects, with the datum of the axes placed at the location of the heart in the human body. However, this technique poses considerable challenges in locating the point of origin (heart) in the human body. A more practical solution has thus been considered for reporting vibration responses, with the coordinate origin conveniently located on the mid-sagittal plane at the interface point between the human body and the vibrating surface (ISO 2631-1, 1997). In the case of a human being seated on a vibrating seat without a back support, the origin may thus be identified below the buttock bones (iscial tuberosities) on the surface of the seat (Griffin, 1990). In this scheme, termed the "basi-centric" coordinate system illustrated in Fig. 1-2, the X-axis denotes fore-aft body motion, the vertical direction originating at the seat-buttock interface is considered as the Z-axis and the horizontal vector orthogonal to the X and Z axes represents the Y direction. The anti-clockwise rotations about the X-, Y- and Z-axes, called respectively, as roll, sagittal-plane pitch and yaw are considered to depict a positive sense.
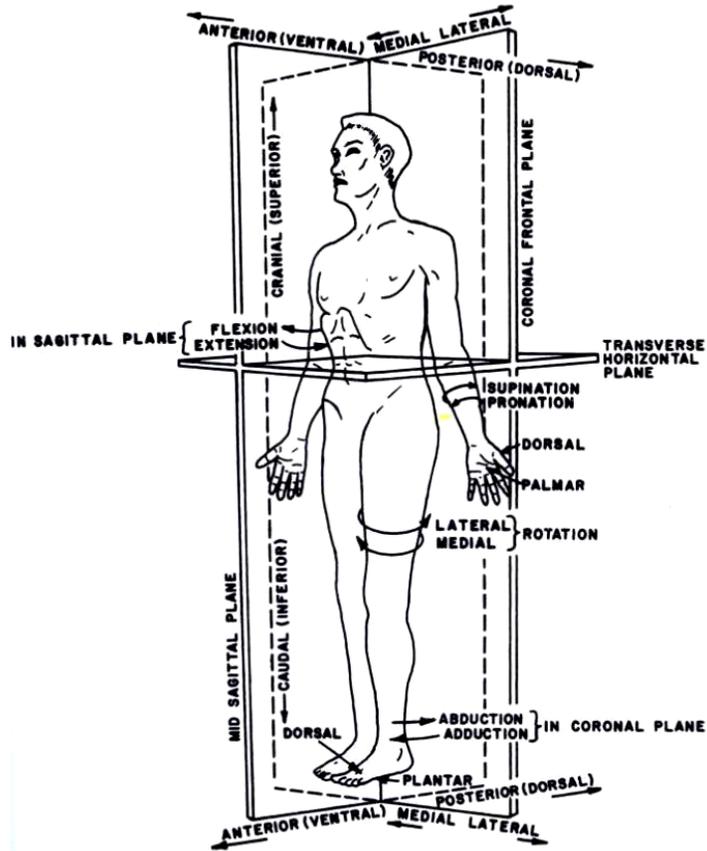
Figure 1-1: Coordinate system used in human biomechanics (Chaffin *et al.*, 1991)

Figure 1-2: The basi-centric coordinate system used for biodynamic measurements of the sitting human body (ISO 2631-1, 1997)

1.2.2 Anatomy of the human spine – in brief

The spine is a musculoskeletal sub-system of the human body that extends from the base of the head (skull) to the hip (pelvis), forming one of the most crucial structural members of the upper body (torso). Figure 1-3 illustrates the skeletal portion of the spine in the upper body. In engineering terms, the spine is the primary load carrying member of the trunk composed of the physical assembly of the vertebral bones with relatively softer elements such as cartilages, vertebral discs, and motion effectors and stabilisers including the muscles, ligaments and tendons. The coordinated functioning of all these systems maintains 'stability' of the biomechanical human system for the performance of physical tasks while minimising tissue damage. The spine, also called the vertebral column, thus has a number of functions, which include: (i) supporting the bulk of the upper body mass; (ii) generating and assisting in functional body movements; and (iii) protecting the spinal column and its nerve roots.

The human spine may be separated into four regions, namely the cervical, thoracic, lumbar and sacral sections, as illustrated in Fig. 1-3. The first three of these sections are flexible, each of these being composed of smaller 'vertebral' bone segments. The cervical spine connects the head to the upper body (torso) and is composed of seven vertebrae denoted by their location from top to bottom as cervical 1 (C1) to cervical 7 (C7). The thoracic section of the spine extends below (or inferiorly) from the C7 to the lower back, near the abdominal diaphragm, and comprises twelve vertebrae (T1 to T12), each connected to a pair of ribs forming the ribcage. The lumbar spine, below the thoracic section, is made up of five relatively large vertebrae (L1 to L5) connecting the upper body to the hip bone (pelvis). The lower regions of the spine, namely the sacrum

and coccyx are fused into one bony mass in the human body, which transfers the body's forces to the pelvis via the sacro-illiac joints and provides stability to the pelvic girdle.
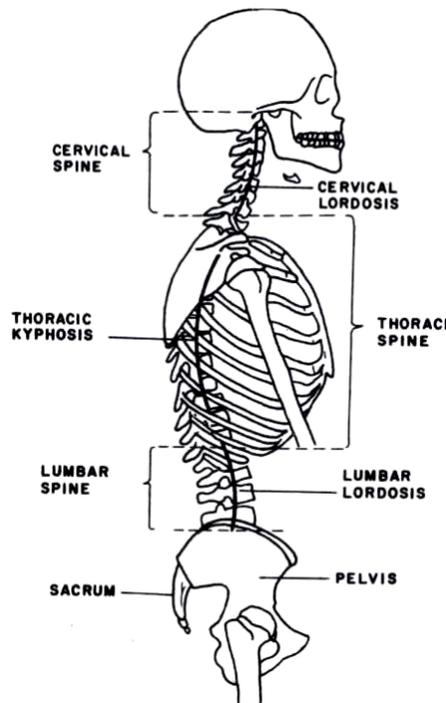
Figure 1-3: Lateral (sagittal) view of the human skeletal spine showing the four major sections with the associated spine curvatures (Chaffin *et al.*, 1991)

The cervical and lumbar regions constitute the most flexible sections of the spine and thus play a vital role in realising, respectively, the movements of the head-neck complex and the trunk segments. A healthy spine is generally symmetric in the frontal view, but in the sagittal (lateral) plane it has four curvatures, as indicated in Fig. 1-3, which determine the paths for the transmission of static and dynamic loads in the upper body. In the standing erect posture, the concave shape of the cervical and lumbar curves is termed 'lordosis', while the convex lines of the thoracic spine and the sacrum are called 'kyphosis.' The cervical and lumbar portions of the spine are however, known to

assume a kyphotic curvature in postures such as forward bending that may alter the nature and path of the loads transmitted along the trunk.

The vertebrae provide flexibility to the entire spine-assembly by permitting relative motion among them. Figures 1-4 (a), (b) and (c) illustrate, respectively, the sagittal, top and three-dimensional views of a single vertebral bone. The vertebral 'body' forms the major structural unit of the vertebral bone, posterior to which bony vertebral arches (pedicles) and laminae form a "spinal canal" that encircles and physically protects the bulk of the nervous spinal column (Fig. 1-4b). Each vertebra has one 'spinous' process, two 'transverse' processes and four 'articular' processes, also called 'facets.' Each vertebra is connected to the subsequent vertebral body via an "inter-vertebral disc", as depicted in Fig. 1-5, which permits constrained relative movement between the two consecutive vertebrae. The human spine is composed of 24 "vertebral units" in the flexible sections (cervical, thoracic and lumbar) that share the body's static and dynamic loads, while providing flexibility to the upper body. The vertebral units in these spine sections have the same structural topology, but generally increase in size and mass towards the lower segments of the body (lumbar) so as to ensure greater spinal strength to withstand the higher inertial loads of the upper body and increased flexibility required in the lumbar spine.

Posterior

(a)

(b)

Posterior

(c)
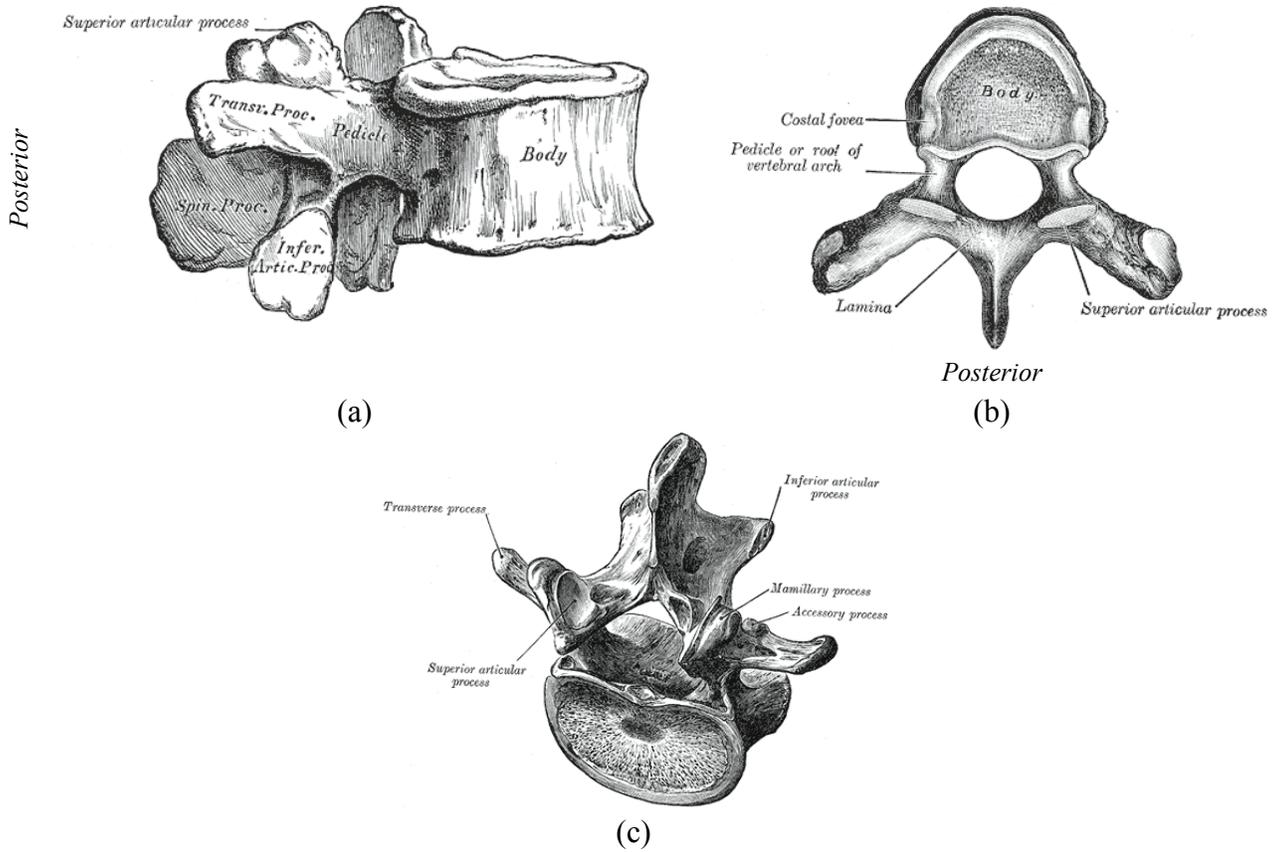
Figure 1-4: The (a) sagittal; (b) top; and (c) three-dimensional views of a typical lumbar vertebra illustrating the different parts of the vertebral bone. (Gray, 1918)
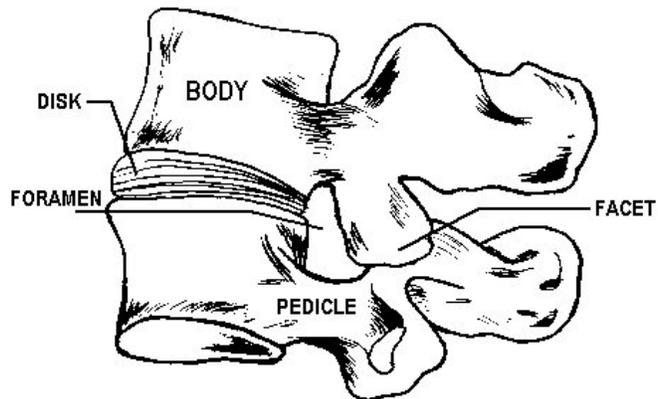
Figure 1-5: The typical functional unit of the lumbar spine showing the assembly of the vertebrae through different types of joints (Pain & Disability)

10

The spine may thus be likened to a biomechanical mechanism composed of multiple rigid bodies (vertebrae) connected through appropriate joints to form a multi-body system with a 'tree' structure. Accordingly, each vertebral unit is composed of a set of three joints, namely the inter-vertebral disc and the upper and lower facet joints, through which the corresponding vertebrae connect and interact. Figure 1-5 illustrates a three-dimensional view of the functional unit of the spine showing the disc and one facet connection. The disc sandwiched between the two vertebral bodies provides a strong connection between the consecutive vertebral bodies in addition to being the primary joint for sharing and transmission of biomechanical loads along the trunk. The inter-vertebral disc is composed of annular rings of fibrous material (annulus fibrosis) enclosing a gelatinous core called the 'nucleus.' The biological state of these elements, the strength and integrity of the annulus and the viscosity of the fluid within the nucleus, determines the disc joint's mechanical characteristics. Thus, from an engineering perspective, the annulus may be assumed as a three-dimensional spring and the nucleus akin to a three-dimensional damping element, albeit with highly non-linear properties (*e.g.*, Markolf, 1970; Panjabi *et al.*, 1976). Opposing pairs of facets from adjacent vertebrae are connected to each other as seen in Fig. 1-5, by smooth cartilages to form what is termed as a "synovial joint." While the facet joints primarily help in constraining the flexural and shear movement between adjacent vertebrae in the spine, these joints, in the cervical and lumbar regions, may share some amount of mechanical loads with the corresponding discs.
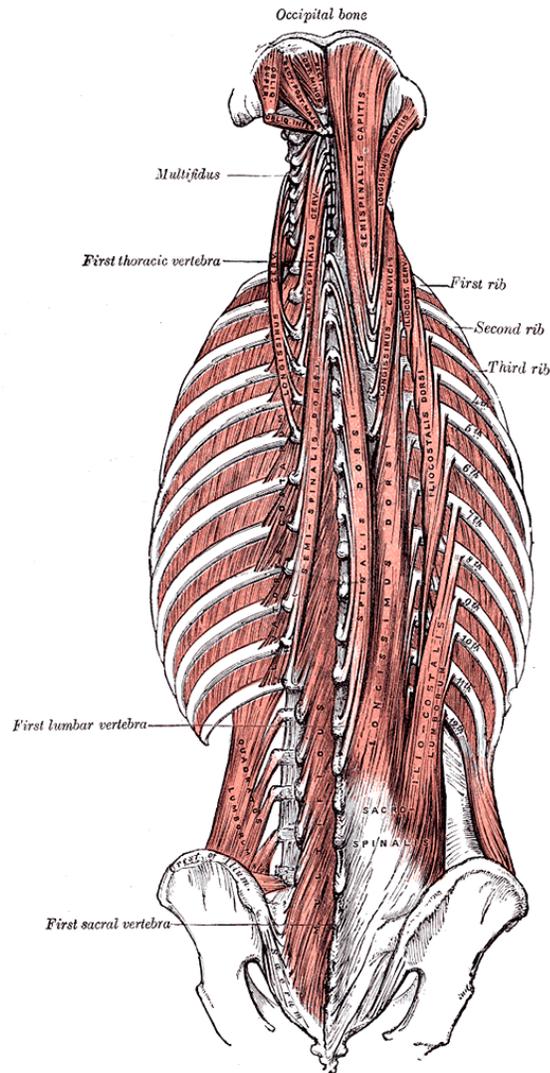
Figure 1-6: Deep musculature of the human back (Gray, 1918)

While the vertebral joints provide geometric and movement constraints to the spine, the relative motion of the functional units is effected by numerous muscular elements connected to the posterior processes among the vertebrae. The isolation of particular trunk muscles and the acquisition of their electrical activity in human subjects is a laborious and complex undertaking demanding another dedicated study, especially under exposure to WBV. In addition, the reported electromyographic studies show very little agreement probably attributable to the high degree of noise in the acquired signals

12

(Basmajian, 1980). Since the scope of this thesis does not involve the study of muscular activity, this description of the spine limits itself to briefly explaining the muscular architecture of the back for gaining a basic level of understanding of the functioning of the spinal substructures. While back muscles may be categorised broadly into two layers, namely the superficial and deep (or intrinsic) muscles of the trunk, the intrinsic musculature is of concern since it is directly in contact with the spinal substructures. Figure 1-6 illustrates the posterior section of the trunk showing the deep muscles of the back interlinking different levels of the vertebral processes. The intrinsic muscles may further be divided into three groups (columns) based on their lateral position relative to the spine as: (i) the *spinalis* (also called the *erector spinae* group, which is closest to the spine); (ii) *longissimus* (intermediate); and (iii) *iliocostalis*, as illustrated in Fig. 1-6. These intrinsic muscles and ligaments, which are passive muscular elements, in addition to other deeper muscles not mentioned here (*e.g.*, *multifidus*, *rotatores* etc.), are attached between the spinous and transverse processes of the vertebrae at different sections of the spine so as to effect and control the trunk movements in multiple axes. Thus, the coordinated movement of sets of vertebrae, due to the synchronised activation of corresponding sets of muscles, constrained by ligaments and vertebral joints, gives rise to functionally useful changes in the spine curvature, very much like an active multi-link mechanism.

The complex human musculoskeletal spine plays a pivotal role in a variety of functions including human locomotion, upper body load-bearing and support, and postural control of the body. In addition, the vertebral arches in each vertebrae form a protective and flexible conduit along the spine that houses the cluster of nerves that

constitutes the spinal column, which forms part of the central nervous system in the human body. While the synchronised functioning of the biological components of the spine in a healthy human being ensures the safe performance of daily voluntary and involuntary activity under normal living conditions, the exposure to harmful vibration and shock could affect various elements of the spine, including the vertebral joints, nervous system and muscular activation, not to mention blood flow in the associated vessels. The human body usually reacts to these external interventions by exhibiting pain around the concerned region, which is a major indicator of a biological abnormality. The subsequent section thus reviews the relevant epidemiological studies on spinal disorders and pain observed among operators of mobile machinery that may be inducing harmful vibrations into the human body.

1.3 Epidemiological findings on the relationship between LBP and WBV

A number of epidemiological studies on low back pain among the vibration-exposed population have been reported. These generally involve surveys conducted with standardised questionnaires in the work site identified with a high risk of back pain and spinal disorders. Statistical conclusions are subsequently made by comparing these field results with those attained for a "control group" not exposed to similar conditions. LBP surveys in relation to machine-induced WBV are generally carried out by identifying symptoms or observable musculoskeletal spine disorders in a chosen subject population exposed to vibration at the workplace. A control group, not exposed to such vibration is usually selected to serve as the reference for the field study results. Agriculture, mining, material handling, transportation–cargo/passenger, forestry, construction and even aviation may be cited as examples for work environments where human operators are

exposed to vibration from machinery (*e.g.*, Bovenzi and Betta, 1994; Bovenzi *et al.*, 2002; de Oliveira *et al.*, 2001). Most epidemiological studies have been undertaken through questionnaires designed to isolate possible causes and risk factors for LBP occurrences and any systematic environmental risk factors (Palmer *et al.*, 1998). Medical observations through magnetic resonance imaging (MRI) of the spine (Luoma *et al.*, 1998) or stadiometric measurement of spinal height before and after a set period of work may also be recorded on the subject group (Pope *et al.*, 2002) to make epidemiological results more quantitative.

A comprehensive review of 17 surveys was presented by Bovenzi and Hulshof (1998) spanning twenty two WBV-exposed occupational groups including crane operators, drivers of fork-lift trucks, tractors, helicopters, wheel-loaders, transportation trucks, buses and subway trains. The cross–sectional study showed increased prevalence of LBP, sciatic pain in lower leg and back disorders in the WBV-exposed versus the non-exposed control groups. Furthermore, studies on farm tractors (Bovenzi and Betta, 1994) and port machinery operators (Bovenzi *et al.*, 2002) showed both WBV and posture to be independent indicators of LBP. In these studies, regression analysis revealed a strong influence of vibration exposure duration and cumulative dosage on the risk for LBP. It was also suggested that awkward postures like bending forward and twisting of the spine may have a long-term adverse effects on spinal health. However, posture alone as a factor could not be correlated with LBP. Exposure–effect relationships were analysed in 388 drivers of different vehicles by Schwarze *et al.* (2002) using questionnaires, and X-ray measurements of affected body locations. This four-year longitudinal study showed greater incidence of spinal disorders in a group exposed to 0.6 m/s^2 (eight-hour energy

equivalent exposure as defined in ISO 2631-1 (1997), while the German guidelines (VDI 2057, 1987) specify a 0.8 m/s^2 threshold for hazardous daily exposure. Although no specific cause could be attributed to the observed lumbar syndromes, it was concluded that long-term vibration exposure has a high probability of causing spinal health effects.

It is known from the biomechanics works that the sagittal-plane orientation of the pelvis is different in the sitting and standing postures (Chaffin *et al.*, 1991). In addition, the lordosis of the lumbar spine usually observed while standing erect, is suppressed in the sitting postures, which may increase intra-discal forces, in this posture. However, the majority of the epidemiological studies seem to concentrate more on the work environment than inherent factors such as posture and seating conditions. A comprehensive review of epidemiological, biomechanical and physiological factors of posture that might cause musculoskeletal problems was presented by Magnusson and Pope (1998). Prolonged sitting in constrained spaces along with WBV was found to increase the risk of LBP. The authors suggested a set of postural and environmental changes that might reduce the risk of muscular pain and disorders. Changes to workspace design so as to decrease postural loading, adoption of certain comfortable postures and avoiding material handling after exposure to WBV were suggested as measures to reduce the risk of LBP in the workforce. A survey of 23 fork-lift drivers by Hoy *et al.* (2005) also corroborated the view that WBV and awkward postures together pose a greater risk for LBP. The study by Rehn *et al.* (2002) reported muscular pain and disorders in the neck, shoulder and thoracic region in operators of forestry and snow-removal equipments (421 subjects totally), attributed possibly to an elevated arm position in some operating conditions since the driver had to constantly lean forward to ensure better visibility.

Interestingly, LBP was significantly high in the control group, which prompted the authors to suggest that WBV alone may not be the most significant factor for the risk of pain.

One common observation from the majority of epidemiological studies is the inability to establish a relationship between WBV and health effects, due to the presence of various confounders. The highly non-linear nature of psychological, physiological and environmental factors makes it impossible to draw definitive conclusions from epidemiological surveys. The subjective nature of the surveys makes them susceptible to human perception errors (psychological). Although this seems trivial, parameters like job satisfaction and mental state of the operator during the survey have been shown to be significant confounders, leading some machine operators to overestimate the pain (Hoy *et al.*, 2005). Physiological differences such as anthropometry and gender, among the surveyed population may cause changes in data even under identical occupational conditions. Some other confounders that deter thorough epidemiological investigations are the age distribution, and variations in the life style such as smoking, eating, drinking and exercise habits, which may have an effect on the neuromuscular responses.

Disregarding a bent–forward posture during prolonged machine operation may underestimate health risk prediction (Seidel, 2005). In addition, it has been reported that WBV exposure interspersed with manual material handling tasks (*e.g.*, lifting) may accelerate the risk of lumbar disorders and LBP (Pope, 1996). Kumar *et al*. (2001) reported no significant change in MRI data between tractor drivers exposed to WBV and the corresponding control group (farming non-drivers). It was suggested that the unexpected result might be due to the equally stressful manual faming jobs that the

control group was involved with. In addition, the duration of daily vibration exposure is usually predicted based on operator judgement and thus may be inaccurate. Furthermore, acceleration weighting factors (ISO 2631, 1997) based on root-mean-square (RMS) averaging of machine excitations are not suited to characterise vibration spectra with high crest factors (greater than 9) typically found in tractors and fork-lift trucks (Nélisse *et al.*, 2008). These transients are reported to have a significant influence on the spine loading (Seidel *et al.*, 1997) as well as back muscle activity (Blüthner *et al.*, 2001), which could well be suppressed by the application of RMS methods.

Epidemiological research needs to be conducted at regular time intervals so as to identify the risks for LBP or other vibration-related work disorders and to understand if a particular intervention strategy is effective in reducing such risks. However, such subjective surveys may also have to be augmented with more quantifiable experimental and modelling studies so as to better understand the phenomena that may be adversely affecting the vibration-exposed human body in the work environment.

1.4 Experimental assessment of human whole-body vibration

Vibration experiments on the human body have shown the subjective perception of discomfort to be dependent on excitation frequency (Whitham and Griffin, 1978). It has also been noticed by clinical follow-up studies after epidemiological surveys that increased discomfort reported by subjects was associated with detrimental effects of WBV (Seidel, 2005). Frequency weightings defined in the international standard, ISO-2631-1 (1997), for the assessment of vibration exposure and safe design of machinery, are primarily based on this assumed relationship between perceived discomfort and the health risk. Although these frequency weighting functions quantify safe operational zones

in vibrating machinery for human safety in terms of excitation magnitude, frequency, discomfort criteria and exposure tolerance time limits; they are primarily founded upon subjective observations. Moreover, the evaluations of comfort in the standards are based on RMS values of weighted acceleration, which may be insufficient for the assessment of vibration with large transients. An assessment parameter based on the fourth-power of weighted acceleration, the Vibration Dose Value (VDV) has also been suggested, which is more sensitive to time-dependent vibration exposure with high crest factors. The VDV expressed in $m/s^{1.75}$, is obtained by taking the fourth root of the time integrated fourth-power of weighted acceleration, which unfortunately fails to make any physical sense for use in the design of machinery. It should be noted that while a few other vibration assessment variables such as Maximum Transient Vibration Value (MTVV) and Dynamic Response Index (DRI), have also been defined to account for the different kinds of excitation conditions, all these methods are based on the subjective performance measures of discomfort due to WBV exposure. Moreover, they do not incorporate information on any form of direct measurement techniques from the human subject.

Alternatively, the human body may be likened to a mechanical system with inherent stiffness and damping properties. The nature of these parameters is, however, difficult to accurately establish due to the high level of non-linearity in tissue properties (Markolf, 1970; Panjabi *et al.*, 1976). On the other hand, it is possible to study the impedance response of the biomechanical human body at certain points of interest. The sitting human is in contact with the mobile machinery (*e.g.*, cranes and trucks), primarily at the seat and thus the force and vibration transmission to the body also happen at the buttock-seat interface: the 'driving-point.' This force is a significant parameter and may

19

reflect the local dynamics and the mechanical properties if the point of interest is close to the seat interface (Sandover, 1998). However, due to the prevalence of LBP in the body segments above the interface, it may be more useful and appropriate to study the vibration responses at different locations on the body.

Although the measurement of internal forces on a live human subject is impossible due to ethical concerns, a few indirect methodologies have been developed to estimate the effects of WBV on the trunk and spinal structures. Long term exposure to heavy lifting or postures like extreme-flexion, found in many material handling facilities, might cause the stretching of spinal units due to 'creep.' This is registered as a change in spine height termed 'stature.' Since the daily dynamic activities such as walking, sitting and lifting involve changes in spinal stature (van Deursen *et al.*, 2005), the exposure to WBV could also be assumed to induce changes in the spine height. The measurement of stature is thus usually performed in-between or after intervals of exposure to vibration, using a 'stadiometer' (Pope *et al.*, 2002). The reported studies have, however, depicted contradictory results establishing no clear link between stature and WBV (Drerup *et al.*, 1999; Bonney and Corlett, 2003). The stadiometric technique is thus usually employed as a means to augment epidemiological results (Pope, 1996). The measurement of biodynamic functions that characterise the force and motion responses of the human have been considered more reliable to study the dynamics of the vibrating human body (Coermann, 1962).

1.4.1 Definition of biodynamic response functions
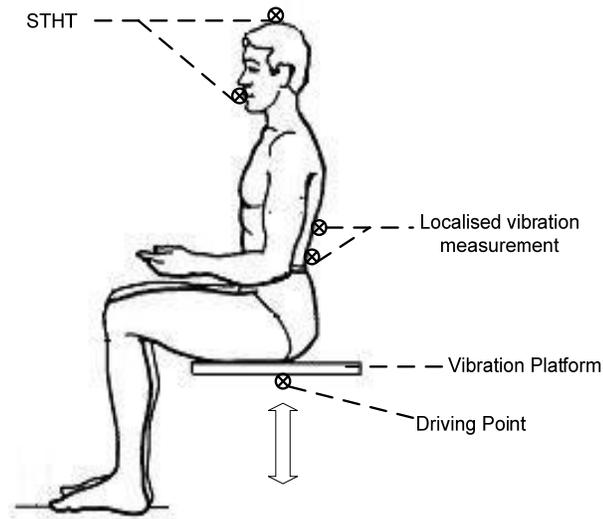
Figure 1-7: General locations for attachment of sensors for the measurement of driving-point and body segment vibration responses of the seated human body (Chaffin *et al.*, 1991).

Biodynamic responses may be generally classified based on (i) the type of variables measured, *viz.*, 'force-motion' and 'motion-motion'; and (ii) the measurement location relative to the vibrating body, as 'driving-point' and 'body-segment' responses. Figure 1-7 illustrates a typical sitting human subject exposed to vibration from a seat in the vertical axis (*Z*). The point of entry of vibration, commonly referred to as the 'driving-point', in this case is the seat-buttock interface. Due to the complexities involved with measurement of forces at different locations on the body, the body force is usually measured at the driving-point. Force-motion responses for the vibrating human body hence primarily refer to the complex driving-point biodynamic functions namely, the seat apparent mass (APMS) and the driving-point mechanical impedance (DPMI) (*e.g.*, Coermann, 1962; Fairley and Griffin, 1989). Alternately, the vibration transmitted through the body may be characterised by the vibration measurements directly at

21

different locations on the body (*e.g.*, Panjabi *et al.*, 1986). The ratio of motion at the body locations and the seat are referred to as 'motion-motion' responses, the most widely reported of these being the seat to head acceleration transmissibility (STHT) (*e.g.*, Paddan and Griffin, 1998). The DPMI, APMS and STHT, respectively, may be mathematically represented as:

$$DPMI: Z(j\omega) = F(j\omega) \Big/ V(j\omega) = G_{FV}(j\omega) \Big/ G_{VV}(j\omega) \qquad (1.1)$$

$$APMS: M(j\omega) = F(j\omega) \Big/ A(j\omega) = G_{FA}(j\omega) \Big/ G_{AA}(j\omega) = Z(j\omega) \Big/ j\omega \quad (1.2)$$

$$STHT: H(j\omega) = H(j\omega) \Big/ A(j\omega) = G_{HA}(j\omega) \Big/ G_{AA}(j\omega) \qquad (1.3)$$

Where, F, A and V represent the force, acceleration and velocity measured at the driving-point, respectively, in the vertical axis. G_{FA} and G_{FV} depict the cross-spectra, respectively, of the aforementioned acceleration and velocity, with the seat force. Similarly, the cross-spectrum of the acceleration at the head with the seat is denoted by G_{HA}. The auto-spectra of the motion quantities, *i.e.*, acceleration and velocity are denoted as G_{AA} and G_{VV}, respectively. The angular frequency of vibration (ω) is expressed in radians per second and the complex phasor is represented by j whose value is $\sqrt{-1}$.

By using a similar approach, the vibration transmissibility (T) of a particular body segment (i) may be expressed by the ratio of the cross-spectrum of the acceleration (A_i) at i and the seat, and the auto-spectrum of the seat acceleration as:

$$T_i(j\omega) = A_i(j\omega) \Big/ A(j\omega) = G_{A_iA}(j\omega) \Big/ G_{AA}(j\omega) \qquad (1.4)$$

Further, the force-motion signals acquired at the driving-point may be utilised to estimate the vibratory power absorbed by the human body (Wang *et al.*, 2004). The power at the seat-body interface is expressed by the product of the dynamic force and velocity, as:

$$P(t) = F(t)V(t) \tag{1.5}$$

The frequency-dependent oscillatory power $P(j\omega)$ may thus be calculated from the cross-spectrum of the force and velocity measured simultaneously at the driving-point (Lundström and Holmlund, 1998) and expressed as the complex quantity:

$$P(j\omega) = C_{VF}(\omega) - jQ_{VF}(\omega) \tag{1.6}$$

Where, $C_{VF}(\omega)$ and $Q_{VF}(\omega)$ are respectively, the real coincident and imaginary quadrature spectral density functions of the cross-spectrum $P(j\omega)$ expressed in Nms^{-1}/Hz. The real component or the co-spectrum of the power determines the energy absorbed by the human body due to internal tissue friction. The quad-spectrum quantifies the energy stored within the body. Interestingly, biodynamic absorbed-power is significantly affected by the magnitude and duration of vibration exposure and hence provides a potential methodology for the quantification of a 'dose' value (Griffin, 1990). However, being a quantity derived from driving-point dynamics alone, it might not be suitable to draw conclusions on the detrimental effects of vibration on the spinal segments. Naturally, the ease of measurement of force-motion functions at the driving-point has led to a number of studies on APMS and DPMI. On the other hand, STHT has been measured through a variety of techniques employing head harnesses such as helmets, caps and other straps, and through a bite bar assembly mounted with accelerometers (Paddan and Griffin, 1988; Wang *et al.*, 2006). Such wide variations in measurement systems and the

unconstrained movement of the head-neck complex have been attributed to the huge

scatter found in STHT responses from different studies (Paddan and Griffin, 1998).
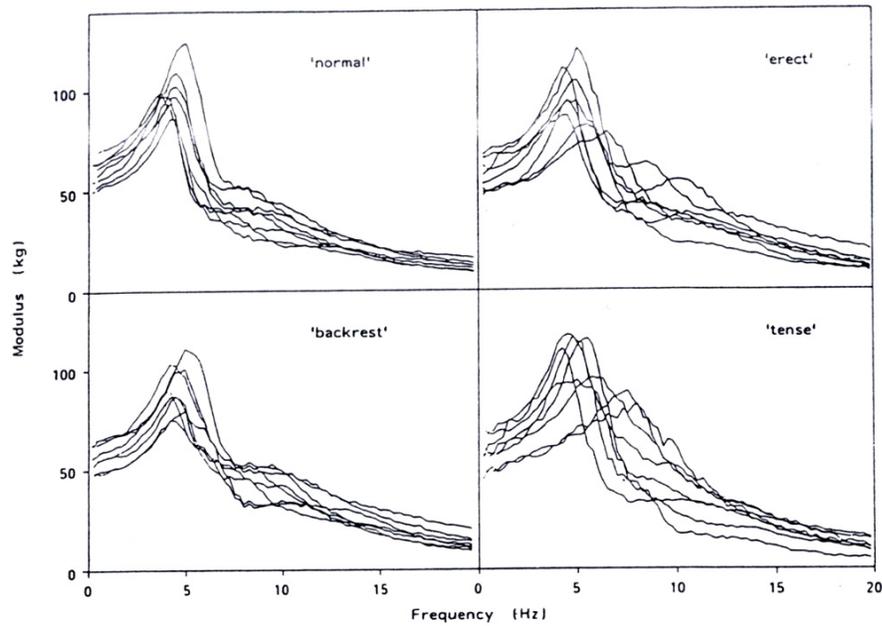
Figure 1-8: Apparent mass measured at the seat by Fairley and Griffin (1989) in various
sitting conditions with subjects exposed to vertical WBV.

Figures 1-8, 1-9 and 1-10 illustrate the reported biodynamic responses of seated

subjects, respectively, in terms of APMS, STHT and absorbed-power under exposure to

vertical WBV. It may be noticed that in the vertical axis, all the three responses show a

peak value around 5 Hz. This characteristic is widely accepted to be caused by a primary

resonance mode of the entire body in the sitting posture (Fairley and Griffin, 1989). Both

the interface forces (APMS) and the acceleration at the head (STHT) tend to peak around

this frequency indicating the presence of a vertical vibration mode of the entire body. In

addition, the peak resonance value of vertical power absorbed (Figs. 1-10 c and f) at the

driving-point is suggestive of significant tissue stress/strain. However, the mechanisms

responsible for resonance are still not fully understood. The considerable fore-aft and

24

pitch transmissibility magnitude at the head even under vertical excitation (Fig. 1-9) around resonance indicate probable multi-dimensional movements of the upper body or the head-neck region. Moreover, measurements at the driving-point and extreme end-point (head) of the human biomechanical system may not be sufficient to characterise the movements of the intermediate segments of the upper body. Hence the measurement of multi-dimensional motion at locations forming the path for vibration transmission through the body may yield better understanding of the dynamic behavior of different segments exposed to WBV.
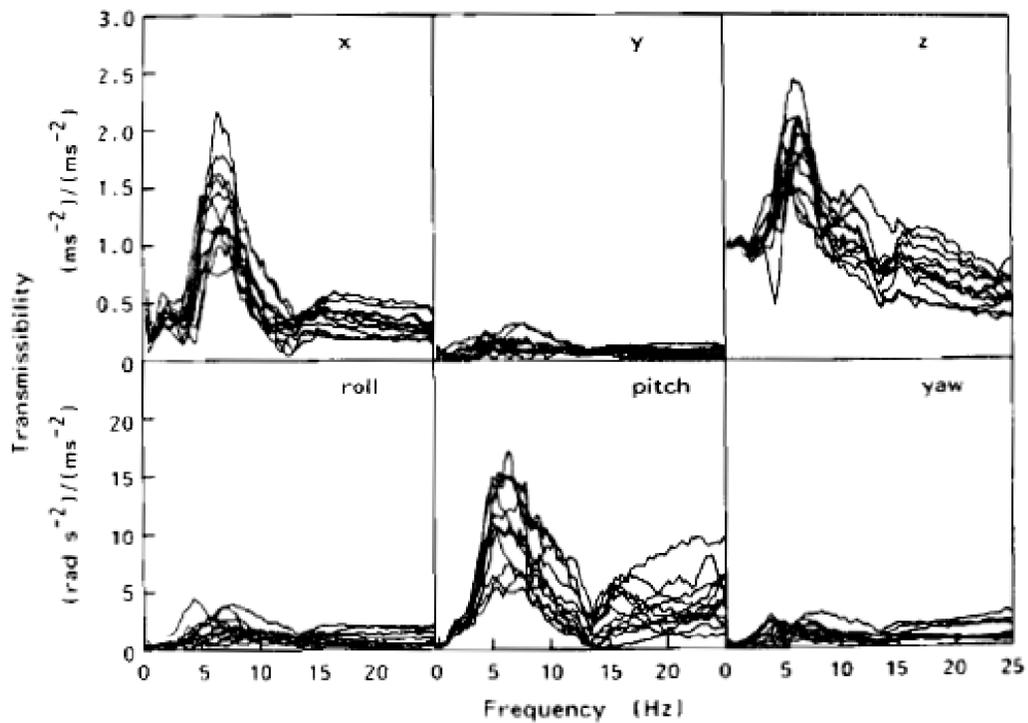
Figure 1-9: Translational and rotational seat to head acceleration transmissibility in three-axes measured with 12 subjects sitting with a backrest and exposed to vertical excitation (Paddan and Griffin, 1988)
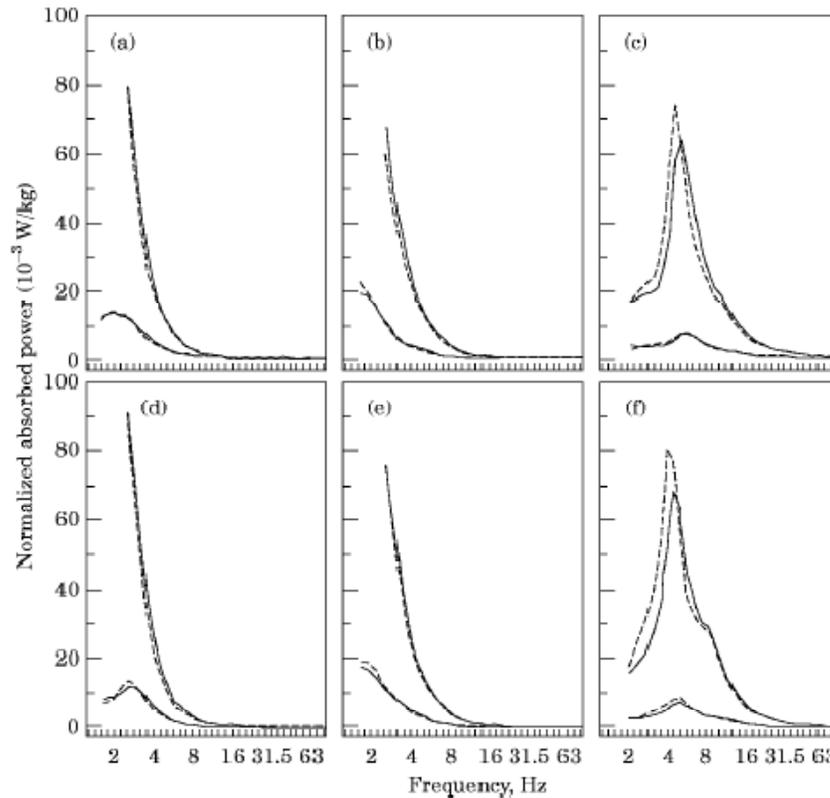
Figure 1-10: Power absorbed male and female (Lundström and Holmlund, 1998)

1.4.2 Measurement of vibration 'through' the body

The segments of the musculoskeletal spine composed of vertebrae, discs, muscles and ligaments provide the path for vibration transmission within the body and in the process undergo relative movements. The stresses generated due to vibration may "load" the spine and lead to irreparable damage of substructures in the long term (Pope *et al.*, 1998). Vertebral endplate failure and/or disc degeneration due to rupture of the nucleus tissue are well known reasons that cause spine disorders (Dolan and Adams, 2001; Wilder and Pope, 1996). It may thus be useful to know the nature of vibration transmission through the spine. However, it is impossible to measure forces in the discs directly in live human subjects. Thus, the study of the transmission of WBV "through the seated human" invariably involves the acquisition of motion parameters at the selected

26

body segments. Body-segment vibration studies may be classified primarily based on the measurement techniques. Motion data may be acquired by surgically or *invasively* inserting relatively rigid but thin wires dorsally into the chosen vertebrae and mounting motion sensors on the wire outside the body (*e.g.*, Zagoski *et al*., 1976; Panjabi *et al*., 1986; Pope *et al*., 1986). Alternatively, transducers may also be *non-invasively* attached to the skin at selected locations, for example over the vertebral spinous process (*e.g.*, Hinz *et al.*, 1988a; Matsumoto and Griffin, 1998). Due to the inaccessibility to deep vertebral locations, invasive studies have been performed on the vibration behaviour of primate spines (Quandieu and Pellieux, 1982; Slonim, 1985). However, it should be noted that although the spinal layout of primates closely resembles humans, vibration data collected on a baboon harnessed and probably drugged may not be comparable to human subjects who could be requested to assume various postures voluntarily. Alternately, human cadavers have been utilised in some experiments to acquire normally inaccessible parameters (*in vivo*) such as disc pressure and acceleration at the vertebral bodies under exposure to vertical random WBV (El-Khatib *et al*., 1998; El-Khatib and Guillon, 2001). While two peaks were observed in the vertical responses around 4 and 9 Hz, in most of the postures, there was considerable inter-subject variability. Due to observable differences among acceleration and disc-pressure measurements, the authors suggested that measurement of vertebral motion variables alone may be insufficient for the assessment of spinal health risks posed by WBV. It must however be noted that the absence of muscle activity in the cadavers may have altered the vibration transmission properties and thus the disc pressure considerably.

27

Table 1-1: Studies reporting vibration response measured at different locations on the seated human body exposed to vertical excitations.

	Study	Purpose (Type of Input Excitation)	Sensor Location on Body (Axes)
Invasive Studies	Zagorski *et al.* (1976)	Measure acceleration at different spine locations (Sinusoidal)	Head, C7, T7, L, S3 (Z)
	Panjabi *et al.* (1986) [†]	K-wire accelerometers to measure vertebral motion directly (Sinusoidal)	L1, L3, Sacrum (X, Z, Pitch)
	Pope *et al.* (1986)	Comparison of LED displacement on skin versus vertebral pins (Sinusoidal)	L3, PSIS (Z)
	Sandover and Dupuis (1987)	K-wire photogrammetric study of vertebral displacement (Sinusoidal)	T12, L1, L2, L3, L4 (X, Z)
	Pope *et al.* (1989) [†]	Measure lumbar vertebral response on cushioned seats (Impact)	L3, Sacrum (Z)
	Pope *et al.* (1991)	Relative shear, axial and pitch movements of lumbar vertebrae (Sinusoidal)	L3, L4, L5 (X, Z, Pitch)
	Magnusson *et al.* (1993) [†]	Analyse the influence of back support on lumbar transmission (Impact)	L3, L4 (X, Z)
	El-Khatib *et al.* (1998) [†]	Measure acceleration vertebral transmission in human cadavers (Random)	L1 – L5, Sternum (Z)
	Pope *et al.* (1998)	Response of lumbar vertebra on different types of seats (Impact)	L3 (Z)
	El-Khatib and Guillon (2001)	Measure intradiscal pressure in lumbar spinal units of cadavers (Random)	Discs: L1 – L5
Non-invasive Studies	Donati and Bonthoux (1983)	Simultaneous measurement of DPMI and thoracic acceleration transmissibility (Random and Swept Sine)	Sternum (Z)
	Seidel *et al.* (1986)	Predict the lumbar stress and strain with acceleration and EMG measurements (Sinusoidal)	Head, shoulder, T5 (Z)
	Hinz and Seidel (1987)	Analyse non-linearity of vibration transmission through the body (Sinusoidal)	Head, Shoulder, T5 (Z)
	Hinz *et al.* (1988a) [†]	Derive functions for correcting tissue effect on skin mounted accelerometers (Sinusoidal)	T5, L3 (Z)
	Hinz *et al.* (1988b)	Bi-dimensional relative motion of lumbar vertebrae (Sinusoidal)	Head, Shoulder, L3, L4 (X, Z)
	Hinz *et al.* (1994)	Predict compressive loads on lumbar vertebra during transient vibration (Half and full Sinusoids)	Acromion, L3, L4 (Z)
	Zimmermann and Cook (1997)	Analyse effect of pelvic tilt on vibration transmission properties of the body (Sinusoidal)	Head, T5, Pelvis (Z)
	Seidel *et al.* (1998)	Predict vertebral loads due to vibration (Field Measured Signal)	T5, T11, S1, S3 (Z)
	Kitazaki and Griffin (1998)	Extract modes of vibration of the human body (Random)	Head, T1, T6, T11, L3, Sacrum (X, Z)
	Matsumoto and Griffin (1998) [†]	Study movement of the seated body (Random)	Head, T1, T5, T10, L1, L3, L5, Pelvis (X, Z, Pitch)
	Mansfield and Griffin (2000)	Analyse pelvic movement under vibration (Random)	Upper and lower abdomen, L3, illiac crest, PS illiac spine (X, Z)
	Matsumoto and Griffin (2002)	Investigation of the effect of excitation magnitude on acceleration at different body segments (Random)	T1, T5, T10, L1, L3, L5, L5 (Z, Pitch)
	Yoshimura and Nakai (2005)	Measurement of vibration at different segments of the body for development of biodynamic model (Random)	L1, L2, L3, L4, L5 (Z)

[†] Study chosen for response comparison in Chapter 4

Table 1-1 provides a list of selected WBV studies that measured vibration parameters at different locations on the spine and body locations. Live human volunteers have been employed in some studies with invasive instrumentation of vertebrae, using thin threaded Kirschner (K) wire under local anesthesia. Motion sensors such as accelerometers, displacement transducers and photogrammetric motion capture markers have been mounted on the K-wire to estimate the vibration transmission to the spinal units in the seated position (*e.g.*, Lange and Coermann, 1965; Christ and Dupuis, 1966; Hagena *et al*., 1986; Panjabi *et al*., 1986).

A peak response in the vertical motion transmissibility around 5-7 Hz has been noticed in most of the measured vertebral locations, which corresponds to the resonance characteristic observed from the seat APMS response under vertical excitation. While Panjabi *et al.* (1986) reported insignificant differences in the vertical acceleration transmitted to different lumbar locations, Sandover and Dupuis (1987) observed relatively larger motion in the horizontal axis between the vertebral combinations T12–L2 and L2–L4. Pope *et al.* (1991) also revealed coupled motions in shear, compression and pitch amongst the L3–L4 and L4–L5 vertebral pairs in subjects exposed to sinusoidal vibration at 5 Hz. This is suggestive of complex bi-dimensional relative motion among the lumbar vertebrae. However, the inter-subject variability within each study and the wide variations in experimental methods between the studies make it difficult to derive generally applicable body segment vibration responses. Moreover, owing to the medical and ethical concerns associated with the insertion of pins into the skeletal structures of the spine, the acquisition of vibration data by mounting transducers on the skin by non-invasive means has been adopted in a number of recent studies.

Such vibration measurements on the skin surface have been undertaken with accelerometers either strapped on or attached by adhesives to the upper body locations and motion capture markers, as listed in Table 1-1. The securing of accelerometers is a challenging task due to a variety of reasons. The location of a particular vertebral spinous process in the back of human subjects is bound to alter slightly with change in postural conditions. Moreover, sensors attached on the corresponding skin location are prone to pick up the relative movement of the dermic tissue and are known to overestimate the vibration at the vertebra (Pope *et al.*, 1986). Appropriate mathematical correction procedures are thus required to extract the actual vibration transmission properties through the skeletal elements of the body (*e.g.*, Kitazaki and Griffin, 1995). In addition, there are other errors that may arise due to misalignment of the sensors from the biodynamic axis due to local tissue curvatures and movement (Hinz *et al.*, 1988a) and sometimes inherent noise in the data acquisition system due to the lengths of cables employed. Despite these complexities, the study of body segment responses may provide valuable information on the nature of WBV "through-the-body" transmission for better understanding and interpretation of human biodynamic responses to WBV.

It is interesting to note that only a few studies have measured the vibration transmitted "through-the-body" simultaneously with established biodynamic functions such as DPMI or APMS. The study by Donati and Bonthoux (1983) revealed a clear peak in all the three simultaneously measured responses namely, the absorbed power, DPMI and vertical vibration transmissibility at the sternum between 4 and 5 Hz, irrespective of the type of excitation. It was suggested that the human body's vertical motion responses could be simplified by a one degree-of-freedom simple lumped parameter model.

However, the human body has been shown to exhibit non-linear biodynamic properties (*e.g.*, Fairley and Griffin, 1989; Paddan and Griffin, 1998). Hinz and Seidel (1987) observed distortion of sinusoidal waveform at the T5 when human subjects were exposed to cyclic excitation at discrete frequencies, even while the APMS at the seat showed no such trends. In addition, the measured vibration transmissibility to the pelvis and the seat APMS responses have demonstrated similar trends in characteristics leading to the hypothesis that the resonance peak observed in the APMS magnitude may be influenced by pelvic rotation and spinal movements (Mansfield and Griffin, 2000). Interestingly, pelvic rotation has been observed by some body-segment studies at a higher frequency (Matsumoto and Griffin, 1998).

Small perturbations in the orientation of the sacro-pelvic unit may alter the spinal curvatures considerably and thus affect the nature of vibration loading on the vertebral units (Chaffin *et al.*, 1991). This phenomenon may have greater effects on the movements of low inertia segments of the spine than directly influencing the global seat APMS parameter. Additionally, Zimmermann and Cook (1997) showed that a static posterior pelvic angle, although having insignificant effect on the vibration transmitted to the thoracic spine (T5), increased the head response at 4.5 and 5 Hz. However, only a few studies have investigated such postural influences on body segment vibration properties, probably due to difficulties in the identification of appropriate locations for motion measurement around the lower lumbar and pelvic regions.

The actual reason for the resonance peak observed in the driving-point response variables such as APMS, DPMI and absorbed power is still unclear. Some studies suggest buttock tissue compression and shear at resonance frequency, while others hypothesise a

variety of spinal movements including lumbar compression-extension, spine bending and pelvic pitching have significant influences. Matsumoto and Griffin (1998) measured vertical, fore-aft and pitch acceleration transmissibility at different locations on the body exposed to vertical seat vibration. A vertical resonance around 5 Hz was observed at all the body locations in majority of the subjects. Although considerable relative axial movement of the spine was not identifiable at resonance, pelvic pitch causing compression and shear of the buttock tissue were reported around the vertical resonant frequency. It was thus hypothesised that multiple vibratory modes may be contributing to the resonance peak observed in the seat APMS. Modal frequencies and shapes were identified for the sitting human body exposed to vertical vibration by Kitazaki and Griffin (1998) from the measured acceleration transmissibility using experimental modal testing techniques. The primary resonance of the seated human body was found to comprise of a whole body axial movement of the spine caused by buttock tissue compression and shear, in phase with a vertical visceral mode, and coupled with bending of the upper thoracic and cervical spine. It was further suggested that spinal forces causing injury may not be appropriately predicted by simple lumped-parameter models that do not account for body motion.

Biodynamic responses at the driving-point and head are known to be considerably influenced by a variety of factors including human anthropometry, the nature and magnitude of input excitation, and postural and support conditions (*e.g.*, Mansfield and Griffin, 2000; Nawayseh and Griffin, 2004; Rakheja *et al.*, 2006; Wang *et al.*, 2006). It follows that the spine directly in the path of vibration transmission through the body should be affected by the presence of these conditions. However, very few studies on the

vibration of body segments have performed such investigations (*e.g.*, Magnusson *et al.*, 1994; Donati and Bonthoux, 1983; Matsumoto and Griffin, 2002). The APMS measured at the seat and backrest seem to suggest a change in the nature of spine loading, increasingly towards a shear mode, due to the interaction of the backrest (*e.g.*, Nawayseh and Griffin, 2004 and 2005; Rakheja *et al*., 2006). However, only a few studies have reported the effect of a back support. The vibration study on human cadavers seated with a backrest (El-Khatib *et al*., 1998, 2001) revealed a broader peak in the vertical lumbar acceleration transmissibility. In another study, female subjects seated with a thoracic backrest and exposed to shock vibration showed only slight decrease in the peak gain in vertical acceleration measured using a vertebral pin (Magnusson *et al*., 1994). Although estimations of lumbar loads have been predicted under static sitting for various postures and support conditions (Chaffin *et al*., 1991), the influence of the backrest on vibration transmission properties through the spine is still unknown. It thus behooves the researcher to (i) perform simultaneous measurements of established biodynamic responses along with body segment vibration; and (ii) study of the effect of significant independent parameters in the experiment matrix so as to better understand the nature of vibration transmission "through-the-seated-body." Further, datasets derived from the measurements of vibration at localised segments may be employed as target functions in the development and validation of analytical anthropometric models of the human body with multiple degrees of freedom, for the study of a variety of parameters such as spinal forces and vibration power absorbed in the body segments.

1.5 Analytical study of the effects of vibration on the human body

The measurement of mechanical vibration parameters of the human body involves expensive hardware and necessitates the exposure of human individuals to excitations either in the actual workplace or in a controlled environment. While biodynamic response signals acquired during the operation of machinery in the work environment are characterised by considerable noise due to inherent extraneous factors, the reach of experimental methods is limited by ethical concerns for the test subjects and the operational range of the vibration simulator employed. Additionally, owing to the variability in the measured responses arising due to the non-linearity in subject physical characteristics and biodynamic behaviour, and experimental variables and data acquisition processes, repetitive measurements and demanding data analyses techniques may be necessary to ensure reliable results. Alternatively, mathematical models may be developed to characterise specific aspects pertaining to the vibration behaviour of the human body. The ideal goal of "biodynamic modelling" may be defined as the development of analytical approaches that eliminate the need for measurements with human subjects. However, as mentioned before, the complexity and non-linearity associated with the human body and the vibration equipment make the accurate response predictions from the models a challenging, if not impossible, task. Hence, the vast majority of biodynamic models have been primarily employed to complement experimental vibration research in order to gain a deeper analytical understanding of the human body's responses to machine-induced vibration.

The acquisition of certain responses such as loads and strains in the spinal substructures such as discs and end plates in live human subjects is not possible directly for ethical reasons, although they may provide information regarding the nature of

34

damage in the biological structures due to WBV. These parameters, however, may be estimated from a mathematical model of the entire body or the biological system of concern, when sufficiently validated with other measurable responses such as the vibration transmissibility to the particular body segment. Bio-modelling has been undertaken in a number of studies in order to understand various aspects of the effects of WBV, concerning the biodynamic responses registered at both the body-seat interface and at different locations of the human body (*e.g.*, Fairley and Griffin, 1989; ISO-5982, 2001; Matsumoto and Griffin, 2001). A classification of such modelling efforts along with the key capabilities of each model-category ensues.

1.5.1 Approaches for biodynamic modelling

A number of mathematical models have been developed to simulate different aspects of whole-body vibration (WBV) over the past few decades either for gaining analytical knowledge or for a specific application (*e.g.*, Boileau *et al.*, 1997; Liang *et al.*, 2007; Seidel and Griffin, 2001). The biodynamic models found in the literature may be classified broadly based on the analytical approaches employed as (i) mechanical-equivalent models; (ii) multi-body dynamic models; and (iii) finite element models. Table 1-2 summarises the key features of the three classes of models mentioned above. While, these approaches and the appropriate application are discussed below, a detailed review of key features of selected models as applicable to this dissertation is elaborated in Chapter 6. Alternative modelling methodologies, such as those developed based on artificial neural networks, fuzzy systems and the like are mostly empirical in nature and thus not the concern of this research study (*e.g.*, Karwowski *et al.*, 2006; Zurada *et al.*, 1997).

Table 1-2: Capabilities of different types of bio-models.

Model Type	Human Anthropometry	Domain		WBV Responses		Health Risk Prediction	
		Time	Frequency	Biodynamic functions	Body modes	Segment Forces	Segment Deformation
Mechanical Equivalent		✓	✓	✓	✓		
Multi-body Dynamic	✓	✓	✓	✓	✓	✓	
Finite Element	✓	✓	✓	✓	✓	✓	✓

Mechanical-equivalent models mainly involve the reproduction of a particular biodynamic response of the human body through simplistic analytical representation(s) of the WBV phenomenon, such as biodynamic responses. Such models are mainly used to enhance our understanding of the fundamental characteristics of the overall biodynamic response of the whole-body, to design and analyse seating systems, and to develop physical human body simulators or mannequins for testing seats and/or anti-vibration devices (*e.g.*, Nélisse *et al.*, 2008). For such applications, the primary concern being the study of the influence of the human body on the seating systems' dynamic behaviour, where the extraction of detailed responses inside the body's substructures is not critical. The mechanical-equivalent models have thus been mostly developed on the basis of the measured biodynamic response property of the human body such as the apparent mass (APMS) and mechanical impedance (DPMI) measured at the seat and backrest driving-points (*e.g.*, Boileau *et al.*, 2002; Fairley and Griffin, 1989). Since the primary goal of the mechanical-equivalent models is the simulation of the overall biodynamic response of the

human body, there is no requirement for such a model to be geometrically representative of the body's structure. However, its simplistic construction makes the mechanical-equivalent model both efficient and cost-effective, and thus a practically feasible approach for building simple human simulators (mannequins). Moreover, the analytical models have also been employed for the estimation of representative driving-point biodynamic response of the seated body of different body masses (ISO 5982, 2001).

While the majority of the mechanical-equivalent models are based on the measured responses such as APMS and DPMI, representing the biodynamic phenomenon at the driving-point, it has been suggested that such measurements at the body-seat interface alone may not account for the existence of pain and disorders in various regions of the human spine (Seidel, 2005). Further, it has also been argued that measurement of acceleration transmitted to the head and segments of the trunk of seated humans exposed to vertical excitation are required for deeper understanding of the nature of vibration transmission "through-the-body" and subsequently for the assessment of health risks to the spinal substructures due to WBV (Wang *et al.*, 2006a). However, owing to the variability in the measured body segment responses arising from non-linearity in human characteristics, experimental variables and the data acquisition processes, repetitive measurements and demanding data analyses techniques may be necessary to ensure reliable results. Alternatively, bio-models including the geometric (anthropometric) and mechanical properties of the human body have been suggested to simulate the vibration-induced biodynamic responses of the body's substructures, especially the musculoskeletal spine (Seidel and Griffin, 2001).

The simplest approach to simulate vibration transmission to different body locations of the human exposed to excitations is the use of a multi-body dynamic (MBD) model of the entire human body, in which the major substructures of the body are represented by individual masses and connected to each other by lumped stiffness and damping elements. In principle, a mechanical-equivalent model may also be developed using a multi-body structure with lumped inertial and force parameters. In this sense, both these models are based on the "lumped parameter" approach, being composed of point-definitions for inertial and force variables. However, the major difference between the two techniques is that the verification of the multi-body model necessitates the comparison of the simulated vibration at a specific body segment with that measured at the corresponding body location. The validity of the majority of the reported multi-body models has been established based on the measured vibration transmissibility to different body locations (*e.g.*, Amirouche and Ider, 1988; Fritz, 1998; Kim *et al.*, 2005). It may be suggested that the reliability of these models, however, may be improved if both the driving-point biodynamic response property and the transmitted vibration are employed to determine the model parameters, especially the joint stiffness and damping values. In addition, due to their anthropometric nature, the MBD models are especially useful to predict the dynamic forces acting on the joints and the distribution of vibration in the body system.

It should be noted that the lumped parameter approach which forms the basis for both the mechanical-equivalent and multi-body models cannot be used to simulate the vibration behaviour of a continuous system such as the human body without appropriate assumptions to simplify its non-linear properties. For example, the prediction of detailed

biodynamic responses such as vibration-induced stresses and strains at the spinal elements including the end plates and inter-vertebral discs is not possible using the aforementioned lumped parameter approach (see Table 1-1). For such applications, the best option is to develop a finite element (FE) model of either the spinal substructures (Natarajan *et al.*, 1994) or the whole body with appropriate representation of the spine (Pankoke *et al.*, 1998). Both these approaches have been attempted and will be elaborated in Chapter 6. However, it may suffice to mention here that due to the immense complexity of the human body it is extremely difficult to determine material properties of its different tissue types, thus making the development of the whole body FE model an expensive and time-consuming affair. Moreover, the accuracy of these models cannot be easily established due to the limited measured data available on tissue behaviour and body-segment vibration, in addition to the large variability associated with such reported data. However, FE models provide the capabilities for assessing stresses and strains in the vertebral body and discs, which may be directly applicable for the prediction of health risks due to vibration (*e.g.*, Pankoke *et al.*, 1998).

Three analytical techniques for biodynamic modelling of the human whole body exposed to vibration have been briefly discussed in this section. The choice of the approach to develop a particular bio-model strongly depends on the purpose of the model and the available computational and financial resources. While a number of simplistic lumped mass-spring-damper models have been developed and employed to reproduce driving-point dynamic parameters, more complex anthropometric multi-body and finite element models are required for the simulation of multi-axes motions of the seated human body exposed to WBV.

1.6   Scope of this research dissertation

Field surveys and epidemiological studies point towards the growing significance of work conditions, including the prolonged exposure to vibration and constrained seating postures, on the prevalence of spinal disorders and pain in the working population interacting with vibrating machinery. A definitive relationship between the observed spinal symptoms and whole body vibration has, however, not been established by these studies due to the presence of multiple confounding factors. The experimental study of the biodynamic behaviour of the seated body exposed to vibration is thus required for a more objective characterisation of WBV.

The majority of controlled experiments in the laboratory have acquired the force-motion relationships of the seated human body at the driving-point (buttock-seat interface) in terms of the apparent mass (APMS) and mechanical impedance (DPMI), or the vibration transmitted to the head (STHT) (*e.g.*, Fairley and Griffin, 1989; Paddan and Griffin, 1998). In addition, these studies have mostly focussed on deriving biodynamic responses under WBV limited to vertical excitation, primarily due to the predominance of excitations in this axis (*e.g.*, Fairley and Griffin, 1989; Coermann, 1962; Paddan and Griffin, 1988). The biodynamic functions obtained from these studies have been considered vital for understanding the nature of vibration transmission to the body (Paddan and Griffin, 1998; VIN, 2001), development of methods for assessing exposure severity (Seidel, 2005) and the construction of anthropodynamic manikins for design and assessment of seats (Nélisse *et al.*, 2008). Both the APMS and STHT responses have shown a peak gain in the frequency range of 4 to 6 Hz for the seated human body exposed to vertical vibration, generally considered as the primary vertical resonance characteristic of significance to ergo-dynamic seat design. It has also been argued that

STHT may be more representative of multiple vibration modes of the upper body than a driving-point response (Wang *et al.*, 2006a).

These measures, however, have not contributed to identification of potential injury risks due to WBV. While the APMS and STHT biodynamic functions are derived from measurements, respectively at the seat and the head, the majority of the vibration–related health disorders at the workplace have been noted in the lower regions of the back (Hoy *et al.*, 2005; Bovenzi *et al.*, 2002). It is widely believed that the high incidences of LBP and spinal disorders among the vibration-exposed working population could actually be attributed to harmful motion in the localised segments of the musculoskeletal spine (Wilder and Pope, 1996). However, the movements of the spinal sub-structures may not be sufficiently reflected by the 'global' force or acceleration measurements at the extreme end points alone. The measurements of responses at various segments of the human body in the seated condition are thus crucial for better understanding of the responses to WBV. These could be applied for developments in anthropometric-biodynamic models for predicting relative deflection and forces, and thus potential mechanisms that may induce LBP.

Moreover, the reasons for the resonance peak observed in the APMS magnitude measured at the seat under vertical vibration (Fairley and Griffin, 1989) are still uncertain partly due to the complex nature of upper body movements. The reported studies have attempted to identify a model or mechanism associated with frequencies corresponding to primary magnitude peaks in the response, while only little agreement could be observed among the reported interpretations. Due to the relatively higher peak frequencies observed in the vertical vibration transmissibility to the sacrum, as compared to the

lumbar vertebrae, Panjabi *et al.* (1986) hypothesised that the actual biodynamic stress-strain region could lie at the junction between the lumbar spine and the sacrum. However, Sandover and Dupuis (1987) suggested that the resonance observed in the apparent mass may be related to bending in the lumbar spine caused by rocking of the pelvis. While such a mode has also been reported by some studies around the frequency range of APMS resonance (Matsumoto and Griffin, 1998; Yoshimura *et al.*, 2005), the measured transmissibility data have also revealed the presence of pelvic pitch and lumbar spine extension-compression either coupled with or independent of the bending modes (Kitazaki and Griffin, 1998). The relationship between the driving-point biodynamics and upper body motion has thus not been clearly established yet. Hence, knowledge of body movements extracted from vibration measurements at different locations of the seated upper body may provide much needed information for the ergo-dynamic design of human interface systems in vibrating machinery.

The acquisition of vibration responses at different locations of the trunk has been reported by a number of studies employing either invasive skeletal measurements (*e.g.*, Panjabi *et al.*, 1986) or by attaching vibration sensors on the skin-surface non-invasively (*e.g.*, Donati and Bonthoux, 1983). Due to the ethical concerns associated with surgical procedures on live human subjects in invasive experiments, and the advancements of analytical techniques to estimate skeletal vibration from measurements on the skin surface, non-invasive measurements are preferred for acquiring vibration transmitted to different locations of the seated human body exposed to WBV.

It must be noted that considerable disagreements are observed in the vibration transmission properties of the upper body measured in both the non-invasive and invasive

studies. This may be attributed to a variety of factors including differences in (a) experimental variables, namely seating conditions, posture, type and magnitude of input excitation; (b) subject parameters such as gender, anthropometry and the number of volunteers used; and (c) the data acquisition procedures including the type of sensor and its mounting and signal processing techniques. The reported data on vibration transmission to segments of the upper body may thus not be directly comparable due to the interplay of these multi-factorial influences.

Majority of the reported data on body-segment vibration have been measured with subjects sitting without a back support with hands usually placed on the lap, which may not be representative of typical vehicle driving conditions. A few studies have clearly established significant influences of the back support conditions on the apparent mass and the STHT biodynamic responses (Nawayseh and Griffin, 2004; Paddan and Griffin, 1998; Wang *et al.*, 2006a). It could thus be deduced that the vibration transmission to the upper body, through the musculoskeletal spine will also be affected by the back support, although such measurements with a backrest have been attempted only in two invasive studies, one using human cadavers (El-Khatib *et al.*, 1998), and the other with a thoracic backrest so as to accommodate the instrumentation at the lumbar vertebrae (Magnusson *et al.*, 1993). Additionally, very few studies have characterised the vibration transmission through the body under varying excitation conditions, while the input excitation type and magnitude are known to have significant non-linear effects on the driving-point and head responses under vertical vibration (Mansfield, 2005; Paddan and Griffin, 1998). A study of the effects of significant independent parameters including the support conditions and input excitation on the seated body's response to WBV may thus be better served by the

43

measurement of vibration transmitted to vertebral locations with the inclusion of more representative seating and excitation conditions.

The APMS and STHT responses synthesised in the international standards: ISO 5982 (2001), suggest notable differences in their primary resonant frequencies, which has been attributed to their acquisition in individual sessions possibly involving different subjects. It is thus essential to acquire all these measures (APMS, STHT and trunk segment vibration), under identical test conditions, preferably simultaneously. In addition, considering the wide differences in the reported data on body segment vibration transmissibility and the lack of knowledge on the influence of back and hands support conditions, it is important to characterise responses of the trunk segments under various experimental conditions in order to derive different sets of target functions essential for the development and validation of reliable biodynamic models. The validity of such models could further be enhanced by considering driving-point APMS and STHT data in addition to the segmental responses.

Although the ideal goal of vibration bio-modelling is the development of analytical approaches that could provide estimates of stresses and strains, and reduce the need for repetitive response measurements on human beings, the complexity and non-linearity of the human body make accurate response predictions from models a challenging task. Hence, the vast majority of models have been primarily employed to complement experimental vibration research and for gaining a deeper analytical understanding of biodynamic responses. Such models could further help in the design of effective intervention mechanisms, such as suspension seats (Pang *et al.*, 2005; Stein and Múča, 2003; Tchernychouk *et al.*, 2000; Wei and Griffin, 1998) and anthropodynamic

manikins for assessing vibration isolation performance of suspension seats (Cullmann and Wölfel, 2001; Toward, 2001). While the majority of mechanical-equivalent biodynamic models do not have any representation of the human body structure (Liang and Chiang, 2006), the detailed finite element models of the whole body (Seidel and Griffin, 2001) pose extreme challenges in the identification of numerous joint parameters and may be computationally demanding. Considering the complex nature of the active human body and the excessive scatter of response data found in the literature (Matsumoto and Griffin, 2001; Panjabi *et al.*, 1986; Pope *et al.*, 1991; Yoshimura *et al.*, 2005), it is desirable to develop sufficiently-, but not overly-, simplified biodynamic models that incorporate representative inertial and anthropometric parameters along with appropriate joint properties.

Visco-elastic parameters of biodynamic models have been widely identified through minimisation of errors between the measured and model responses (Fairley and Griffin, 1989; Griffin, 2001; Tchernychouk *et al.*, 2000; Yoshimura *et al.*, 2005). The choice of the error function, however, may have significant influences on the identified parameters and the performance of the model (Wang *et al.*, 2008). An appropriate error function coupled with a simplified multi-body model representing the human structure could help to identify more reliable visco-elastic parameters in an efficient manner. A model thus developed and thoroughly validated could then be employed to derive vibration responses that might be significant but inaccessible to conventional non-invasive measurement techniques.

This dissertation is expected to contribute substantially to research in WBV by generating much needed information on the nature of vibration transmission through the

segments of the human body in the seated posture. Additionally, the outcome of the research study is aimed at providing measurement and analyses methodologies, and an analytical tool for potential applications in the design of seating and body support systems.

1.7   Objectives established for the research dissertation

The overall goals of this research are to study the responses of the seated human exposed to vertical seat vibration through the characterisation of the biodynamic responses of the total body and the body segments as a function of certain seating and excitation conditions, and the development of a mathematical human body model for predicting responses that may be related to potential injury risks. The specific objectives of the proposed study are formulated as follows:

- Perform a thorough literature survey on the reported biodynamic measurements that characterise the transmission of vibration "through-the-body", which would help develop sound measurement methods and identify the key influencing factors.

- Develop measurement methods for non-invasive experimental measurements of seated human subjects' biodynamic responses, including the force-motion and the motion-motion behaviour of the human body, under test conditions representative of vehicular vibration environments and configurations.

- Characterise the human body's biodynamic responses in terms of the measured vibration transmitted to different locations of the upper body in the vertical and fore-aft directions, in addition to the driving-point Apparent Mass at the seat and backrest, with the subjects exposed to vertical seat excitations.

- Analyse the vibration transmission responses of the seated body segments so as to understand the nature of body motions under vertical vibration.

- Analyse the influence of experimental factors including the back-rest condition, hands position and the excitation magnitude on the vibration transmission properties of body segments.

- Identify and analyse the inter-relationships between body segment vibration transmissibility and the driving-point APMS responses in relation to the aforementioned influencing factors, and propose minimal number of target datasets in terms of the simultaneously measured body segment vibration transmission functions and APMS responses for model development.

- Develop an anthropometric multi-body model so as to simulate the sagittal-plane vibration responses of the seated human body exposed to vertical seat excitations.

- Evaluate the distributed vibration energy responses of the model for assessing the effects of vertical vibration on different body segments.

1.8   Organisation of this dissertation

This dissertation is written in 7 chapters. The first chapter is a general introduction to the issue of low back pain, whole-body vibration, and an overview of the experimental and analytical approaches to the study of WBV. The last chapter concludes this dissertation research. The remaining chapters of the dissertation may be separated into two themes, namely: experimental and analytical studies. While chapters 2, 3, 4 and 5 involve the experimental and data analyses sections of the dissertation, chapters 6 and 7 are the analytical parts.

Chapter 2 presents an elaborate literature review on the transmission of vibration through the seated human body exposed to vertical vibration with in-depth discussions on the observed trends in the measured responses and the influence of significant contributory factors. Chapter 3 presents in-detail the experimental design, test methodology, data acquisition and analyses procedures used for the simultaneous measurement of driving-point and body-segments biodynamic functions, which form the experimental part of this research study. Chapter 4 discusses the vibration transmissibility results and analyses the role of the major experimental contributory factors on the measured responses. Chapter 5 expands on the simultaneous measurement of driving-point and body-segment biodynamic responses, discussing the relationships among them in the presence of the influencing factors and proposes a set of target datasets for the development and validation of biodynamic models.

The case for the development of an appropriate model for the simulation of WBV is made in Chapter 6 through a detailed literature survey on the available biodynamic model types. The chapter also presents the work done in this research dissertation in developing a multi-body anthropometric model of the seated human exposed to vertical vibration, by employing the target datasets extracted from measurements in the previous chapter. The application of the developed biodynamic model in predicting the power absorbed by the human body under WBV is also detailed in this chapter.

Finally, the highlights and contributions of this research dissertation, conclusions derived, and the recommendations for future studies are presented in Chapter 7.

2. Seated Body Responses to Vertical Vibration: Literature Review

2.1 Introduction

Most work environments involve human beings operating some form of machinery that generates mechanical vibrations, the exposure to which is known to produce a variety of health effects among the human operators (Lings and Leboeuf-Yde, 2000). Considerable work is being undertaken to study the human responses to whole-body vibration (WBV) exposure so as to identify injury mechanisms and to seek better methods to assess potential injury risks. The major proportion of the efforts is being directed at characterisation of the biodynamic responses of the seated body to WBV through measurements under controlled conditions. The measurement of biodynamic responses have mostly focused on the seat-buttock interface, although most of the workplace-related medical disorders have been found in the lower back and neck regions (Wikström *et al.*, 1994). Consequently, the findings of the biodynamic responses at the driver-seat interface have met with only very little success in quantifying potential WBV injury effects. Alternately, a few studies have explored the transmission of vibration to various body segments in order to identify localised deflections (Sandover, 1998). The segments of the musculoskeletal spine composed of vertebrae, discs, muscles and ligaments provide the path for vibration transmission within the body and in the process undergoes relative movements. The stresses generated due to vibration may "load" the spine and lead to irreparable damage of substructures in the long term (Pope *et al.*, 1998). Vertebral endplate failure and/ or disc degeneration due to rupture of the nucleus tissue are well known reasons that cause spine disorders (Wilder and Pope, 1996). It may thus be useful to know the nature of vibration transmission through the spine.

The measurement of vibration at localised segments of the body, however, poses some many unique problems associated with identification of appropriate measurement locations, sensitivity of low-inertia substructures to a variety of external factors, limitations of the non-invasive measurement systems and sometimes even ethical concerns in employing human test subjects. In spite of these issues a number of studies have measured WBV transmission to different locations on the body. These may be classified based on the nature of the measurement technique employed. Vibration data may be acquired by surgically or *invasively* instrumenting the selected vertebrae (*e.g.*, Panjabi *et al.*, 1986) or by transducers *non-invasively* attached to the skin at selected locations (*e.g.*, Hinz *et al.*, 1988a). The reported studies under vertical (*z*) axis excitation have invariably shown that the dominant vertical vibration transmissibility at most of the body locations occurs in the 4-7 Hz frequency range. However, the relationship between the observed resonances at different body locations and in the established biodynamic variables such as APMS, DPMI and STHT is still unclear, since most studies do not measure these two groups of responses simultaneously. In addition, there is considerable variability among the corresponding body segment responses in the reported studies. This has been attributed primarily to the wide variations in the experimental conditions employed in different studies (VIN, 2001a). The differences in test subject characteristics, the type of excitation, vibration magnitude and duration, the support and postural conditions employed, and the data acquisition equipment and error correction techniques, are also believed to be among the major factors contributing to the variability in the measured responses. Hence, there is a need to collate and analyse the reported studies, so as to extract and understand the vibration transmission properties of the seated human body.

Operation of mobile machinery involves the exposure to a wide variety of vibration waveforms, and human interaction with the seat and the backrest, while operating controls with hands and sometimes the feet. However, only a few studies have attempted to study the influences of such practical factors on the biodynamic responses, limited only to the driving-point (APMS) and head vibration responses (STHT). These have shown substantial influences of the excitation magnitude, back support condition and hands position on the above parameters (*e.g.*, Mansfield and Griffin, 2000; Nawayseh and Griffin, 2004; Rakheja *et al.*, 2006; Wang *et al.*, 2006). It follows that the spine being directly in the path of vibration transmission should be affected by the presence of these external conditions. However, very few studies on the vibration of the spine have employed some form of a support condition (*e.g.*, Donati and Bonthoux, 1983; Magnusson *et al.*, 1993). It thus behooves the researcher to (i) study the body's responses to vibration through simultaneous measurements of established biodynamic responses including the body segment vibration; and (ii) incorporate significant independent parameters, representative of the workplace environment, in the experiment matrix so as to study their effects to better understand the nature of vibration transmission "through the seated body."

This chapter summarises reported studies on vibration measurements performed at different locations on the human body, primarily under vertical excitation. A comprehensive list of invasive and non-invasive studies is enumerated and their significant features and contributions are discussed. The reported studies are further examined to identify the influences of various independent factors including subject anthropometry, excitation magnitude and support conditions. The issues involved in the study of vibration at the spine and body segment level are also highlighted. The analyses

herein form the basis for the design of the test matrix and experimental methodology to be adopted in this dissertation research.

2.2   Human biodynamic responses to WBV

Exposure to vehicular WBV has been widely associated with various health and safety risks among operators of work vehicles, particularly due to injuries related to the spine and the supporting structures (Seidel, 2005). Many epidemiological surveys have shown a strong relationship between prolonged WBV exposure and the symptoms of LBP among the drivers of various vehicles (*e.g.*, Bovenzi and Beta, 1994; Schwarze *et al.*, 2002; Pope, 2005). However, it is still not possible to state from these studies conclusively if WBV alone is a major contributing factor to LBP or that it is merely an additional risk factor in conjunction with other influences (Lings and Leboeuf-Yde, 2000). Consequently, one of the multi-facetted approaches to understanding the effects of workplace vibration on human health and discomfort has been through objective characterisation of the human body through controlled experimental studies of test subjects exposed to WBV on a vibration simulator. In order to represent the postural state of the majority of mobile-machine operators, these studies have been mostly performed with human subjects seated on a vibration platform and exposed to WBV. Such experiments are mostly concerned with the acquisition of mechanical responses such as forces and acceleration at the seat and other body locations so as to derive frequency-dependent biodynamic functions of the seated human exposed to vibration. The reported biodynamic responses under WBV characterise one or more of the following functions: (i) the force-motion frequency response at the body-seat interface in terms of apparent mass (APMS) or driving-point mechanical impedance (DPMI) (*e.g.*, Fairley and Griffin,

1989; Coermann, 1962); (ii) the acceleration transmissibility from the seat to the head (STHT) (*e.g.*, Paddan and Griffin, 1998) (iii) transmission of seat vibration to different body segments (*e.g.*, Matsumoto and Griffin, 1998); and (iv) absorption of vibration power derived from the force-motion relations at the driving point (*e.g.*, Lundstrom *et al.*, 1998). The definitions of these functions have been presented in Chapter 1.

Owing to the sensitivity of the human body to the nature of exposed vibration (ISO 2631-1, 1997), different sets of biodynamic responses have been extracted through measurements under various magnitudes, types and directions of vibration. Due to the predominance of vibration in the pitch-plane due to tyre-terrain interactions and intermittent acceleration-deceleration of most work vehicles, a number of studies have measured biodynamic functions either with vibration input in a single-axis (*e.g.*, Coermann, 1962; Fairley and Griffin, 1989; Paddan and Griffin, 1998; Rakheja *et al.*, 2008), or with excitations in multiple axes (*e.g.*, Mansfield and Maeda, 2007). While considerable variability has been observed among studies measuring responses under fore-aft vibration, there is very little understanding on the relationships within biodynamic responses measured in different axes with multi-directional input.

The vast majority of the measurements have focussed on acquiring biodynamic responses of the seated human body under vertical WBV (*e.g.*, Fairley and Griffin, 1989; Coermann, 1962; Paddan and Griffin, 1988), primarily due to the predominance of workplace vibration in this axis and the relatively lower levels of non-linearity exhibited by the human body to vertical inputs. The biodynamic functions obtained from these studies have been considered vital for understanding the nature of vibration transmission to the body (Paddan and Griffin, 1998; VIN, 2001), the development of methods for assessing exposure severity (Seidel, 2005) and the construction of anthropodynamic

manikins for design and assessment of seats (Nélisse *et al.*, 2008). The review in this research dissertation is limited to studies employing single-axis vertical excitation to derive various types of biodynamic functions.

2.2.1 Driving-point measures

The driving-point measures such as seat apparent mass (APMS) and mechanical impedance (DPMI) are the most widely reported biodynamic functions primarily due to their relative ease of measurement, since they do not necessitate the physical instrumentation of the human subject. In addition, mathematical techniques have also been developed to conveniently derive the vibration power absorption from either of the aforementioned driving-point responses (Lundström and Holmlund, 1998; Wang *et al.*, 2006b). A number of studies have reviewed the reported driving-point measures (*e.g.*, Mansfield, 2005; Boileau *et al.*, 1998; Zhang, 2006). It is observed from the literature that there are considerable differences among the reported studies in their experimental parameters, including the biological characteristics of the tested population and seating conditions. However, irrespective of the test conditions, a prominent peak in the magnitude of driving-point measures occurring in the frequency range of 4-6 Hz is widely believed to represent the primary resonance of the human body exposed to vertical vibration (Fairley and Griffin, 1989). The excellent repeatability of this characteristic in the measured seat apparent mass has been particularly useful for the development of simplified analytical lumped-parameter models that are capable of representing the driving-point biodynamic behaviour of the human body. However, models validated only on such single-point measures have failed to reproduce the multi-dimensional motion of the human body segments, hypothesised to be one of the reasons for spinal disorders (Seidel, 2005). Additionally, physical anthropodynamic manikins

constructed on the basis of seat APMS measurements have shown limited capabilities in characterising the driving-point measures on the seat cushion (Nélisse *et al.*, 2008), largely due to the unknown nature of interactions at the human tissue-cushion interface. Furthermore, the effects on the driving-point biodynamic function due to factors such as vibration type and magnitude, subject characteristics, and seating and support conditions have been demonstrated in some studies (*e.g.*, Mansfield, 2005; Nawayseh and Griffin, 2004, 2005; Wang *et al.*, 2004). Some of these contributory factors and reported interpretations are discussed in Section 2.4.

2.2.2 STHT measures

It is widely believed that a "through-the-body" biodynamic function involving the measurement of vibration transmitted to at least one location on the body in addition to the driving-point could yield more information on the nature of body modes under WBV. The measurement of vibration at the head has been widely performed primarily due to the ease of positioning a harness with a sensor on the head. Moreover, the seat to head vibration transmissibility response (STHT) is considered to represent the overall behaviour of vibration transmission through the body.

A wide variety of methodologies have been employed in the reported STHT studies including the use of a bite-bar at the mouth, helmet or cap and head harnesses (*e.g.*, Paddan and Griffin, 1998; Wang *et al.*, 2006a). It is widely accepted that owing to the high sensitivity of head motion to measurement techniques and differences in experimental conditions, the STHT responses from different studies exhibit wide variability, as illustrated in Fig. 2-1. However, it is also evident from the reported literature that under single axis vertical seat excitation, while there is considerable fore-aft vibration of the head, insignificant lateral motion is observed (Paddan and Griffin,

1998). This is suggestive of vertical translation and pitch rotation of the head-neck segment either independently or due to pitching of the upper body about the lower torso regions. Moreover, the primary peak observed in seat APMS magnitude, under exposure to vertical vibration, is also evident in the vertical STHT function when the two biodynamic variables are measured simultaneously (Rakheja *et al.*, 1998). Furthermore, some studies have shown a clear effect of hands and back support conditions on the vertical and fore-aft STHT responses, which is indicative of the influences of the body support on the upper body modes (Wang, 2006). These claims, however, cannot be substantiated without extracting the motion variables at intermediate body segments of the trunk. The primary focus of this research dissertation is thus the study of vibration transmission through the segments of the upper body. The published literature on vibration responses measured at different body locations on the trunk are reviewed in the following sections together with discussions on the effects of various influencing.
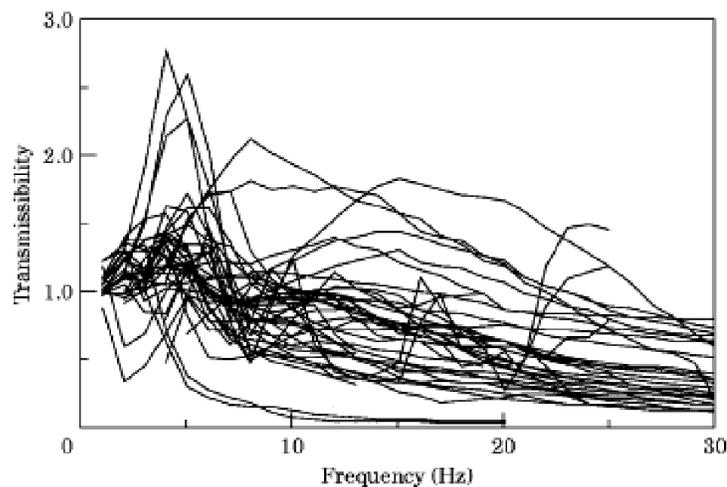
Figure 2-1: An illustration from Paddan and Griffin (1998) demonstrating the variability in mean vertical head acceleration transmissibility from 48 experimental studies.

Table 2-1: A list of significant reported studies on vibration measurement at different locations on the human body exposed to vertical WBV.

	Study	Purpose (Type of Input Excitation)	Sensor Location on Body (Axes)
Invasive Studies	Zagorski *et al.* (1976)	Measure acceleration at different spine locations (Sinusoidal)	Head, C7, T7, L, S3 (Z)
	Panjabi *et al.* (1986) [†]	K-wire accelerometers to measure vertebral motion directly (Sinusoidal)	L1, L3, Sacrum (X, Z, Pitch)
	Pope *et al.* (1986)	Comparison of LED[1] displacement on skin versus vertebral pins (Sinusoidal)	L3, PSIS (Z)
	Sandover and Dupuis (1987)	K-wire photogrammetric study of vertebral displacement (Sinusoidal)	T12, L1, L2, L3, L4 (X, Z)
	Pope *et al.* (1989) [†]	Measure lumbar vertebral response on cushioned seats (Impact)	L3, Sacrum (Z)
	Pope *et al.* (1991)	Relative shear, axial and pitch movements of lumbar vertebrae (Sinusoidal)	L3, L4, L5 (X, Z, Pitch)
	Magnusson *et al.* (1993) [†]	Analyse the influence of back support on lumbar transmission (Impact)	L3, L4 (X, Z)
	El-Khatib *et al.* (1998) [†]	Measure acceleration vertebral transmission in human cadavers (Random)	L1 – L5, Sternum (Z)
	Pope *et al.* (1998)	Response of lumbar vertebra on different types of seats (Impact)	L3 (Z)
	El-Khatib and Guillon (2001)	Measure intradiscal pressure in lumbar spinal units of cadavers (Random)	Discs: L1 – L5
Non-invasive Studies	Donati and Bonthoux (1983)	Simultaneous measurement of DPMI and thoracic acceleration transmissibility (Random and Swept Sine)	Sternum (Z)
	Seidel *et al.* (1986)	Predict lumbar stress and strain with acceleration and EMG measurements (Sinusoidal)	Head, shoulder, T5 (Z)
	Hinz and Seidel (1987)	Analyse non-linearity of vibration transmission through the body (Sinusoidal)	Head, Shoulder, T5 (Z)
	Hinz *et al.* (1988a) [†]	Derive functions for correcting tissue effect on skin mounted accelerometers (Sinusoidal)	T5, L3 (Z)
	Hinz *et al.* (1988b)	Bi-dimensional relative motion of lumbar vertebrae (Sinusoidal)	Head, Shoulder, L3, L4 (X, Z)
	Hinz *et al.* (1994)	Predict compressive loads on lumbar vertebra during transient vibration (Half and full Sinusoids)	Acromion, L3, L4 (Z)
	Zimmermann and Cook (1997)	Analyse effect of pelvic tilt on vibration transmission properties of the body (Sinusoidal)	Head, T5, Pelvis (Z)
	Seidel *et al.* (1998)	Predict vertebral loads due to vibration (Field Measured Signal)	T5, T11, S1, S3 (Z)
	Kitazaki and Griffin (1998)	Extract modes of vibration of the human body (Random)	Head, T1, T6, T11, L3, Sacrum (X, Z)
	Matsumoto and Griffin (1998) [†]	Study movement of the seated body (Random)	Head, T1, T5, T10, L1, L3, L5, Pelvis (X, Z, Pitch)
	Mansfield and Griffin (2000)	Analyse pelvic movement under vibration (Random)	Upper and lower abdomen, L3, illiac crest, PS illiac spine (X, Z)
	Matsumoto and Griffin (2002)	Investigation of the effect of excitation magnitude on acceleration at different body segments (Random)	T1, T5, T10, L1, L3, L5, L5 (Z, Pitch)
	Yoshimura and Nakai (2005)	Measurement of vibration at different segments of the body for development of biodynamic model (Random)	L1, L2, L3, L4, L5 (Z)

[†] Studies included in Fig. 4-8, Chapter 4. [1] Light Emitting Diode, [2] Posterior-Superior Iliac Spine.

Table 2-2: Experimental conditions and reported measures of studies on localised response to vertical WBV: Invasive methods.

Authors	Subject and Seating Conditions			Measurement Location	Input Excitation			Responses Reported	Characteristic Frequencies (Hz)
	Subjects, Gender (M/F)	Body mass (kg)[†]	Posture(s)[∞]		Axis, Type	Level, Duration	Frequency Range (Hz)		
Panjabi *et al.* (1986)	5 (Not reported)	59	Erect – NB Hands in lap Feet supported[£].	L1, L3, Sacrum	Z, Sinusoidal	1, 3 m/s^2, 30 sec/trial, 3 hrs total	2 – 15	Mean lumbar X, Z and Pitch transfer functions	Z: 4.4 (lumbar) 4.76 (sacrum)
Sandover and Dupuis (1987)	1 (Not reported)	Not reported	NB	T12, L1, L2, L3, L4	Z, Sinusoidal	Displacement 10 mm (peak-peak), 4 hrs	2, 3, 3.5, 4, 4.5, 5, 6, 7	Vertebral X, Z and Pitch displacement	Z: 4 X: 3, 4
Pope *et al.* (1989)	3 (F)	63.7	NB, Relaxed, Erect, Valsalva, Sitting on cushion	L3, PS iliac spine [∈]	Z, Impact	-	2 – 30 (impact)	Acceleration gain at L3 with different cushions	Z: 4-6
Pope *et al.* (1991)	3 (F)	61.7	NB, supported by arms	L3, L4, L5	Z, Sinusoidal	0.29–1.67, m/s^2 RMS	5, 8	Relative vertebral displacement X, Z, Pitch	Coupled motion: 5
Magnusson *et al.* (1993)	3 (F)	55	B, NB, Hands on SW, Feet supported	L3, L4	Z, Impact	6 m/s^2 peak, Irregular intervals	0 – 32 (impact)	Vertebral X, Z acceleration gain	Peak: 4.5-6.7, Valley: 8-10
El-Khatib *et al.* (1998)	1 (F) 6 (M)	58.1	Erect – NLS, Erect – LS[$], Car back – NLS, Car back – LS	L1 – L5, Sternum. (Cadaver)	Z, Random	1.5 m/s^2 RMS, 5 min/trial	0.8 – 25	Vertebral Z transmissibility	Lumbar : 6.3, 13.6 Sternum: 7.3

* X – Fore-Aft, Y – Lateral, Z – Vertical Axes, [†] Unless stated, body mass is reported by the average across subjects, [∞] B and NB – With Backrest and No Backrest, SW – Steering Wheel, [$] LS, NLS – With and without Lumbar Support. LB–low back, not a full-length backrest, [£] Foot support indicates the foot rest was moving with the seat pan, [∈] PSIS: Posterior-Superior Iliac spine.

Table 2-3: Experimental conditions and reported measures of studies on localised response to vertical WBV: Non-invasive methods.

| Authors | Subjects and Seating Conditions | | | Measurement Location | Input Excitation | | | Responses Reported | Characteristic Frequencies (Hz) |
	Subjects, (Gender)	Body mass (kg)	Posture(s)		Axis, Type	Level (m/s²), Duration	Frequency Range (Hz)		
Donati & Bonthoux (1983)	15 (M)	62.9	Erect – NB, Hands on SW	Thorax (sternum)	Z, Random and Sine	1.6, 275 s	1 – 10	Seat to Thorax transmissibility, DPMI, Pabs	Z Thorax and DPMI: 4
Hinz & Seidel (1987)	4 (M)	76.25	Moderately erect, NB, anatomically shaped seat	Head, acromion (shoulder), T5	Z, Sine	1.5, 3, 30 s, 1 min/ trial	2 – 12	APMS, transmissibility to locations	Z: 4.5
Hinz et al. (1988a)	1 (M)	68	Erect – NB	C7, T1, T3, T5, T7, T9, T12, L1, L3, L5, S1	Z, Sine	1.5, 1 min/trial	4.5, 8	Skin correction functions	NA
Hinz et al. (1988b)	3 (M)	68	Erect–NB, anatomically shaped seat	Head, acromion L3, L4	Z, Sine	1.5, 3, 1 min/ trial	4.5, 8	Relative acceleration L3-L4 in X and Z	4.5, 8
Hinz et al. (1994)	5 (M)	74.2	Moderately Erect–NB	Acromion, L3, L4	Z, Sine and Half Sine	1.3-4.14, not reported	2, 4, 8	Z acceleration and estimated force at vertebrae	NA
Zimmermann & Cook (1997)	30 (M)	77.6	NB, Feet supported but not moving	Head, T5, Pelvis (potentiometer)	Z, Sine	1, not reported	4.5, 5, 6, 8, 10, 12, 16	Pelvic rotation, trunk acceleration transmissibility	Z: 6
Kitazaki & Griffin (1998)	8 (M)	74.6	Erect, Normal, Slouched	Head, T1, T6, T11, L3, Sacrum (S2)	Z, Random	1.7, 1 min/trial	0.5 – 35	Extracted modal properties of the upper body	1.1, 2.2, 3.4, 4.9, 5.6, 8.1, 8.7, 9.3
Matsumoto & Griffin (1998)	8 (M)	63 – 83	Upright – NB, Feet hanging	Head, T1, T5, T10, L1, L3, L5, Pelvis	Z, Random	1, 1 min/trial	0.5 – 20	APMS, X, Z and Pitch acceleration transfer functions	APMS: 4.75-5.75
Mansfield & Griffin (2000)	12 (M)	68.3	Upright – NB, Feet supported and vibrated	Upper and lower abdomen, L3, iliac crest, PSIS ϵ	Z, Random	0.25, 0.5, 1, 1.5, 2, 2.5, 1 min/trial	0.2 – 20	APMS, X, Z transmissibility to all locations	APMS: 5
Yoshimura & Nakai (2005)	1 (M)	Not reported	Upright – NB	Forehead, mouth-bite bar, C7, T1, T4, T8, L1 to L5, Sacrum	Z, Random	0.7, 1 min/trial	Up to 20 Hz	Z transmissibility to L1, L2, L3, L4 and L5	6.6, 11.8 (extracted modes)

2.3 Transmission of vertical WBV to body segments

The study of the transmission of WBV to different segments of the seated human body invariably involves measurements of motion parameters at the respective segments. Owing to the complexities associated with the measurement systems and its installations, only a few studies have attempted such measurements. Table 2-1 lists some of the significant experimental studies that measured vibration at different segments on the human body together with the study objective and the measurement locations. It is evident that the studies involving invasive measurements considered either sinusoidal or shock inputs, with the exception of those using cadavers, which employed random excitations. A large number of studies using non-invasive measurements, on the other hand, were conducted under random vertical vibration. The reported studies may be classified primarily based on the measurement techniques employed. The experimental conditions and the reported response measures are summarised in Tables 2-2 and 2-3 for studies employing invasive and non-invasive methods, respectively. The tables also list the characteristic frequencies observed from the measured data. Vibration data may be acquired surgically or *invasively* by inserting relatively rigid but thin wires dorsally into the chosen vertebrae and mounting motion sensors on the wire outside the body (*e.g.*, Zagoski *et al*., 1976; Panjabi *et al*., 1986; Pope *et al*., 1986). Alternately, transducers may also be *non-invasively* attached to the skin at selected locations, for example over the vertebral spinous process (*e.g.*, Hinz *et al.*, 1988a; Matsumoto and Griffin, 1998). Some of the early invasive experiments were carried out on primates (baboons), which were harnessed to the vibration platform in a seated posture (Quandieu and Pellieux, 1982; Slonim, 1985). The measured signals revealed considerable noise making the results

unreliable and difficult to interpret. Although the spinal layout of primates seems to resemble humans, the vibration data collected on a baboon harnessed and probably drugged may hardly be considered comparable to those of the human subjects who could assume various desired postures voluntarily.

On the other hand, it is quite difficult to measure spinal movement parameters directly in a live human subject due to the ethical concerns associated with the insertion of a sensor into the vertebral structures, while being exposed to vibration. However, changes in parameters such as disc compression and pressure due to WBV may provide valuable information on the effects of vibration exposure on some of the most injury-prone elements of the spine like the vertebral endplates and discs (Sandover, 1998). A few studies have reported these parameters in human cadavers exposed to vibration. Sagittal plane acceleration transmissibility in the fore-aft and vertical axes was measured by El-Khatib *et al*. (1998) at all the lumbar vertebrae and sternum of 7 cadavers exposed to random vertical seat excitation. A variety of postures including a lumbar support and backrest were employed. While two peaks were observed in the vertical responses around 4 and 9 Hz, in most of the postures, there was considerable inter-subject variability. Interestingly, insignificant differences were found in the responses at different lumbar levels. The effect of the lumbar support was considerable in that it increased the resonant response frequency while slightly decreasing the peak magnitude. The same cadaveric subjects when used to elicit lumbar intra-discal pressure revealed cyclic loading of the vertebral discs (El-Khatib and Guillon, 2001). Although insignificant amplification of vibration from L5 to L1 was observed in the previous study (El-Khatib *et al*., 1998), the disc pressure variations in this region were considerable. Additionally, the interactions with the lumbar support resulted in greater pressure distribution above L3 but lower

pressure in the lower discs. Due to these differences among vibration and disc-pressure measurements, the authors suggested that measurement of vertebral motion variables alone may be insufficient for the assessment of spinal health risks posed by WBV. It must however be noted in these studies that the subjects lacked the abdominal viscera, which was taken out so as to instrument the vertebrae. Moreover, the absence of muscle activity in the cadavers may be the prime reason for their registering similar vibration responses at all the lumbar vertebrae. Furthermore, the deep muscles connected to the facets of the vertebrae may play a major role in controlling both the relative movement of the spinal units and consequently the disc pressures.

2.3.1 Assessment of injury risks to the spine and its mechanical properties

One of the most common medical symptoms among operators of mobiles machines is the damage to the spine, including failure of the vertebral endplate and/or rupture of the annulus tissue encasing the disc's nucleus. It is known that damage to the endplate may lead to degeneration of the associated vertebral disc (Sandover, 1998). Likewise, compressive loads are known to alter hydration patterns in the annulus tissue and nucleus contents adversely changing the physical properties of the vertebral unit (Dolan and Adams, 2001). While the measurements of vibration transmitted to various spine segments have provided considerable knowledge on the deflection modes of the vibration-exposed body, such measurements do not yield a direct assessment of the spinal injuries caused by WBV. The estimates of forces in the vertebral unit under WBV have thus been considered for quantifying the spinal loads associated with vibration. Consequently, a few studies have considered detailed models for estimating the spine loads. The stress and strain in the lumbar spine were estimated by Seidel *et al*. (1986) through a biomechanical model with force estimates from measured back muscle activity

(electromyography) and vertebral accelerations on the skin. Interestingly, compression in the lumbar spine was evidenced for sinusoidal vibration at 4.5 Hz in both upward and downwards trunk motions. The authors suggested frequency-dependent muscle activity (Blüthner *et al.*, 1995) to be responsible for this response behaviour. In a similar study by Hinz *et al.* (1994) the effects of transient vibration were reported in terms of estimated dynamic peak-to-peak compressive force at the lumbar spine. The values in the order of 400 to 1000 N between 4-8 Hz under vertical vibration were found to be close to the upper borderline for long-term exposure to repetitive loading of the lumbar vertebrae, without risk of injury (Brinckmann *et al.*, 1989). A systematic study on spinal loading by Seidel *et al.* (1998) employed multiple approaches including photogrammetry, force and acceleration measurements and EMG at different locations on the back. The 12-subject population classified according to body build as 'frail', 'intermediate' and 'robust' were exposed to vertical vibration having the spectral characteristics of earth moving equipment. Posture was found to be a significant contributor to static and dynamic forces on the discs estimated using a simple biomechanical model of the considered spine sections. While such simplistic models may provide a quick approach for estimating the loads at different spine levels, the understanding of the nature of localised loading patterns in the spinal substructures such as discs and endplates is a more intricate process necessitating the development of finite elements models of the spine sections. The reliability of such complex models, however, strongly depends on the accurate description of mechanical properties of the spinal substructures. The identification of such properties in a reliable manner is a highly complex task. A number of studies have characterised the mechanical properties of the spinal substructures through in vitro measurements on the cadaver spines (Sandover, 1998). These property values may be

incorporated in analytical models of the human body, which may be further utilised for the prediction of spine loads.

Stiffness properties of the thoracic spinal units, removed from fresh cadavers and subjected to mechanical load tests, were reported in all the three axes by Panjabi *et al.* (1976) including the cross-axis components as shown in Fig. 2-2. The figure illustrates the (6x6) flexibility matrix of the thoracic vertebrae derived from the measured force/moment-deflection properties along the three translational and rotational axes. Other studies have also attempted measurements of stiffness and damping properties (White, 1969; Markolf, 1970) of the vertebral units at different locations. These parameters have been widely used as nominal values for the development of occupant bio-models with multiple-degrees-of-freedom (DOF) (Amirouche and Ider, 1988). Additionally, the therapeutic treatment of spinal disorders has led to the development of simple lumped-parameter models from experimental load-deformation data (Nicholson *et al.*, 2001; Keller *et al.*, 2002). In the study by Garder-Morse and Stokes (2004), the lumbar spine stiffness was expressed in terms of "equivalent" structural elements such as trusses and beams, which may be directly incorporated into multi-dimensional (finite element) models of the human body exposed to WBV (Kitazaki and Griffin, 1997). Although these models may have significant applications for the prediction of transmitted vibration and loads in inaccessible areas of the spine, they require thorough validation with dynamic data acquired through measurements of vibration at corresponding locations on the body.

$$\begin{bmatrix} K_{11} & 0 & 0 & 0 & K_{15} & K_{16} \\ & K_{22} & K_{23} & K_{24} & 0 & 0 \\ & & K_{33} & K_{34} & 0 & 0 \\ & & & K_{44} & 0 & 0 \\ & \text{Symmetric} & & & K_{55} & K_{56} \\ & & & & & K_{66} \end{bmatrix}$$
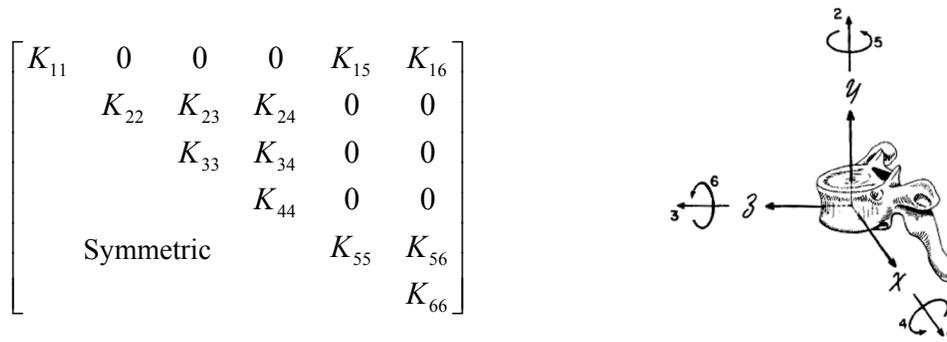
Figure 2-2: Three-dimensional flexibility matrix for the thoracic vertebra (on right) derived from force-deflection experiments by Panjabi *et al*. (1976). The coordinate subscripts: 1, 2, 3 and 4, 5, 6 in the matrix represent vertebral x, y, z translation and pitch, roll, yaw rotations, respectively.
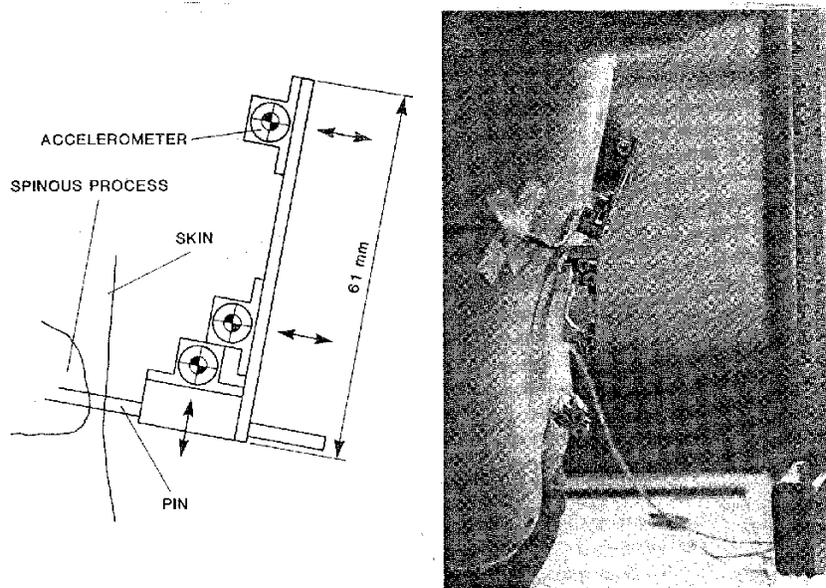
Figure 2-3: The plane-motion accelerometer transducer (PAT) system employed for the invasive vibration measurements by Panjabi et al. (1976)

2.3.2 Measurement of transmitted vibration using invasive methods

Live human volunteers have been employed in some studies involving invasive instrumentation of vertebral locations, generally using threaded Kirschner pins (or K-wire) under local anesthesia, as shown in Fig. 2-3. A variety of motion sensors such as accelerometers, displacement transducers and photogrammetric motion capture markers have been mounted on K-wires to estimate the vibration transmission to specific spinal units in the seated position (e.g. Lange and Coermann, 1965; Christ and Dupuis, 1966; Hagena *et al*., 1986).

Utilising the instrumentation illustrated in Fig. 2-3, Panjabi *et al*. (1986) measured the seat acceleration transmitted to the L1, L3 and sacrum of five human subjects exposed to vertical sinusoidal excitations. A clear resonance peak was observed at 4.4 Hz in the mean vertical responses of the subjects. However, no clear differences were found between the vibration transmitted to L1 and L3 under 1 m/s^2 vertical excitation. Additionally, while insignificant horizontal response magnitudes were registered at all the lumbar levels, the large inter-subject variability in vertebral pitch made it impossible to conclude on the presence of any lumbar rotational modes in the sagittal plane. Sandover and Dupuis (1987), on the other hand reported relatively larger motion in the horizontal axis between the vertebral combinations T12–L2 and L2–L4. The study measured the relative vertical displacements among lumbar vertebrae under vertical sinusoidal seat excitations along the horizontal, vertical and pitch axes. A number of sources of errors were identified including the effects due to accelerometer orientation. It was suggested that displacement and acceleration be measured simultaneously so as to estimate/monitor the attitude of the accelerometer. It was concluded that the reason for resonance may be lumbar spine bending and not buttock compression. Similar

measurements by Pope *et al.* (1991) revealed coupled motions in shear, compression and pitch amongst the L3–L4 and L4–L5 vertebral pairs. In this study, greater levels of relative movements were reported under vertical sinusoidal excitations at 5 Hz than at 8 Hz, which also showed higher peak response under a higher excitation.

A number of invasive studies have also been performed to understand the behaviour of lumbar vertebrae to sudden shock/impact inputs on seated test subject (*e.g.*, Pope *et al.*, 1998; Wilder and Pope, 1996). Under impact loads, a gain of about 3 dB in vibration transmitted to the lumbar region has been reported between 4 and 5 Hz. Subjects sitting on different cushions seats revealed lower peak response magnitudes than a baseline measurement with a rigid seat, when exposed to impact excitation in the vertical direction (Pope *et al.*, 1989). The soft cushion seats were also hypothesised to reduce the rotational modes by damping the pelvic pitch mode in the 7-8 Hz frequency range. In another impact study, the vertical vibration transmitted to the L3 vertebra was found to be insignificantly affected by a thoracic backrest (Magnusson *et al.*, 1993). The back support resulted in slightly lower peak magnitude and the corresponding frequency in the vertical axis, while the fore-aft motion although completely attenuated without a backrest, showed levels comparable to the vertical response between 4 and 8 Hz in the back-supported posture with backrest inclination of 120°.

2.3.3 Measurement of transmitted vibration using non-invasive methods

It is generally experimentally difficult to employ subjects for invasive methods to study the influences of a backrest. Moreover, owing to the medical and ethical concerns associated with the insertion of pins into the skeletal structures of the spine, acquisition of vibration data by harnessing transducers on the skin by adhesive or other non-invasive means has been adopted in a number of studies. The vertical transmissibility between the

pelvis and thoracic torso was measured by Donati and Bonthoux (1983) using an accelerometer strapped to the upper body and positioned on the sternum of subjects exposed to separate vertical random and swept-sinusoidal waveforms. Simultaneously, the DPMI and vibration power absorbed at the driving-point were also derived from force-motion measurements at the seat-body interface. A clear peak in all the three measured responses was observed between 4 and 5 Hz, irrespective of the type of excitation. It was concluded that while simple SDOF systems may be sufficient to represent the thorax response, the DPMI may require more complex models.

In a similar study with 4 male human subjects exposed to sinusoidal excitations, Hinz and Seidel (1987) presented the apparent mass at the seat along with vertical vibration transmissibility measured non-invasively at the head using a strapping device, shoulder (acromion) and T5 vertebra. Two sources of non-linearity were identified namely, the excitation magnitude and the location of the transducer on the body. The widely reported softening trend of decreasing resonant frequency with higher vibration levels (Mansfield and Griffin, 2000) was also observed in this study with slightly larger variability around the peaks in all the responses. The second non-linearity occurred in the form of non-sinusoidal patterns observed at the shoulder, possibly due to interactions of the muscular activity (Blüthner *et al*., 2001). The authors drew particular attention to the possible underestimation of stress and strain in the vertebral structures calculated from the RMS quantities due to this non-sinusoidal phenomenon. However, it should be noted that spine motion is realised by a combination of vertical, shear and rotational movements of the vertebral units as reported in a number of studies (*e.g.*, Hinz *et al*., 1988b; Pope *et al*., 1991). However, the coupled motions among the vertebrae, which may elicit

controlled fore-aft movements of the upper body in the sagittal plane even under vertical excitation, have been measured only in a few studies.
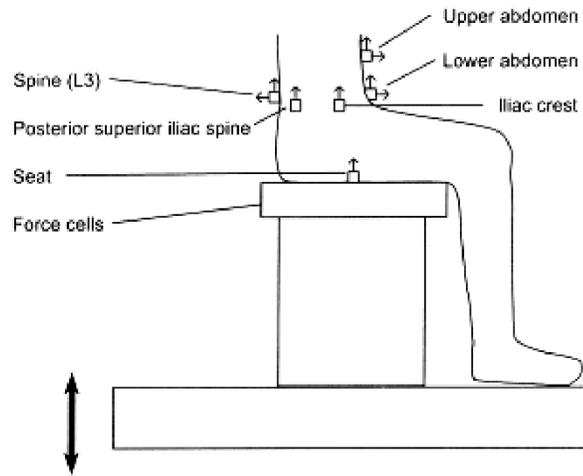
Figure 2-4: Illustration from Mansfield and Griffin (2000) depicting the sensor placements for the simultaneous measurement of APMS and vibration transmissibility to different locations around the lower body.

Mansfield and Griffin (2000) reported the simultaneously measured seat APMS, and fore-aft and vertical vibration transmitted to selected locations enveloping the anterior, lateral and dorsal faces of the lumbar-pelvic torso, and discussed the effect of vertical vibration magnitude on these responses (Fig. 2-4). A general trend of higher peak response magnitude and a reduction in the corresponding frequency with increase in input vibration magnitude was observed in both the APMS and vertical transmissibility. It should be noted that the inter-subject variability in the reported fore-aft responses was quite high. The lower abdominal wall exhibited both vertical and fore-aft resonances around 6 Hz. However, it was argued by the authors that this body unit, constituting only 7% of the total body mass (Synder and Cook, 1975), may not entirely be responsible for the observed non-linearities in the APMS. Similarity in the characteristics observed among the responses at the sacro-pelvic unit and the driving-point led to the authors concluding that the APMS peak may be influenced by pelvic and spinal movement

mechanics. However, in another study involving vertical seat excitations, the effect of vibration magnitude on the seat apparent mass was observed to be greater than pelvic rotation (Mansfield and Griffin, 2002). Additionally, pelvic response showed a peak around 12 Hz. Movements of the sacro-pelvic unit may have greater effects on the movement of low inertia segments of the spine compared to that on the global APMS response. However, only a few studies have studied such influences probably due to the difficulties associated with motion measurement around the lower lumbar region.
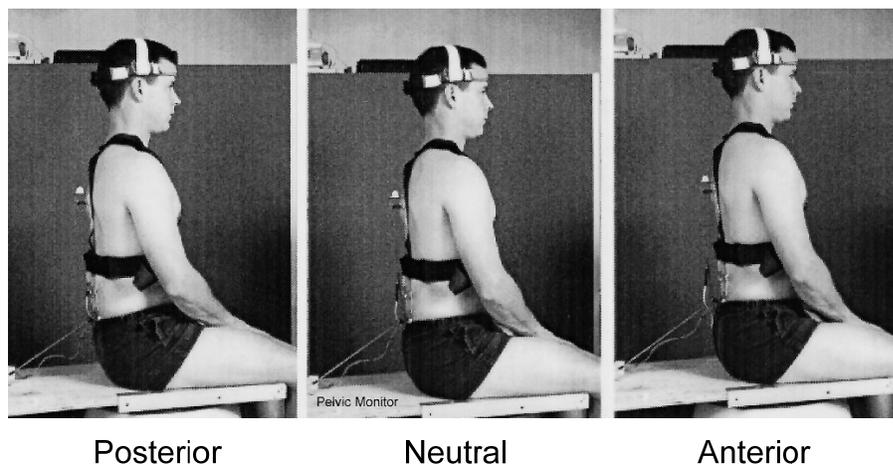
Figure 2-5: Pictorial illustrated from Zimmermann and Cook (1997) showing the subject instrumented with a pelvic monitor, seated with three different pelvic orientations (indicated at the bottom of each picture) for the WBV experiments.

The effects of static pelvic orientation on vertical transmissibility at the head and torso (T5) were studied by Zimmermann and Cook (1997) with 30 male subjects instrumented with accelerometers attached to the head and T5 through appropriate harnesses (Fig. 2-5). Pelvic position, including anterior, posterior and neutral orientations, showed significant effects on the head and trunk responses, especially below 6 Hz. The anterior and neutral orientations of the pelvis showed an increase in vibration

70

at the trunk. Posterior pelvic angle, although having insignificant effect at the trunk level, increased the head response at 4.5 and 5 Hz.
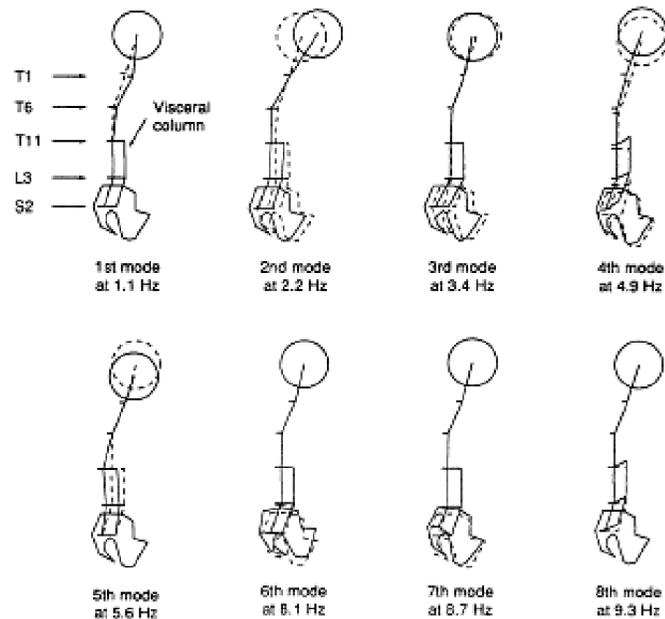
Figure 2-6: Vibration modes extracted from measured vibration transmissibility by Kitazaki and Griffin (1998) showing the presence of 8 modes below 10 Hz for the seated body.

The human body may thus be assumed to have multiple modes of vibration at the different segmental levels that permit relative motion. Using experimental modal testing techniques, Kitazaki and Griffin (1998) extracted eight modes below 10 Hz from the measured acceleration responses at the vertebral levels of seated male subjects exposed to vertical vibration. A number of modes were identified from the synthesis as depicted in Fig. 2-6. The primary resonance was found to comprise of a whole body axial movement of the spine caused by buttock tissue compression and shear, in phase with a vertical visceral mode, and coupled with bending of the upper thoracic and cervical spine. The second significant characteristic was attributed to pelvic pitch along with a secondary

71

visceral mode. It was suggested that spinal forces causing injury may not be appropriately predicted by simple lumped-parameter models that do not account for body motion. Furthermore, Matsumoto and Griffin (1998) measured vertical, fore-aft and pitch acceleration transmitted to different locations on the body exposed to vertical seat vibration. A vertical resonance around 5 Hz was observed at all the locations in majority of the subjects. However, distinct peaks in the fore-aft transmissibility were visible only at the head and T1 while all the other trunk locations depicted insignificant motion in this axis. The translational and pitch transmissibility peaks occurred at a slightly higher frequency than the trunk vertical responses. Slight rocking of the thoracic torso about the lower thoracic and lumbar spine was visible from the measured transmissibility. Although considerable relative axial movement of the spine was not identifiable at resonance, pelvic pitch causing compression and shear of the buttock tissue was observed at this frequency. Hence, it was hypothesised that multiple modes may be contributing to the resonance peak observed in the seat APMS.

2.4   A critical analysis of the reported biodynamic responses and the contributory factors

It is obvious from the literature that the study of vibration transmitted to different segments of the body is quite significant in order to understand the mechanisms causing detrimental effects on the spine. However, the inaccessibility of much needed information on the physical properties of the spinal substructures and the nature of spinal movements under WBV make it quite difficult to conclude on the exposure-effect relationship for the human body subjected to mechanical vibrations. In addition, considerable variability is observed in the measured responses among the studies reporting body-segment vibration, which often lead to contradictory conclusions. This

has been attributed primarily to wide variations in the experimental conditions employed in these studies (VIN, 2001a). The differences in test subject characteristics, the induced vibration type, magnitude and duration, the support and postural conditions employed, and the data acquisition equipment and techniques could all be factors contributing to the variability in the measured responses. The reported data and their interpretations are thus further examined in this section to understand the nature of vibration transmission through the upper body and to analyse the effects of selected significant factors on the reported biodynamic responses in order to formulate an appropriate experiment design.

2.4.1 Movement of the upper body exposed to vertical WBV

The reasons for resonance in the seated body exposed to vertical vibration, generally identified by the peak in seat APMS magnitude (Fairley and Griffin, 1989), are still uncertain due to the complex nature of the multidimensional movements of the upper body. The reported studies have attempted to identify a model or mechanism associated with frequencies corresponding to primary magnitude peaks in the response, while only little agreement could be observed among the reported interpretations. The relationship between the driving-point biodynamics and upper body motion has not been understood yet. Hence, knowledge of body movements may provide much needed information for the ergo-dynamic design of human interface systems in vibrating machinery. However, the reported studies on measurement of vibration transmission to different locations of the upper body have employed widely varying experimentation conditions as seen in Tables 2-2 and 2-3. These mostly employed subjects sitting upright with no backrest contact, while the responses display a peak around 5 Hz in magnitudes of both the seat APMS and the vertical transmissibility responses at all the segments (Fairley and Griffin, 1989; Matsumoto and Griffin, 1998). It has thus been widely assumed that resonance in

73

the vertical axis is comprised of a whole body vertical vibration mode responsible for the dynamic forces at the seat-body interface (Coermann, 1962). However, the prevalence of pain and vibration disorders in the spinal units have necessitated the measurement of motion in the low-inertia vertebrae so as to better understand the nature of vibration transmission through the upper body.

Resonant frequencies observed from the vertical vibration transmissibility were slightly higher for the sacrum when compared with that for the lumbar vertebrae (Panjabi *et al.*, 1986). It was thus hypothesised that the lumbar region (L1 to L5) could be considered as one rigid segment for vibration assessment, while higher stress and strain could lie at the junction between the lumbar spine and the sacrum. Impact tests performed by Pope *et al*. (1989) hypothesised that the resonance characteristic may be due to pitch of the pelvis in addition to buttock-tissue compression. Sandover and Dupuis (1987), however, suggested that pelvic rocking causes bending in the lumbar spine which could be responsible for the peak in the apparent mass magnitude. While lumbar bending has been reported by some studies in the frequency range of 4-6 Hz (*e.g.*, Sandover and Dupuis, 1987; Pope *et al*., 1991), pelvic rotation was observed at higher frequencies, 8-12 Hz (Kitazaki and Griffin, 1998).

On the other hand, lumbar compression-extension has also been associated with vertical body resonance. A few studies on body segment acceleration transmissibility have revealed the presence of pelvic pitch and lumbar spine extension-compression either coupled with or independent of the bending modes (Zimmermann and Cook, 1997; Kitazaki and Griffin, 1998). Additionally, relative motions of the lumbar vertebrae have been registered in the vertical direction in *invasive* vibration measurements although with a high degree of variability (Sandover and Dupuis, 1987). Furthermore, some studies

have observed coupling between the horizontal and vertical inter-vertebral movements in the lumbar region (Hinz *et al*., 1988b; Pope *et al*., 1991). The considerable magnitudes of fore-aft motion in the upper thoracic, cervical region and the head under vertical seat excitation seem to support a rocking of the upper body about the lower thoracic/lumbar spine (Matsumoto and Griffin, 1998). However, the fore-aft head response should probably be treated with caution since the head-neck complex in itself might also be subjected to pitching, independent of the torso due to the relatively unconstrained head-neck joint.
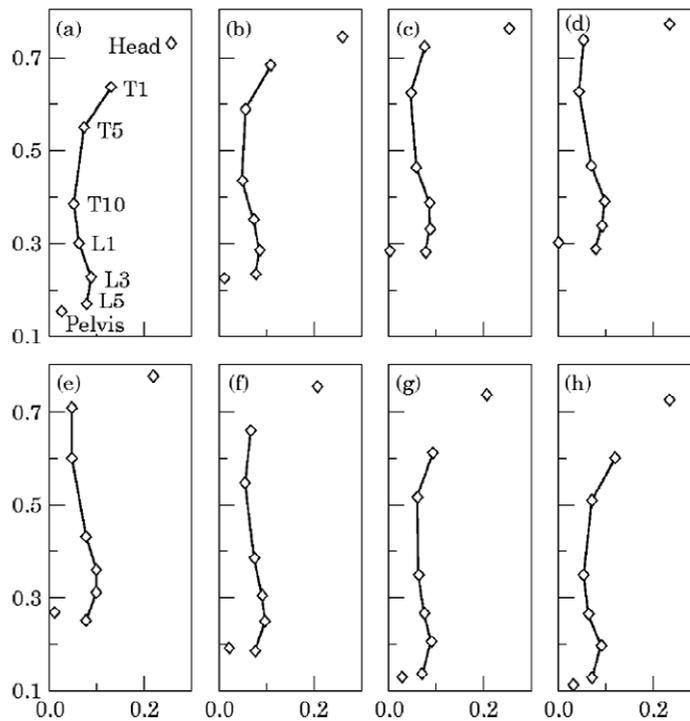
Figure 2-7: Body movements reported for one subject by Kitazaki and Griffin (1998) at 5 Hz. Figures (a) through (h) represent one complete cycle.
The units of both axes are metres.

75
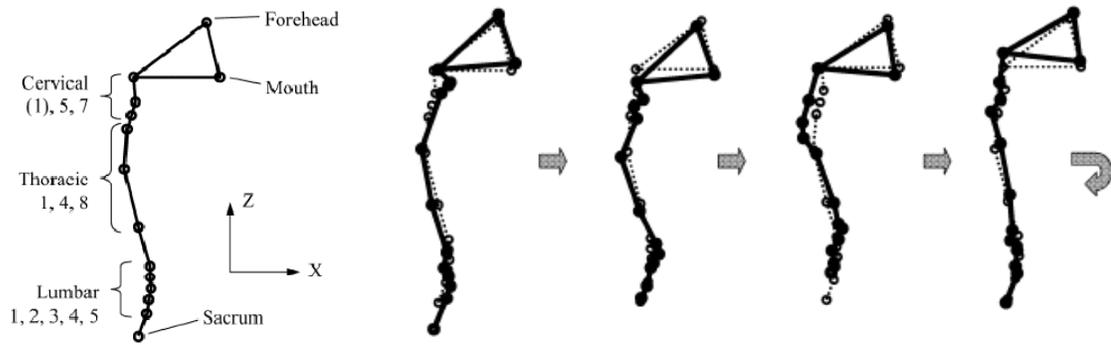
Figure 2-8: Spinal movements extracted from measured body-segment vibration data reported by Yoshimura and Nakai (2005) at the dominant mode (6.6 Hz) for every quarter period of one cycle.

Figures 2-7 and 2-8 show the deflection modes of the spinal structure and the head over one complete cycle of oscillation reported in two studies at the corresponding resonant frequencies of 5 Hz (Kitazaki and Griffin, 1998) and 6.6 Hz (Yoshimura and Nakai, 2005). Head pitch is clearly observed in both the figures. Figure 2-7 shows slight extension of the upper thoracic spine, lumbar bending and pelvic pitch within one cycle of movement, while Fig. 2-8 depicts greater bending in the lumbar spine coupled with bending in the upper thoracic/cervical complex. In addition to bi-dimensional spinal movements, some studies have also suggested that dynamic forces developed due to deflection of the abdominal viscera may play a role in determining the driving-point dynamics (Matsumoto and Griffin, 2001; Pankoke *et al.*, 1998). Visceral motion is not only observed at body resonance, but is also reported at higher frequencies, possibly responsible for the secondary peak in seat APMS magnitude around 8-12 Hz (Mansfield and Griffin, 2000; Matsumoto and Griffin, 1998). It is thus evident that the apparent mass biodynamic response alone may not be sufficient for understanding the complex pitch-plane movements that may be responsible for the disorders in the spine.

2.4.2 Anthropometric effects

The influence of subject mass has been reported in a number of studies that measure driving-point force-motion responses (*e.g.*, Failey and Griffin, 1989; Mansfield and Griffin, 2000; Patra *et al.*, 2008; Rakheja *et al.*, 2002; Wang *et al.*, 2004). A larger body mass has been found to result in greater contact area allowing for a more uniform force distribution at the body-seat interface thus altering the driving-point responses (Nawayseh and Griffin, 2005). In general, an increase in peak APMS magnitude accompanied by a reduction in resonant frequency is observed with increasing body mass. Hence, the grouping of driving-point responses based on body mass has been undertaken in many studies. Figure 2-9(a) demonstrates the mean vertical APMS responses reported by Patra *et al.* (2008) for male subjects within three mass categories around 55, 75 and 98 kg. There is wide variation in the responses among the three groups. The normalisation of APMS with respect to either seated mass or APMS at a low frequency has been widely performed to study the influences of other factors (*e.g.*, Fairley and Griffin, 1989; Mansfield 2005). Interestingly, it may be seen from Fig. 2-9(b) that the body mass dependence in both the peak magnitude and resonant frequency cannot be eliminated through such normalisation. Wang *et al.* (2004) measured the vertical APMS of seated subjects under various postures including different backrest and seat pan geometries and concluded that the vertical APMS magnitude at various frequencies is linearly correlated with the body mass.

The effects of subject anthropometry on vibration transmitted to the head (STHT) and other segments of the body have been reported only in a few studies. The studies that analysed the influence of body mass on vertical STHT were unable to establish any definite relationships primarily due to the high level of inter-subject variability in the

measured responses (Griffin and Whitham, 1978; Paddan and Griffin, 1998,). It may also be observed from Tables 2-2 and 2-3 that the size of the test population, employed in most of the studies examining vibration at different body locations, seems to be insufficient for analysis of such effects. Donati and Bonthoux (1983) observed higher vertical acceleration transmissibility to the sternum of taller subjects at 2, 3 and 4 Hz, while the correlation coefficients were in the low range of 0.5-0.6.
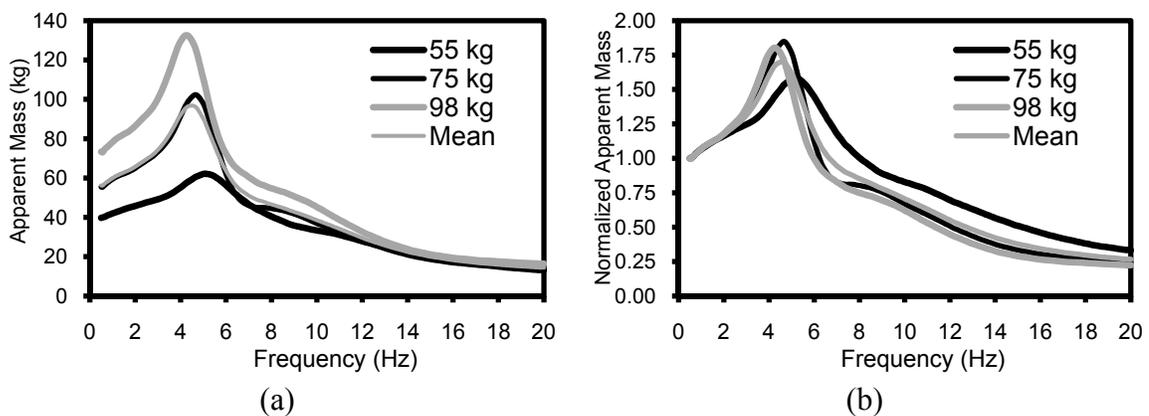
Figure 2-9: Effect of subject mass on the vertical (a) apparent mass; and (b) normalised apparent mass magnitude measured at the seat under vertical vibration (Patra *et al.*, 2008)

The contribution of anthropometry to the degree of spine loading is still not established. It may be assumed that larger upper body mass and inertia in heavier subjects may lead to greater compressive forces in the spine. However, the study by Seidel *et al*. (1998), which classified subjects based on body build as 'frail', 'intermediate' and 'robust', reported greater static and dynamic pressure in the frail subjects attributable to the decreased inter-vertebral disc diameter. The vertically-excited human body considered akin to an inverted pendulum may well be affected in the horizontal direction due to anthropometric properties like the height and upper body inertia. However, the degree of inter-subject variability reported by most studies in this axis makes it quite

difficult to isolate influences on the responses related to stature and weight. Human participants thus need to be recruited carefully in order to study the anthropometric effects or to minimise the anthropometric effects.

2.4.3 Influence of vibration type and magnitude

Laboratory measurements of WBV have been conducted with excitations along the vertical axis using one of the following types of waveforms: (i) band-limited white noise; (ii) sinusoidal; (iii) shock or impulse; and (iv) excitations synthesised from field measurements. The human body has been considered sensitive to a variety of factors including the vibration type and magnitude. However, the driving-point response magnitudes have been reported to show only slight differences around the resonant frequency between sinusoidal and random vibrations. Mansfield and Maeda, (2005) observed minimal changes in the apparent mass magnitude measured with random and sinusoidal vibration around the primary resonance, while some influences were shown in the corresponding phase above 8 Hz. Donati and Bonthoux (1983) concluded insignificant effect of excitation type on the DPMI magnitude except only slightly higher response magnitude due to sinusoidal vibration, around the resonance. This may be attributable to the frequency dependence of back muscle activity (Blüthner *et al.*, 1995; Seidel *et al.*, 1986).

On the other hand, a vast majority of the studies seem to report a non-linear dependence of driving-point response on the vibration magnitude (*e.g.*, Mansfield, 2005) while the phenomena responsible for this non-linearity is yet to be established. This may to a large degree be due to our limited knowledge of the precise mechanics associated with resonant forces at the seat interface and the associated movements elicited in the upper body. Additionally, the intervention of other contributory factors such as subject

anthropometry, posture and support conditions makes it more difficult to isolate the causative factors for non-linearity. Under random vibration, the driving-point variables consistently show the characteristics of a 'softening' system identifiable by only a slight increase in peak magnitude with a simultaneous reduction in the resonant frequency with increasing input vibration (*e.g.*, Failey and Griffin, 1989; Mansfield and Griffin, 2000). Most of the studies consistently report greater shifts in the resonant frequency at lower excitation magnitudes, *e.g.*, 0.25-1 m/s^2 (Boileau *et al.*, 1998; Mansfield and Griffin, 2000; Wang *et al.*, 2004; Zhang, 2006), while the effect tends to diminish under magnitudes greater than 1 m/s^2. However, there are differences among the reported studies in the degree of variation in both the peak magnitude and frequency.
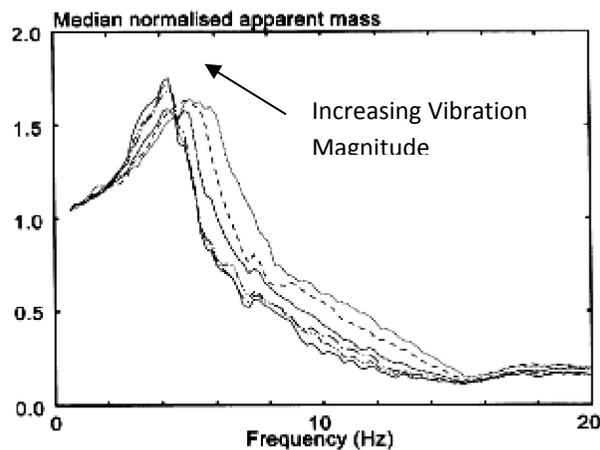
Figure 2-10: Median normalised vertical APMS at the seat showing the decrease in resonant frequency and increase in peak magnitude with increasing vibration magnitude (Mansfield and Griffin, 2000).

Only a few studies have reported the effect of excitation magnitude on the vibration transmission properties 'through' the body. Vertical STHT responses have shown to depict a softening effect at both the primary and secondary peaks (Hinz and Seidel, 1987; Wang *et al.*, 2006), similar to the APMS response. In addition, the study by

Hinz and Seidel (1987) showed a uniform decrease in resonant frequency of vertical acceleration responses measured at the shoulder and T5 with increase in vibration intensity. The effects of vibration magnitude were studied at different locations around the lumbar region by Mansfield and Griffin (2000) (Fig. 2-4, and Tables 2-2 and 2-3). Although softening was observed in the vertical APMS (Fig. 2-10) and the lower body transmissibility responses, greater changes were observed towards the lower excitation range (0.25-1 m/s^2). However, such consistent trends were not evident in the median fore-aft responses at the abdominal wall, although a slight reduction in resonant frequency was somewhat identifiable. Reductions in resonant frequency have been reported on the basis of measured vertical and pitch transmissibility responses at different locations in the thoracic and lumbar regions with increase in random vibration magnitude (Matsumoto and Griffin, 2002). While the study showed an increase in the peak vertical transmissibility magnitude, the peak pitch transmissibility magnitudes were lower with increase in the excitation magnitude. It may be concluded that the seated body shows somewhat similar softening characteristics in the pitch-plane incorporating the vertical and fore-aft motions. This hypothesis is further corroborated by the fact that the upper body undergoes bi-dimensional movements even under exposure to pure vertical WBV (Hinz *et al.*, 1988b; Pope *et al.*, 1991; Matsumoto and Griffin, 1998; Kitazaki and Griffin, 1998).

2.4.4 Effects of Back Support Condition

It is known from a number of studies that an inclined backrest tends to take up a greater proportion of the seated upper body mass and thus may reduce the stresses in the trunk (Andreoni *et al.*, 2002; Magnusson *et al.*, 1994). Additionally, under static sitting, both the intra-discal pressure and electromyographic activity of the back musculature are

known to reduce considerably with the use of a back support (Andersson *et al.*, 1974; Chaffin *et al.*, 1991). However, the influence of vertical and inclined backrests has been studied only in a few studies measuring the seat and upper-body backrest apparent mass response under vertical vibration (Rakheja *et al.*, 2002; Nawayseh and Griffin, 2004; Mansfield and Maeda, 2007; Patra *et al.*, 2008). In general, the backrest tends to suppress the peak vertical APMS magnitude while increasing the response beyond resonance. As a consequence, the bandwidth of the force-motion frequency response is slightly higher suggestive of greater dissipation of vibratory energy in a body leaning on the backrest as seen in Fig. 2-11 for the body seated with hands in lap and on the steering wheel (SW) (Wang *et al.*, 2004). The figure compares the APMS magnitudes corresponding to sitting without a back support (NVF), against a vertical back support (BVF) and an inclined (12°) back support (BIF). The results show only slight shifts in the APMS resonance frequency with backrest interaction. Patra *et al.* (2008) showed slight reduction in the resonant frequency in the mean seat APMS response for subjects in the 55 and 75 kg body mass group, while the 98 kg subjects group displayed the opposite trend.

The body is known to undergo bi-dimensional movements even under vertical seat excitation (Hinz *et al.*, 1988b). The addition of a back support may have significant influences on the forces developed at the body-backrest interface. However, only a few studies have attempted the measurement of the force-motion responses at this additional driving-point. The studies by Nawayseh and Griffin (2004; 2005) and Rakheja *et al.* (2006) illustrated considerable forces at the vertical backrest which additionally increased with the inclination angle suggestive of greater coupling between the upper body motions in the vertical and fore-aft axes. Similar trends were reported by Mansfield and Maeda

(2006) under vertical excitation. These results tend to depict a change in the nature of spine loading, increasingly towards a shear mode, due to the interaction of the backrest.
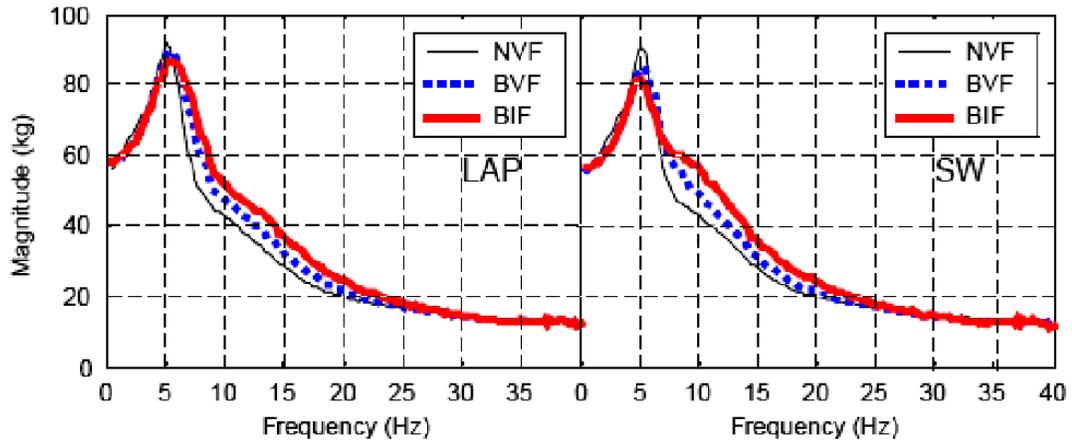
Figure 2-11: Effect of back support condition and hands position on mean vertical seat APMS of 27 subjects under exposure to vertical vibration. Back support conditions include NVF: None; BVF: Vertical; and BIF: Inclined (12°). Hands are either placed on lap (LAP) or holding a steering wheel (SW). (Source: Wang *et al.*, 2004)
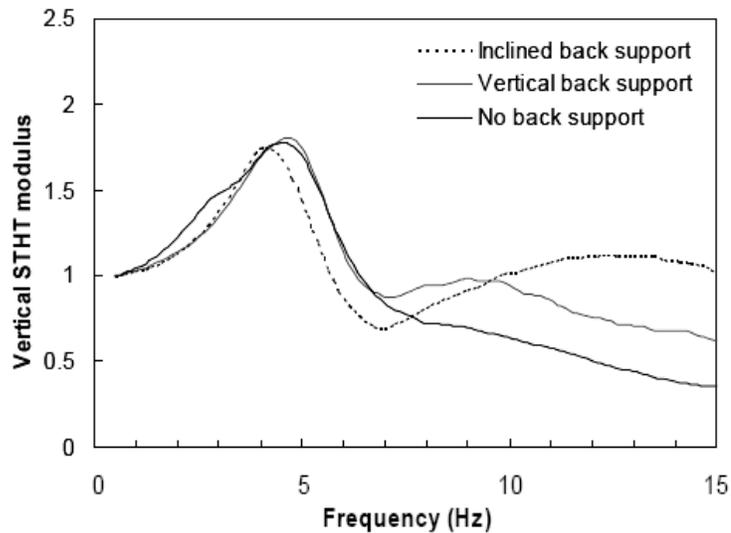
Figure 2-12: Effect of back support on vertical head (STHT) transmissibility (Wang *et al.*, 2006)

Interestingly, there are only a few studies that elaborate on the effect of a backrest on the vibration transmissibility through the body. Paddan and Griffin (1988a; 1988b; and 1998) analysed the STHT responses along the three axes under vertical, horizontal and lateral excitations, applied individually. Under vertical vibration with the interaction of an inclined backrest, slightly higher vertical STHT peak magnitudes were reported with considerable increase in the corresponding frequency. However, such frequency shifts have not been noticed in other comparable studies. Additionally, Hinz *et al*. (2002) showed a reduction in peak vertical STHT magnitude with the back support. Wang *et al*. (2006) also reported significant changes in STHT magnitude around 3 Hz and beyond 7 Hz with vertical and inclined back supports (Fig. 2-12). Moreover, the interaction of a backrest, irrespective of the inclination angle, reduces the fore-aft motion at the head (Wang *et al*., 2006). It follows that the motion of the body segments may also be substantially influenced by the back support condition. However, it may be observed from Tables 2-2 and 2-3 that only two studies have extracted measurements at intermediate segments with some form of a back support. The vibration study on human cadavers seated with a backrest (El-Khatib *et al*., 1998; and 2001) revealed a broader peak in vertical lumbar acceleration transmissibility. The absence of muscular activity in the cadaveric subjects makes the data unreliable for comparisons with *in vivo* results. In another study, female subjects seated with a thoracic backrest and exposed to shock motions showed only slight decrease in the peak gain in vertical acceleration measured using a vertebral pin (Magnusson *et al*., 1994). Although estimations of lumbar loads have been predicted under static sitting for various postures and support conditions (Chaffin *et al.*, 1991), the influence of the backrest on vibration transmission properties through the spine is still unknown.

2.4.5 Effects of Hands Position

The seated posture with hands in the lap reported in the vast majority of biodynamic studies may not be considered representative of the driving posture assumed in most work vehicles. In addition, international standards such as ISO-5982 (2001) and DIN-45676 (1992) define the values of vertical DPMI, APMS and STHT only for the hands-in-lap condition, while sitting without a back support. Although only a few studies have employed some form of a hands support (Donati and Bonthoux, 1983; Pope *et al.*, 1991; Wang *et al.*, 2006) there could be effects on the vibration characteristics of the seated body due to the additional constraint imposed by the hand controls. Static studies have shown the significance of hand positions on the muscle fatigue and disorders (*e.g.*, Chaffin *et al.*, 1999; Magnusson and Pope, 1998). Hands holding the steering wheel in a vibrating cab may introduce excitation into the upper body altering the acceleration transmission properties through the body and thus the biodynamic responses at the seat and the backrest. This phenomenon may be of particular interest when there is relative movement between the seat and the hand controls, for example, while using a suspended seat. The static and dynamic forces on the seat may also be reduced on the seat pan due to the inertia of the hands being partially supported by the steering wheel and the supportive muscular activity provided by the gripping action (Rakheja *et al.*, 2002). Further, pelvic rotation, which is found to influence biodynamic responses (Zimmermann and Cook, 1997), may also be altered by the hand constraints.
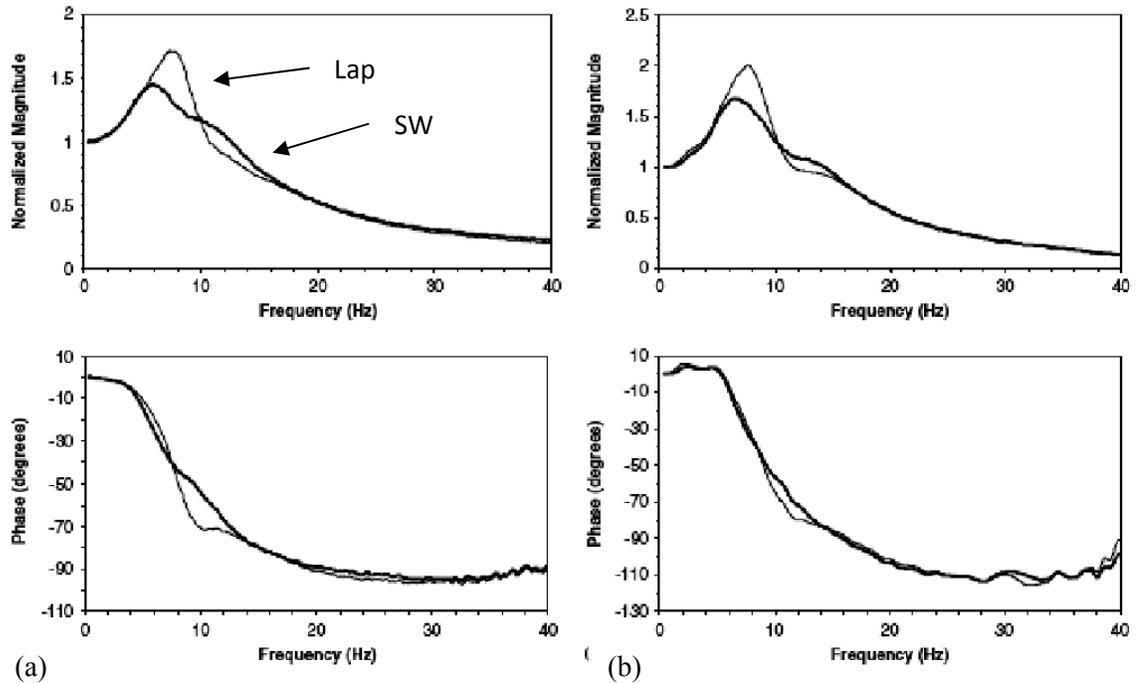
Figure 2-13: Influence of hands position on measured (a) vertical seat APMS; and (b) cross-axis backrest APMS. Lap: Hands on Lap, SW: Hands holding Steering Wheel (Adapted from Rakheja *et al.*, 2006)

Rakheja *et al.* (2006) noticed significant differences in measured APMS responses between hands on a steering wheel versus the lap, while sitting in a rigid automotive seat with full back support (Fig. 2-13). There was considerable decrease in peak response magnitude and a reduction in resonant frequency due to the steering wheel support in both the vertical seat- and upper-body backrest-APMS measurements. Additionally, a higher frequency secondary mode was also accentuated in the hands-supported posture. However, such trends have not been reported in other studies. Wang *et al.* (2004) reported significant influences of the steering wheel hands position on the vertical APMS mainly with an inclined backrest, as in the case of an automotive seat, which showed a pronounced secondary mode around 10 Hz. However, Patra *et al.* (2008) noted no substantial changes in seat pan APMS due to hands position irrespective of the

86

back support, which was most likely due to the relatively small backrest inclination, in the order of 12°. The studies seem to show noticeable changes on the vertical APMS with hands on the steering wheel mainly in the presence of a back support. However, there seem to be inconclusive inferences on the influence of hands position on transmissibility to the head. Interestingly, Wang *et al*. (2005) showed the hands position to be slightly significant ($p<0.05$) around the resonance frequency range of both vertical and fore-aft STHT magnitudes in the erect posture without a back support. Without a backrest contact, the hands holding the steering wheel resulted in increase in the resonant frequency in both the fore-aft and vertical transmissibility of the head. This may be due to the stiffening of the seated body due to the additional hand constraints. However, it may be observed from Table 2-3 that only one WBV study performed measurements on various segments of the human body with the steering-wheel hands position (Donati and Bonthoux, 1983). Further efforts are thus required to investigate the effects of hands support coupled with a back support.

2.5   Summary of critical issues and impediments

The relevant reported studies on transmission of whole body vertical vibration to the seated body have been reviewed in order to gain an understanding of human response to vibration, measurement techniques and to identify most significant contributory factors, so as to formulate the scope of the experiment design in the present dissertation. Selected studies reporting responses at different body locations are particularly emphasised from the point of view of gaining insight into the reasons for resonances, sagittal-plane movements reported and the modes of vibration of the seated upper body. Although most of the studies report a response peak around 4-6 Hz at all body locations,

when exposed to vibration in the vertical axis, there is wide variability in the responses from different studies. This may be attributed to a variety of factors including the differences in (a) experimental variables, namely seating conditions, posture, type and magnitude of input excitation; (b) subject population, gender and anthropometry; and (c) data acquisition and analysis procedures, including the type of sensors and their mounting. The reported data on vibration transmission to segments of the upper body may thus not be directly comparable due to the interplay of these multi-factorial influences. The reported studies have thus been systematically reviewed to isolate and understand these effects. A definite increase in maximum seat APMS coupled with a decrease in resonant frequency is generally observed with increasing body mass. However, no clear relationships between subject characteristics and vibration transmission properties could be established from the reported studies. The excitation magnitude seems to show similar influences on the driving-point and trunk biodynamic response parameters. However, only a few studies have attempted the analysis of the effects on the localised responses.

The back support condition and hands position also show a significant effect on seat APMS and STHT. Hands holding the steering wheel seem to reduce peak APMS and STHT magnitude, while the effect appears to be strongly coupled with the backrest support. The back support by itself revealed significant influences on the APMS and STHT functions in the fore-aft and vertical directions. While the APMS peak magnitude is decreased with a backrest along with an increase in resonance bandwidth, the vertical STHT responses show considerable increase at higher frequencies with a back support. An inclined backrest, on the other hand, could yield low peak STHT magnitude and lower resonant frequency. The interaction with a backrest, irrespective of the inclination

angle, has been shown to reduce fore-aft motion at the head. It follows that the motion of body segments may also be substantially influenced by the back support condition. These results tend to depict a change in the nature of spine loading, increasingly towards a shear mode, due to greater interaction with a backrest. However, only a few studies seem to have extracted measurements at intermediate body segments with some form of a back support. Other than one cadaveric study revealing a broader peak in vertical lumbar acceleration transmissibility, the influences of the backrest on vibration transmission properties through the body are still unknown.
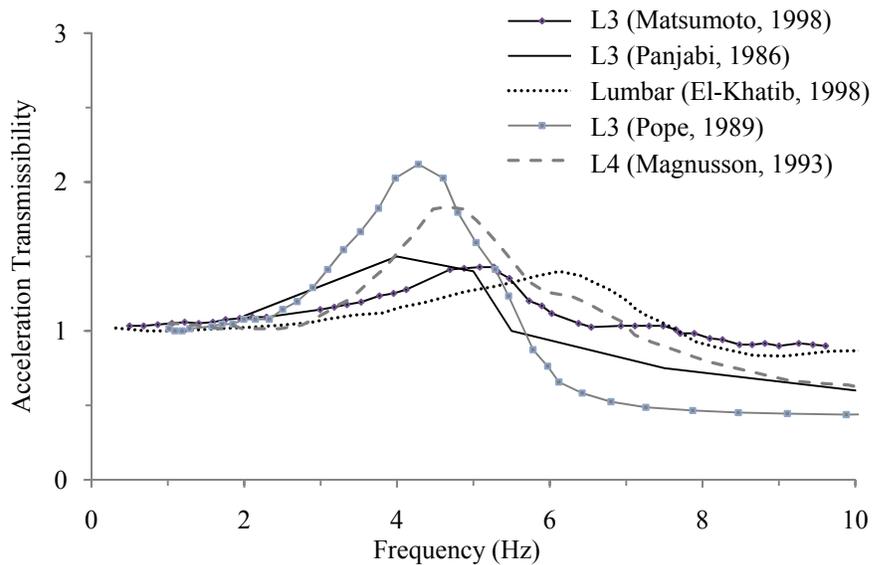
Figure 2-14: Comparison of reported vertical acceleration transmissibility responses measured in the lumbar spine.

Additionally, even among the reported studies on the properties of vibration transmission through the human body sitting without a back support, considerable disagreements are evident. As an example, Fig. 2-14 illustrates the comparison of reported vertical transmissibility data at the lumbar vertebrae, where the curves are denoted by the first authors of the corresponding study. While most of the responses

show maximum transmissibility in the 4-6 Hz range, there are wide variations in the peak magnitude and the bandwidth of the measured responses, which may be attributed to a variety of factors including differences in (a) experimental variables, namely seating conditions, posture, type and magnitude of input excitation; (b) subject population, gender and anthropometry; and (c) data acquisition and analysis procedures including the type of sensor and its mounting. The reported data on vibration transmission to segments of the upper body may thus not be directly comparable due to the interplay of these multi-factorial influences. Furthermore, it may be inappropriate to utilise such a wide range of responses for deriving target datasets for formulation and validation of anthropometric biodynamic models for representation of multidimensional body movements, as it is observed in the idealised ranges of the APMS and STHT values presented in ISO-5982 (2001). It is thus necessary to isolate some of the confounders and also apply appropriate correction procedures, where possible.

A number of anomalies have been identified in the measured data that necessitate cautious interpretations or additional measurements in order to ensure reliable body-segment response datasets for further analyses. The estimation of movement at the vertebral body from the skin-mounted transducer data particularly involves careful scrutiny. Errors in the measurement may be introduced by the orientation of the sensor and by the angular acceleration at the skin location. This acceleration error may be partly compensated by considering the distance between the vertebral centroid and the sensor location. On the other hand, inclination of the skin transducer due to the curvature of the local body location may result in the sensor registering signals in its localised coordinates that may differ from the responses in the biodynamic and basi-centric axes. This could lead to considerable errors in estimating the acceleration transmitted to the corresponding

90

body segment (Sandover and Dupuis, 1987). Such orientation errors have been addressed by Dong *et al.* (2002) for measurements at the palm of a gloved hand subject to hand-transmitted vibration. Coordinate transformation was employed to correct for angular misalignment of the accelerometers. A similar methodology has also been utilised in some of the WBV studies involving vibration measurements at different body locations (e.g. Magnusson *et al.*, 1993; Matsumoto and Griffin, 1998).

The relative movement of the local skin and the endodermic tissue over which the sensor is mounted may lead to erroneous conclusions on the vibration at the internal skeletal structures (Hinz *et al.*, 1988a; Sandover, 1998). It has been found that skin-mounted transducers could overestimate vertebral bone displacements (Pope *et al.*, 1986) Mathematical techniques have been developed both in the time and frequency domains so as to estimate and subsequently correct for tissue effects in the responses measured at the skin surface. Most studies derive tissue mechanical properties, namely natural frequency and damping ratio, from the free response tests of the skin-sensor system and employ the inverse transfer function of the skin as a correction, assuming a single degree of freedom (DOF) behaviour of the skin and the tissues (Hinz *et al.*, 1988a; Kitazaki and Griffin, 1995). The single DOF skin tissue model displays excessive attenuation at higher frequency and may thus reduce accuracy at these frequencies. An alternative approach using a two part transfer function was proposed by Morrison *et al.* (1995) for the corrections at low and high frequencies. The measurement of vibration at localised segments is thus sensitive to a number of errors, which need to be considered and addressed appropriately. However, it should be noted that despite all these complexities the reported studies could provide valuable information on the nature of vibration transmission "through-the-body" for better understanding and interpretation of human

biodynamics. However, considering the wide discrepancies among the reported data, additional measurements under carefully controlled representative conditions are vital for deriving target response sets and reliable bio-models of the seated human body exposed to vertical WBV. In addition, the study of the effects of significant independent parameters like seating and postural conditions and input excitation on the seated body response to WBV may thus be better served by the measurement of vibration transmitted to vertebral locations with the inclusion of more representative seating and excitation conditions.

3. Simultaneous Measurement of Body Segment Vibration and Driving-Point Biodynamic Response

3.1 Introduction

The most widely reported driving-point measures of seated body biodynamics have provided considerable knowledge on human response to vibration and contributed to the development of biodynamic models. It has been acknowledged that additional biodynamic measures in terms of vibration transmitted to the body segments could yield enhanced knowledge on human response to vibration and provide essential data for identifying more reliable biodynamic models (Seidel and Griffin, 2001). The measurement of whole-body vibration transmitted to segments of a seated body, however, has been extremely challenging due to a number of influential factors, including the selection and mounting of instrumentation, orientation errors, skin effects and the interplay of other inherent measurement errors (Sandover, 1998). The surgical insertion of sensors into the body may also raise some ethical concerns. Consequently, measurements of transmitted vibration have been mostly limited to the head or mouth of the seated human body, while only a few studies have measured vibration transmitted to various other segments. These data generally exhibit significantly large inter-subject variability, which is mostly attributable to the above-mentioned influencing factors.

Additionally, varied experimental conditions used in the reported studies have resulted in very little agreements in the measured vibration transmission responses (Paddan and Griffin, 1998; Pranesh *et al.*, 2010). Owing to the potential differences attributable to anthropometry of subjects used in different studies, it is also essential to acquire all of the desired biodynamic measures simultaneously or sequentially in a given laboratory under identical test conditions. Only a few studies, however, have performed

simultaneous measurements of the widely reported driving-point biodynamic responses such as apparent mass, mechanical impedance or absorbed power, and body segment vibration transmissibility (*e.g.*, Donati and Bonthoux, 1983; Kitazaki and Griffin, 1998; Matsumoto and Griffin, 1998).

It also needs to be emphasised that the reported biodynamic measures may not correspond to situations associated with typical vehicle driving. For instance, the driving-point measures have been invariably, with the exception of a recent study (Hinz *et al.*, 2006), measured for the body seated on a rigid seat. Furthermore, the vast majority of studies have measured biodynamic responses for the body seated without a back support with hands resting on the lap. The operators of mobile machinery in the actual workplace tend to utilise a backrest and hold hand controls. However, the influence of the back support and/or vibrating hand controls has been investigated only in a few studies measuring responses at multiple driving-points (Rakheja *et al.*, 2006; Wang *et al.*, 2004) and transmitted head vibration (Wang *et al*., 2006; Magnusson *et al*., 1993). The influence of a back support on the vibration transmitted to the upper body has not yet been attempted, primarily due to measurement difficulties. Significant changes in the vibration transmitted to the head in both the vertical and horizontal axes with the interaction of a vertical or an inclined backrest suggest strong influence of the back support on the nature of vibration transmission through the body (Wang *et al*., 2006). Considering that vehicle driving generally involves the use of a backrest, it would be desirable to characterise the biodynamic responses of the human body seated with a back support and subsequently derive biodynamic models for seeking improved designs of intervention mechanisms and seating evaluation methods.

This chapter details the experimental procedures employed to simultaneously measure the seated body's responses to vertical vibration in terms of: (i) apparent mass responses at two driving-points formed by the buttock-seat and upper body-back support interfaces; (ii) vertical and fore-aft vibration transmissibility at the occupants' head; and (iii) vertical and fore-aft vibration transmitted to selected vertebrae. The experiment design is presented that comprises a combination of postures involving the back support condition and hands position along with three different magnitudes of random vertical excitation. The hardware and the processes used for vibration data acquisition and for rectification of measurement errors that may arise due to inherent experimental conditions are systematically explored and discussed. The statistical techniques used for analyses of the data are also described.

3.2   Experimental Methods

An experiment design was formulated to simultaneously acquire multiple biodynamic response measures of seated adult male subjects exposed to vertical whole body vibration. These included: the force-motion relations at the buttock-seat and upper body-back support driving-points (in the presence of a back-support contact); vertical (z) and fore-aft (x) axis vibration transmitted to the head; and z and x axis vibration transmitted to selected locations of the spine (C7, T5, T12, L3 and L5). The experiment design also included the study of representative influencing factors, namely the back support condition, hands position and magnitude of vibration excitation. The experiments thus involved factorial design of two back support conditions (none and vertical), two levels of hands position (in the lap and on a steering wheel) and three levels of broad-band vertical vibration in the 0.5 to 20 Hz range.

3.2.1 Subject selection and instrumentation

A total of twelve healthy adult male human subjects in the age group of 25 to 38 with no known back problems were recruited for the study. The vast majority of these volunteers came from the student population at Concordia University, and had fairly athletic body build. Although, the subject masses varied from 63 to 95.4 kg, ten of the twelve candidates were in the mass range of 65 to 80 kg (mean mass = 75.57 kg; and standard deviation (SD) = 10.15 kg) and mean standing height of 1.75 m (SD 0.05 m), closely resembling the 50th percentile male anthropometry. The sitting height of each subject was also measured as the vertical distance from the seat pan to the top of the skull, which ranged from 0.83 to 0.97 m (mean = 0.88 m, SD = 0.04 m). The subject's sitting weight at the seat-buttock interface under static conditions was also acquired (mean = 58.32 kg; SD = 6.43 kg). Table 3-1 summarises some of the physical characteristics of the selected population. Each subject was advised about the experimental method and the safety procedures, and was asked to sign a consent form approved by the Human Research Ethics Committee at Concordia University, prior to commencement of the experiment. Subsequently, the subject was instrumented with accelerometers located mid-sagittally at the selected locations on the back.

For measurements of the force-motion relations at the body-seat interfaces, an instrumented rigid seat was used. The design of this seat is described in Section 3.2.2. A tri-axial accelerometer (Analog Devices ADXL05 EM-3) mounted on a light-weight (300 gms) head strap with a ratchet mechanism for tension adjustments, developed by Wang *et al.* (2006), was used to measure the vibration transmitted to the head along the three translational axes. Figure 3-1(a) illustrates a pictorial view of the head acceleration measurement system installed on the subject seated on the vibration simulator. The

subject was permitted to adjust the tension so as to achieve a firm and comfortable mounting. The orientation of the accelerometer was finally corrected by the experimenter to achieve measurements along the basi-centric *x*-, *y*- and *z*- axes.

Table 3-1: Characteristics of the subjects recruited for the experimental study.

n = 12	Age (yrs)	Total Weight (kg)	Sitting Weight (kg)	Standing Height (m)	Sitting Height (m)
Min	25	63	48.60	1.69	0.83
Max	38	95.40	70	1.84	0.97
Mean	30.27	75.57	58.32	1.75	0.88
SD	5.12	10.15	6.43	0.05	0.04
Median	28.00	74.00	58.60	1.74	0.88

A total of five three-axis micro-accelerometers were utilised on the seated subject's back to measure transmitted vibration. These were mounted near the seventh cervical (C7), fifth and twelfth thoracic (T5, T12), and third and fifth lumbar (L3, L5) vertebrae. The choice of these vertebrae involved a variety of factors encompassing the incidences of spinal disorders and pain (Bovenzi *et al.,* 1998; Hoy *et al.*, 2005; Kjellberg *et al.,* 1994; Magnusson *et al.*, 1998), and the availability of comparable vibration results in the published literature (e.g., Panjabi *et al.*, 1986; Magnusson *et al.*, 1993). Owing to the significant effect of the sensor mass on the measured responses, micro-accelerometer chips (10x10mm * 4mm thick) weighing 5 gms (Analog Devices ADXL-330) were affixed to the skin near the target locations, as illustrated in Fig. 3-1(b). The measurements of the vibration transmitted, however, were limited only to the fore-aft (*x*) and vertical (*z*) axes, since the vibration transmitted along the lateral (*y*) axis is known to be relatively small (Paddan and Griffin, 1988; Nawayseh and Griffin, 2004; Wang, 2006).
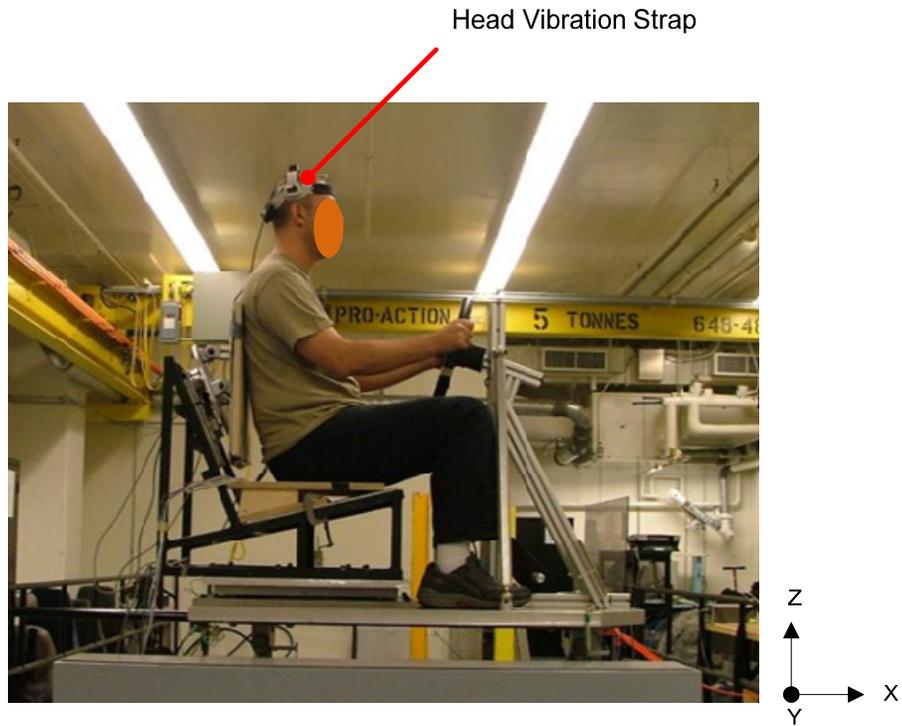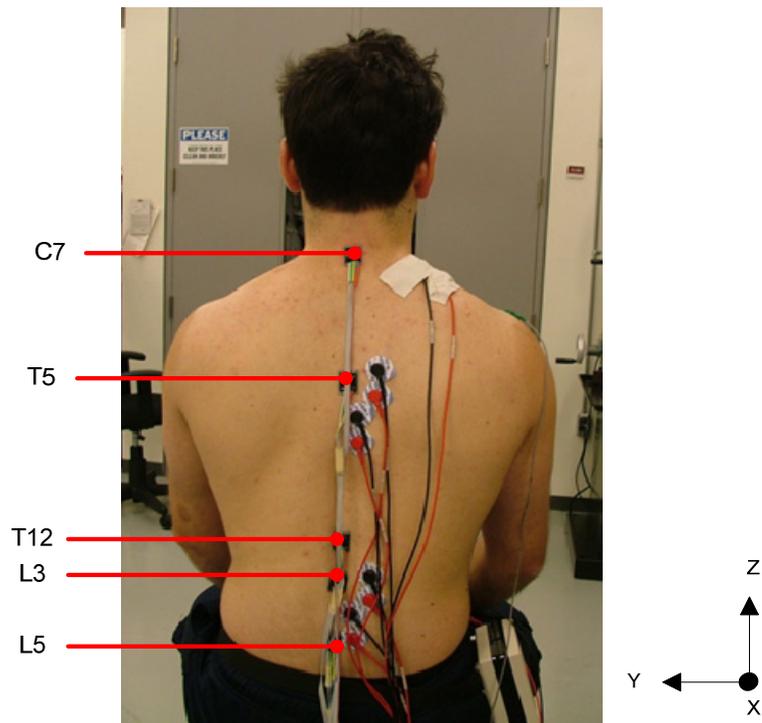
Figure 3-1: Pictorial views illustrating (a) the light-weight adjustable head acceleration measurement system mounted on the subject; and (b) the location of skin-mounted micro accelerometers at the selected vertebral levels.

The posterior face of the spinous process for each of the above vertebrae was identified by palpation and the corresponding location marked on the skin in the upright sitting posture. Body hair and dead tissue over the skin were removed around each of the marked location (20x20 mm) by shaving and using an abrasive nail file, respectively. The selected locations were subsequently cleaned with alcohol wipes so as to provide an adequately smooth surface for mounting the transducer. The accelerometers were then mounted on the skin near the selected locations using double-sided adhesive tape. Electrical wires from the transducers were appropriately harnessed so as to avoid discomfort to the test subject as well as to reduce noise in the measured signals. Before starting the experiments a free vibration response test was performed on each of the miniature accelerometers mounted on the subject's back so as to characterise the frequency response behaviour of the skin-transducer system, which is described in Section 3.3.2.

3.2.2 Whole-body vibration simulator and test conditions

This study utilised the Whole Body Vertical Vibration Simulator (WBVVS) installed in the research facility at the Concordia Centre for Advanced Vehicle Engineering (CONCAVE). Figures 3-2(a) and (b) depict, respectively, the pictorial and schematic views of the simulator mounted with a seat fixture and a steering column. The setup comprised of a rigid aluminium base plate (100x100*25 mm) excited vertically by two electro-hydraulic actuators with peak to peak displacement of 300 mm. The vibration controller for the WBVVS was equipped with a number of safety features including limits for peak displacement (< 125 mm) and peak acceleration (< 2 m/s^2). Additionally, five emergency stop switches, including one on the steering wheel for the test subject, were installed at various locations in the system.
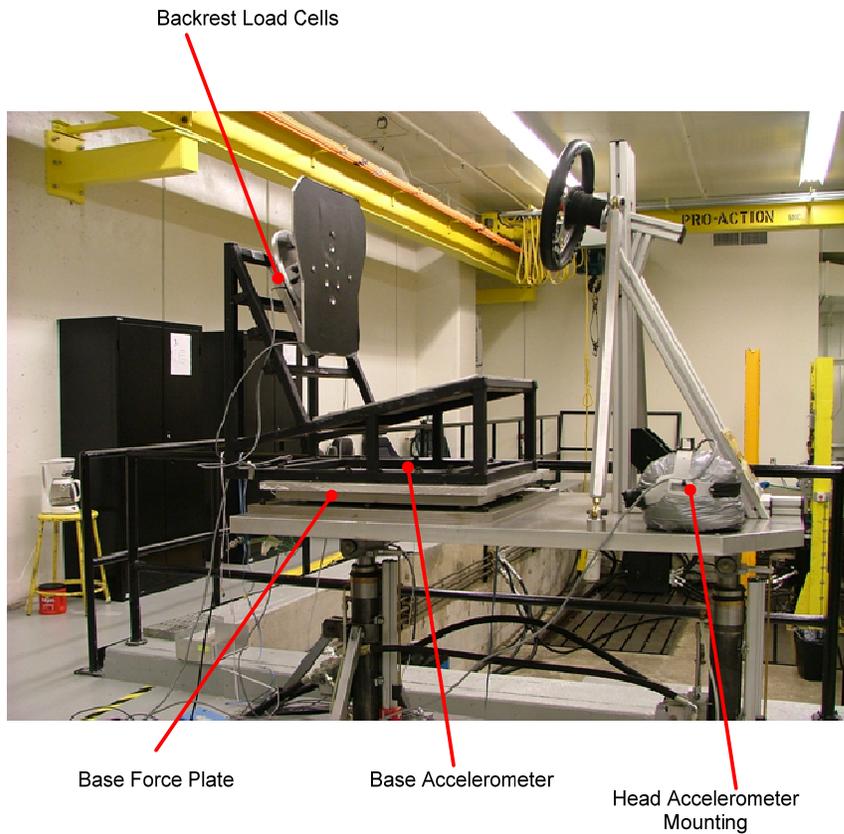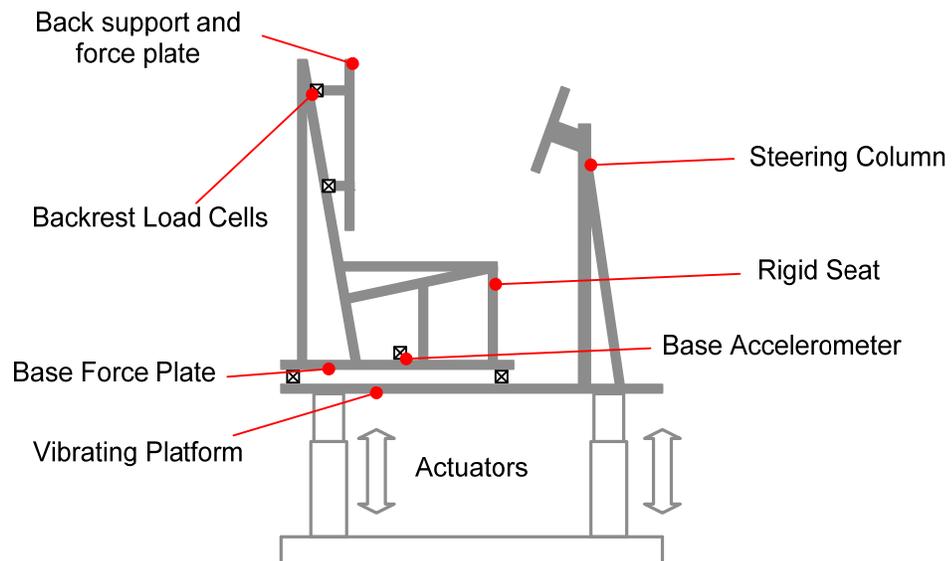
Figure 3-2: (a) Pictorial view; and (b) schematic representation of the Whole Body Vertical Vibration Simulator (WBVVS) showing its components and instrumentation.

A rigid seat was mounted on the platform through a force plate with four capacitive Kistler load cells to measure the dynamic force at the seat base. A single-axis accelerometer (B&K 4370) was attached to the force plate to measure vertical driving-point acceleration. The original seat was designed to achieve a configuration representative of automotive seats (Rakheja *et al.*, 2006), wherein the aluminium plate (450x450*6 mm) serving as the seat pan was installed at an inclination of 13º from the horizontal axis. It has been shown in earlier studies that biodynamic responses are affected by seating conditions including posture and seat pan geometry (Wang *et al.,* 2004; Rakheja *et al.*, 2006). However, since most reported experiments have been conducted on a horizontal seating surface, the automotive seat pan geometry was modified by clamping a wooden fixture (450x450*25 mm) to obtain a horizontal seat pan configuration.

An aluminium backrest plate with two 222 N strain-gauge load cells (Omegadyne, LCHD-100) was also fastened to the seat frame and adjusted so as to realise a vertical backrest angle. The force plate provided the measurement of driving-point force at the upper body-backrest interface in a direction normal to the back support. Initial pilot tests with human subjects sitting with upper body-backrest contact revealed adhesion of the miniature accelerometers fixed at the T5, T12 and L3 vertebral levels to the back plate. This phenomenon was identifiable from the flat unity vertical transmissibility in addition to almost insignificant horizontal responses at these trunk locations. Considering one of the primary goals was to study the effect of a backrest constraint on the vibration transmissibility properties through the upper body, a relatively large area of the trunk supported by the backrest was deemed necessary while avoiding accelerometer adhesion with the back plate. Subsequently, the backrest was modified, as shown in Fig. 3-3, by

fixing two wooden panels so as to form an elongated cavity for the back accelerometers to be accommodated without contacting the vibrating surface. Subsequently, trials showed significant differences in the vibration transmissibility responses with different slot sizes, most probably due to local skin-tissue stretching. A width of 30 mm provided the required leeway for independent skin-sensor movements while ensuring sufficient back contact area.
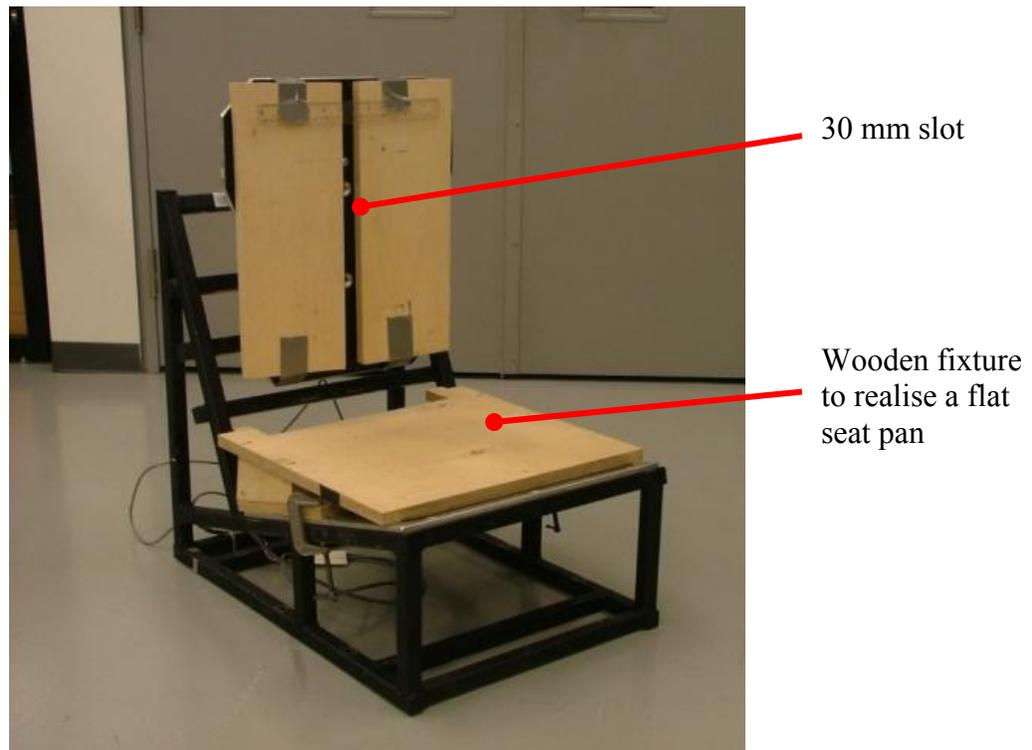
Figure 3-3: The rigid seat with a vertical backrest modified with a central slot to avoid adhesion of trunk accelerometers in the back-supported postures.

The experiments involved four different sitting postures assumed by the subjects, which were realised through combinations of two back support conditions and two hands positions, as shown in Fig. 3-4. Each subject sat either with the backrest in contact with the upper body (B) or upright without a back support (NB). The hands were either resting on the lap simulating a passenger-like sitting condition (L) or placed on the steering

wheel representative of the driving condition (SW). The four postural conditions considered in the study are denoted as: L-B, L-NB, SW-B and SW-NB, and illustrated in Fig. 3-4. The experiments were performed under three different magnitudes of white-noise vertical excitation with constant acceleration power spectral density (PSD) characteristics. Three different vibration signals were thus synthesised using a programmable vibration controller (Vibration Research: VR 8500) so as to produce seat acceleration waveforms with RMS (root mean square) values of 0.25, 0.5 and 1 m/s^2 in the frequency range of 0.5 to 20 Hz. Figure 3-5 illustrates the PSD spectra of the three random excitation signals synthesised for the experiments and measured at the seat base.
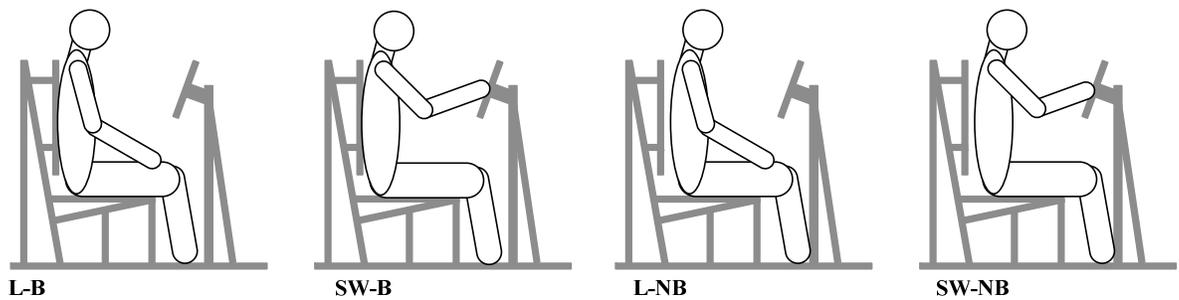
Figure 3-4: Schematic of the postures assumed by test subjects in this study. (L–Hands in Lap; SW–Hands on Steering Wheel; B, NB–with and without Back contact, respectively).

The test matrix used for each subject in this study is summarised in Table 3-2 showing the 12 conditions resulting from the factorial combinations of four support conditions (back and hands support) and three excitation magnitudes. Three trials were performed for each of the test condition and the data was examined so as to ensure acceptable repeatability. The experiment design thus constituted a total of 36 trials of 96 s duration each, for each subject. The order of experiments was randomised to reduce any counter balancing effects of the influencing factors on the response data. The subjects

were given sufficient rest between trials (minimum: 2 mins between successive trials) and were requested to dismount the simulator and walk within the lab at regular intervals so as to reduce discomfort and the possibility for cramps. The experimental procedures for each subject took approximately 5–6 hours, dictated primarily by the subject's comfort condition, while the total exposure was limited to a maximum of 60 minutes.
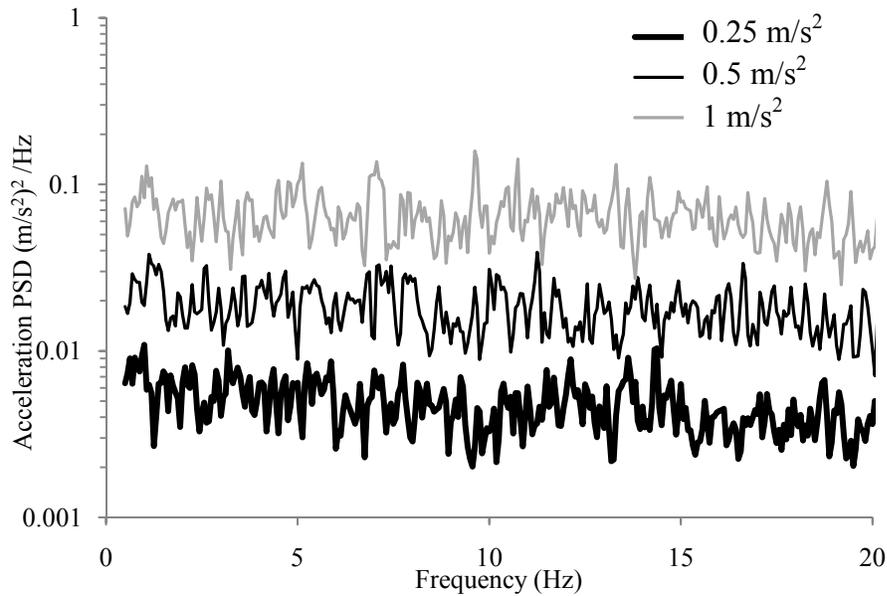
Figure 3-5: Acceleration power spectral density (PSD) of the broad-band random excitation signals synthesised to realise three vibration magnitudes (0.25, 0.5 and 1 m/s² RMS).

Table 3-2: Test matrix

Back support	Hands support	Excitation magnitude (m/s² RMS)			Notation
		0.25	0.5	1	
None	Lap	✓	✓	✓	L-NB
	SW	✓	✓	✓	SW-NB
Vertical	Lap	✓	✓	✓	L-B
	SW	✓	✓	✓	SW-B

3.3   Data acquisition (DAQ) and processing

Signals from the accelerometers and load cells installed on the WBVVS and the human subject were acquired using a multichannel spectral analysis system (B&K PULSE 11.0). Through preliminary measurements and data analyses, performed with only one subject, it was concluded the acquired data over the duration of 96 s per trial provided sufficient number of averaging windows, using a 50 Hz bandwidth with a resolution of 0.0625 Hz. Total force at the seat was obtained by summing the signals from the four load cells integrated within the seat base force plate. In a similar manner, the driving-point force at the backrest was obtained by summing outputs of the two strain gauge load cells supporting the vertical backrest. The total force signals together with the seat and body-mounted accelerometers signals were acquired by the PULSE front-end, and subsequently analysed to derive biodynamic measures.

Acceleration signals from the upper body including the head and five trunk locations (skin-mounted) along the fore-aft (x) and vertical (z) axes were used to derive fore-aft and vertical acceleration transmissibility from the seat base to the corresponding body locations, respectively. The vibration transmission from the seat to a particular body location was calculated using the H$_1$ function (in B&K PULSE) involving the complex ratio of the cross-spectrum between the excitation and response and the auto spectrum of the vertical seat acceleration, such that:

$$T_{Sx}^*(j\omega) = \frac{G_{SxA}(j\omega)}{G_{AA}(j\omega)}; \quad T_{Sz}^*(j\omega) = \frac{G_{SzA}(j\omega)}{G_{AA}(j\omega)} \tag{3.1}$$

Where $T_{Sx}^*(j\omega)$ and $T_{Sz}^*(j\omega)$ are the complex vibration transmissibility functions computed in the accelerometer's mid-sagittal local coordinates for a particular location or body segment S along the x- and z-axis, respectively. The x-axis is the axis normal to the local plane of the skin-accelerometer attachment and z is the axis along this plane.

105

$G_{SxA}(j\omega)$ and $G_{SzA}(j\omega)$ are the cross-spectra of measured x- and z-axis responses, respectively, at a specific location S, namely head, C7, T5, T12, L3 and L5, and $G_{AA}(j\omega)$ is the auto-spectrum of vertical seat acceleration. Here, j denotes the imaginary phasor whose value is $\sqrt{-1}$ and ω is the excitation frequency in radians/s.

The total biodynamic force measured at the seat base along the vertical axis and at the backrest plate along the axis normal to the back support were utilised in conjunction with the vertical base acceleration to calculate the respective direct and cross-axis apparent masses, respectively, such that:

$$M_P^*(j\omega) = \frac{G_{F_pA}(j\omega)}{G_{AA}(j\omega)}; \quad M_B^*(j\omega) = \frac{G_{F_bA}(j\omega)}{G_{AA}(j\omega)} \tag{3.2}$$

Where $M_P^*(j\omega)$ and $M_B^*(j\omega)$ are the complex direct and cross-axis apparent mass functions, denoted as "seat APMS" and "backrest APMS", respectively. $G_{F_pA}(j\omega)$ and $G_{F_bA}(j\omega)$ represent the cross-spectra of the vertical seat acceleration (A) and the force signals from the seat (F_p) and the backrest (F_b), respectively. Table 3-3 summarises the list of response functions derived simultaneously in this study along with the corresponding correction techniques applied, which are described in the following sub-section.

For all the aforementioned frequency responses, *i.e.* the apparent masses (APMS) and acceleration transmissibility to the six body locations, the corresponding coherence functions were also derived and monitored during the experiments. The frequency-dependent coherence function of the two signals used for calculating transmissibility assumes a value from 0 to 1, denoting the level of correlation between them. The coherence of the two signals is computed as the ratio of the square of the absolute value of cross-spectral density and the product of the auto-spectra of the two signals considered.

The coherences for the seat and backrest APMS are related to the auto-spectra of the seat and backrest force, G_{F_p} and G_{F_b}, respectively:

$$\gamma_P^2(j\omega) = \frac{\left|G_{F_pA}(j\omega)\right|^2}{G_{F_p}(j\omega)G_{AA}(j\omega)}; \quad \gamma_b^2(j\omega) = \frac{\left|G_{F_bA}(j\omega)\right|^2}{G_{F_b}(j\omega)G_{AA}(j\omega)} \tag{3.3}$$

Where γ_P and γ_b, define the coherence of seat and backrest APMS responses, respectively. Similarly, the auto-spectra of acceleration measured at a particular body location S in the z- and x-axes, were employed to derive the respective coherence functions γ_{Sz} and γ_{Sx} as:

$$\gamma_{Sz}^2(j\omega) = \frac{\left|G_{SzA}(j\omega)\right|^2}{G_{Sz}(j\omega)G_{AA}(j\omega)}; \quad \gamma_{Sx}^2(j\omega) = \frac{\left|G_{SxA}(j\omega)\right|^2}{G_{SxA}(j\omega)G_{AA}(j\omega)} \tag{3.4}$$

The computed coherence functions were consistently monitored during each experiment. A particular trial was rejected if the coherence magnitude in the 0.5 to 20 Hz frequency range occurred below 0.7.

Table 3-3: Frequency response functions calculated from the acquired signals and corresponding corrections

Measurement Location	Notation	Axes	Magnitude and Phase	Coherence	Mathematical Corrections
Apparent Mass					
Seat Base	Seat APMS	z	✓	✓	Rigid mass cancellation
Backrest	Backrest APMS	x	✓	✓	
Vibration Transmissibility to body locations					
Head	Head	x, z	✓	✓	Sensor misalignment (x, z); skin movement correction (z only)
Cervical 7	C7	x, z	✓	✓	
Thoracic 5	T5	x, z	✓	✓	
Thoracic 12	T12	x, z	✓	✓	
Lumbar 3	L3	x, z	✓	✓	
Lumbar 5	L5	x, z	✓	✓	

3.3.1 Inertial correction of the apparent mass responses

Before commencing the experiments with the human subjects, the force-motion responses at the seat and the backrest alone were recorded with the simulator excited with the three synthesised random excitation waveforms of magnitude 0.25, 0.5 and 1 m/s^2 RMS. Figures 3-6(a) and (b) illustrate, respectively, the apparent mass magnitude and phase responses of the components assembled on the load cells in the seat force plate and the backrest plate under the 1 m/s^2 excitation. Nearly identical responses were attained under the other two excitations, while the phase responses were nearly zero. The simulator assembly demonstrated acceptable rigid mass properties in the frequency range of 0.5 to 20 Hz. However, the backrest load cell unit showed non-linear behaviour above 15 Hz with respect to the response magnitude, which was attributed to a fore-aft resonance of the backrest plate near 16 Hz. Hence, the upper limit of frequency for the backrest APMS was limited to 15 Hz. The total seat and backrest APMS magnitudes were observed to be near 100 kg and 4 kg, respectively, which were nearly identical to the masses of the components supported by the force plates. The measured APMS responses of the seat structure alone were subsequently applied to those of the coupled seat-occupant system, $M_P^*(j\omega)$ and $M_B^*(j\omega)$, in order to perform the inertial correction and extract the biodynamic responses of the occupant alone. For this purpose the complex APMS functions obtained for the simulator alone were utilised in real time during the acquisition of the driving-point forces with the human subjects to cancel out the inertial effect due to the rigid masses, such that (*e.g.*, Matsumoto and Griffin, 1998; Wang *et al.*, 2004):

$$M_P(j\omega) = M_P^*(j\omega) - M_{Po}(j\omega)$$

$$M_b(j\omega) = M_b^*(j\omega) - M_{bo}(j\omega) \tag{3.5}$$

In the above correction, $M_{Po}(j\omega)$ and $M_{bo}(j\omega)$, refer to the complex APMS responses measured at the seat base and the backrest, respectively, due to the seat structure alone.
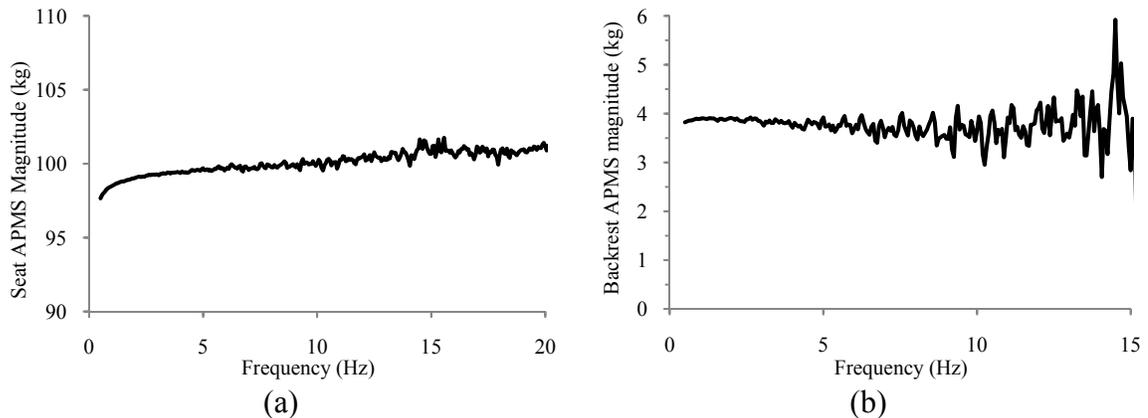
Figure 3-6: Apparent mass magnitude of rigid components of the simulator without a human subject measured at the (a) force plate; and (b) backrest.

3.3.2 Extraction of skin tissue properties and skin movement correction

The errors induced by the mechanical characteristics of the skin and certain endodermic tissue on the biodynamic responses measured using skin-mounted sensors has been acknowledged in a number of studies (*e.g.*, Hinz *et al.,* 1988a; Sandover, 1998). Additionally, acceleration measured at the skin surface may differ considerably from that at the vertebrae. Mathematical techniques have been developed both in the time and frequency domains in order to estimate and subsequently correct for tissue response effects in the measured results (*e.g.,* Hinz *et al.,* 1988a; Kitazaki and Griffin, 1995; Lafortune *et al.,* 1995; Pankoke *et al.,* 2001). One of the widely used methods involves characterisation of the mechanical properties of the skin tissue, namely the natural frequency and damping ratio, which are conveniently derived from the free-vibration response of the skin-accelerometer system. An inverse vibration transfer function of the skin tissue is subsequently formulated and implemented as a correction function to the

109

vibration responses measured at the skin surface. A similar approach was employed in this study. The skin-mounted miniature accelerometer at each location on the back was pulled and released to simulate a damped free-response test with an initial displacement of approximately 10 mm (Kitazaki and Griffin, 1995). The tests were performed along the vertical and horizontal directions, and the time histories of acceleration responses were acquired and analysed in a signal processing software (DADisp 6.0). The Fourier spectra of the measured signals were obtained over the bandwidth of 100 Hz with a frequency resolution of 0.195 Hz. The centre frequency (f_0) of the Fourier transform of the measured data was considered as the natural frequency of the skin-sensor system, assuming a single-DOF response. The damping ratios (ζ) of the tissue at various body locations were estimated using the difference in frequencies of the half-power points ($\Delta f_{\pm}$), such that:

$$\zeta = \mp \frac{1-(1\pm\Delta\beta)^2}{2(1\pm\Delta\beta)} \tag{3.6}$$

Where $\Delta\beta$ is the frequency ratio $\Delta f_{\pm}/f_0$. The transfer function H_S of the skin-sensor system was subsequently formulated as:

$$H_S(j\omega) = \frac{1+j\left[2\zeta\left(\frac{f}{f_0}\right)\right]}{1-\left(\frac{f}{f_0}\right)^2+j\left[2\zeta\left(\frac{f}{f_0}\right)\right]} \tag{3.7}$$

The above transfer function was applied to the acceleration transmissibility derived from the vibration signals at the skin surface to compensate for the skin effects and to obtain the estimates of the transmitted vibration to the bones, such that:

$$T'_{Si}(j\omega) = \left(H_{Si}(j\omega)\right)^{-1}T^*_{Si}(j\omega); \quad i = x, z \tag{3.8}$$

Where $T^*_{Si}(j\omega)$ is the measured vibration transmitted at a selected location along the axis i ($i = x, z$), as described in Eq. (3.1) and $T'_{Si}(j\omega)$ is the corresponding corrected

vibration transmissibility. The application of the inverse transfer function to the corrected data revealed significant contribution due to skin effects to the vertical vibration transmissibility but very small influence on the fore-aft responses. This was attributed to relatively higher skin stiffness along the fore-aft direction. The correction for the fore-aft vibration transmission, therefore, was not attempted during the subsequent measurements such that:

$$T'_{Sx}(j\omega) = T^*_{Sx}(j\omega) \tag{3.9}$$

The measurements showed considerable inter-subject variability in the skin natural frequencies and damping ratios identified from the vertical free-vibration responses of the subjects, irrespective of the measurement location. Figure 3-7 illustrates the range and inter-quartiles of the estimated skin-tissue natural frequencies and damping ratios along the vertical direction at different locations for the twelve subjects. The range of identified natural frequencies measured near the lower segments was generally higher compared to those of the higher locations, being the highest at L5. The median values of the skin-tissue natural frequencies generally occurred between 15 and 20 Hz. The central value of the damping ratios at different locations were observed to occur in the range of 0.51 to 0.62. The range of identified frequencies is considerably lower than the median frequency of around 40 Hz reported for the L3 vertebra by Kitazaki and Griffin (1995), while the damping ratios lie in a similar range. On the other hand, Hinz *et al.* (1988a) reported the tissue frequencies between T5 and L3 in the 5-11 Hz and 6-12 Hz ranges, respectively. Although the reasons for these differences are unclear, the weight of the accelerometer, the type and characteristics of the mounting adhesive, the area of skin contact, etc., are believed to be the major contributory factors (Kitazaki and Griffin, 1995).
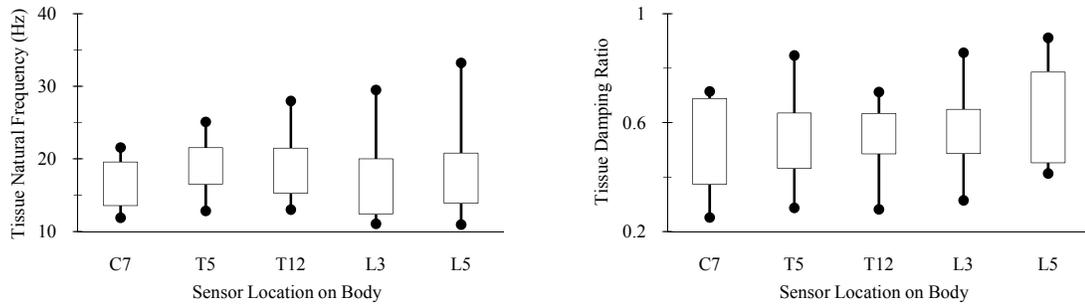
Figure 3-7: Ranges of skin-tissue natural frequencies and damping ratios calculated from free-vibration (pull) tests of the skin-mounted accelerometers at different measurement locations of 12 subjects.

3.3.3 Corrections for misalignments of the skin- and head-mounted accelerometers

Owing to the curvature of the spine, the surface-mounted accelerometers near the selected vertebral spinous processes may yield considerable orientation errors. Furthermore, the misalignment of the head band accelerometer may also contribute to certain errors. Inclinations of the back accelerometers due to the contour of the spinous processes or postural adjustments by the seated subject could induce errors in measurement due to relative change in the sensor's orientation from the biodynamic axis. Sandover and Dupuis (1987) suggested that "knowledge of accelerometer attitude could lead to much better accuracy." It was also shown by Dong *et al.* (2002) that misalignment of an embedded accelerometer for assessing the anti-vibration properties of gloves could cause measurement errors in excess of 20%. Therefore, the horizontal and vertical transmissibility responses in the basi-centric biodynamic axes, $T_{SX}(j\omega)$ and $T_{SZ}(j\omega)$ respectively, may be obtained by transformation of the response-axes, as shown in Fig. 3-8, using the complex components of the skin-corrected x- and z-axis transmissibility functions, such that:

112

$$\begin{bmatrix} T_{SX}(j\omega) \\ T_{SZ}(j\omega) \end{bmatrix} = \begin{bmatrix} \cos \propto & \sin \propto \\ -\sin \propto & \cos \propto \end{bmatrix} \begin{bmatrix} T'_{Sx}(j\omega) \\ T'_{Sz}(j\omega) \end{bmatrix}$$ (3.10)

The accelerometer orientation ($\propto$) with respect to fixed basi-centric axis system is estimated from the measured acceleration transmissibilities at a very low frequency of 0.5 Hz, such that:

$$\propto = tan^{-1} \left[\frac{T'_{Sx}(j\omega)}{T'_{Sz}(j\omega)} \right]; \qquad \omega = 2\pi(0.5) \text{ rad/s}$$ (3.11)

In the above formulation, it is assumed that the body dynamic yields negligible horizontal motions of the head and the upper body at the low frequency of 0.5 Hz. The skin-corrected acceleration transmissibility responses of individual subjects were analysed to determine the mean and standard deviation of the accelerometer orientations at the selected measurement locations. The orientation angle of the head accelerometer system was visually monitored and rectified prior to each trial. The correction due to orientation error was thus not attempted for the head acceleration responses such that:

$$T_{HeadX}(j\omega) = T'_{Headx}(j\omega); \text{ and } T_{HeadZ}(j\omega) = T'_{Headz}(j\omega)$$ (3.12)
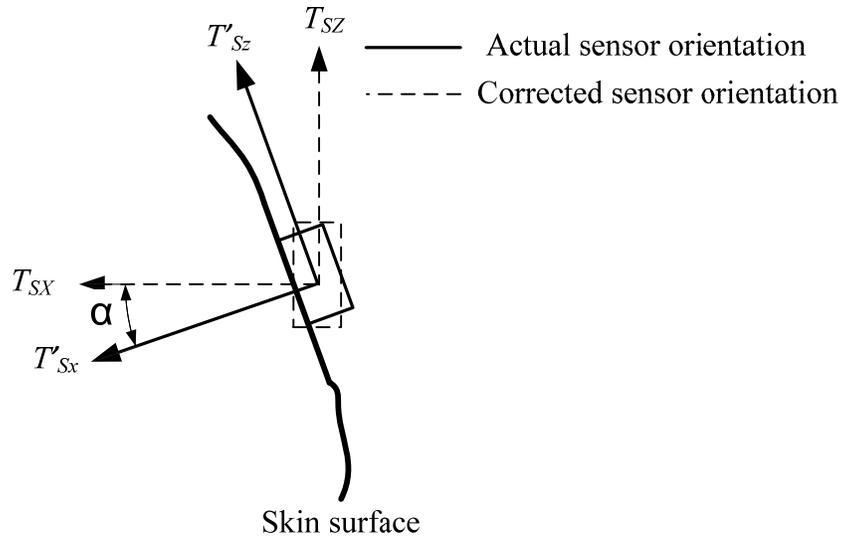
Figure 3-8: Illustration of the trunk accelerometer's coordinate transformation to the basi-centric axis.

Table 3-4 summarises the mean and coefficient of variation (CoV) of the mean estimated accelerometer orientations, derived for the 12 subjects at different measurement locations for the four sitting postures considered. The results suggest considerable misalignments of the accelerometers mounted at different locations of the trunk, particularly near the C7 and T5 locations, which showed significant orientation angles. The response data for the T12, L3 and L5 locations required correction in the opposite sense ($-\propto$). The posterior deviation from the basi-centric axis system was considered negative in this study.

Table 3-4: Mean and coefficient of variation (CoV) values of accelerometer orientation angles at the measured trunk locations

Location	C7	T5	T12	L3	L5
Posture	Mean (CoV) values of accelerometer orientation angles (degrees) [†]				
L-B	35 (0.19)	17 (0.3)	-6 (0.58)	-6 (0.43)	-13 (0.46)
L-NB	35 (0.19)	18 (0.29)	-7 (0.46)	-7 (0.23)	-9 (0.48)
SW-B	34 (0.14)	14 (0.41)	-6 (0.66)	-7 (0.56)	-12 (0.48)
SW-NB	34 (0.14)	14 (0.41)	-6 (0.66)	-7 (0.56)	-12 (0.48)

[†] Negative values indicate posterior (backward) orientation of the sensor

The lower thoracic and lumbar regions showed relatively less sensor orientation angles with lesser variation amongst the segments, probably because of the erect posture assumed by the subjects. The maximum mean deviations in sensor orientation occurred in the upper torso region (C7), in excess of 30º, irrespective of the sitting posture. The static sensor misalignment at the T12 and L3 locations were relatively small for all the postures considered in this study and may produce only negligible effect of the misalignment error. The SW-B posture was observed to lower static anterior rotation at the T5 level probably due to the two motion constraints provided by the steering wheel and the backrest.

The mean orientation angles obtained for individual subjects were applied to perform the orientation error corrections using Eq. (3.10). As an example, Fig. 3-9 illustrates the comparison of the vertical and fore-aft vibration transmission magnitudes at the selected vertebral locations obtained with and without the orientation corrections. The results are presented for the L-NB posture and 1 m/s^2 vertical seat excitation. The results show notable effects of the orientation error corrections, particularly in C7 fore-aft transmissibility and in the vertical acceleration transmissibility to all the locations. The results show that the low frequency (0.5 Hz) magnitudes of the uncorrected fore-aft and vertical acceleration transmissibility at the C7 lie near 0.6 and 0.8, respectively. These low frequency values are also considered as the static values to estimate the accelerometer orientation angle, which correspond to anterior sensor misalignment of about 37º from the fixed basi-centric axis. The application of the orientation error correction resulted in remarkable influences on both the peak magnitude and the corresponding frequency of the C7 fore-aft transmissibility. The correction also resulted in considerably higher peak magnitude of the C7 vertical transmissibility. The application of the correction resulted in nearly unity value of the low frequency vertical acceleration transmissibility, as it would be expected, and very low magnitudes of the fore-aft transmissibility. The correction also caused a slight increase in the frequency corresponding to the peak vertical response at C7, while the corrected responses at the T12 and L3 levels display the opposite trend. Additionally, the correction for the misalignment errors altered the transmissibility responses almost in the entire frequency range and resulted in greater attenuation of vertical vibration beyond 5 Hz at all the locations except at L5. The comparisons clearly suggest the need for mathematically correcting the misalignment errors in the skin-mounted accelerometers.
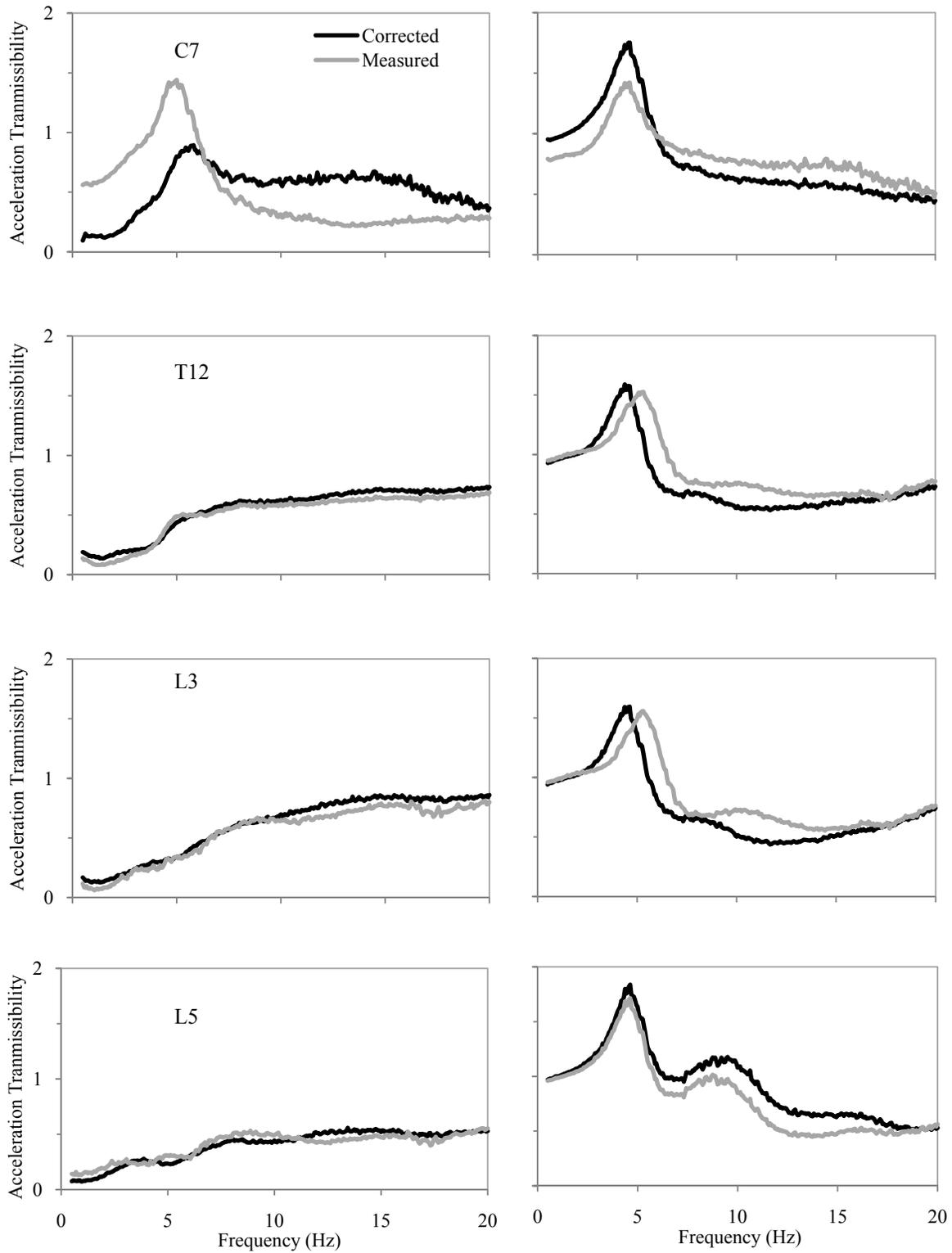
Figure 3-9: Comparisons of acceleration transmissibility responses measured at the C7, T12, L3 and L5 locations with and without the accelerometer orientation error corrections. (a) fore-aft; and (b) vertical transmissibility.

The results clearly demonstrated that the misalignments of the accelerometers, either due to the curvature of the back or the postural changes in the seated body, strongly alter the magnitude and frequency characteristics of the measured transmissibility responses. Magnusson *et al.* (1993) reported a maximum deviation of 4º in the orientation of the pin (K-wire) accelerometer inserted into the L3 vertebra with a vertical back support. In the present study, the postures with a backrest, *i.e.*, L-B and SW-B, showed a mean misalignment of 7º at L3 (Table 3-4). Additionally, the mean transducer inclination at the C7, observed in the order of 35º, is comparable to the 20-35º range reported by Matsumoto and Griffin (1998) at a close location, T1, for the 8 male subjects seated without a backrest. It may therefore be concluded that body segment transmissibility responses need to be derived in the basi-centric axes prior to further analyses on the data. On the other hand, changes in transducer orientation may also occur due to involuntary postural adjustments by the subjects for reasons of enhanced stability or comfort during the exposure, especially while sitting without a back support. Unfortunately, apart from the experimenters ensuring consistency in the subject's posture, the contributions due to such additional orientation errors could not be considered.

3.3.4 Data reduction and statistical analyses methods

The human body's responses to WBV were characterised in terms of (i) the apparent mass responses, corrected for inertial effects at the backrest and seat base; and (ii) the vibration transmissibility functions to the six body locations in the vertical and horizontal biodynamic axes, with the application of appropriate mathematical corrections for the skin effect and accelerometer misalignment. As mentioned earlier, a total of 12 test conditions for each subject were employed due to a combination of three input vibration levels, two back conditions and two hands positions. Additionally, three trials

of data acquisition were performed in each condition so as to ensure reliability of the measurements. For every subject, the three trials for a particular response function, for example seat APMS magnitude, were compared so as to ensure repeatability of the measurement and identify major differences, if any, among them. A particular trial, judged as an outlier was subsequently removed from the dataset. Such outliers, however, could be rarely identified due to the care taken by the experimenters in monitoring the seating conditions during the data acquisition, and in providing sufficient rest periods for the subjects between the successive trials. The average of the data acquired during the trials for a particular response was then considered as representative of the corresponding response and utilised for further data analyses. Subsequently, the data was averaged across subjects in order to extract single biodynamic response datasets for the 50th percentile male human body. The data analyses procedures employed are discussed in the following chapter. Owing to the considerable inter-subject variability found in the measured responses of the 12 subjects, statistical techniques were employed in an attempt to better understand the effects of different independent parameters and their relative significance. Multi-factorial analyses of variance (ANOVA) were performed on the horizontal and vertical body vibration response magnitudes, and apparent mass magnitudes using SPSS to identify the statistical significance of the selected main factors including the back support condition, hands position and excitation magnitude, and the interactions among them. The effects of these influence factors are discussed in terms of the significance level ($p < 0.05$) and the observed trends in the responses in the subsequent chapters so as to extract representative datasets.

3.4 Summary

This chapter describes the experimental procedures utilised to simultaneously measure the driving-point apparent mass and vibration transmissibility of the selected segments of twelve adult male human subjects exposed to random vertical vibration in the frequency range of 0.5 to 20 Hz. Six locations including the head, C7, T5, T12, L3 and L5 were chosen to mount accelerometers for measurements in the horizontal and vertical axes. While the head accelerometer was secured using a head-strap device, the trunk accelerometers were affixed to the vertebral skin locations using double-sided adhesive tape. The vertical backrest mounted on the vibration platform was modified with a central slot to accommodate the trunk sensors and avoid their adhesion to the backrest. The test matrix consisted of four postures involving a combination of two hands positions (in lap and holding a steering wheel) and two back support conditions (with vertical backrest and without), and three excitation magnitudes (0.25, 0.5 and 1 m/s^2 RMS). Damped free response tests of the skin-mounted trunk accelerometers were performed on every subject at each vertebral location to derive the frequency response correction functions so as to eliminate the effect of the skin-tissue on acquired data at the vertebral locations. The central values of the resulting tissue natural frequencies and damping ratios were in the range of 15-20 Hz and 0.51-0.62, respectively. It was also observed that misalignments of the trunk accelerometers from the basicentric axes induced considerable errors at the C7, T5 and L5 vertebrae. Consequently, appropriate mathematical corrections were performed on the transmissibility responses at all the trunk locations to derive the responses along the basi-centric coordinate system. The sensor at the C7 vertebral level showed the maximum orientation of around 35˚ comparable with other reported values. The corrected data were further utilised for

statistical analyses (ANOVA) with main factors including the back support condition, hands position and excitation magnitude, and the interactions among them. The results and inferences from the corrected biodynamic responses are presented and discussed in the Chapters 4 and 5.

4. Measured body segment vibration transmission properties and the influence of factors

4.1 Introduction

Characterising the behaviour of the seated human body exposed to whole-body vibration (WBV) has been of interest over the past five decades, from its first applications in defence sectors (Coermann, 1962) to the present issues of spinal disorders and low back pain (LBP) among the operators of heavy vehicles in various work environments (Hoy *et al.*, 2005; Bovenzi *et al.*, 2002). Considering the vibrating human body as a mechanical system, biodynamic functions such as the apparent mass (APMS) and seat to head acceleration transmissibility (STHT) have been experimentally derived to enhance knowledge of the human body's response to vibration (*e.g.*, Fairley and Griffin, 1989; Paddan and Griffin, 1998). Although both the APMS and STHT responses show a peak gain between 4 and 6 Hz for the seated human body exposed to vertical vibration, it has been argued that STHT may be more representative of multiple vibration modes of the upper body rather than a seat-pan driving-point response such as APMS (Wang *et al.*, 2006).

While the two biodynamic functions described above are derived from measurements at the seat or the head under laboratory vibration testing using human subjects, the majority of the vibration-related health disorders at the workplace have been noted in the lower regions of the machine operators' back (Hoy *et al.*, 2005; Bovenzi *et al.*, 2002). It is widely believed that the high incidences of LBP and spinal disorders among the vibration-exposed working population could be attributed to local effects in the musculoskeletal spine (Wilder and Pope, 1996), which may not be sufficiently

reflected by the 'global' force or acceleration measurements at the extreme end points alone. Additionally, target datasets based only on the APMS and/or STHT functions have proven inadequate for the development and verification of analytical bio-models capable of depicting multiple vibration modes of the human body (Fairley and Griffin, 1989; Rakheja *et al.*, 2006; Boileau *et al.*, 2002).

The characterisation of responses at various segments of the human body in the seated condition is thus crucial for better understanding of the potential mechanisms that may induce LBP. However, the multiple contributing factors and sources of errors have led to wide variability among the reported body-segment vibration data (see Section 2.5). Moreover, the reported studies may not be directly comparable with each other since these have employed widely varying experimental conditions. While most of the studies that measure body-segment vibration were conducted with subjects seated on a flat seat pan with no consideration of the back support condition and with hands resting on the thighs or in the lap, a typical mobile-machinery driving posture may include a backrest and the hands supports. A few studies have suggested important influences of the back support and hands position on the measured force-motion biodynamic responses (Wang *et al.*, 2006; Mandapuram *et al.*, 2005). Even fewer studies have commented on such postural effects on the vibration transmitted to the spine (*e.g.*, Magnusson *et al.*, 1993, El-Khatib *et al.*, 1998). A thorough study of the effects of significant independent factors including seating and postural conditions representative of the work environment, on the vibration transmitted to vertebral locations is thus vital for identifying the roles of such factors in view of the potential injury effects.

In this chapter, the transmission of vertical seat vibration through the spine to the head of the seated body measured along the fore-aft and vertical axes are presented. The

experimental procedures have been elaborated in Chapter 3. The acquired driving-point responses at the seat and the backrest in terms of APMS are discussed in the subsequent chapter, since the main focus of this study is the vibration transmission "through the body." The measurements were performed on 12 male seated subjects using miniature accelerometers attached on the skin at locations over the spinous processes of selected vertebrae and at the head. The inter-subject variability of the measured data are analysed with respect to the postural conditions and the input vibration magnitude. Subsequently, the mean data are used to illustrate the effects of support conditions and input excitation level on the transmitted vibration. The level of significance of these independent parameters on segmental acceleration transmissibility is further analysed through statistical multi-factorial analysis of variance (ANOVA). Finally, the measured body segment responses are compared with the corresponding datasets reported by localised body measurements.

4.2   Characteristics of vibration transmitted to body segments

While a number of studies have reported vertical vibration transmitted to various locations of the body (Tables 2-2 and 2-3), only a few have been performed with postural and seating conditions representative of the work environment, especially using a backrest (*e.g.*, Magnusson *et al.*, 1993; El-Khatib *et al.*, 1998). The backrest and hands position are known to significantly affect the driving-point and head responses of the human body exposed to vertical vibration (*e.g.*, Wang *et al.*, 2006). A thorough study of the effects of significant independent factors including seating and postural conditions representative of the work environment, on the vibration transmitted to vertebral locations is thus vital for identifying the roles of such factors in view of the potential injury effects.

As mentioned earlier in Section 3.2.2, the test matrix employed in this study comprises a total of 12 test conditions for each subject, due to a combination of three input vibration levels, two back conditions and two hands positions. Additionally, three trials of each experimental measurement were performed in each condition so as to ensure reliability of the measurements. For every subject, the three trials for a particular response function, say vertical STHT, were examined so as to identify any major differences among them. A particular trial judged as an outlier was subsequently removed from the dataset, and the average computed from the remaining trials was then considered as representative of the corresponding response and utilised for further data analyses. The trials generally revealed very good repeatability, while the maximum intra-subject variability was below 20%, attributable to the care taken by the experimenters in monitoring the seating conditions during data acquisition, and the sufficient rest periods provided to the subjects between trials. The trial-averaged responses acquired for each subject were corrected for skin effects using the inverse transfer function approach, described in Section 3.3.2, which was established for each location for each individual. The data were then corrected for the sensor orientation error, as enumerated in Section 3.3.3. The means of the corrected data obtained across the test subjects were subsequently analysed to evaluate the segmental transmissibility responses and major influencing factors. These discussions and further analyses, described in Chapter 5, lead towards the ultimate goal of extracting target response datasets for the 50th percentile male human body for the development of multi-body biodynamic human models.

The measured vibration transmissibility responses revealed considerable scatter in the data in the entire frequency range, while the peak magnitudes generally occurred within relatively narrow frequency bands. As an example, Fig. 4-1 illustrates the trial-

averaged, vertical, $T_{SZ}(j\omega)$, and fore-aft, $T_{SX}(j\omega)$, vibration transmissibility response magnitudes corrected for the skin effect and sensor misalignment at the measured body locations of the 12 subjects sitting in the L-NB posture (hands in lap and no back support) and exposed to 1 m/s² vertical random base excitation. Although this is the most widely reported posture in the reported studies on localised vibration measurements (see Tables 2-2 and 2-3), the discussions in the following sections are not limited to these conditions alone. The results illustrated in Fig. 4-1 show consistent trends in the magnitude responses at all the locations. With the exception of the fore-aft transmissibility at the head and C7, and vertical transmissibility at T5 and L5, the responses generally show relatively smaller inter-subject variability. Such dispersions are attributable to a number of contributory factors such as subject anthropometry, variations in the sitting posture, involuntary movements and the individual's physical state. Additionally, a few candidates showed markedly different trends from the other test subjects at some of the body segments. For example, in Fig. 4-1, the fore-aft responses at the C7 vertebrae of subjects 4 and 6, and the vertical transmissibility to L3 and L5 of subjects 8 and 11, differed considerably from those of the remaining population. Such differences caused noticeable changes to the corresponding standard deviation (SD) errors about the mean responses of the population. While the SD error of the peak C7 fore-aft response magnitude around 5.4 Hz for the population was 0.57 (L-NB posture), the corresponding magnitude of subject 4 was found to be 0.32, close to two times the SD error. Such anomalies were addressed by considering these subjects as outliers and removing the respective magnitude and phase responses from the particular dataset. It should be noted that this procedure was adopted taking into consideration the transmissibility magnitudes only, since the vertical phase responses showed relatively less scatter below 10 Hz, as

could be observed further in Fig. 4-3. Additionally, the vertical phase responses alone are presented in this study due to the excessive scatter and fluctuations observed in the fore-aft transmissibility phase at almost all the locations, especially in the lower frequency range of 1 to 4 Hz. The mean and standard deviations were thus computed across the subjects for the vertical transmissibility magnitude and phase, and the fore-aft response magnitude at each measurement location and presented in Figs. 4-2 and 4-3 for the same excitation and postural conditions depicted in Fig. 4-1. While Fig. 4-2 illustrates the mean response magnitudes and SD (about the mean) for body-segment acceleration transmissibility in the vertical and for-aft axes, Fig. 4-3 presents the vertical transmissibility phase.

In the L-NB posture, the peak magnitudes in vertical vibration transmissibility at all the body locations tend to occur in the narrow frequency band of 4 to 6 Hz (Figs. 4-1 and 4-2) when exposed to random vertical vibration of 1 m/s^2 RMS. A second peak is also discernible in this posture in the range of 7-12 Hz in the vertical transmissibility responses of the head, T12, L3 and L5 for most of the subjects, although this peak is far more pronounced at L5, both in individual subject data as well as in the mean curves. Three of the subjects' responses revealed significantly lower magnitude of the secondary peak around 10 Hz at the L5 level (Fig. 4-1), which contributed to high dispersion of the data in this frequency range, as seen in Fig. 4-2. The fore-aft vibration responses of the body segments show varying trends across the measured locations. While the data presented in Figs. 4-1 and 4-2 clearly show peaks in the fore-aft vibration transmission to the head and C7 for most subjects between 5 and 6 Hz, such characteristics are not distinctly observable in the fore-aft axis at other locations in the L-NB posture. Insignificant fore-aft motion is noticeable at the T5 in the entire frequency range for

subjects seated without the back support (Figs. 4-1 and 4-2). The mean fore-aft transmissibility of L5 in the L-NB posture (Figs. 4-2) shows three slight peaks around 3, 7.5 and 13 Hz. Interestingly, the mean fore-aft magnitude curves for both the head and L5 seem to show a clear characteristic peak at 3 Hz in the absence of a backrest, although their respective magnitudes are considerably different. Additionally, the magnitude of SD error noticed in the head is significantly lower than that at the L5. Wide variability among the subjects' data is also evident in the L5 transmissibility phase presented in Fig. 4-3. In order to ensure greater confidence in the measured data and the averaging process, the inter-subject variability in the transmissibility data are thus further investigated in the subsequent sub-section before utilising the mean data for analysing the effects of the different experimental conditions.

4.2.1 Inter-subject variability

The reported responses on localised vibration transmissibility measured from different subjects under similar postural conditions have typically exhibited greater variability when compared to the driving-point APMS (*e.g.*, Matsumoto and Griffin, 1998). While the reasons for these variations are as yet not quantified, it is widely believed that the intervention of the back musculature under WBV may play a significant role in introducing such non-linearities in the segmental responses (Seidel, 2005). However, due to the difficulties associated with measurement of muscle activity under WBV, this study discusses the variability in the measured segmental vibration responses and the influence of support conditions and the excitation magnitude on the same.
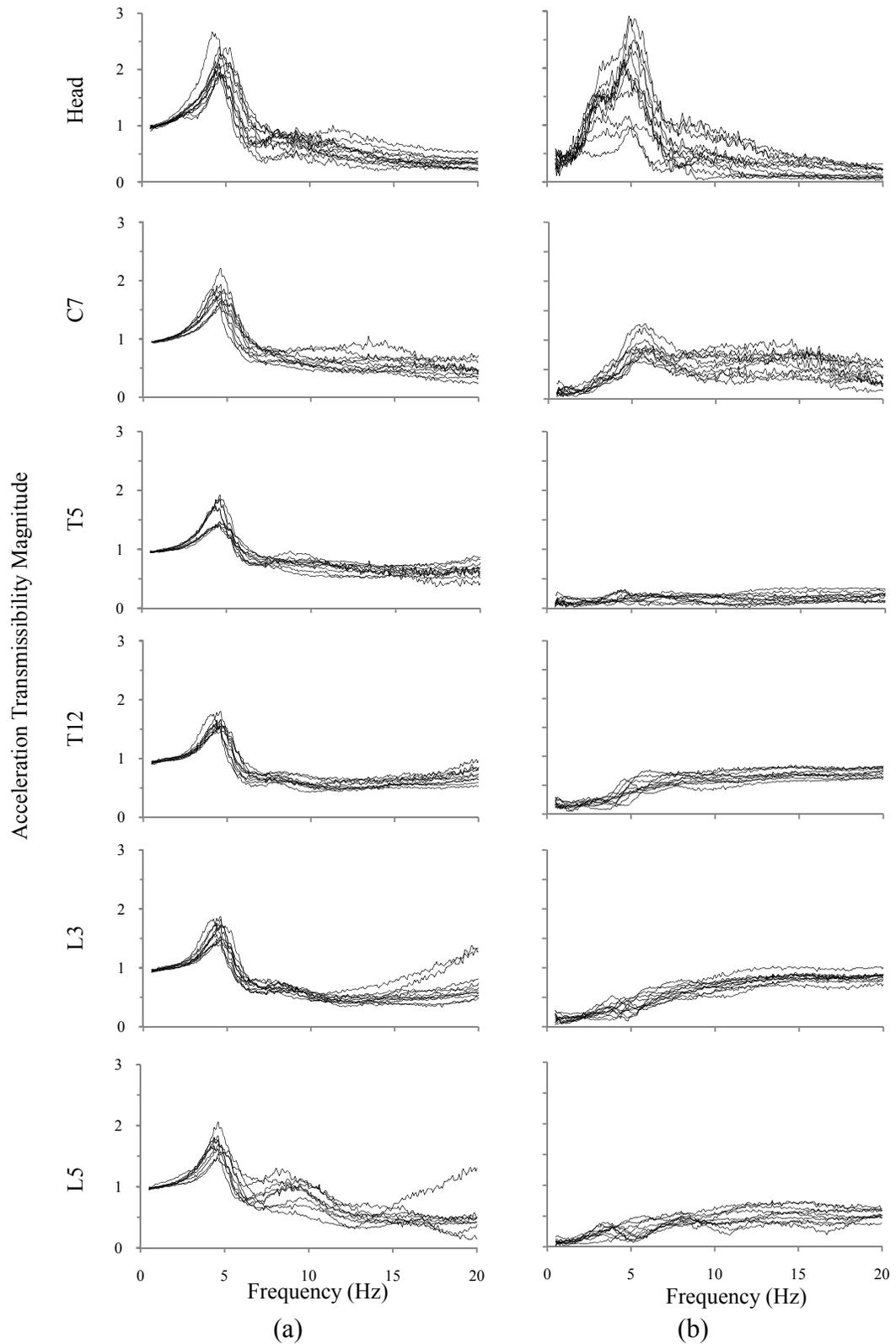
Figure 4-1: (a) Vertical and (b) fore-aft acceleration transmissibility magnitudes measured at different locations of 12 male subjects seated in the L-NB posture and exposed to 1 m/s^2 random vertical vibration. (L-NB: Hands in lap and no back support)
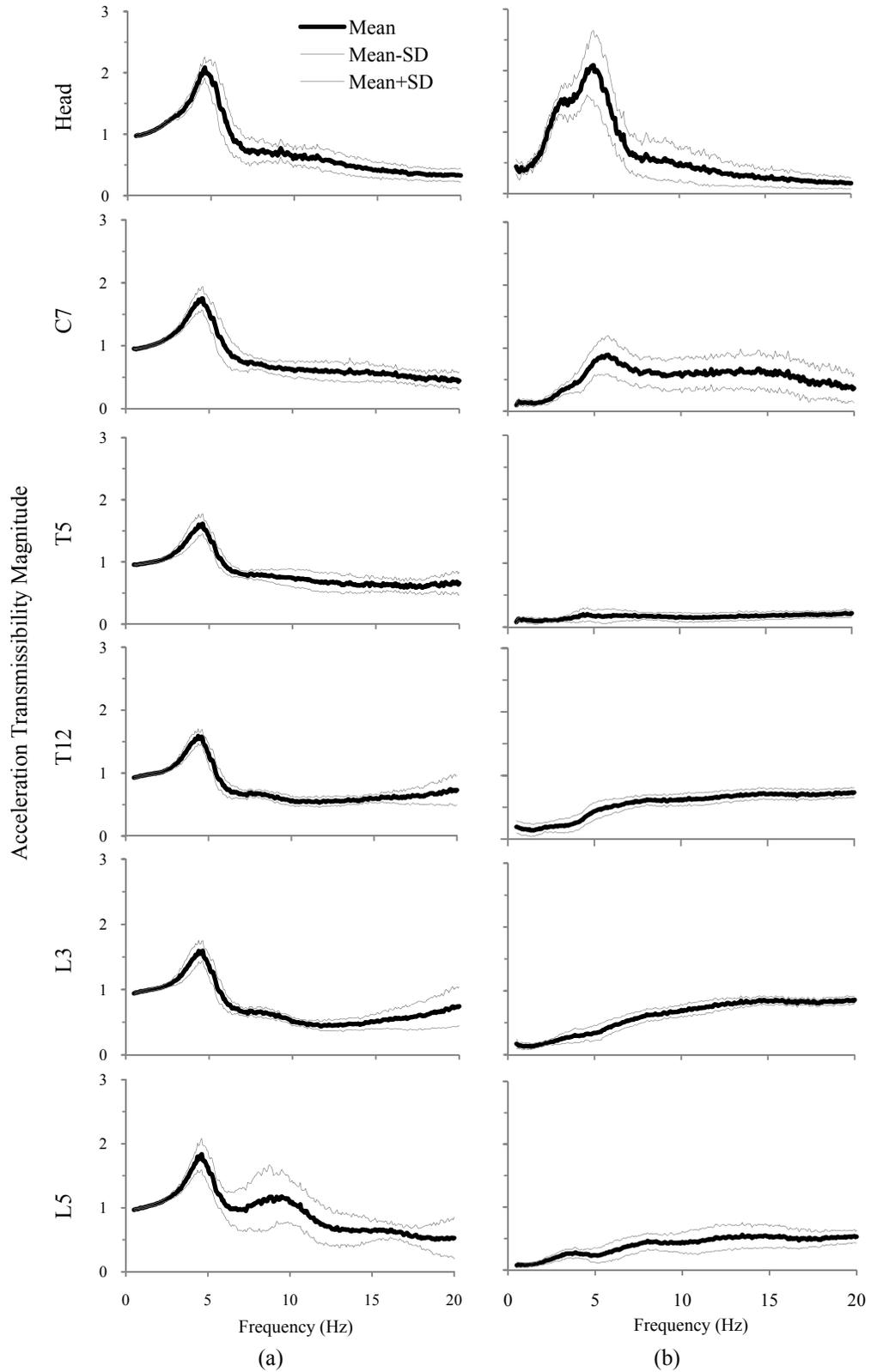
Figure 4-2: Mean and standard deviation of acceleration transmissibility magnitudes at measured body locations across 12 subjects seated in the L-NB posture and exposed to 1 m/s^2 vertical excitation: (a) vertical; and (b) fore-aft transmissibility magnitudes.
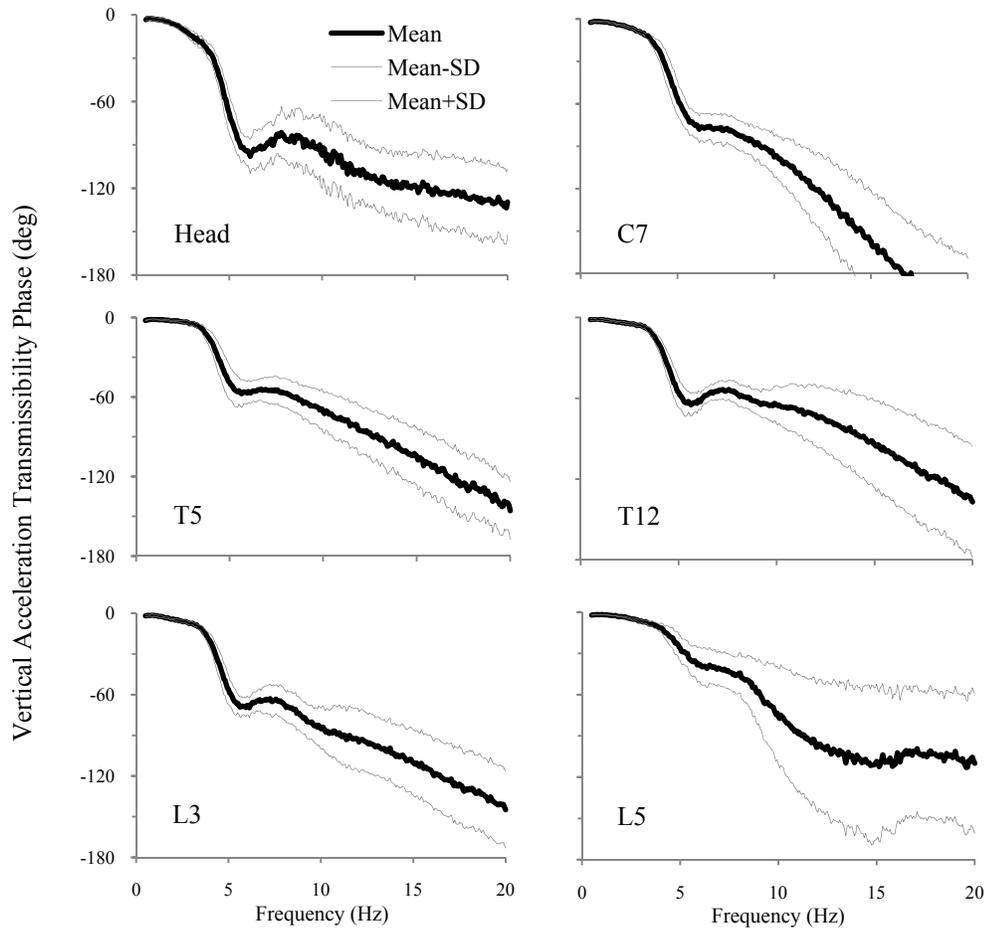
Figure 4-3: Mean and standard deviation of vertical acceleration transmissibility phase (degrees) at measured body locations across 12 subjects seated in the L-NB posture and exposed to 1 m/s^2 vertical excitation.

The standard deviations about the mean vertical phase responses shown in Fig. 4-3 depict a relatively small degree of scatter below 10 Hz, while the corresponding coefficients of variation (CoV) were in the order of 20% for all locations with the exception of the L5. This is suggestive of similarities in the damping properties of the spinal structures primarily due to the non-activated ligaments, inter-vertebral discs and skeletal structures. The highest scatter with CoV in the order of 40% was observed in the fore-aft response magnitude of the head for all postures in the frequency range of 3-8 Hz.

The reported STHT acceleration transmissibility data also show excessive variations in the fore-aft axis, which may be attributed to involuntary head motion (Paddan and Griffin, 1998; Wang *et al.*, 2006a). Additionally, wider scatter has been reported with lower magnitudes of excitation in the driving-point, STHT and segmental vibration responses attributable to the highly non-linear behaviour of the back muscles with lower vibration inputs (Paddan and Griffin, 1998). In this study, although wider scatter was observed at all the measured locations with lower levels of vibration (0.25 and 0.5 m/s^2), the postural conditions showed greater effects on the nature of vibration transmitted to the body segments. Hence, the transmissibility responses measured under vertical seat vibration 1 m/s^2 are mostly used to discuss the inter-subject variability in this section.

The scatter in the transmissibility magnitudes in all the postures were generally considerably less in the vertical axis when compared to the fore-aft responses of the trunk segments, except at L5, which may be caused by variations in the muscle tension of the subjects, apart from differences in their body build. While the change in posture strongly influenced the variability among the vertical responses of subjects primarily at L3 and L5, the dispersion in horizontal vibration transmissibility to all the segments was observably affected by the back support condition and in certain cases additionally by the hands position. Significantly greater inter-subject variability (maximum CoV: 50%) was obtained in the data acquired with backrest contact postures in the vertical magnitude responses at L3 and L5 between 4 and 12 Hz. In the same frequency range, the dispersion in the horizontal vertebral vibration transmission magnitude was greater with the back support. This trend has also been reported in the vertical STHT responses of subjects seated with a back support (Wang *et al.*, 2006). The higher level of variability in the vertical responses with back support is attributable to variations in the contact area of the

upper body with the back support. Backrest interaction also yields an additional source of vibration to the upper body, which probably contributed to higher magnitudes of the fore-aft transmissibility.

Overall, greater inter-subject variability was observed around the primary resonance characteristic in both the vertical and horizontal vibration transmissibility magnitudes at most locations. However, the highest dispersions were observed in the fore-aft motion at the head and C7, and the vertical transmissibility to L5 in all the postures. Matsumoto and Griffin (1998), under the L-NB posture, also reported large inter-subject variability in the horizontal axis at the head and hypothesised that it may be due to the relatively unconstrained motion of the head-neck complex under vertical excitation. To illustrate the effect of the seating conditions on the scatter in the measured body segment vibration data, the mean and SD (about the mean) of vertical and fore-aft transmissibility magnitudes of selected body segments are, respectively, illustrated in Figs. 4-4 and 4-5 for the four sitting postures, *i.e.* L-B, L-NB, SW-B and SW-NB, under 1 m/s^2 seat excitation. The body locations showing the greatest data scatter are alone considered here for exemplifying and discussing the inter-subject variability. The figures show the transmissibility magnitudes in the vertical axis at the C7, L3 and L5 (Fig. 4-4), and the fore-aft axis at the head, C7 and T5 (Fig. 4-5).

Except at L3 and L5, the back support tended to have insignificant effect on scatter in the vertical responses at all the measured body locations (Fig. 4-4). It is clearly evident from the figure that the responses at the lower torso segments may be extremely sensitive to the experimental conditions, especially in the presence of a backrest. In the vertical responses at L5, greater effect of the back support conditions on the inter-subject variability is noticed in the vicinity of the secondary peak around 8 Hz. The NB posture

reduces scatter considerably at both the peaks around 5 and 8 Hz. This may be attributable to a dominant compression-extension mode of vibration of the lumbar spine segments around 5 Hz, in the absence of a back support. The interaction of the backrest could alter the pelvic orientation differently in the subject population due to variations in anthropometry and posture. This may elicit different kinds of responses at the lower lumbar level leading to the higher dispersion in the data in the highly flexible lower lumbar region (Zimmermann and Cook, 1997).

In the fore-aft axis, both the back support condition and hands position significantly affected the dispersions in response magnitudes at the head and C7 (Fig. 4-5). For the fore-aft motion at the C7, the back supported sitting postures (L-B, SW-B) revealed greater deviations when compared to that observed in the response with no backrest contact (L-NB, SW-NB). Additionally, the placement of hands on the steering wheel (SW) reduced the variability in the fore-aft axis responses at the C7, irrespective of the back support condition (B, NB), particularly at frequencies below 10 Hz. The steering wheel is generally considered to introduce an additional source of vibration into the seated body. However, it may also be conceptualised as an additional musculoskeletal constraint for the upper thoracic region. This may elicit activity in the muscles of the hands and upper torso so as to stabilise the fore-aft motion of the body and thus reduce scatter in the horizontal response at C7.
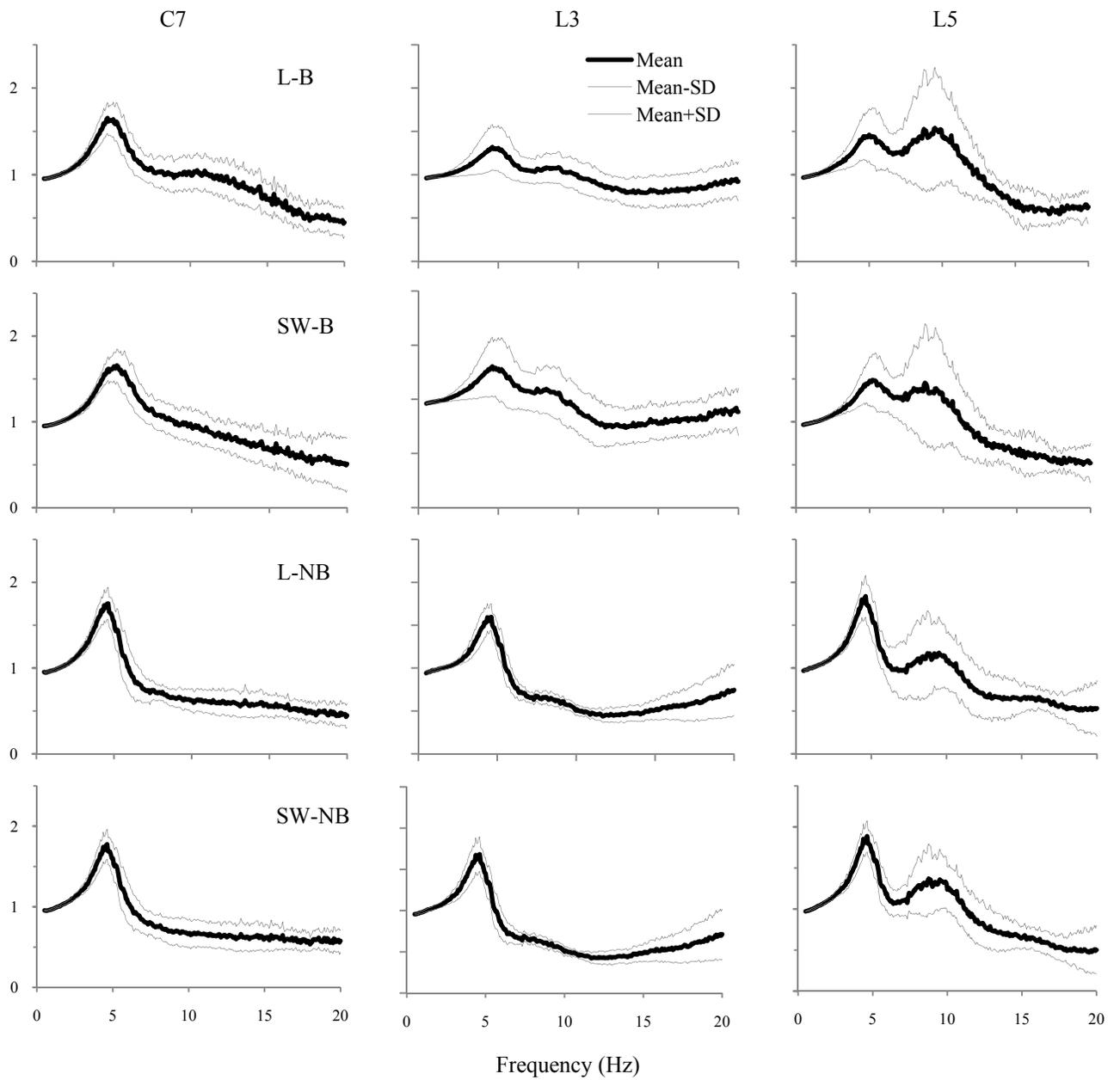
Figure 4-4: Influence of postural conditions on the inter-subject variability in vertical acceleration transmissibility magnitude at the C7, L3 and L5 under exposure to 1 m/s2 seat excitation. Postural conditions include L-B: Back supported (B) with hands in lap (L); SW-B: Back supported with hands on steering wheel (SW); L-NB: Hands in lap and no back support; SW-NB: Hands on SW and no back support.
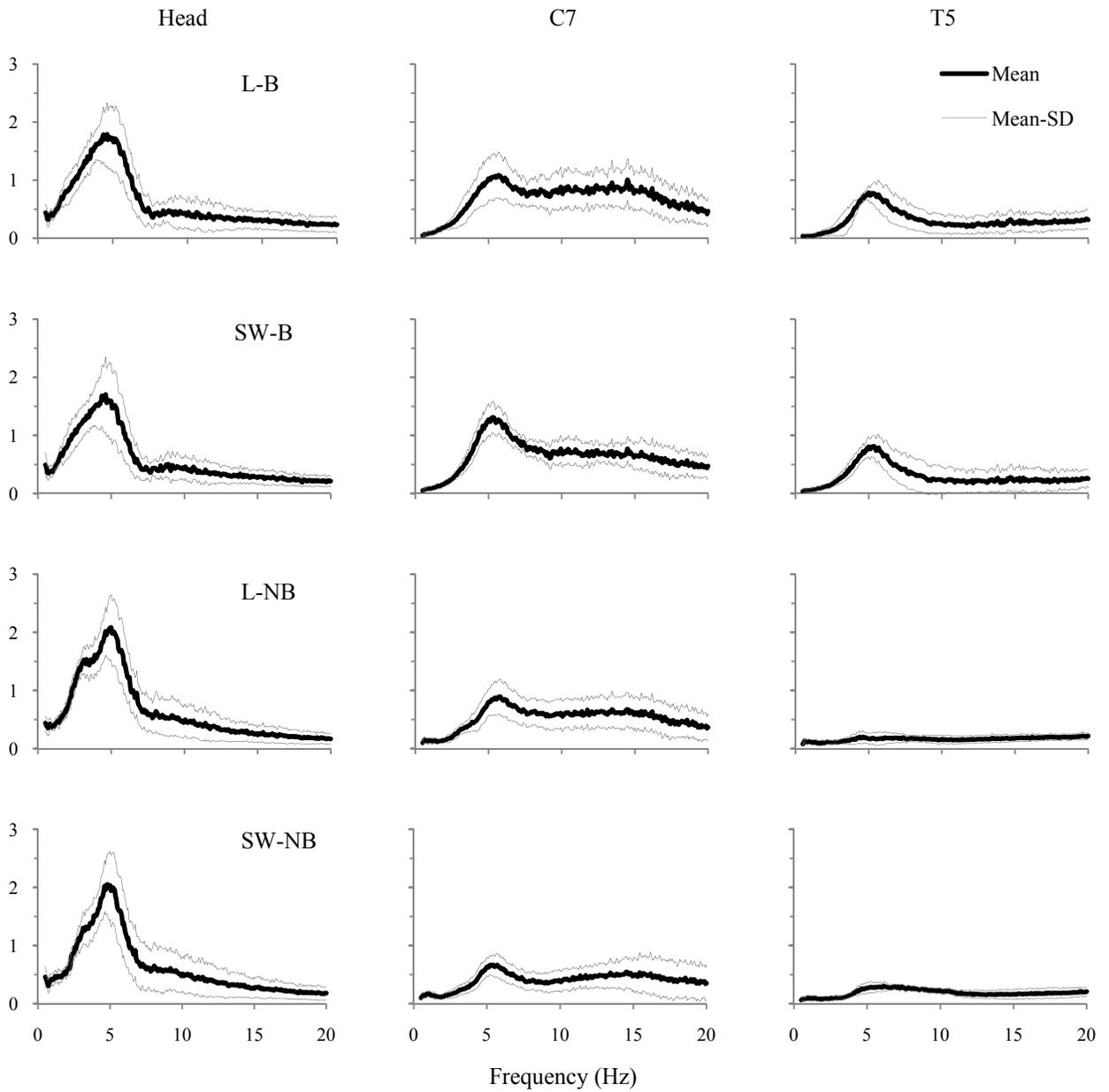
Figure 4-5: Influence of postural conditions on the inter-subject variability in fore-aft acceleration transmissibility magnitude at the Head, C7 and T5 under exposure to 1 m/s2 seat excitation. Postural conditions include L-B: Back supported (B) with hands in lap (L); SW-B: Back supported with hands on steering wheel (SW); L-NB: Hands in lap and no back support; SW-NB: Hands on SW and no back support.

The discussions above suggest significant effects of the support conditions on the nature of vibration transmitted to various segments of the human body, which are additionally sensitive to other independent parameters such as subject characteristics and excitation conditions. Since the subject pool was mostly restricted within a narrow body mass and height range representative of the 50th percentile male human body, the influence of postural and excitation conditions employed in this study are first examined in this chapter, using the mean measured body segment transmissibility data. However, owing to the considerable scatter in the measured data at certain locations, caution should be exercised in employing segmental responses for the assessment of vibration transmission through the body and for the development of analytical human models.

4.3   Effects of support conditions on vibration transmission properties

While most studies reporting the motion of localised body-segments under seated WBV have been performed with subjects sitting on a flat seat pan with no consideration of the back support condition, usually with hands resting on the lap, a typical mobile-machinery driving posture may include a backrest and the hands supports. The magnitudes of normal forces measured at the backrest under vertical vibration suggest a fore-aft motion of the upper body in the primary resonance region around 5 Hz. Additionally, significant effects of the back support conditions and hands position have been reported on the vertical seat APMS, and vertical and fore-aft STHT functions (Wang, 2006), suggestive of changes in body motions in the trunk segments due to these support conditions. The body segment acceleration transmissibility responses measured and averaged across the subjects in this study are thus examined to identify the influences of support conditions on the vibration transmitted to the selected locations. Figure 4-6 illustrates comparisons of the mean body-segment vertical and fore-aft acceleration

transmissibility magnitudes corresponding to the four sitting postures, *viz.*, L-B, L-NB, SW-B and SW-NB, assumed by the subjects exposed to 1 m/s^2 vertical vibration. The results clearly show that the back support has significant influence on the vibration transmission properties through the upper body. This influence is pronounced in the vertical vibration transmitted to all the body-segments, while the effect on the fore-aft responses measured at the lower regions of the torso, namely T12, L3 and L5, are notable generally below 5 Hz. The influence of the hands position is generally relatively small, although the effect is quite important in the fore-aft motion at C7 and vertical L5 movements. The results show that the use of a back support tends to slightly reduce the fore-aft transmissibility to the head, while the peak fore-aft responses at the C7 and T5 vertebrae increase considerably. A secondary mode around 3 Hz is also evident in the horizontal transmissibility to the head while seated assuming the L-NB posture, which seems to be slightly attenuated when the hands are supported by the steering wheel (SW). However, this mode is neither observed in the fore-aft head motion with a back support nor in the vertical responses at all the other segments.

Interestingly, all the four postures show considerably different fore-aft vibration tendencies at the C7 level. Backrest contact increases the peak fore-aft transmissibility magnitude at the C7 around 6 Hz, which tends to be lower with hands in lap compared to the hands holding the steering wheel. An opposite effect of hands position on the fore-aft vibration at C7 is observed when the back is not supported, which tends to considerably lower the peak fore-aft magnitude at this location. The fore-aft response at C7 also reveals a broad secondary peak around 15 Hz, irrespective of the support condition.
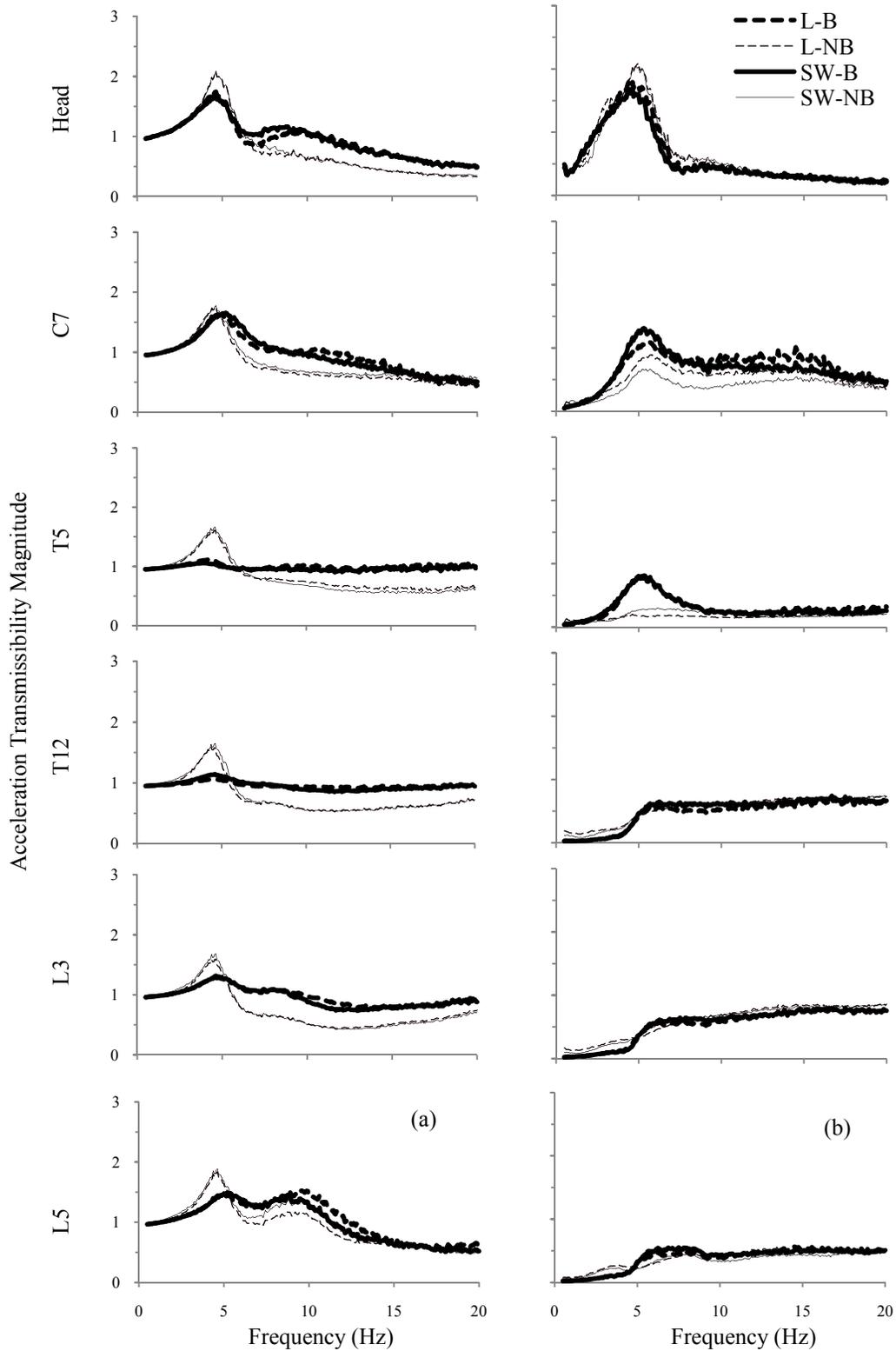
Figure 4-6: Influences of back and hands supports on the mean transmissibility magnitudes measured at the body segments under 1 m/s² vertical excitation. (L-B: Back supported with hands in lap; SW-B: Back supported with hands on steering wheel (SW); L-NB: Hands in lap and no back support; SW-NB: Hands on SW): (a) vertical; and (b) fore-aft axis.

Although the reasons for this phenomenon at the C7 may not be deducible from the measured data alone, it may be hypothesised that the backrest contact and the associated additional vibration input may cause enhanced pitch of the upper body about the mid-thoracic region and lead to greater fore-aft motion at the lower cervical spine. Similarly, the constraint provided by the hands support (SW) could act as another source of vibration directly transmitted to the lower cervical region through the hands and shoulder, thus further amplifying the fore-aft vibration at the C7 in the presence of a back support. This argument is further corroborated by the significantly higher fore-aft motion at the T5 around the primary resonance frequency near 5 Hz. The fore-aft transmissibility magnitude at the T5 shows a distinct peak near 5.4 Hz in the back supported postures (L-B, SW-B), which is not clearly evident without backrest contact. The absence of such clear effects of the back support in the fore-aft responses at the lower body locations (T12 and L3) suggest the amplification of a pitch or shear mode about the lower thoracic spine due to a back support.

Slight effects of the back support are also observable in the fore-aft motion at L5 in the 3-8 Hz frequency range. The horizontal responses at L5 display noticeable peaks near 3 and 8 Hz when seated without a back support, while the peak around 3 Hz is generally suppressed with backrest contact. The bandwidth of the second peak in the fore-aft motion at L5 (around 8 Hz), however, increases with the back support. Overall, the fore-aft transmissibility responses tend to display a slight shear/pitch mode around 5 Hz in the lower lumbar region probably due to pelvic pitch (Zimmermann and Cook, 1997) that is transmitted up towards the lower thoracic spine. The intervention of the backrest tends to significantly affect fore-aft motion above T12, hypothesised here as the amplification of a pitch mode about this spine region. Furthermore, the hands supports

significantly affect the head-neck fore-aft motion by introducing an additional source of vibration at the steering wheel.

In Fig. 4-6, it is seen that the back support tends to reduce peak transmission magnitude along the vertical axis to all the segments near the primary resonance frequency around 5 Hz. This most significant effect of the backrest is seen in the responses at T5, T12, L3 and L5. While the vibration characteristics at the thoracic and L3 locations may be partly attributed to isolation of the accelerometers from the bony spinous processes due to stretching of the local skin surface due to backrest contact, the sensor at L5 was generally not in contact with the backrest in most subjects. However, due to the absence of any comparable WBV response studies under similar back support conditions (El-Khatib *et al.*, 1998; Magnusson *et al.*, 1993), it is difficult to conclusively state the effect of the back support on the vertical responses at T5, T12 and L3. The backrest amplifies a significant secondary vertical magnitude peak around 9 Hz at the head and L5, and in the 10-15 Hz frequency range at C7. As mentioned earlier, in the back supported postures (L-B, SW-B), the C7 is not in direct contact with the backrest.

The back support also yields higher frequency corresponding to the peak vertical responses at C7, T12, L3 and L5, suggesting the stiffening of the human body in the vertical axis due to contact with a vertical backrest. The vertical vibration response at C7 exhibits noticeable shift (increase) in the primary resonant frequency with the back supported postures, while the corresponding peak magnitude change is insignificant. In addition, the back support tends to yield a broader vertical transmissibility peak at C7. The trends at the C7 suggest relatively greater damping effect due to backrest contact, which results in lower peak magnitude coupled with greater transmissibility at higher frequencies (up to 15 Hz). Furthermore, in the L-B posture a broad peak is also observed

in the vertical transmissibility at C7 around 12 Hz, somewhat similar to the corresponding fore-aft response in the range of 10-15 Hz, suggestive of coupled vertical and pitch motions.

The vertical transmissibility responses of the thoracic segments (T5 and T12) depict nearly unity magnitude over majority of the frequency range in the back supported postures (SW-B and L-B), which may be attributable to the aforementioned dynamics of the stretched skin at these accelerometer locations. This may not be attributable to adhesion of the measurement regions with the backrest, since the fore-aft responses shows significant peaks. Interestingly, the back support introduces a higher frequency secondary peak, around 9 Hz, in the vertical vibration at the lumbar region (L3 and L5) and the head. It may be observed that the vertical transmissibility peak magnitude at L5 around this frequency is comparable to that of the primary resonance peak around 5 Hz suggestive of the presence of two dominant modes of vibration in the lower lumbar-pelvic region in the presence of a vertical back support. Additionally, the vertical responses at the L5 reveal interesting contributions of the hands supports to the secondary mode around 9 Hz.

While the back support condition (B and NB) shows insignificant effects on the peak vertical L5 transmissibility around 9 Hz in the presence of a SW hand constraint, the hands in lap posture depicts considerable sensitivity to the back support conditions in this frequency range. The backrest tends to increase the magnitude of this second response peak considerably when compared to the NB condition with the hands placed on the lap. Although pelvic rotation was not measured in this study, it is believed that sacro-pelvic rotations in the sagittal plane under vertical excitations may influence the local dynamics of the lower lumbar region in the seated posture (Mansfield and Griffin, 2002).

Additionally, a number of analytical studies with multi-body biodynamic models have shown the presence a pelvic pitch mode around 10 Hz. The hands support in conjunction with the stiffening of the back musculature while holding the steering wheel may be constraining the subject's pelvic movements and thus limiting the induced motion in the L5 due to the sacro-pelvic pitch around 9 Hz, irrespective of the back support condition. However, with the hands placed on the lap, the reduced constraint on the pelvis may accentuate its effect on the lower lumbar region. In addition, contact with a backrest with the hands in lap (L-B) may be constraining only the upper body while the vertical movements in the lower lumbar region induced by the pelvic pitch may actually be greater, akin to the dynamic movement of a vibration absorber mass. These characteristics in the lower lumbar region may have significant concerns for potential injury in the associated biological tissue and need to be further investigated possibly by instrumentation of the pelvis (Zimmermann and Cook, 1997).

4.4   Effects of input vibration magnitude

Many studies have shown nonlinearity in the biodynamic responses due to varying excitation magnitudes. The exact nature of the non-linearity, however, may be difficult to establish due to the multiple influence factors including subject characteristics, postural and excitation conditions (Seidel, 2005). While the nature of the non-linearity arising due to the excitation magnitude has been mostly reported on the basis of the driving-point parameters such as APMS and DPMI, very few studies have systematically examined the effect of vibration magnitude on the nature of vibration transmission through the body (Wang, 2006, Matsumoto and Griffin, 2002).

The results obtained from this study also revealed noticeable influences of the excitation magnitude on the vertical and fore-aft vibration transmitted to most of the

measured body segments, insignificant effects were observed due to changes in vibration level in the fore-aft responses in the thoracic and lumbar locations. Figure 4-7 illustrates the mean vertical and fore-aft acceleration transmissibility of 12 subjects obtained under three different magnitudes of vertical vibration: 0.25, 0.5 and 1 m/s^2. Since most of the reported studies have been performed with subjects sitting erect without a backrest (Tables 2-2 and 2-3), the results in the figure also depict the measured segmental responses for the L-NB posture. The influence of input excitation is clearly identifiable in the vertical responses at all the body locations (Fig. 4-7a) and in the fore-aft axis for the head and C7 (Fig. 4-7b). The frequency corresponding to the primary magnitude peak (primary resonance) around 5 Hz for the aforementioned responses decreases with increase in the vibration magnitude. The vertical responses show relatively greater decrease in the primary resonant frequency when the excitation magnitude is increased from 0.25 to 0.5 m/s^2, compared to that observed when the seat vibration is increased from 0.5 to 1 m/s^2. Additionally a slight increase in peak vertical transmissibility magnitude due to higher excitation levels is observed in most of the segmental transmissibility responses.

A similar non-linear "softening" effect due to increase in the vertical excitation magnitude has been reported in a number of studies in both the seat APMS and vertical STHT responses (Mansfield, 2005; Mansfield and Griffin, 2000; Paddan and Griffin, 1998; Wang *et al.*, 2006). However, the magnitude of the secondary peak in the vertical vibration transmitted to L5, in the vicinity of 9-12 Hz, progressively decreases and the corresponding peak frequency also decreases with increasing vibration magnitude (Fig. 4-7a). This is suggestive of increase in damping in addition to the softening effect, most likely due to a localised vibration mode in the lower lumbar region, as discussed in

Section 4.3. The fore-aft responses at the head and C7 also reveal a similar effect with increase in excitation level (Fig. 4-7b). Additionally, a secondary peak in the fore-aft STHT responses around 3 Hz occurs more prominently under 0.25 and 0.5 m/s^2 excitation.

The non-linearity in the fore-aft responses, however, may be largely due to the changes in vibration-dependent muscle activity in the upper thoracic and cervical regions of the body (Blüthner *et al.*, 1995). It is interesting to note only minimal influence of the vibration level on the fore-aft transmissibility magnitudes at the thoracic and lumbar regions in the postures without a back support (L-NB and SW-NB). However, sitting with backrest contact (especially the SW-B posture), showed slight reduction in peak frequencies in the fore-aft responses at the thoracic and lumbar locations due to increase in vibration levels but with insignificant change in the corresponding peak magnitudes. These results strongly suggest that the human body responses to vertical vibration comprise coupled modes of vibration in the pitch-plane possibly including vertical extension-compression, shear and pitch rotations of the various spinal segments. In addition, the non-linearities in the segmental responses may arise due to a variety of reasons including the vibration-dependent muscular activity and the inherent mechanical properties of the biological tissue.
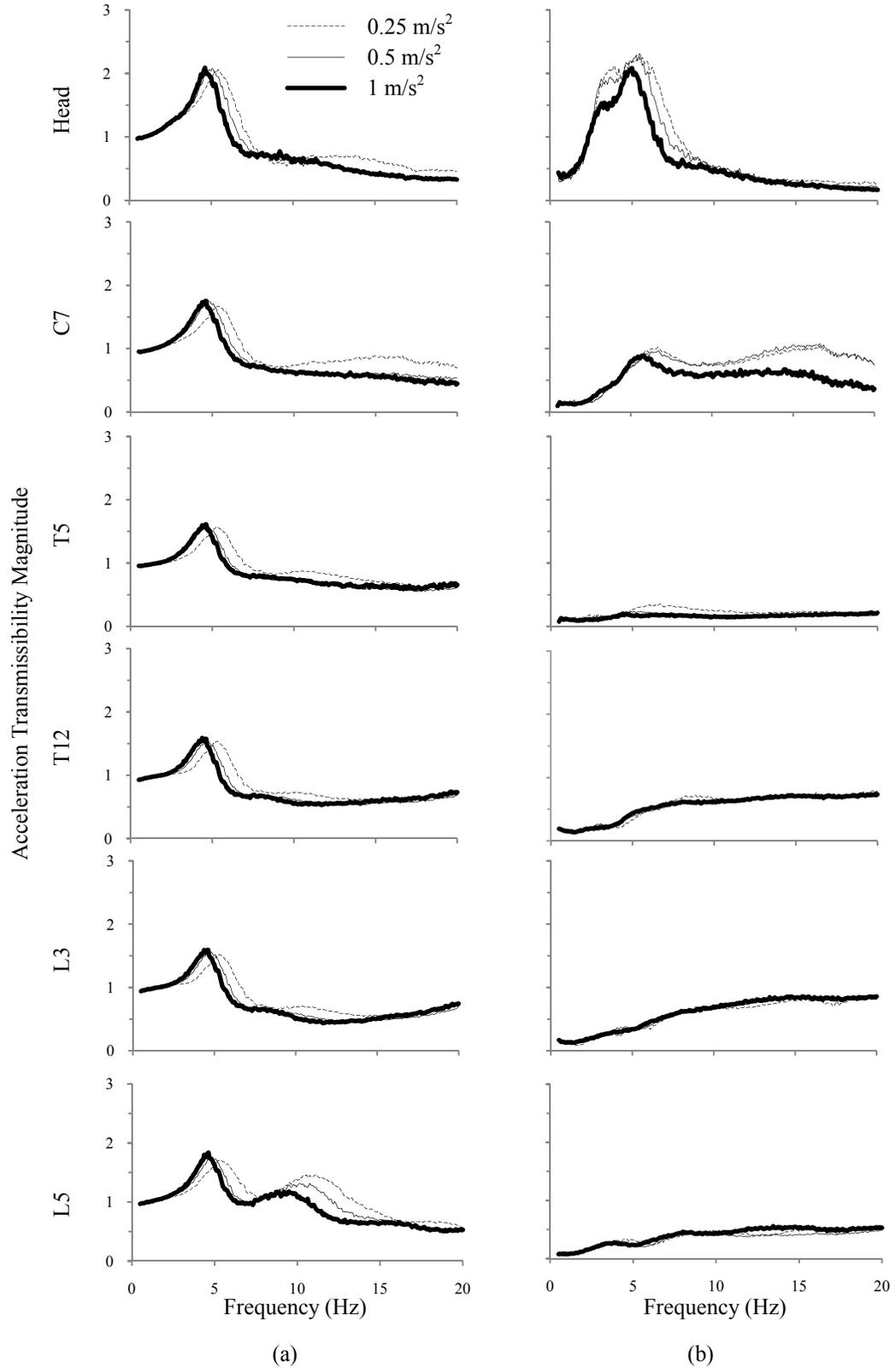
Figure 4-7: Influence of excitation magnitude on the mean (a) vertical and (b) fore-aft transmissibility magnitude measured at the body locations of 12 subjects seated in the L-NB posture.

4.5 Statistical significance of contributory factors on vibration transmission properties

The mean segmental responses in terms of vertical and fore-aft acceleration transmissibility at the measured body locations (Sections 4.3 and 4.4) depict a clear dependence on the support conditions and input vibration magnitude. However, the considerable scatter among subjects' data necessitates further analyses so as to establish validity of the averaging process and to gain confidence in the observed trends. Individual subject data at selected discrete frequencies are thus further analysed to study the statistical significance of the major influencing factors including the back support condition, hands position and the vibration magnitude. Tables 4-1 and 4-2 summarise the significance levels in terms of 'p' values obtained through multi-factorial ANOVA with factors including the back support condition and input excitation level, respectively, on the fore-aft and vertical transmissibility magnitudes at the measured locations for each hands position. A factor at a discrete frequency was considered to have statistically significant influence on the chosen response if its confidence interval was greater than 95% (*i.e.*, $p<0.05$).

The results presented in Table 4-1 suggest very strong influences ($p<0.001$) of the back support on fore-aft responses at C7 and T5 over almost the entire frequency range, irrespective of the hands position (L and SW). Similar influences are observed for frequencies below 5 Hz for the fore-aft transmissibility of T12, L3 and L5 ($p<0.001$). This is also evident from the mean fore-aft transmissibility magnitudes illustrated in Fig. 4-6b, particularly at frequencies below 4 Hz. Furthermore, the back support reveals strong statistical influence on the fore-aft motion of the head between 4 and 9 Hz, and the L5 lumbar vertebra in the frequency range of 5-10 Hz ($p<0.05$), which also correspond to

observable differences in the fore-aft transmissibility characteristics at the head and to some extent at the L5 due to the back support (Fig. 4-6b). The results obtained from statistical analyses of the postural conditions on the fore-aft vibration at the T12, L3 and L5 vertebrae, however, need to be interpreted with caution since the magnitudes of fore-aft motion are relatively low at these locations. Vertical vibration transmission to all the segments seems to be significantly affected in nearly the entire frequency range above 2.5 Hz by the back support condition ($p<0.05$), as seen in Table 4-1, especially with the subjects holding the steering wheel. This is further confirmed by the observed changes in vertical vibration transmission properties due to the back support, as shown in Fig. 4-6a. However, the statistical values illustrating the significance of back support on the vertical transmissibility at the thoracic (T5 and T12) and L3 vertebrae may be unreliable considering the wide variations in the responses corresponding to B and NB postures, which may in-part be attributable to possible isolation of the sensors from the bony spinous processes due to stretching of the local skin-surface in contact with the backrest (L-B, SW-B postures), as described in Section 4.3.

When compared to the back support condition, the hands position seems to have relatively less statistical influence on the vibration transmitted to the body segments in both the fore-aft and vertical axes. Further, effects of the hands support (SW) are observable with some consistency primarily on the fore-aft responses, as discussed in Section 4.3. The table of p values for the influence of hands position is thus omitted in this dissertation due to the minimal effects observed therein. Additionally, since the observed significances were mostly in the postures without a back support, the ANOVA results pertaining to horizontal transmissibility in the NB posture alone are discussed here. The analyses suggest strong influence of hands position on the fore-aft response at C7 in

the absence of a backrest (p<0.001). In corroboration, the mean horizontal responses of C7 (Fig. 4-6b) reveal the differences due to the Lap and SW hands positions at almost all frequencies above 3 Hz. The T5 fore-aft transmissibility, although of small magnitude in the NB postures, seems to be slightly greater above 5 Hz with hands holding the steering wheel. However, ANOVA results portraying a corresponding influence in the frequency range of 6-10 Hz (p<0.05) has to be treated with caution due to the very low magnitudes of fore-aft transmissibility at the T5. In the vertical axis, transmissibility to the L5 showed some influences in the frequency range of 8-14 Hz, that was also supported by the trends in the vertical vibration transmitted to this location (Fig. 4-6a).

The decrease in resonant (peak) frequencies of mean transmissibility responses at most of the measured body locations, particularly in the vertical axis, with increasing vibration level (Fig. 4-7) was further examined through the statistical analysis of the data acquired for individual subjects. The results summarised in Table 4-2 show that the fore-aft transmissibility magnitude is strongly affected by excitation magnitude at the head (p<0.001) and C7 (p<0.05) primarily in the frequency range above 5 Hz. However, this influence seems to be slightly greater at higher frequencies for the C7 for the hands-in-lap condition (p<0.05). Additionally, the results show that the fore-aft response at the head in the hands-in-lap posture is strongly affected by excitation magnitude near 2.5 and 4 Hz (p<0.05). This is also evident from the mean fore-aft vibration transmissibility of the head under exposure to a vibration magnitude of 0.25 m/s^2 (Fig. 4-7). Table 4-2 also depicts some influence (p<0.05) of input vibration levels on the fore-aft transmissibility responses at the T5, T12 and L5 generally around 5 Hz, with the hands holding the steering wheel. These results, however, could be considered relatively insignificant due to the very small differences observed in the transmissibility characteristics at these

locations with changes in the seat vibration levels (Fig. 4-7). On the other hand, strong influence of vibration magnitude ($p < 0.001$) is evidenced, in agreement with observed resonant frequency and magnitude shifts, in the range of 5-6 Hz for the vertical transmissibility at all the measured body locations in all the postures. Furthermore, the softening effects on the vertical transmissibility peaks, observed in Fig. 4-7 for the thoracic and lumbar vertebrae, seem to correlate well with the ANOVA results ($p < 0.001$) at 10 Hz for T12 and L3, and 12.5 Hz for L5 (Table 4-2).

The results of the statistical analyses suggest clear influence of both the back support condition and input excitation magnitude individually on the bi-dimensional motion of the upper body exposed to vertical seat vibration. The hands position, however, seems to exhibit discernible effects only in the fore-aft axis at the C7 and vertical response at L5, and especially while sitting erect with no backrest. Further, while the vibration level affects the primary resonance (peak) frequencies with some influence on the peak magnitude (in the vertical responses) of segmental vibration transmissibility, the back support considerably alters the vibration transmission properties "through the body." It may thus be hypothesised with a comfortable level of confidence that in order of importance for the understanding of body movements under vertical vibration, the back support condition assumes prime significance followed by the excitation magnitude and the hands position.

Table 4-1: ANOVA results in terms of 'p' values showing the influence of the backrest condition on fore-aft and vertical responses at various body locations (in both the hands positions)

Frequency (Hz)	Head	C7	T5	T12	L3	L5
Significance in terms of p values on Fore-aft acceleration transmissibility magnitude						
1	0.387	**0**	**0**	**0**	**0**	**0**
2.5	0.873	**0**	0.930	**0**	**0**	**0**
4	**0.033**	**0.001**	**0**	**0**	**0**	**0**
4.5	**0.044**	**0**	**0**	**0**	**0**	**0**
5	**0.022**	**0**	**0**	**0.010**	**0.019**	0.188
5.5	**0.028**	**0**	**0**	0.136	0.791	0.196
6	**0.039**	**0**	**0**	0.779	0.050	**0.003**
7.5	**0.022**	**0**	**0**	0.512	0.133	**0**
9	**0.034**	**0**	**0**	**0.010**	**0.018**	0.146
10	0.650	**0**	**0**	**0.048**	**0.033**	0.301
12.5	0.375	**0**	**0**	0.265	0.604	0.067
15	**0.004**	**0.040**	**0**	0.924	0.660	**0.014**
1	0.166	**0**	**0**	**0**	**0**	**0**
2.5	**0.000**	**0.002**	0.521	**0**	**0**	**0**
4	0.129	**0**	**0**	**0**	**0**	**0**
4.5	**0.020**	**0**	**0**	**0**	**0**	**0**
5	**0.003**	**0**	**0**	**0.009**	**0.001**	0.924
5.5	**0.004**	**0**	**0**	0.066	0.228	**0.025**
6	**0.012**	**0**	**0**	0.281	0.612	**0.001**
7.5	**0.015**	**0**	**0**	0.142	0.294	**0.001**
9	**0.014**	**0**	**0**	**0.016**	0.133	0.130
10	0.182	**0**	**0**	0.092	0.215	0.115
12.5	0.765	**0**	**0**	0.467	0.878	0.061
15	0.087	**0.041**	**0**	0.367	0.417	0.043
Significance in terms of p values on Vertical acceleration transmissibility magnitude						
1	0.871	0.220	0.054	0.514	0.989	**0.007**
2.5	**0**	**0.002**	**0**	**0**	**0.001**	**0.001**
4	0.411	**0.001**	**0**	**0**	**0**	**0**
4.5	**0**	**0**	**0**	**0**	**0**	**0**
5	**0**	0.116	**0**	**0**	**0**	**0.002**
5.5	**0.001**	0.095	**0**	**0**	0.382	0.377
6	**0.031**	**0**	**0.001**	0.985	**0.001**	**0**
7.5	0.072	**0**	**0**	**0**	**0**	**0**
9	**0**	**0**	**0**	**0**	**0**	**0**
10	**0**	**0**	**0**	**0**	**0**	**0**
12.5	**0**	**0**	**0**	**0**	**0**	**0**
15	**0**	**0**	**0**	**0**	**0**	**0.010**
1	0.468	0.273	0.150	**0**	**0.028**	**0.001**
2.5	**0**	**0.001**	**0**	**0**	**0**	**0**
4	0.115	**0**	**0**	**0**	**0**	**0**
4.5	**0**	**0**	**0**	**0**	**0**	**0**
5	**0**	**0.005**	**0**	**0**	**0**	**0.008**
5.5	**0**	0.325	**0**	**0**	**0.046**	0.217
6	**0**	**0**	**0**	**0**	0.053	**0**
7.5	**0.007**	**0**	**0**	**0**	**0**	**0**
9	**0**	**0**	**0**	**0**	**0**	**0**
10	**0**	**0**	**0**	**0**	**0**	**0**
12.5	**0**	**0**	**0**	**0**	**0**	**0**
15	**0**	0.404	**0**	**0**	**0**	**0.002**

Row group labels: "Hands in Lap" and "Hands on Steering Wheel" apply to the first and second 12-row blocks of the Fore-aft section, and to the first and second 12-row blocks of the Vertical section, respectively.

Table 4-2: ANOVA results in terms of 'p' values showing the influence of the excitation magnitude on fore-aft and vertical responses at various body locations

	Frequency (Hz)	Head	C7	T5	T12	L3	L5
Significance in terms of p values on Fore-aft acceleration transmissibility magnitude							
Hands in Lap	1	0.922	0.581	0.411	0.270	0.343	0.709
	2.5	**0.041**	0.197	0.570	0.520	0.091	0.871
	4	**0.016**	0.176	**0.028**	0.480	0.081	0.541
	4.5	0.361	0.348	0.321	0.331	0.639	0.102
	5	0.569	0.760	0.662	**0.036**	0.063	0.222
	5.5	**0.006**	0.175	0.119	0.057	**0.018**	0.108
	6	**0**	**0.005**	**0**	0.718	0.249	0.092
	7.5	**0**	**0**	**0**	0.582	0.978	0.893
	9	0.290	**0.005**	**0**	0.263	0.908	0.157
	10	0.653	**0.015**	**0**	0.638	0.774	0.204
	12.5	0.220	**0.010**	**0.002**	0.393	0.216	0.355
	15	**0.010**	**0.002**	**0.000**	0.177	0.201	0.253
Hands on Steering Wheel	1	0.740	0.774	0.984	0.417	0.858	**0.017**
	2.5	0.561	0.304	0.122	0.198	0.566	0.145
	4	0.604	**0.015**	**0**	0.617	0.603	0.464
	4.5	0.672	**0.018**	**0**	0.094	0.287	**0.004**
	5	0.877	0.119	**0.039**	**0.002**	**0.001**	0.070
	5.5	**0.003**	0.103	0.295	**0.003**	**0.000**	**0.036**
	6	**0**	**0.005**	**0.006**	0.407	**0.046**	0.437
	7.5	**0**	**0**	**0.001**	0.951	0.730	0.439
	9	0.350	**0.002**	**0**	0.820	0.993	**0.003**
	10	0.659	**0.009**	**0**	0.857	0.943	**0.010**
	12.5	0.071	0.139	**0**	0.597	0.496	0.988
	15	**0.005**	**0.030**	**0.001**	0.312	0.222	0.651
Significance in terms of p values on Vertical acceleration transmissibility magnitude							
Hands in Lap	1	**0.001**	0.076	0.541	0.872	0.550	0.816
	2.5	**0.034**	**0.001**	**0.008**	0.221	0.122	0.087
	4	**0.006**	**0**	**0.001**	**0**	**0**	**0**
	4.5	**0.001**	**0**	0.064	**0.004**	**0.010**	**0.002**
	5	0.528	0.167	0.418	0.069	0.735	0.453
	5.5	**0**	**0**	**0**	**0**	**0**	**0.008**
	6	**0**	**0**	**0**	**0**	**0**	**0**
	7.5	0.749	0.203	**0.001**	**0.048**	0.065	0.813
	9	0.211	0.992	0.098	**0.002**	**0.015**	0.699
	10	0.649	0.830	0.072	**0**	**0**	0.330
	12.5	**0**	**0.022**	**0.002**	0.165	**0.001**	**0**
	15	**0**	**0**	0.111	0.785	0.599	**0.032**
Hands on Steering Wheel	1	0.139	0.101	0.366	0.714	0.298	**0.019**
	2.5	0.116	**0.005**	0.092	0.174	0.141	**0.004**
	4	**0.020**	**0**	**0.008**	**0**	**0.001**	**0**
	4.5	0.067	**0**	0.151	**0.007**	**0.010**	**0**
	5	0.955	**0.043**	0.226	0.716	0.602	**0.006**
	5.5	**0**	**0.001**	**0**	**0**	**0.001**	**0.025**
	6	**0**	**0**	**0**	**0**	**0**	**0.004**
	7.5	0.810	0.260	**0.003**	**0.015**	0.070	0.889
	9	0.173	0.483	**0.029**	**0.001**	**0.003**	0.356
	10	**0.010**	0.739	**0.025**	**0**	**0**	0.149
	12.5	**0.001**	0.994	**0.017**	0.440	**0.002**	**0**
	15	**0**	0.910	0.128	0.924	0.705	**0.003**

4.6 Comparison of measured vibration transmissibility with reported data

When compared to established biodynamic responses such as driving-point APMS and vertical STHT, there are only a few studies on vibration transmission to the spine. The experimental conditions and responses of studies examining human body segment and spine vibration under vertical excitation on seats have been reviewed in Section 2.3 and summarised in Tables 2-1 to 2-3. It may be observed that most of these studies have been performed with subjects sitting in an erect posture without a backrest. However, the few experiments that included some form of a back support seem to show conflicting results. For example, while Magnusson *et al.* (1993) reported negligible change in vertical responses of the L3 due to a backrest, El-Khatib *et al.* (1998) showed significant contributions of a lumbar support to vertical vibration transmitted to the lower torso in the frequency range (around 5 Hz) of vertical resonance. The two studies employed considerably different experimental conditions ranging from shock inputs on human subjects to random vertical vibration of cadavers. Additionally, owing to the lack of sufficient published data in similar postures, the studies reporting body-segment response to vertical seat vibration with subjects sitting without a back support have been considered for comparison with the vertical response magnitudes measured in the L-NB posture in this study. In addition since most of the selected studies employed excitations of 1 m/s^2 or higher, the measured responses in this study corresponding to the highest random excitation level (1 m/s^2 RMS) are chosen for comparisons.

Figures 4-8 (a) and (b) illustrate the mean vertical transmissibility magnitudes measured at the T5 and L3, respectively, for the 12 subjects in this study under exposure to 1 m/s^2 random vibration in the L-NB posture, along with those reported in other comparable studies. The response curves from the published studies are denoted by their

152

first authors in the legends. Further, these studies have been specifically identified in Table 2-1 (Chapter 2) by the superscript (†). It should be noted that while all the response data presented in Fig. 4-8 were acquired with no backrest interaction, some reported experiments may have been performed with excitation levels, hands positions or subject body mass categories different from those considered in this study (see Table 2-1). These also include the vertical transmissibility measured at L3 of subjects seated on a cushioned seat (Pope *et al.*, 1989).

a.)   b.)
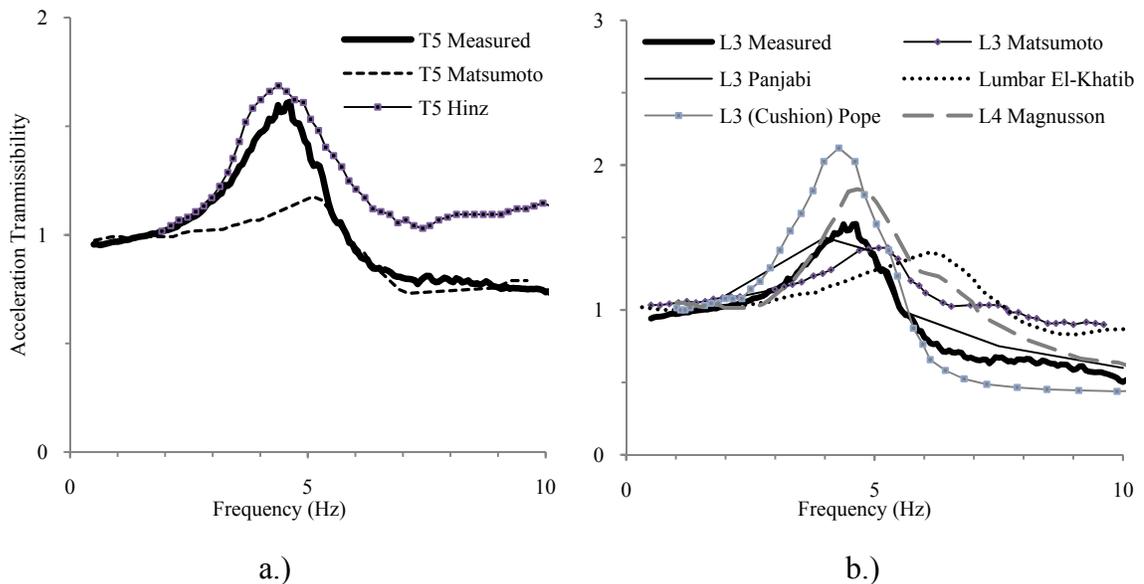
Figure 4-8: Comparison of mean measured vertical transmissibility responses at T5 and L3 with the reported data on vibration transmitted to the spine to the (a) thoracic, T5; and (b) lumbar region, L3 and L4.

Irrespective of the differences in the experimental conditions, the majority of the results indicate vertical resonance at the thoracic and lumbar regions of the spine in the narrow range of 4-5.5 Hz, except for the data acquired from the human cadaver study by El-Khatib *et al.*, (1998), which shows the peak frequency near 6 Hz (Fig. 4-8b). While there are acceptable differences in the vertical transmissibility at the T5 (Fig. 4-8a) in the

0.5-5 Hz range between the results of the present study and that reported by Hinz *et al.* (1987), the measured data in the same frequency range is considerably different from that reported by Matsumoto and Griffin (1998), which employed excitation conditions close to this study (1 m/s^2). Additionally, there are observable differences both in resonant frequency and peak magnitude between the transmissibility at L3 reported by Matsumoto and Griffin (1998) and this study. However, three of the five lumbar transmissibility datasets from the literature presented in Fig. 4-8b show peak magnitudes around 1.5 close that found in this study (Magnusson *et al*, 1994; Matsumoto and Griffin, 1998; Panjabi *et al*, 1986). Furthermore, the measured lumbar response shows good agreement with the invasive measurements of Panjabi *et al.* (1986), which employed sinusoidal excitation, and a good match in resonant frequencies with those reported by Magnusson *et al*, (1994) and Pope *et al.* (1989), although the latter study was performed on female subjects sitting on cushion seats and exposed to vertical shock motions. It is evident from the figures that further experimental efforts are needed to obtain sufficient numbers of comparable datasets so as to confidently characterise the multi-dimensional motion of the seated human body exposed to vibration for subsequent efforts in deriving reliable biodynamic models. Furthermore, owing to significant influences of the hands and back support conditions on the vibration transmission properties of the upper body, it may also be concluded that separate sets of segmental biodynamic functions need to be extracted for different postural conditions so as to identify the contributions of the specific independent parameters. The datasets thus obtained may then be utilised for comparisons across different research studies and as target functions for the development and validation of anthropometric bio-models for simulation and virtual testing.

4.7   Summary

This chapter presents the results of the WBV experiments in terms of vibration transmissibility in the fore-aft and vertical axes measured at selected vertebral locations on the trunk (C7, T5, T12, L3 and L5) and head of 12 male seated human subjects exposed to random vertical vibration. Independent factors including the hands position (hands placed on lap and gripping a steering wheel) and back support condition (vertical backrest and no backrest), and three different levels of input excitation magnitude (0.25, 0.5 and 1 m/s^2 RMS) were employed so as to study the influence of these factors on the body's responses. The mean body-segment responses of the twelve subjects depicted a clear dependence on the support conditions, particularly on the back support condition.

The effect of input vibration magnitude was also significant but relatively weaker than that of the backrest. The vertical back support tends to either reduce or have insignificant effect on the scatter in the vertical vibration transmissibility at all the measured locations. The backrest, however, induced greater deviations in the fore-aft responses, especially at the thoracic and lumbar locations. Additionally, hands holding the steering wheel tended to reduce the dispersions attributable to the introduction of an additional constraint on the vibrating human body. The back support resulted in greater attenuation of vibration in the vertical axis to all the measurement locations, while increasing the fore-aft transmissibility at C7 and T5. Additionally, statistical analyses of main factors including the back and hands support conditions, and excitation magnitude showed greater influence of the back support condition on the vertical transmissibility to all the segments, irrespective of the hands position. The hands support condition generally showed a relatively smaller effect; but hands holding the steering wheel increased peak vertical response magnitude at C7 and L5. However, the results also

155

suggested a strong influence of the hands position on the fore-aft response at C7 in the absence of a backrest. The decrease in resonant frequencies ("softening") with increasing excitation magnitude, usually reported for the APMS and STHT functions, was also observed in the measured vertical transmissibility data at all the segments of the upper body, while the effect on the fore-aft responses was seen only at the head and C7.

The results and analyses suggest that in order of importance for the understanding of body movements under vertical vibration, the effects of the back support condition assume prime significance followed by the excitation magnitude and the hands position. Owing to the significant influences of these parameters on the vibration transmission properties of the upper body, it may also be concluded that separate sets of segmental biodynamic functions need to be identified for different postural conditions so as to represent the unique contribution of the specific independent parameters. The datasets thus obtained may then be utilised as target functions for the development and validation of anthropometric bio-models for simulation and virtual testing.

5.   Identification of target datasets

5.1   Introduction

Although the epidemiological surveys have established a strong relationship between prolonged WBV exposure and the symptoms of low back pain (LBP) among the drivers of various vehicles (*e.g.*, Bovenzi and Beta, 1994; Schwarze *et al.*, 2002; Pope, 2005), it is not possible to conclude that WBV alone is a major contributing factor to LBP (Lings and Leboeuf-Yde, 2000). Consequently, one of the multi-facetted approaches to understanding the effects of workplace vibration on human health and discomfort has been through controlled experimental studies of test subjects exposed to WBV. Such experiments have mostly focussed on acquiring the biodynamic responses of the seated human body under WBV in terms of one or more of the following functions: (i) the force-motion frequency response at the body-seat interface in terms of apparent mass (APMS) or driving-point mechanical impedance (DPMI) (*e.g.*, Fairley and Griffin, 1989; Coermann, 1962); (ii) the acceleration transmissibility from the seat to the head (STHT) in a particular axis (Paddan and Griffin, 1998) (iii) transmission of seat vibration to different body segments (*e.g.*, Matsumoto and Griffin, 1998); and (iv) absorption of vibration power derived from the force-motion relations at the driving point (*e.g.*, Lundstrom and Holmlund, 1998). The measured biodynamic response data have provided valuable knowledge on resonance frequencies of the body and have been employed for deriving frequency-weightings for assessment of WBV exposure (Lundstrom and Holmlund, 1998; Rakheja *et al.*, 2008; Mansfield, 2005; ISO-2631-1, 1997). These measures, however, have not contributed to identification of potential injury risks of WBV.

The biodynamic models incorporating a biomechanical structure derived on the basis of the measured responses, on the other hand, could offer considerable potential to evaluate the injury risks due to WBV exposure. The effectiveness of a biodynamic model, however, strongly relies upon the type of biodynamic measure considered and its structure. A large number of lumped-parameter, multi-body dynamic and finite element models of the seated body have been developed, where the model parameters are identified using different measured biodynamic responses (*e.g.*, Boileau *et al.*, 1997; Seidel and Griffin, 2001). The APMS is the most widely used measure for deriving the biodynamic models due to the ease of its measurement, particularly for the lumped parameter models (*e.g.*, Wei and Griffin, 1998). However, lumped-parameter models generally lack the biomechanical structure and thus the responses cannot be interpreted in terms of dynamic loading and deflections of various joints and substructures. Furthermore, the models derived on the basis of the apparent mass alone may not yield reliable information on the deflections of the upper body segments. Some of the lumped-parameter and multi-body dynamic models have also employed the STHT biodynamic measure, either by itself (deCraeker, 2003) or in conjunction with the APMS (Wu, 1998; Kim *et al.*, 2005; Pranesh *et al.*, 2008). The STHT measure, however, has been applied in far fewer studies, partly due to very large inter-subject variability in the data and extreme differences among the data reported by various investigations (Paddan and Griffin, 1998).

While both the driving-point and head transmissibility responses are generally accepted as representative of the resonance behaviour of the vibrating whole human body, the majority of the related injuries in the workplace have been registered in the lower back region, specifically in the musculoskeletal spine (Bovenzi and Betta, 1994). The vertical APMS and STHT functions, being acquired at the seat interface and head,

respectively, may not fully account for the multidimensional movements of the intermediate structures of the seated upper body (Matsumoto and Griffin, 1998). The models with essential representations of the human body's subsystems are thus considered promising for identifying deflections and loading of various subsystems (Seidel and Griffin, 2001). Although a number of such complex bio-models with multiple DOF's have been developed, the majority have been validated primarily on the basis of the driving-point response functions (*e.g.*, Pankoke *et al.*, 1998; Seidel *et al.*, 2001). Such models could be significantly enhanced through consideration of additional responses of significant substructures, such as spine segments. Only a few studies, however, have reported the transmission of vertical WBV to different locations of the cervical, thoracic and lumbar spine, measured either by surgical and non-invasive techniques (Sandover, 1998; Seidel, 2005). Moreover, the extreme variabilities of the reported data limit their applicability for deriving reliable models. It is thus desirable to define responses of the critical substructures, which would facilitate the formulation of reliable multi-body or finite element models for predicting the deflections and dynamic loads imposed on the substructures of the joints.

This chapter presents target functions in different biodynamic measures acquired in a non-invasive manner so as to facilitate the development of reliable biodynamic models and further be useful for validation of the existing models. The measured biodynamic and vibration responses to vertical WBV are analysed to identify target functions applicable under particular postures considered. These include the apparent mass responses at the two driving-points (backrest and seat pan), and acceleration transmissibility to the measured segments of the human body in the fore-aft and vertical directions. The measured data are processed so as to analyse the significance of the major

contributing factors and to identify a minimal number of unique target datasets through statistical analysis.

5.1.1 Brief critical comments on the suitability of available biodynamic datasets

Apparent mass acquired at the body-seat interface is the most widely reported biodynamic response function due to its relative ease of measurement. Furthermore, it may be characterised using simplistic linear and lumped-parameter models, often with a single degree-of-freedom (DOF) (*e.g.*, Boileau *et al.*, 1997; Fairley and Griffin, 1989). The reported APMS data suggest a strong influence due to the body mass but relatively smaller effect of the vertical excitation magnitude (*e.g.*, Fairley and Griffin, 1989, Mansfield and Griffin, 2000; Mansfield, 2005; Patra *et al.*, 2008). The idealised ranges of APMS response of the seated body exposed to vertical WBV have been defined in the international standard: ISO 5982 (2001) on the basis of synthesis of the reported data under vibration levels up to 5 m/s^2. A three DOF lumped-parameter model has also been defined in the standard for possible applications in the coupled seat-operator system, and for development of physical mannequins for seat testing. Such analytical models and anthropodynamic dummies, however, have shown limited prospects due to non-linearities in the nature of body-seat interactions (Nélisse *et al.*, 2008). On the other hand, STHT has been argued to be more inclusive of the multiple modes of vibration of the human body (Wang *et al.*, 2006) and necessitates the incorporation of at least two DOF in a phenomenological model for the vertical axis (Boileau *et al.*, 1997). However, only limited success has been achieved in reliably representing the vertical head vibration properties through lumped-parameter models, especially in conjunction with the APMS. Additionally, larger variability, compared to the APMS responses, is observed in the measured STHT data due to its relatively higher sensitivity to measurement systems and

methods that are still evolving, and the possible unconstrained movements of the head-neck unit (Paddan and Griffin, 1998).

The primary resonance peaks in the seated body's APMS and STHT functions measured under vertical WBV are generally found to occur in the vicinity of 5 Hz. The ranges of the synthesised responses in the ISO 5982 (2001), however, show a shift in the frequencies corresponding to peak APMS and STHT, which is not observed in the data reported in a few studies that measured these variables simultaneously (Hinz and Seidel, 1987; Wang, 2005). This is most probably due to the wide variations in the experimental conditions and the anthropometry of subjects used in the studies involving measurements of APMS and STHT. In addition, most of the aforementioned measurements have been performed with subjects seated in an upright posture without a back support with their hands usually placed on the lap. Actual work conditions, however, involve the interaction of a seat-backrest and hand controls, which may also serve as additional sources of vibration to the body. A few studies have shown that the back support affects both the APMS and STHT responses, while the effect of hands position may be moderately significant to the vibration transmitted to the head, especially in the fore-aft axis (Wang *et al*., 2006; Rakheja *et al*., 2006). The idealised ranges defined in the standard (ISO 5982, 2001), however, are limited to the body sitting without the back and hands supports.

While simplistic analytical derivations satisfying the APMS and STHT biodynamic variables may not require anthropometric resemblance (Boileau *et al.*, 1997), the biomechanical models with detailed representations of the human body's subsystems may necessitate additional experimental data on the movement of individual body segments for their verifications (Amirouche and Ider, 1988; Seidel and Griffin, 2001). Although a number of complex bio-models with multiple DOF's have been developed,

these have been primarily validated using the driving-point response functions alone (*e.g.*, Pankoke *et al*., 1998; Seidel *et al*., 2001). The validity of such models may thus be questioned, particularly for predicting the distributed vibration responses. These models have thus met only limited success in predicting the vibration transmissibility to the spinal structures and for estimating the responses of the coupled seat-occupant system. Further, the advantages of employing datasets derived from measured vibration transmissibility responses, over the driving-point measures, for the identification of multi-body model parameters have been demonstrated only in a few studies through response matching (Kim *et al*., 2005; Pranesh *et al.*, 2008). Even so, the dearth of sufficient numbers of datasets of localised vibration responses measured under comparable experimental conditions poses difficulties for deeper investigation of the mechanisms causing low back pain and vibration-related injuries (VIN, 2001).

When compared to the number of studies reported on APMS and STHT measures, the measurement of body-segment vibration responses, primarily at the vertebrae of sitting human subjects has been performed only in a few studies employing both surgical and non-invasive techniques, as summarised in Chapter 2. However, there seems to be little agreement among the reported responses, possibly due to wide variations in their experimental methods (*e.g.*, Matsumoto and Griffin, 1998; Magnusson *et al.*, 1993). The few studies reporting comprehensive datasets on body-segment vibration seem to be undertaken with little considerations of actual workplace support conditions, the vast majority being performed without a backrest (Hinz and Seidel, 1987; Kitazaki and Griffin, 1998) and sometimes with feet hanging freely from the vibration platform (Matsumoto and Griffin, 1998). Owing to the well-established influences of the support conditions on the reported traditional biodynamic responses (Rakheja *et al.*, 2006; Wang *et al.*, 2006), it

would be reasonable to speculate that the vibration transmission in the upper body through the musculoskeletal spine will also be affected by the back and the hand supports, in addition to the characteristics of the input excitation. Hence, the measurement of responses at different segments of the human body with the interactions involving support elements is necessary for furthering our understanding of the human body's responses to WBV. The biodynamic response datasets extracted from these studies under specific conditions may then be utilised for the development of analytical models for the corresponding conditions.

The focus of this chapter is the extraction of an optimal number of datasets that could be useful for the development and validation of multi-body models of the seated human exposed to vertical vibration. The measured localised vibration responses, presented in Chapter 4, together with the simultaneously acquired APMS responses at the seat and the backrest are analysed to study the relationships among them. Further, the interplay of the major contributing factors including subject anthropometry, support conditions and vibration magnitude is analysed for both the response categories (driving-point APMS and body-segment transmissibility). Subsequently, the appropriate mean APMS and body-segment transmissibility functions are chosen from the measured array of responses so as to extract an optimal number of unique target datasets that may be employed for the development and/or validation of analytical multi-body bio-models under the specific influential conditions.

5.2   Characteristics of measured seat and backrest APMS responses

A number of studies have reported the total biodynamic forces at the body-seat interface in terms of apparent mass (APMS), especially under exposure to vertical vibration (e.g., Fairley and Griffin, 1989; Mansfield, 2005; Patra *et al.,* 2008). These

163

driving-point measures alone may not be sufficient to characterise the pitch-pane motion of the upper body under vertical excitation (Matsumoto and Griffin, 1998). In addition, most of these studies generally involve the measurement of APMS at a single driving-point measure, namely the rigid seat-pan, which is not representative of the majority of vehicle driving postures involving a cushion seat and a backrest. The few studies that investigated the effects of backrest interactions reported their considerable effects on the seat APMS responses (Rakheja *et al.*, 2004; Wang *et al.*, 2004). In addition, considerable forces have been registered at the backrest along the axis normal to the plane of back contact (*e.g.*, Nawayseh and Griffin, 2004), suggestive of significant upper body movement in the for-aft axis, probably due to pitching about the lower torso. It is thus necessary to acquire the APMS at multiple points of body-machine contact, representative of driving conditions in addition to the measurement of vibration transmitted to different upper body segments. This section discusses the nature of the measured APMS responses at the seat pan and the backrest for different postural and excitation conditions described in Section 3.2.2 so as to aid in the selection of appropriate target driving-point functions for the development of an analytical biodynamic human model.

Figure 5-1 illustrates the APMS responses of the 12 subjects sitting with hands in the lap measured at the seat (L-NB, L-B) and the backrest (L-B), respectively, in the vertical and fore-aft axes, under a random vertical excitation magnitude of 1 m/s^2. It should be noted that some reported studies employ the term "cross-axis" to indicate the APMS measured at the backrest normal to the plane of contact (*e.g.*, Wang, 2006). This research dissertation, however, refers to the backrest measure as "backrest APMS" or "upper body backrest APMS." This is to avoid confusion with the term "cross-axis"

164

which may also be used to denote driving-point functions with respect to the axis of excitation (Mansfield and Maeda, 2007). While both the magnitude and phase responses of the vertical apparent mass measured at the seat are presented in Fig. 5-1(a) and (b), the backrest APMS data are presented only in magnitude since the data revealed large fluctuations in the data. This is attributable to expected variations in the contact force of the upper body against the backrest. The APMS responses for the other postures, namely SW-B and SW-NB, are discussed further on in this section.

Interestingly, in all the postures, except for subjects 2 and 6, with total body masses of 91.2 and 95.4 kg, respectively, the data exhibit vertical seat APMS magnitude peaks around 5 Hz, which is widely accepted as the primary resonance characteristic of the human body in the vertical mode (Fairley and Griffin, 1989). A slight peak in the magnitude is also seen around 10 Hz for some of the subjects, which is believed to be caused by movements of the abdominal viscera (Matsumoto and Griffin, 2001; Mansfield and Griffin, 2000). Additionally, the phase responses of the seat APMS also shows a lag of about 90° at frequencies above 5 Hz, indicative of at least one resonance mode in this frequency range. The upper body APMS responses obtained at the back support (Fig. 5-1(c)) also show magnitude peaks around 6 Hz, which is slightly higher than that observed in the vertical APMS data (Fig. 5-1(a)). This is possibly due to the pitching of the upper body as reported in some studies under vertical excitation (Nawayseh and Griffin, 2004, Matsumoto and Griffin, 2001). A second mode around 2 Hz is also noticeable in the backrest APMS responses. It may be noted that inter-subject variability is greater for the backrest APMS response than in the vertical direction at the seat. This is attributable to considerable variations in the upper body contact with the backrest, which is also dependent upon the individual's sitting habit and posture, and possibly on the involuntary

movements of the upper body. Similar trends in variability were also observed by Wang

(2005) in a study with twelve male human subjects sitting with a vertical back support.
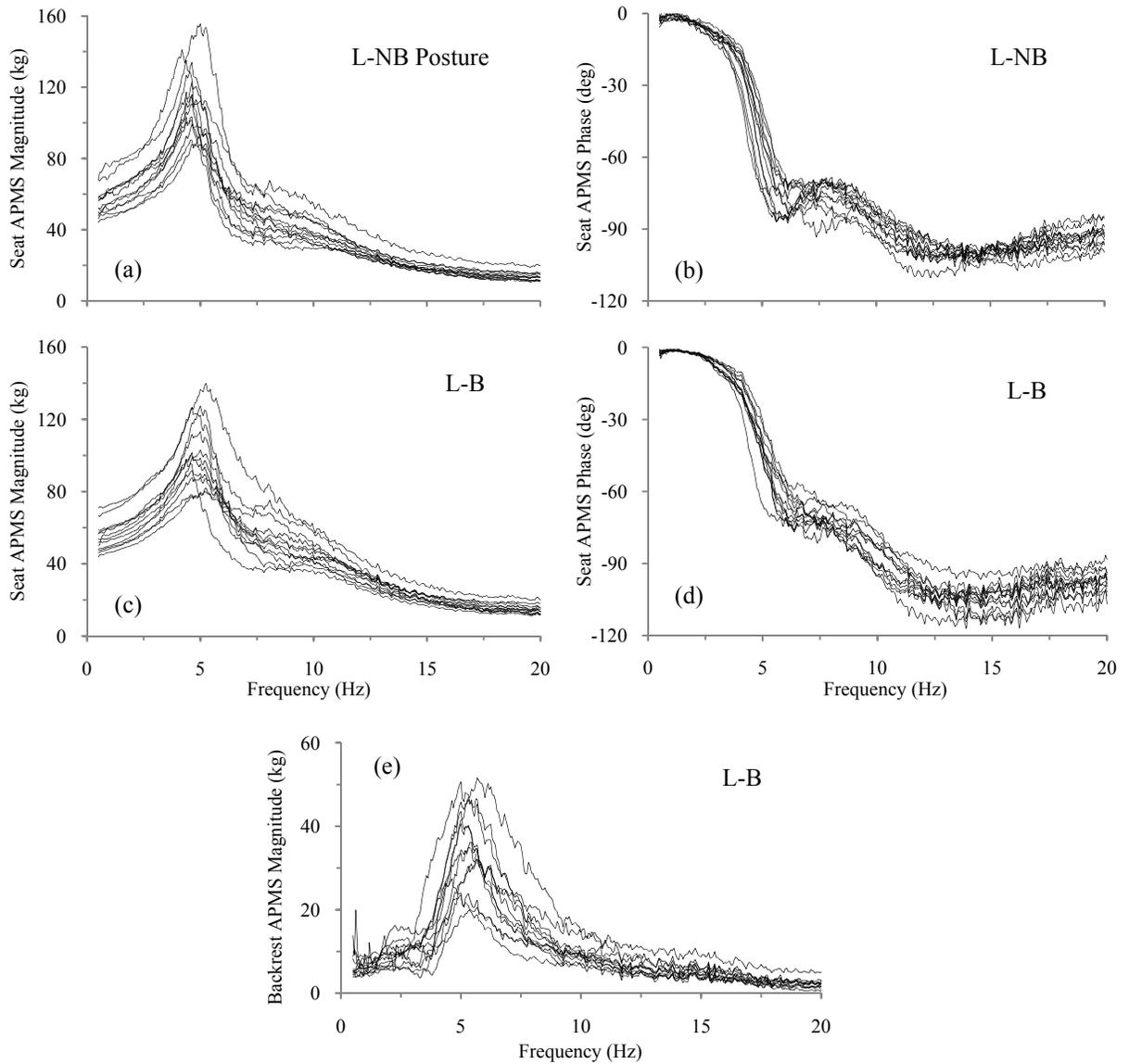
Figure 5-1: Apparent mass responses of 12 male subjects seated with hands placed on the lap and exposed to 1 m/s^2 random vertical seat excitation under different back support conditions. Vertical seat apparent mass (a) magnitude; and (b) phase in the L-NB posture. (c) Backrest apparent mass in the L-B posture.
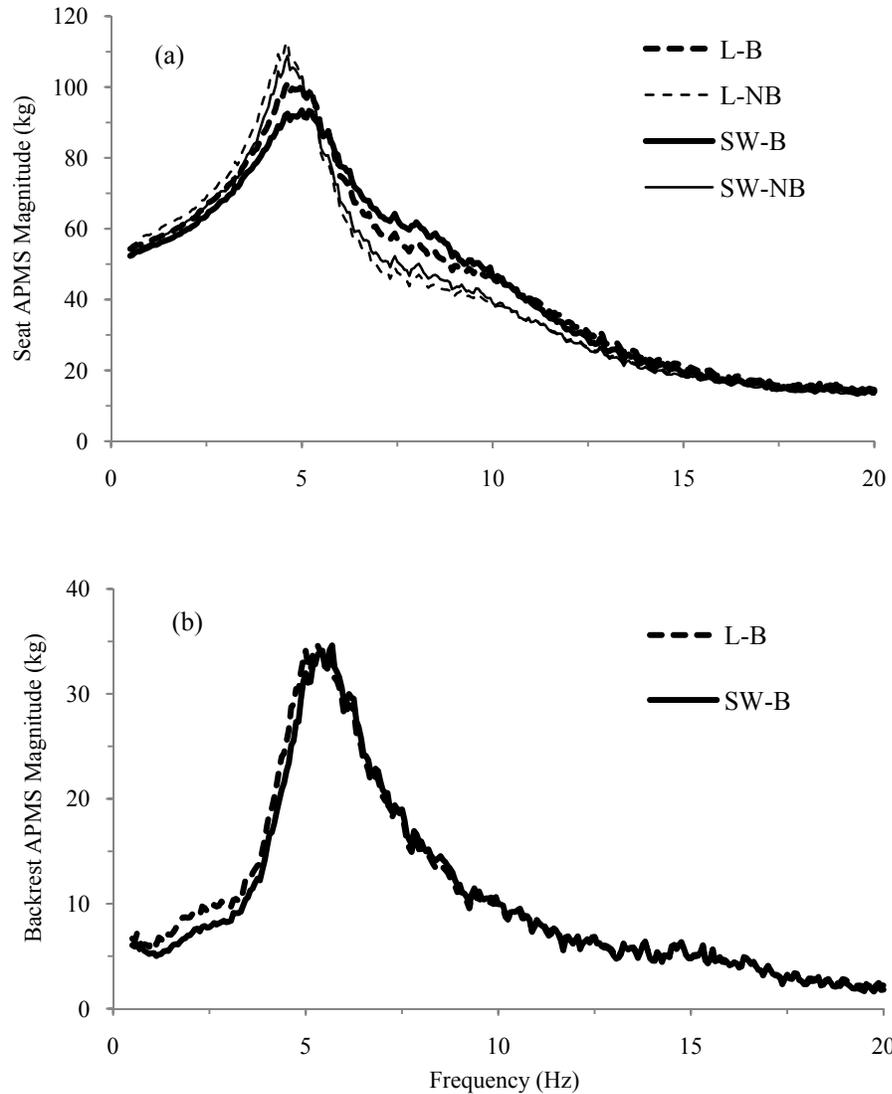
Figure 5-2: Comparison of mean magnitudes of (a) vertical seat; and (b) upper body backrest apparent mass from 12 subjects seated in various postures and exposed to 1 m/s2 random vertical seat excitation. Postural conditions include L-B: Back supported (B) with hands in lap (L); SW-B: Back supported with hands on steering wheel (SW); L-NB: Hands in lap and no back support; SW-NB: Hands on SW and no back support.

The differences observed in the data acquired with subjects 2 and 6, with respect to the remaining data, are most likely caused by their greater mass values. This is also evident from the higher APMS magnitudes near 0.5 Hz. Considering that their body mass deviates considerably from that of the 50th percentile male human body, the mean APMS responses were computed after removal of these subjects' data APMS responses. Figures 5-2 (a) and (b) present comparisons of the means of the seat and backrest APMS responses of the remaining 10 subjects for the four sitting postures: L-B, L-NB, SW-B, SW-NB, under 1 m/s^2 random vertical excitation. It is evident from the figure that the back support tends to have a significant effect on both the peak magnitude and the primary resonant frequency of the vertical seat APMS. In addition to reducing the peak vertical APMS magnitude (Fig. 5-2(a)), the back support seems to accentuate the secondary mode around 10 Hz. Furthermore, the results show considerable effects of the hands position on the seat APMS magnitude in the presence of a back support.

The backrest contact causes an increase in resonant frequency along with a reduction in the peak APMS magnitude measured at the seat pan, which can be observed in the SW-B condition in Fig. 5-2(a). The hands position, however, does not seem to significantly influence the backrest apparent mass magnitude as seen in Fig. 5-2(b). The backrest in conjunction with the hands support (SW) may be causing local effects in the lower lumbar-pelvic regions restraining the pelvic pitch with associated increase in forces at the driving-point. The vibration transmitted to the L5, discussed earlier in Section 4.3, also showed similar effects of the SW-B posture. While the general trends in the mean vertical APMS characteristics with the back and hands supports seem to be in agreement with those described in the few reported studies under similar conditions (Rakheja *et al*., 2002; Wang *et al*., 2004), the hands holding a steering wheel have been reported to

attenuate backrest APMS at resonance and increase the corresponding magnitude in the frequency range beyond (Rakheja *et al*., 2006). The reported measurements, however, were obtained for human occupant seated on an automotive seat geometry with 12° degree inclination of the backrest and exposed to considerably lower vibration.

The results in Fig. 5.2 present the APMS responses to vertical vibration magnitude of 1 m/s^2, which is perhaps the most commonly used excitation magnitude in the reported studies. A number of studies, however, have shown some effects of excitation magnitude on the measured APMS responses (*e.g.*, Mansfield and Griffin, 2001; Rakheja *et al.*, 2002). These studies have generally shown an increase in peak response magnitude with a simultaneous reduction in the corresponding frequency under a higher vibration level (*e.g.*, Fairley and Griffin, 1989; Mansfield, 2005; Mansfield and Griffin, 2000). Generally, the characteristics of a "softening" spring have been attributed to the seated body's driving-point biodynamic responses, although a quantitative relationship for the influence has not been established due to wide variations in the experimental conditions among the studies.

The data acquired under the other lower excitation levels (0.25, 0.5 m/s^2) were also analysed in a similar manner to derive the mean responses. These responses suggested certain influences of the excitation magnitude on the measured driving-point responses.

Figure 5-3 presents the mean seat and backrest APMS responses attained under three different magnitudes of vertical vibration considered in the study for the L-NB and L-B postures. The responses corresponding to the other postures (SW-B and SW-NB) have been since the responses depicted similar effects of the vibration magnitude. The decrease in the primary resonant frequency, with increase in vibration magnitude, was

evident in both the seat and the backrest apparent mass, irrespective of the posture. However, while the NB posture revealed an increase in peak apparent mass magnitude at the seat with increasing vibration level, the back supported postures (SW-B, L-B) showed decrease in the corresponding peaks from 0.25 to 1 m/s^2 vibration magnitude. This 'softening' effect reported in a number of studies due to increase in excitation level (Mansfield, 2005) is also evident in the backrest APMS response, suggestive of a direct relationship between the fore-aft motion in the upper body and the reasons for whole-body resonance under vertical seat vibration (Matsumoto and Griffin, 2001 and 2002). The secondary magnitude peaks identified around 2 Hz and 10 Hz, respectively, for the backrest and the seat APMS responses are also significantly reduced under higher vibration levels. These changes could be related to the reduction in muscular activity of the trunk with higher levels of vibration (Blüthner et $al.$, 1995; Seidel et $al.$, 1986). In corroboration, the statistical analyses (ANOVA) of the APMS response of the population also suggested strong influences of the vibration level on the magnitudes of seat apparent mass ($p<0.001$: 5-15 Hz frequency range and $p<0.05$: 7.5-9 Hz and 10-15 Hz), irrespective of the support condition. While the general trends of the APMS responses measured at the seat pan and backrest are presented here, the results are further discussed in the following sections with the ultimate aim of extracting appropriate target datasets applicable for the development of biodynamic models.
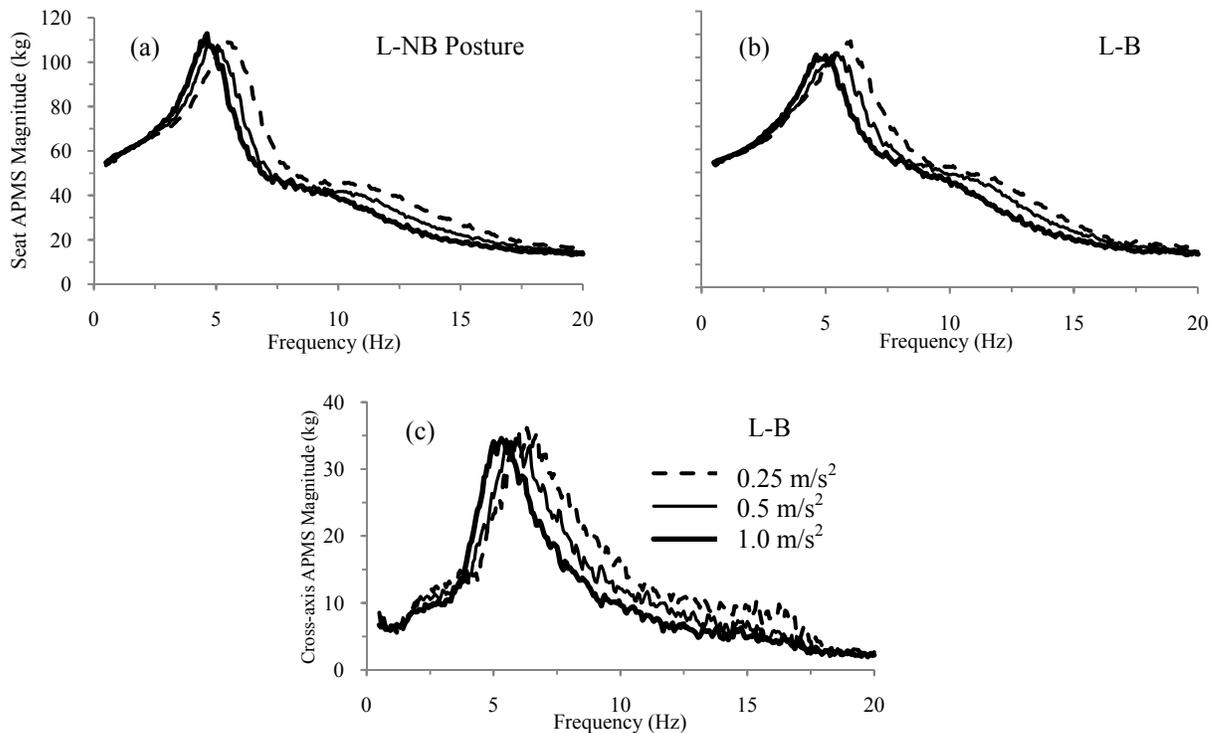
Figure 5-3: Comparison of the mean seat apparent mass measured in the (a) L-NB; and (b) L-B postures, and the (c) backrest apparent mass response in the L-B posture with the 12 male seated subjects exposed to 0.25, 0.5 and 1 m/s^2 random vertical seat vibration.

The uniqueness of this research study lies in the simultaneous measurements of driving-point biodynamic variables (APMS) at both the seat pan and the backrest, and the vibration transmitted to different segments of the body along the spine, with the inclusion of different postural and excitation conditions. The body segment vibration in terms of vertical and fore-aft acceleration transmissibility measured at different locations of the human body in the four tested postures and excitation conditions were presented in the previous chapter, along with the detailed discussions on the observed variabilities in these responses and the statistical influences of the postures. These body-segment measures are utilised in the following sections, along with the APMS acquired at the seat and backrest, for further analyses so as to identify the relationships among them with respect to the

171

various contributory factors, and subsequently extract response datasets for the development and verification of biodynamic human models.

5.3   Discussions on response peaks and characteristic frequencies

It is known from biodynamic responses at the driving point and the head that various contributory factors influence the nature of vibration transmitted to and through the body (*e.g.*, Mansfield, 2005; Paddan and Griffin, 1998). However, considerable ambiguity exists on the nature of vibration transmission through the segments of the seated human body exposed to vertical vibration. Further, only a few studies have attempted a systematic study of influencing factors on the vibration measured at localised segments. To this effect, the significance of the back and hands support conditions, and the excitation magnitude was established in the previous chapter through the use of statistical analyses on the body segment vibration transmissibility in the fore-aft and vertical axes. The wide variations in the responses with the postural conditions suggest that datasets corresponding to each particular posture need to be extracted for the development of biodynamic human models. The influences of possible contributory factors on the mean responses including the segmental acceleration transmissibility, and the apparent mass at the seat and backrest are thus initially investigated so as to identify the most significant factors in order to minimise the number of target datasets. The analyses include the effects due to anthropometric variables, the aforementioned support conditions and vibration magnitude.

5.3.1 Effects on subject anthropometry on response magnitude peaks

The strong dependence of driving-point variables, such as APMS, DPMI and vibration power absorption, on certain anthropometric variables of the test subjects has

been acknowledged in a few studies (*e.g.*, Smith, 1993, Rakheja *et al.*, 2002, Wang *et al.*, 2004, Nawayseh and Griffin, 2004). It has been found that the peak vertical APMS increases considerably with the subject body mass. Similar effects have also been reported for the backrest apparent mass (Wang, 2005). The grouping of the data for subjects within narrow mass ranges has been suggested for sufficiently large test populations so as to enable the study of non-anthropometric influence factors within a narrow mass range (Rakheja *et al.*, 2006). In line with this approach, a recent study has proposed the APMS datasets for three subject groups with mean body masses of 55, 75 and 98 kg (Patra *et al.*, 2008). It should, however, be noted that in the present study attempts were made to limit the subject pool to the 50th percentile anthropometric scale in order to reliably compare segmental responses. Slight differences in the individuals' body mass, however, permitted limited analysis of the body mass effect, while the influence of the sitting height could be investigated more thoroughly.

Figures 5-4 and 5-5 depict the effects of body mass and sitting height of subjects, respectively, on the peak magnitude of the mean apparent mass and selected transmissibility functions, in both the vertical and horizontal axes, through linear correlations. The peak magnitudes mostly occurred in the vicinity of the primary resonant frequency (near 5 Hz). The influences observed due to the subjects' total body mass on the peak magnitudes of all the responses were similar to that due to the individuals' static sitting mass measured on the seat (73-78% of total body weight for most subjects). Due to its ease of measurement, the total subject weight is thus chosen to illustrate the anthropometric mass effect on the peak responses in Fig. 5-4. The peak vibration transmissibility magnitudes at most of the body segments did not show significant influence of the total body mass. Only the vertical responses at L5 and fore-aft at the

173

head revealed noticeable influences of the body mass, as shown in the Fig. 5-4. Furthermore, owing to the relatively larger inter-subject variability observed in responses at the lower vibration magnitudes (0.25 and 0.5 m/s^2), the results corresponding to 1 m/s^2 excitation level alone are discussed in this sub-section.
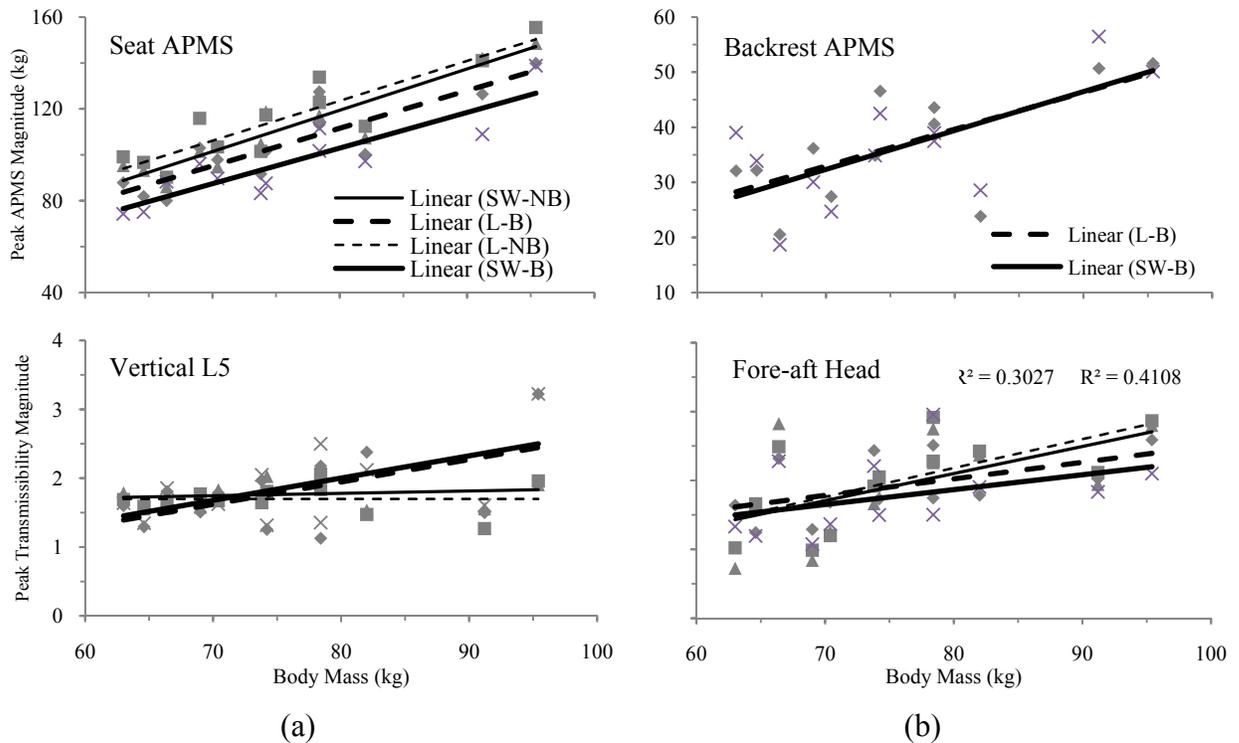
Figure 5-4: Peak magnitude values of selected apparent mass and body segment vibration transmissibility responses in the (a) vertical; and (b) fore-aft axes, expressed as a function of body mass of 12 subjects seated in various postures exposed to 1 m/s^2 vertical seat excitation.
♦ L-B; ■ L-NB; × SW-B; and ▲ SW-NB.

The body mass demonstrated expectedly strong influences (Mansfield, 2005) on the peak vertical seat apparent mass (R^2 ranging from 0.77 to 0.85), in all the postures, and slightly less significant contributions to backrest APMS (R^2: 0.45-0.47) in the SW-B and L-B conditions. Both the responses showed positive correlation with the body mass, irrespective of the postural condition considered. However, the subject weight did not display definite trends on the measured transmissibility peaks at most locations.

Consequently, the variations in the peak transmissibility at these locations are not presented. The peak fore-aft movement of the head in the NB postures (R^2: 0.16-0.41) and vertical transmissibility to L5 with backrest interaction (R^2: 0.32-0.37) revealed increasing trends with body mass, although a definite relation could not be estimated due to the relatively high degree of inter-subject variability. The similarity in the trends observed among the peak magnitudes of the L5 transmissibility and the seat APMS in the vertical axis, especially with the back supported, is suggestive of a direct relationship between dynamic forces registered at the seat-buttock interface (APMS) and the motion in the lower torso segments under vertical WBV. The behaviour of the L5 in the back unsupported postures is quite ambiguous. Although the subject population in this study is primarily constrained to the 50th percentile male body, the APMS at the seat and backrest show significant dependence, while the same cannot be definitely stated for the vibration transmissibility responses.

In comparison to the body mass, the sitting height of subjects, illustrated in Fig. 5-5, showed relatively greater effects on the vibration transmitted to the body segments. Interestingly, while the peak vertical vibration transmitted to the thoracic (T5 and T12) and cervical (C7) locations showed very little effect of the subjects' sitting height, the head and C7 fore-aft motion displayed relatively higher dependence on the trunk height. The discussions are thus limited to these transmissibility responses in addition to the APMS at the seat and the backrest. The vertical vibration peaks at L5 displayed noticeable dependence on the sitting height of the subjects (R^2: 0.54-0.66) in the presence of a backrest, while the effect is insignificant for the back unsupported postures. The vertical L3 and the fore-aft head transmissibility peak magnitudes also showed, albeit to a much lesser degree (R^2 around 0.3), a similar trend due to the upper body height of

subjects sitting with a back support. The dependence of the fore-aft head motion may be related to rotational motions of the upper body about the lower torso (Matsumoto and Griffin, 2001). However, the relatively high variability in the backrest APMS peaks suggest the need for an independent model of the fore-aft head motion, probably due to pitching of the head about the upper neck. In corroboration, the small effects of sitting height on the fore-aft movement at C7 suggest possible out of phase rotations of different substructures of the trunk. Similar, and sometimes even smaller, influences were registered in the other body segment responses and hence not presented.

In summary, the results presented in this subsection need to be treated with reservation since the anthropometric variables of the subject pool varied in a narrow range and may not be sufficient for the conclusions on the anthropometric effects on the to- and through-the-body biodynamic responses. Further efforts are thus needed to acquire individual sets of biodynamic functions, especially in terms of vibration transmitted to different body segments, for different anthropometric body types (*e.g.*, 5th, 50th, 95th percentile). However, for the purpose of extracting target datasets in this study for the development of the biodynamic model, the mean responses of the 10 subjects may be considered sufficient.
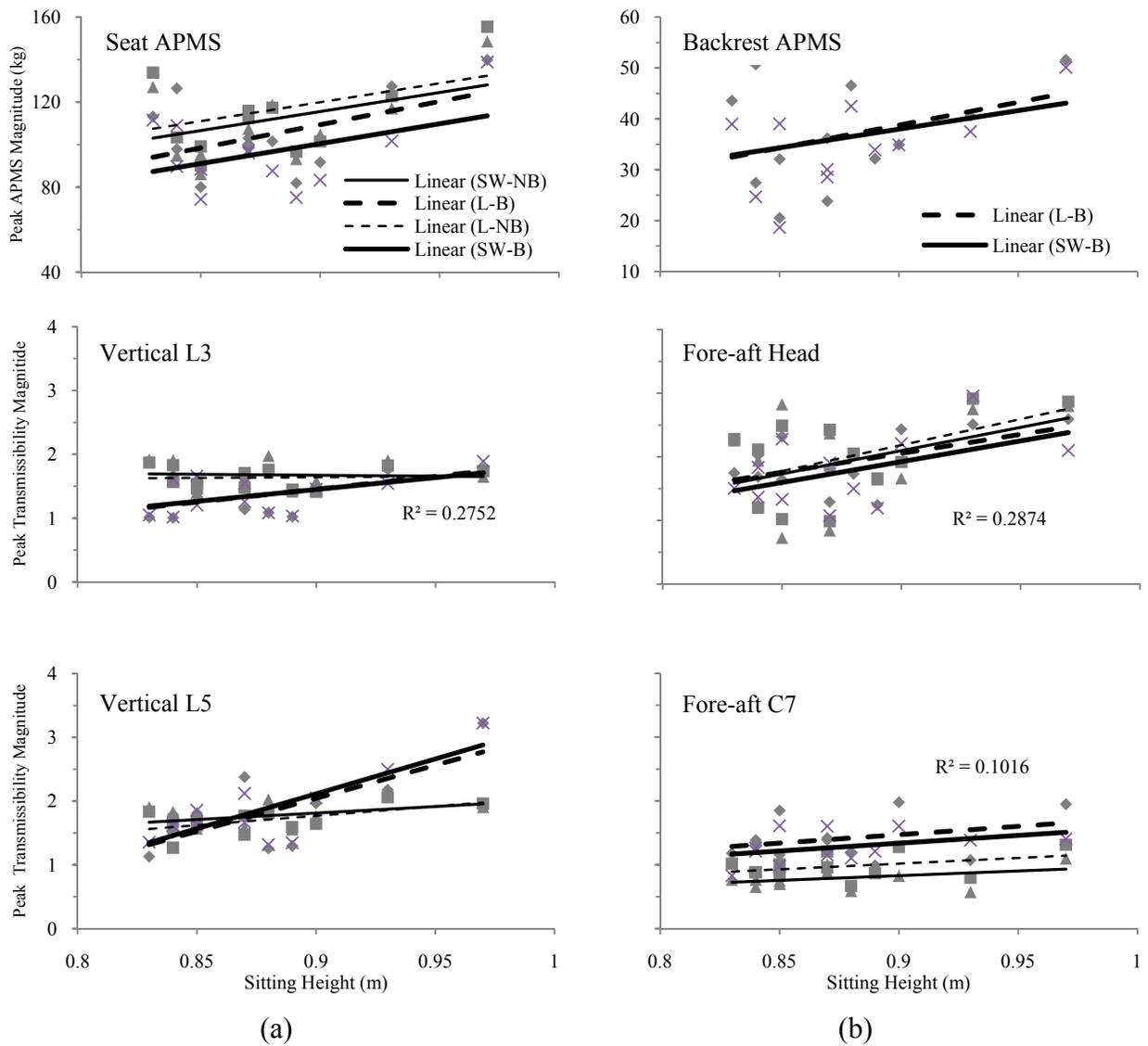
Figure 5-5: Peak magnitude values of selected apparent mass and body segment vibration transmissibility responses in the (a) vertical; and (b) fore-aft axes, expressed as a function of sitting height of 12 subjects seated in various postures exposed to 1 m/s^2 vertical seat excitation.
♦ L-B; ■ L-NB; × SW-B; and ▲ SW-NB.

5.3.2 Influences of support conditions and vibration magnitude on the characteristic frequencies

The influence of postural variations, back support condition and hands position, on the vibration transmitted through the body were evaluated using statistical analyses (ANOVA) in the previous chapter. The vibration transmissibility responses at various body segments measured in the fore-aft and vertical axes were also compared for different postures in Fig. 4-6. The results suggested that the use of a back support attenuates the vibration transmission through the body in the vertical axis at all the chosen segments but causes higher fore-aft motion at C7 and T5. Additionally, the results obtained from the statistical analyses revealed significant contributions of the back support to the accelerations measured at all the locations. The hands position, however, showed relatively smaller effects on the vertical transmissibility to all the segments, but demonstrated significant influence on the fore-aft responses at the C7. While the previous analyses were mostly performed on the response magnitudes, considerable shifts in the frequencies corresponding to the peak magnitudes in the vertical and fore-aft responses could be observed (Fig. 4-6) at many locations due to postural variations, primarily due to the back and the hands supports. The measured magnitude datasets are thus further examined to identify the shifts in characteristic frequencies corresponding to the magnitude peaks and valleys in the frequency range of 0.5 to 15 Hz. The characteristic frequencies are extracted from the mean apparent mass and vibration transmissibility response magnitudes of the 12 subjects for each of the postural condition and the vibration level employed in the study. These characteristic frequencies are summarised in Tables 5-1 and 5-2, respectively, for the vertical and fore-aft axes responses in apparent mass and vibration transmissibility. The observed changes in the characteristic

178

frequencies of the selected responses are analysed to explore relationships that may exist among the measured responses, which are subsequently utilised for making decisions on the selection of appropriate target datasets in Section 5.4 for the development of a biodynamic model of the human body.

Table 5-1 summarises the characteristics frequencies observed in the mean response magnitudes of the seat apparent mass and the vertical body segment transmissibility. The vertical APMS reveals two characteristics frequencies around 5 and 10 Hz in all the postural conditions, which correspond, respectively, to the primary and secondary peaks in the apparent mass observed in Fig. 5-2, irrespective of the postural condition. While the first characteristic frequency has been widely attributed to a whole body vibration mode (Fairley and Griffin, 1989), the secondary characteristic frequency is believed to be due to resonance of the abdominal viscera (Mansfield and Griffin, 2000). The backrest was shown to noticeably attenuate seat APMS peak magnitude (Fig. 5-2; $p<0.001$) with considerable statistical significance in the vicinity of the secondary peak ($p<0.001$ in the 7.5-10 Hz frequency range). Similarly, the shifts in characteristic frequency associated with the secondary mode (around 10 Hz) are also strongly affected by the back support condition (Table 5-1). Additionally, the shifts in frequencies due to hands position, for both the primary and secondary peaks, are greater with the presence of backrest contact (SW-B, L-B) as depicted in the ANOVA results ($p<0.001$: 4.5-5 Hz, and 7.5-12.5 Hz). As observed earlier, the backrest in conjunction with the hand support may be causing local effects in the lower trunk regions constraining the pitch motion of the pelvis and thus reducing the associated forces at the driving-point.

Similar to the seat APMS responses, the vertical acceleration transmissibility magnitudes at majority of the body locations also show at least two characteristic

frequencies in the vicinity of 5 and 10 Hz, corresponding to the primary and secondary response peaks observed Fig. 4-6 (Table 5-1). It is, however, interesting to observe slightly higher characteristic frequencies for the vertical transmissibility at L5, especially for the postures with a back support. This may be caused by the presence of vibration modes in the lower lumbar and sacro-pelvic units (Mansfield and Griffin, 2000).

The results presented in the previous chapter reveal that the back support can considerably attenuate the peak vertical vibration transmissibility magnitudes at all the body locations (p<0.001: 4-6 Hz). In addition there is a slight shift (increase) in the primary peak frequency at most of the body locations due to the back support probably due to the additional stiffness provided to the vertical body motion by the backrest contact. On the other hand, the effects of the hands position on the vertical vibration transmitted to different body segments are more clearly noticeable in the graphical results illustrated in Fig. 4-6(a) than that observed from the characteristic frequencies. The effect of the back support is quite considerable on the secondary mode around 10 Hz registered for the vertical responses at the head (Table 5-1). While the back supported postures (L-B and SW-B) in the table show secondary frequencies for vertical head motion in the vicinity of 10-11 Hz (p<0.001), no such mode is evident in the NB postures in the table and Fig. 4-6(a). This is suggestive of a separate head-neck vertical vibration mode in this frequency range introduced by the backrest contact.

While significant effects of the support conditions are observed in the vertical axis motions at C7 and L5, nearly complete attenuation of vertical vibration at the thoracic locations (p<0.001: 2.5-15 Hz) does not permit further examination of the latter responses. Additionally, the possible errors that may be introduced by stretching of the local skin tissue at T5 and T12 due to backrest contact, may pose questions on the reliability of the

thoracic datasets in the SW-B and L-B postures. Omitting these two datasets for each of the excitation levels, it is seen that the hands position does not seem to have major effects on the characteristic frequencies of vibration transmitted to the thoracic locations. The back support, however, increases both the resonant frequency and the bandwidth of the vertical vibration peak at C7 as seen in Fig. 4-6(a) (p<0.05: 4-5 Hz). In addition, it may be seen from Table 5-1 that the backrest contact introduces a secondary vertical mode around 10 Hz, similar to that at the head, further suggestive of a separate head-neck vertical vibration mode in this frequency range.

Similarly, two characteristic frequencies are seen in the vertical transmissibility measured at the lumbar vertebrae (L3 and L5), around 5 and 10 Hz. The considerable increase in the primary resonant frequency at both the lumbar locations in the L-B and SW-B postures is possibly due to the aforementioned stiffening of the body due to backrest contact. However, the insignificant shift in the lumbar secondary characteristic frequencies, around 9-11 Hz especially at the L5, due to variations in postural conditions suggests a distinct vibration mode not directly associated with the vertical spinal resonance. This higher frequency mode has been hypothesised to be caused by the pelvic pitch (Mansfield and Griffin, 2000) and movements in the abdominal viscera (Matsumoto and Griffin, 2001). It is evident that shifts in the characteristic frequencies in the vertical axis are dominated more by the back support conditions than the hands position, irrespective of the excitation level.

Table 5-1: Characteristic frequencies identified from measured vertical responses of seat APMS and body-segment transmissibility.

Excitation Magnitude	0.25 m/s²				0.5 m/s²				1 m/s²			
Posture/ Measurement Location	L-B	L-NB	SW-B	SW-NB	L-B	L-NB	SW-B	SW-NB	L-B	L-NB	SW-B	SW-NB
Seat APMS	5.63	5.19	6.95	5.44	5.19	4.63	5.38	4.94	4.63	4.34	5	4.63
	11.25	10.44	9.88	10.19	10.19	9.69	9.13	9.25	8.81	8.2	7.75	8.06
Head						2.38		2.8				
	5.31	5.19	5.19	5.25	4.75	4.69	4.56	4.81	4.56	4.38	4.56	4.38
	11	10.81	10.25	10.88	10.31		9.25		9.38		9.06	
C7	5.94	5.44	5.88	5.38	5.25	4.81	5.75	4.94	4.88	4.63	5.19	4.56
	13.38		10.25		11.81		11.75		10.88			
T5	5.69	5.31	5.56	5.44	4.69	4.69	4.56	4.88	4.38	4.5	4.13	4.56
		10.88	10.13	10.56		10.75	9.44	10.38				
T12		2.25				2.56						
	5.31	5.31	5.38	5.31	4.68	4.5	5.06	4.81	4.56	4.44	4.63	4.25
		10.44				9.06		9		7.81		8.13
L3								2.63				
	5.75	5.38	5.94	5.25	5.56	4.69	5.69	4.88	4.81	4.38	5	4.56
	10.19	10.63	9.88	10.56	9.5	9.38	9.38	9.38	8.88	8.25	8.44	7.81
L5	6	5.38	6.31	5.5	5.75	4.88	5.88	5.06	5.06	4.56	5.31	4.56
	11.06	11.19	11	11.25	10.25	10.38	10.13	10.31	9.5	9.44	9.06	9.31

Table 5-2: Characteristic frequencies identified from measured backrest APMS and fore-aft body-segment transmissibility.

Excitation Magnitude	0.25 m/s^2				0.5 m/s^2				1 m/s^2			
Posture/ Measurement Location	L-B	L-NB	SW-B	SW-NB	L-B	L-NB	SW-B	SW-NB	L-B	L-NB	SW-B	SW-NB
Cross-axis APMS	2.19	-	1.94	-	1.88	-	2.06	-	1.56	-	1.81	-
	3.63		3.63		5.63		5.94		5.19		5.19	
	5		5.06									
	6		6.06									
Head	2.5		2.5	1.31	1.93		1.94					
	3.38	3.63	3.56	3.75		3.06		3		2.88		3.13
	4.57		4.38									
	5	5.06	5.44	5.25	4.75	5.13	4.75	5.06	4.56	4.81	4.44	4.81
					9.25		9.56		8.44		8.63	
C7	2	1.06	2	1.38	2.19	1.38	2.13	1.69				0.75
	6.38	6.56	6.44	6.31	6.44	6.44	6.44	6.31	5.63	5.88	5.38	5.44
T5		2.5		2.31				2.31				
	6	6.25	6.38	6.31	5.56	5.06	5.94	5.94	4.81	4.13	5.25	5.38
T12	3.82	3.13	3.75	3.38		3		2.75		2.32		2.88
	6.75	7.94	6.75	7.88	6.38	6.38	6.44	6.31	5.75	5.69	5.88	6
L3	3.94	2.94	3.9375	3.63		2.94		3.69	3.38		3.69	3.31
		5.19	5	4.94	4.25	4.56	4.13			4		
	7.88		7		7.25		7.06		6.38		6.38	
L5			3.88									
	4.06	4.69	4.81	4.69	4.13	3.87	4.13	3.88		3.69	3.44	3.19
	6.63	9.88	6.8	8.43	6.38	8.94	6.38	8.94	5.63	8.13	5.63	8.13

Table 5-2 summarises the characteristic frequencies identified from the mean fore-aft transmissibility magnitude at the measured body locations along with the apparent mass registered at the backrest in the L-B and SW-B postures. In comparison with the characteristic frequencies presented in Table 5-1, it may be observed that the primary peaks of both the backrest APMS and fore-aft vibration transmissibility at most of the body locations (Table 5-2) generally occur at a slightly higher frequency (near 6 Hz) than the corresponding vertical responses (near 5 Hz). It may also be noticed that most of the secondary modes in the fore-aft responses occur at frequencies below primary resonance, as opposed to the trend in the vertical axis.

It is evident from the tables that the hands position alone (SW or L) does not have a significant influence on the frequency characteristics of both the backrest APMS and fore-aft vibration transmissibility to the selected body locations, although fore-aft transmissibility magnitudes of some segments such as the head and C7 showed sensitivity to both the hands position and the back support condition. Similarly, the backrest was shown to suppress fore-aft vibration at the head, irrespective of the hands position (Fig. 4-6a) in the frequency range below 10 Hz ($p<0.001$: 2.5 Hz, $p<0.05$: 4.5-9 Hz), although no significant trends were observed in the corresponding characteristic frequencies. The primary resonant frequencies (near 6 Hz) identified in Table 5-2 for the fore-aft motion at the measured cervical, thoracic and lumbar locations of the trunk are noticeably higher than that at the head (around 5 Hz). A characteristic frequency around 2 Hz is evident from the C7 response, which is identifiable in all the postures, in addition to the primary resonance peak near 6 Hz, suggestive of low-frequency pitch modes of the head-neck system independent of the trunk at low vibration levels (0.25 and 0.5 m/s^2). Moreover, the back support condition also considerably increases these secondary characteristic

184

frequencies at 0.25 m/s^2 vibration (for example, from 1.06 in the L-NB to 2 Hz in the L-B posture), indicative of the significance of the constraint posed by the backrest driving-point.

The substantial difference in the peak fore-aft vibration magnitude at the T5 (near 6 Hz) due to backrest contact (Fig. 4-6b) suggests a probable change in the nature of vibration transmission through the upper body due to the back support (p<0.001: 4-15 Hz). However, no noticeable change in the corresponding characteristic frequencies could be observed (Table 5-2). The lower thoracic and lumbar levels display similar horizontal response characteristics in all the postures with the back support increasing the magnitude around 6 Hz especially at L5 (p<0.05: 6-7.5 Hz). Contact with the backrest seems to suppress a low frequency peak (2-3 Hz) visible under 0.5 and 1 m/s^2 excitations in the T12 an L3 responses (p<0.001: 2.5 Hz). While the T12 and L3 vertebrae show very similar magnitude characteristics, the L5 responses reveal a marked influence due to the back support in the form of a broader peak from 6 to 9 Hz (Fig. 4-6b). Sitting erect without a backrest seems to produce a slight horizontal peak between 8 and 9 Hz at the L5, which is not comparable with any other body movement in this axis (Table 5-2). The attenuation of horizontal vibration with the hands positioned on the steering wheel is also identifiable from the L5 responses.

The results obtained from statistical analyses of the data acquired with the subject population, presented in the previous chapter, also showed strong influences of the vibration magnitude on the acceleration transmissibility around the primary and secondary peak magnitudes of the majority of body segments. The same discussion is extended here to further include the driving-point responses, but from the perspective of the characteristic frequencies presented in Tables 5-1 and 5-2. The frequencies

185

corresponding to the primary and secondary peaks for all the response magnitudes occur in the range of 8-12 Hz for the vertical responses and between 2 and 4 Hz in the fore-aft responses. The frequencies generally decrease with greater excitation magnitude, irrespective of the postural condition. A higher secondary mode frequency, between 8-13 Hz, identifiable in the vertical transmissibility of the T5, T12, L3 and L5 (Fig. 4-6a), is progressively suppressed ($p<0.05$: 9 Hz) and the corresponding peak frequency decreased with increasing vibration magnitude, as seen in Table 5-1. While an increase in peak vertical response due to higher excitation levels was observable in most of the segments' responses, the head and neck horizontal responses near the primary resonant frequency depicted an opposite trend ($p<0.05$: 5.5-7.5 Hz), registering a decrease in the resonant frequencies. This is additionally observable as a secondary peak in the fore-aft STHT around 3 Hz under 0.25 and 0.5 m/s^2 excitations ($p<0.05$: 2.5-4 Hz), as seen in Table 5-2. This is attributable to changes in vibration-dependent muscle activity which is known to reduce under certain vibration magnitudes (Blüthner *et al.*, 1995; Seidel *et al.*, 1986). The vibration magnitude may thus be hypothesised as having relatively less influence on the apparent mass and vibration transmissibility responses in comparison with that caused by support conditions.

In summary, the backrest condition exhibits considerable influence on both the vertical and fore-aft peak magnitudes and characteristic frequencies identified from the measured apparent mass and vibration transmissibility responses. Although the hands position seems to affect peak vibration magnitudes at certain body segments such as C7 and L5, its overall effect on the characteristic frequencies is insignificant. It must however, be understood that the fore-aft vibration transmissibility results from the lower thoracic and lumbar body locations need to be treated with reservation due to the high

186

degree of variability in the measured data. With these findings, the case for the identification of a reduced number of datasets is made in the next section, which may be utilised for a variety of purposes including the development and verification of biodynamic model parameters and for comparisons among different measured datasets.

5.4 Extraction of target datasets from measured responses

This research dissertation involved 12 male seated subjects who were subjected to three levels of random vertical excitations (0.25, 0.5 and 1 m/s^2) from a vibration simulator while seated in combination of two support conditions that led to 4 postural conditions. The test matrix involved the simultaneous acquisition of force-motion functions (APMS) at two driving-points, the seat base and the backrest, and vibration transmissibility to six locations on the body in two axes, namely fore-aft and vertical. The number of biodynamic responses for the study thus totals to 2016 datasets. Systematic analyses of these datasets, presented in the previous section, were essential to identify reduced number of datasets that could: (i) effectively describe the significance of the influencing factors; and (ii) be applied for the development and verification of biodynamic models.

A number of studies have identified a strong effect of body mass on the driving-point biodynamic functions (Mansfield, 2005), although the APMS data applicable for particular body masses have been presented only in a few studies (DIN 45676, 1992; Patra *et al.*, 2008). The data acquired in the present study also revealed dependence of peak vertical APMS magnitude on the body mass (Fig. 5-4), although the attempts were made to recruit subjects within the 50th percentile body mass. The observed dependence was mostly due to two volunteers weighing more than 90 kg. The exclusion of the datasets of these two subjects revealed only minimal differences among the magnitude

peaks. Additionally, it was also observed that the body mass and sitting height exhibit only relatively small effect on the measured transmissibility responses at majority of the upper body locations, also characterised by wide scatter in the peaks (maximum $R^2 < 0.35$; Fig. 5-4 and 5-5). The relatively insignificant anthropometric effects may thus be omitted, and the mean response functions of the 10 subjects may be taken to be sufficiently representative of the response characteristics of the seated human body exposed to random vertical vibration.

The resulting mean responses revealed significant influences of the back support and notable effects of hands support, and the input vibration magnitude. All the responses in the vertical axis depicted a 'softening' tendency with increasing input vibration (Figs. 4-7 and 5-3; and Table 5-1), while a secondary mode of vibration was noticeable in some of the fore-aft body segment responses under the 0.25 m/s^2 excitation magnitude, which may be attributed to changes in vibration-dependent muscular activity (Seidel *et al.* 1986; Blüthner *et al.*, 1995). In addition, relatively lower inter-subject variability was observed with increase in input vibration magnitude. Considering the relatively smaller effects of excitation magnitude, the mean APMS and transmissibility responses measured under 1 m/s^2 random vibration are considered for further analyses for extraction of the target datasets in the fore-aft and vertical directions. The number of datasets is thus reduced to 54 biodynamic datasets in magnitudes, which is still large for extraction of target functions for the development and verification of bio-dynamic models. On the other hand, the characteristics frequencies (Table 5-1 and 5-2) identified from the APMS and segmental transmissibility responses demonstrate the presence of multiple modes of vibration for different body segments. Hence, it is necessary to exercise care in the

selection of appropriate target functions based on postural conditions while reducing the number of redundant datasets.

5.4.1 Selection of target datasets

Figures 5-6 and 5-7 illustrate, respectively, the mean vertical and fore-aft segmental transmissibility magnitudes at the measured locations on the upper body together with the mean APMS in the corresponding axes with subjects exposed to 1 m/s^2 vertical vibration. The figures show the vertical and fore-aft responses corresponding to four assumed postures including the back support condition and hands position. The results illustrated reiterate the strong influence of the postural conditions in determining the nature of vibration transmitted to segments of the upper body of the seated human. The influence of the hands position is mostly significant when the backrest is in contact with the trunk (SW-B). The SW-B posture reduces peak vertical responses to the head and the secondary peak magnitude at the L5. However, while the fore-aft transmissibility at the C7 is increased in this posture, the opposite trend is observed at the C7 with SW-NB condition. It may thus be concluded that other than the horizontal responses at the head and C7, and vertical responses at the head and L5, the hands position may be considered relatively insignificant for defining target datasets.

Seat APMS and vibration transmissibility in the vertical axis clearly show similar resonance characteristics while sitting erect without a back support (Fig. 5-7). There is also a good match in the primary resonant frequency between the driving-point and body segment transmissibility functions in the vertical axis in the NB postures (Tables 5-1 and 5-2). Among the vertical responses, only the L5 displays a secondary peak in the NB postures around 10 Hz, which is also slightly identifiable in the corresponding seat APMS function. The interaction of the backrest, however, shows interesting

189

characteristics on the responses in the vertical axis. Although the back support reduces the primary magnitude peak near 5 Hz in both the vertical APMS and vibration transmitted to the segments, it does not attenuate the transmissibility above 6 Hz at the thoracic and L3 vertebrae. While there are only little differences in the vertical resonant frequencies amongst the segments' responses in the NB postures, the trunk responses with a back support clearly show differences in the corresponding characteristic frequencies. Interestingly, the primary resonance peak of the vertical APMS in the presence of a backrest (L-B and SW-B) seems to be aligned with those of the C7 and L5 rather than the head, suggesting that the whole body vertical vibration mode responsible for APMS magnitude peak may have greater relationship with the movement of trunk segments than the vertical motion.

The mean responses in Fig. 5-7 further show that sitting erect without a backrest (NB postures) seems to elicit relatively less fore-aft upper body motion except at the head and to a lesser degree at the C7 as suggested in a few reported studies (Matsumoto and Griffin, 1998). However, in the presence of back support, there is an overall increase in the trunk fore-aft transmissibility magnitude, although with considerably lower head fore-aft movement, suggestive of a change in the nature of vibration transmission. Additionally, while the fore-aft transmissibility magnitude at T5 is insignificant in the NB postures, contact with a back support considerably increases the fore-aft motion at the T5 around 6 Hz suggesting upper body pitch about the lower thoracic region in the back supported postures. Similar to the trends observed in the vertical response magnitudes with backrest contact (Fig. 5-6), the peak fore-aft head transmissibility magnitude occurs at a lower frequency than those observed from both the trunk and backrest APMS responses in the L-B and SW-B postures. Furthermore, the peak frequency of backrest

APMS magnitude comparable to those of the fore-aft C7 and T5 resonant frequencies (Fig. 5-7 and Table 5-2) in the back supported postures. These findings suggest a possible change in the nature of vibration transmission through the upper body in the presence of the back support.

Overall, the backrest and hands position are of greater significance to both the vibration transmission properties through the upper body, and the force-motion dynamics at the body-seat interfaces, than the excitation magnitude and anthropometric parameters of the population tested in this study. From this stand-point, an array of target functions based on apparent mass at the seat and backrest, and segmental translational vibration transmissibility in the vertical and fore-aft axes of the male upper body may be extracted from the measured responses emphasising the uniqueness of the most significant factors.

Table 5-3 summarises this matrix derived with the intention of minimising the number of datasets. A total of 26 magnitude-datasets are extracted, 16 in the vertical and 10 in the fore-aft axes. Due to their high sensitivity to both the support conditions, the vertical response at L5 and fore-aft movement at C7 necessitate 4 unique datasets each, for all the four postural conditions tested. Separate datasets for the L-B and SW-B postures have also been extracted for the seat APMS and vertical head and C7 transmissibilities. In most cases, since there was no significant influence of the hands position while sitting erect with no back support, the number of datasets has been reduced to one each for the following responses: vertical – APMS, head, C7, T5, T12 and L3; and fore-aft – head, T5, T12, L3 and L5. Additionally, since the results showed very small inter-vertebral movement in the vertical axis among certain locations in the thoracic and lumbar region (T5, T12 and L3), these datasets were also reduced appropriately, taking into account the back support condition. A similar approach was adopted for the

horizontal responses at T12, L3 and L5. The Appendix summarises the extracted datasets in the form of the mean measured response magnitudes along with their corresponding standard deviations at specific one-third octave frequencies below 20 Hz for each of the four postural conditions considered in this study. The one-third octave scheme was chosen to represent the datasets so as to reduce the number of data points in each response in order to facilitate comparison with other datasets as well as to ensure lower computational requirements when these datasets are employed for development or verification of WBV biodynamic models.

Table 5-3: Response magnitude datasets extracted from the measured apparent mass and body-segment transmissibility functions.

| | Posture | Number of Response Magnitude Datasets | | | | |
| | | Back | | No Back | | Total |
		Lap	SW	Lap	SW	
Vertical Axis	Seat APMS	1	1	1		3
	Head	1	1	1		3
	C7	1	1	1		3
	T5	1 (T5-Lap)		1 (T5-SW)		3
	T12					
	L3	1				
	L5	1	1	1	1	4
Fore-aft Axis	Cross-axis APMS	1		*NA*		1
	Head	1		1		2
	C7	1	1	1	1	4
	T5	1		1		2
	T12	1 (T12-Lap)				1
	L3					
	L5					
					Total	**26**

5.5 Summary

The measured biodynamic responses are systematically analysed in this chapter in order to extract a reduced number of target datasets for development and verification of analytical human body models capable of predicting multi-dimensional movements. The influences of experimental conditions including subject anthropometry, support conditions and excitation magnitude on the measured variables are analysed so as to extract the most appropriate set of target functions. While subject mass showed influences on the peak vertical APMS magnitude, it was found that this was primarily due to a few individuals outside the 70-80 kg mass category. Except at a few segments, both the body mass and sitting height of subjects depicted insignificant effects on the peak APMS and vibration transmissibility responses. Hence the mean response functions of the 12 subjects, with the outliers removed, was considered to be sufficiently representative of the test population which was similar to 50th percentile population in view of body mass. Furthermore, from the apparent mass and transmissibility results in the vertical axis, the human body was found to behave akin to a 'softening' system with increasing vibration input. However, due to the relatively larger inter-subject variability in the responses at the lower excitation levels and the greater potential for injury of biological tissue with increase in vibration magnitude, the mean APMS and transmissibility responses measured under the vibration level of 1 m/s^2 were considered for subsequent analyses, which comprised a total of 54 datasets.

The postural variables including the back support condition and hands position showed varying effects both in response magnitudes and characteristics frequencies. Taking into account the conclusions from the analyses of statistical significance of the support conditions (ANOVA), an array of target functions based on apparent mass at the

193

seat and backrest, and segmental translational vibration transmissibility in the sagittal-plane of the upper body has been extracted from the mean measured responses emphasising the uniqueness of the most significant factors. A total of 26 target functions were extracted from the mean measured magnitude data of 12 subjects exposed to 1 m/s^2 random vertical vibration: 16 in the vertical and 10 in the fore-aft axes. The horizontal responses of the lower thoracic and lumbar torso were small and showed insignificant differences to postural conditions and hence were reduced to one dataset. Similarly the hands position was found to be negligible in the vertical axis at the thoracic and L3 levels, and thus brought down the total number of curves. However, the head and C7 responses necessitated four unique datasets for each of the postural combinations (*viz.*, L-B, L-NB, SW-B and SW-NB) in the vertical and fore-aft axis, while the L5 also showed similar trends only in the vertical motion.

6.   Development of a biodynamic model for vertical WBV simulation

6.1   Introduction

Drivers of work vehicles are commonly exposed to comprehensive magnitudes of low frequency whole-body vibration (WBV), which predominate along the vertical axis in majority of the vehicles. Epidemiological field studies suggest strong relationships between WBV exposure and various health-effects (*e.g.*, Bovenzi *et al.*, 2002; Bongers *et al.*, 1998; Bovenzi and Zadani, 1992), although a definite dose-effect relationship has not yet been identified due to the presence of a variety of confounders (Seidel and Heide, 1986; Lings and Leboeuf-Yde, 2000). It has been widely suggested that biodynamic models of the human body need to be developed for predicting the body's responses to WBV, which could lead to a viable frequency-weighting and exposure risk-assessment methods (*e.g.*, Seidel, 2005). Such models could further help in the design of effective intervention mechanisms, such as suspension seats (*e.g.*, Tchernychouk *et al.*, 2000) and anthropodynamic manikins for assessing vibration isolation performance of suspension seats (*e.g.*, Toward, 2001).

The formulation of effective vibration bio-models, however, necessitates thorough understanding and characterisation of biodynamic responses of the body to WBV, which are known to depend on various anthropometric, postural and vibration-related factors (Wang *et al.*, 2004; Mansfield and Griffin, 2002). These responses have been widely studied experimentally under broad ranges of vibration and postural conditions, and have been expressed by: (i) the force-motion relations at the driving-point (DP), namely, mechanical impedance (DPMI), apparent mass (APMS) and absorbed vibratory power (*e.g.*, Fairley and Griffin, 1989; VIN, 2001a; Wang *et al.*, 2006b); and (ii) functions

describing the flow of vibration "through the body", such as seat-to-head (STHT) and body-segment acceleration transmissibility (*e.g.*, VIN, 2001a; Matsumoto and Griffin, 2001; Paddan and Griffin, 1998). These measurements have provided considerable information on the mechanical properties of the human body exposed to WBV, the influences of posture and vibration-related variables on the properties, resonance frequencies and probable modes of vibration, potential injury mechanisms and frequency-weightings for exposure assessments (Wang *et al.*, 2004; Fairley and Griffin, 1989; Hinz *et al.*, 2002; Mansfield and Maeda, 2005; Rakheja *et al.*, 2006).

A range of biodynamic models of the standing and seated human body have been formulated on the basis of the aforementioned biodynamic responses, namely APMS or DPMI and/or STHT and body segment vibration transmissibility (Fairley and Griffin, 1989; Rakheja *et al.*, 2006; Mertens, 1979; Fritz, 2005; Pankoke *et al.*, 2001; Boileau and Rakheja, 1998). These models may be broadly classified based on the analytical technique employed as being mechanical-equivalent, multi-body dynamic (MBD) models and finite element (FE) models. These analytical categories have been discussed earlier in Section 1.5.1 in this research dissertation in relation to their application(s). The properties and prediction abilities of the reported lumped-parameter mechanical-equivalent models have been reviewed by Boileau *et al.* (1997) and Liang and Chiang (2006). Multi-body and finite element models have been used for predicting vibration-induced relative deflections and stresses in some of the body substructures (Fritz, 2000; 2005; Pankoke *et al.*, 2001; Liu *et al.*, 1998), which are currently impossible to measure *in vivo*.

Owing to their simplicity, the lumped-parameter models have been traditionally applied for the design and assessment of seats, and the development of anthropodynamic manikins (Lewis, 2005; Mansfield and Griffin, 1996). Such models, however, are

considered valid only in the vicinity of conditions upon which their target biodynamic functions had been defined (Boileau *et al.*, 1997; Liang and Chiang, 2006). Moreover, their model structures do not relate to human anatomy and thus cannot yield information pertinent to the deformations of particular substructures or the effects of vibration intensity. It is thus desirable to develop simple and credible mechanical-equivalent biodynamic models of the seated body primarily to be applied for the development of anthropodynamic manikins and coupled seat-occupant simulations.

More complex FE models have been employed to observe deformations and stresses in the vertebrae and inter-vertebral discs (Pankoke *et al.*, 1998; Seidel *et al.*, 2001). Such models, however, have shown limited validity in predicting biodynamic responses of the seated body to WBV and are perhaps not suited for developing anthropodynamic manikins for assessment of seats. Moreover, FE models pose extreme complexities in identification of biological parameters, particularly the dissipative properties.

Alternatively, some multi-body dynamic models have been proposed to study human body movements under WBV. These models generally incorporate anthropometric inertial and visco-elastic properties of selected body substructures and joints (*e.g.* Amirouche and Ider, 1988; Fritz, 1998). The MBD models have been utilised for a variety of applications including the study of upper body responses to shock loads (Luo and Goldsmith, 1991), obtain estimates of frequency-dependent muscle activity (Fritz, 2005), and predict relative displacements between the lumbar vertebrae (Yoshimura *et al.*, 2005). More complex MBD formulations have also been attempted to study inter-vertebral forces (*e.g.* de Craeker, 2003; Verver *et al.*, 2003). It should be noted that the validity of the majority of MBD models in predicting the driving-point and

body segment vibration transmissibility responses, however, has not been thoroughly demonstrated. Moreover, the visco-elastic parameters of the reported models exhibit vastly different properties.

Considering the complex nature of the active human body and the excessive scatter of measured response data found in the literature, it is desirable to develop sufficiently-, but not overly-, simplified biodynamic models that incorporate representative inertial and anthropometric properties along with lumped joint properties. In the seated condition, uniaxial vertical excitation at the seat induces vertical and fore-aft body movements in the sagittal plane (Matsumoto and Griffin, 2001). A sagittal-plane model may thus suffice to enhance our understanding of the two-dimensional movements of the upper body under vertical vibration.

Visco-elastic parameters of biodynamic models have been widely identified through minimisation of errors between the measured and model responses (Griffin, 2001). The choice of the error function, however, may have significant influences on the identified parameters and the performance of the model (Wang *et al.*, 2008). An appropriate error function coupled with a simplified model representing the human structure could help to identify more reliable visco-elastic parameters in an efficient manner. A model thus developed and thoroughly validated could then be used to derive certain responses that might be significant but inaccessible to conventional non-invasive experimental techniques.

This chapter discusses the development of an anthropometric multi-body biodynamic model of the seated human body to study its responses to vertical WBV. A detailed literature survey is presented first based on the aforementioned classification of biodynamic models so as to establish and justify the appropriate technique to be

employed in this research dissertation. The development of the multi-body biodynamic human model is then systematically presented followed by discussions on its results and possible applications.

6.2 Survey of selected biodynamic models of the seated human body

A large number of mathematical models of the seated human-body exposed to WBV have been developed for applications in seating dynamics and for analyses of distributed responses for identified potential risks (*e.g.*, Boileau *et al.*, 1997; Liang *et al.*, 2007; Seidel and Griffin, 2001). These models may be broadly classified based on the analytical technique employed as mechanical-equivalent models, multi-body dynamic models and finite element models. These analytical categories were briefly discussed in Section 1.5.1 in relation to their application for biodynamic modelling. The subsequent sections discuss important features and limitations of selected models in view of their applicability, and to build upon the criterion for deriving a more effective model in this dissertation research.

6.2.1 Mechanical-equivalent models

The simplistic analytical approach in WBV has been to reproduce the measured biodynamic responses through mathematical derivations rather than represent the complex geometry of the human body (*e.g.*, Fairley and Griffin, 1989; ISO-5982, 2001). Such 'phenomenological' models are generally composed of point-masses connected by linear mass-less spring and damping elements. While most of these lumped-parameter models have no anthropometric representation, a few biomechanical models with link-segment definitions have been employed for simulating the body movements (Kim *et al.*,

2003; Matsumoto and Griffin, 2001) and for prediction of spine forces under quasi-static conditions (Hinz *et al.*, 1994; Seidel *et al.*, 1997).

Boileau *et al.* (1997) analysed the relative performance of several reported formulations, where the DPMI and STHT functions extracted from selected models were statistically compared to the biodynamic response data synthesised in the international standard, ISO 5982 (2001). It was found that only a few of the reviewed models yielded a sufficiently acceptable match with the responses synthesised from the measurements. Similarly, it was also shown in a comprehensive study by Liang and Chiang (2006) that only a few of the reported multiple degrees-of-freedom (DOF) mechanical-equivalent vertical-axis models (Muksian and Nash, 1974; Wan and Schimmels, 1995) could reproduce the corresponding biodynamic functions. These studies suggest that only a few of the reported models could be considered suitable for further applications in WBV (e.g., simulating pregnant women, Liang *et al.*, 2007). The differences among the measured and model responses may, in large part, be due to the inability of the model to represent the experimental conditions employed in the acquisition of the corresponding target datasets (*e.g.*, Nawayseh and Griffin, 2004).

The majority of the mechanical-equivalent models have been constructed with little or no consideration for human anthropometric or postural parameters (Liang and Chiang, 2006), which seriously limits the applicability of these models. However, with the inclusion of information in the form of link-lengths between the lumped inertial segments, these models may be expanded to reproduce planar coordinates. Selected mechanical-equivalent models with multiple DOF's which are of interest to the development of the biodynamic model in this study are discussed further in this section, and the important features of these models are summarised in Table 6-1.

Table 6-1: Summary of the features of selected mechanical-equivalent and Finite Element models from the literature.

	Author	No. of inertial bodies	Interface(s) S: Seat, B: Back	Posture	Anthropometry source (mass in kg)	Joint Parameter Identification	Responses reported (axis)	Resonance frequencies (Hz)	Datasets used for parameter identification
Mechanical-equivalent Model									
	Cho & Yoon (2001)	3	S, B	Inclined	Model response matching and literature (≈ 56.8)	Optimisation: Genetic Algorithm	Head (Z), Cushion Seat and Back (Z)	≈ 4	Responses: Head, hip, back
	Matsumoto & Griffin (2001)	4	S	Erect	Databases and reported studies (83.6)	Optimisation: non-linear search	APMS (Z), body segment (X, Z)	5.66	APMS, segment transmissibility (Matsumoto and Griffin, 1998)
	Keller et al. (2002)	7	-NA-	-NA-	Reported studies (representative of 70 kg male)	Reported studies.	Displacement transmissibility (PA, FE, Axial)*	4.2	Impact and PA* lumbar data
	Kim et al. (2003)	4	S, B	Normal inclined	Taken from seat mannequin (63.92)	Measured on components of mannequin	Hip (Z)	5.5, 7.5	Hip response of seat mannequin
Finite Element Model									
	Kitazaki & Griffin (1997)	33	S	Erect, normal, slouched	Reported studies (60.046)	Reported studies	APMS, STHT (Z), L3 (X, Z) Mode shapes below 10 Hz	5.25 (Erect posture)	APMS and body-segment transmissibility
	Pankoke et al. (1998), Seidel et al. (2001)	14	S	Standard, bent forward, relaxed	Reported databases (74.97)	In vitro studies and fitting DPMI, STHT	DPMI, L4, dynamic force at L5-S1 joint	≈ 5	DPMI
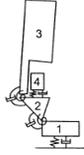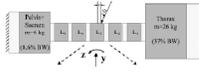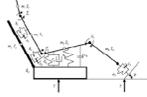
* Terms specific to biomechanics. PA: Posterior Anterior (Biodynamic X-Axis), FE: Flexion-Extension (Pitch), Axial (Z).

A number of mechanical-equivalent model structures with multiple DOF's were attempted by Matsumoto and Griffin (2001) before arriving at two configurations for representing the measured pitch-plane movement of the seated human body under exposure to vertical vibration (Matsumoto and Griffin, 1998). An optimisation approach based on the error-minimisation of seat apparent mass response employed to identify the visco-elastic parameters of the joints yielded a good match with the measured APMS. However, when compared with vibration transmissibility measured at different locations (Matsumoto and Griffin, 1998), the models seemed to overestimate vibration transmitted to the body segments and showed poor phase response results.

Adopting a similar optimisation-based technique, a coupled seat-human model was developed by Cho and Yoon (2001) to represent the pitch-plane motion of the human body seated on a cushioned seat with backrest interaction. The location of the visco-elastic cushion-body interfaces at the seat and backrest were obtained from static pressure concentration areas identified on the seat with seated human subjects. Measured responses in terms of acceleration transmissibility at the head, back and hip were utilised in the error function to identify visco-elastic joint parameters in the model. Although the authors observed that inclusion of force elements at the backrest-body interface significantly improved the performance of the model, no biodynamic responses in the fore-aft axis were reported. It must be noted that even while these models are not structurally comparable to the human anatomy, such low order formulations may help in understanding the nature of biodynamic responses from a whole-body perspective with relative ease. Sufficiently validated mechanical-equivalent models may then be applied for studying the interaction of human-seat interface and for design of seating systems (Boileau *et al.*, 1997).

The analytical approach for the simulation of a human mannequin on a cushion seat proposed by Kim *et al.* (2003) involved a biomechanical model with four distributed masses connected to each other by rotational springs. The stiffness and damping values of the joints were extracted from a physical "H-point" dummy used for seat testing. Additionally, coefficient values for the translational visco-elastic elements at the seat and backrest interfaces were obtained from static pressure measured with human subjects at the seat interface. However, the analytical model validated using static deflections of the physical dummy has yet to prove its applicability to dynamic inputs. In addition, the comparison of initial equilibrium conditions with another simple physical dummy model may be insufficient for representation of the nonlinear human body exposed to WBV.

Majority of the mechanical-equivalent models developed for WBV applications are not only phenomenological in nature, but also do not directly account for experimental parameters including postural, seating and excitation conditions. In addition, the multi-dimensional movements of different body segments are difficult to capture using such simple derivations (Matsumoto and Griffin, 2001; Wei and Griffin, 1998). Nevertheless, the inherent simplicity of such formulations requiring very little computational power offers considerable ease in realising quick solutions in order to extract important resonance characteristics. Owing to these feature, a variety of mechanical-equivalent models have been developed and successfully employed for applications in clinical therapeutics (*e.g.*, Keller *et al.*, 2002; Nicholson *et al.*, 2001) and exercise biomechanics (*e.g.*, Kim *et al.*, 1994; Liu and Nigg; 2000; Nigg and Anton, 1994). While the direct application of such biomechanical models to WBV may be inappropriate, some of the analytical techniques employed therein may be found useful in the development of more effective formulations for the study of whole-body vibration

biodynamics. For example, the interesting joint architectures proposed and the parameter values derived by some of the studies in biomechanics (*e.g.*, Keller *et al.*, 2002; Nicholson *et al.*, 2001) may be incorporated into biodynamic models.

6.2.2 Finite element models

At present, the finite element (FE) method is the only analytical approach available to observe localised deformations and stresses in biological structures (Table 1-2). This feature is considerably significant to the understanding of the nature of damage to spinal tissue due to WBV and the associated health-risk factors (Dolan and Adams, 2001). However, along with this enhanced ability come the challenges involved with modelling highly non-linear biological elements. In addition, the high degree of scatter in the published data on measured tissue properties such as stiffness and damping values of vertebral discs (*e.g.*, Berkson, 1977; Markolf, 1970; Panjabi *et al.*, 1976), widely used for verification of finite element bio-models, poses a considerable impediment to making reliable judgments based on the results from such models. While a number of FE biomechanical models with varying levels of complexity have been put forth, the vast majority of these have been primarily concerned with the development of highly-refined representations of the individual vertebral units to study localised phenomena such as the nature of loading and fracture of end-plates (*e.g.*, Natarajan *et al.*, 1994; Shirazi-Adl *et al.*, 1986; Shirazi-Adl, 1991 and 1992; Yan and King, 1984). Additionally, the FE models of the spine that incorporate muscle force prediction capabilities (*e.g.*, Bazrgari *et al.*, 2008; Rohlmann *et al.*, 2006) have been developed for simulating quasi-static movements in biomechanics and are thus limited in their application to WBV. The features of the few finite element models of the entire human body that have been developed specifically for WBV applications are summarised in Table 6-1 and discussed in this section.

The finite element bio-model developed by Buck and Wölfel (1996; 1997) with detailed vertebral elements was originally formulated with capabilities for expansion into different anthropometric categories. Enhancements to this model were further made by Pankoke *et al.* (1998) by introducing individual vertebral and visceral elements in the lumbar region. The visco-elastic parameters of the model were obtained from the then available literature (Berkson, 1977; Schultz, 1979) and by fitting the model's biodynamic responses to human subject measurements. While the model showed acceptable DPMI responses below 7 Hz there were considerable deviations in the predicted STHT and high frequency responses. These response errors could be attributable to oversimplifications in the form of modal damping values and linearisation of muscle force elements. This reduced model, however, has been employed for a wide range of applications including the extraction of vibration responses at different body segments and estimation of vertebral forces (Pankoke *et al.*, 2001). Furthermore, Seidel *et al.* (2001) exploited the versatility of the model to systematically study the effects of posture and anthropometry on vibration responses and the prediction of possible health risks. Groups of seated human models of five different body sizes were developed in this study (Seidel *et al.*, 2001) to calculate the static and dynamic vertebral force components under vertical WBV. Considerable dependence of the shear loads was observed on the body height and mass properties, while the STHT response magnitude was primarily determined by the postural condition. In addition, the levels of internal forces at the lumbar region suggested overloading of the spinal units, a potential health risk factor.

The whole-body FE formulation developed by Belytschko and Privitzer (1978) with lumped nodal properties was modified by Kitazaki and Griffin (1997) in order to identify the vibration modes of the seated body exposed to vertical seat excitation. The

visco-elastic parameters of this sagittal-plane model were adjusted to match the measured apparent mass responses and experimentally computed body modal parameters (Kitazaki and Griffin, 1998). Two principal resonances at 5.06 and 8.96 Hz were observed in the modified model with coupled visceral movements around the latter frequency mode. Due to the formulation of the spine as a continuous system and the absence of other body elements such as the upper and lower extremities, this model offers limited scope for further applications such as the investigation of influences due to support conditions.

In summary, the complexity of the FE approach poses substantial challenges to the identification of reliable parameter values for the, sometimes numerous, force elements incorporated therein to represent the biological tissues. In addition, most of the FE models are yet to be validated in a comprehensive manner due to the lack of reliable experimental data on localised vibration responses. With our present level of understanding on the reasons for low back-pain and spinal injuries due to vibration exposure and postural conditions, FE models may have limited applicability, not to mention computationally very demanding, for the study of whole body biodynamics.

6.2.3 Multi-body dynamic models

Multi-body dynamic (MBD) models are composed of discrete inertia segments connected by kinematic joints sometimes incorporating force elements. While the majority of MBD models of the human body have been developed for the study of occupant responses to vehicular crash using rigid inertia segments (*e.g.*, ERL, Jödicke, 2001; TNO Automotive, 2001), a number of kinematic models have also been formulated for the study of body movements for occupational applications (*e.g.*, BHMS; Judic *et al.*, 1993; Reed and Schneider, 1996; Safeworks; Technomatix-Jack; van der Meulen and Seidl, 2007). Although these models possess the necessary anthropometric parameters to

represent the human structure, most of them are inapplicable for the derivation of biodynamic responses due to insufficiencies in the joint architecture. On the other hand, a number of multi-body models with visco-elastic and nonlinear definitions for spinal joints have also been developed for body movement studies, such as gait analysis, primarily for commercial applications (*e.g.*, Härtel and Hermsdorf, 2006; McGuan, 2001). Although some of these human-body biomechanics models have been modified for use in WBV environments (*e.g.*, Verver *et al.*, 2003), dedicated MBD formulations of the whole-body have also been developed specifically for biodynamic studies. This section discusses selected multi-body models applicable to WBV studies.

Table 6-2 summarised the key features of the selected MBD formulations. Using anthropometric data from an automotive crash test dummy (Wisman, 1983), a 13-segment pitch-plane sitting human model was developed by Amirouche *et al.* (1988) with linear joint stiffness and damping properties. The values for the visco-elastic parameters were chosen so as to match acceleration transmissibility measurements at the lumbar level reported by Panjabi *et al.*, (1986). The optimised model revealed a whole-body vertical vibration mode at 4.8 Hz and a trunk pitch mode near 2 Hz, about the lower lumbar region. A similar approach has been adopted in a recent study for the analysis of postural effects on biodynamic responses (Teng *et al.*, 2006), which showed higher peak values for transmissibility magnitudes to the head and lumbar segment while sitting erect, in comparison to a relaxed posture.

Table 6-2: Summary of the features of selected multi-body dynamic (MBD) models from the literature.

	Author	No. of inertial bodies	Interface(s) S: Seat, B: Back	Posture	Anthropometry source (mass in kg)	Joint Parameter Identification	Responses reported (axis)	Resonance frequencies (Hz)	Datasets used for parameter identification
	Amirouche & Ider (1988)	13	S	Erect	Hybrid III crash test dummy (74.05)	Chosen to match experimental responses	Head (Z), Lumbar segment (Z, pitch)	2.18, 4.86	Lumbar responses (Panjabi *et al.*, 1986)
	Fritz (1998)	16	S, Steering Wheel	Erect	Cadaver data (74)	*In vitro* spine properties (modified)	APMS, dynamic force at vertebrae (Z).	4-5	Lumbar responses (Panjabi *et al.*, 1986)
	De Craeker (2003)	18 (no head)	S	Erect	Cadaver data (50th percentile male)	*In vitro* spine properties	Head (Z)	≈ 6	STHT-Z
	Verver *et al.* (2003)	Spine-RAMSIS Model	S, B	Normal	MADYMO human model (75.7)	In-built in RAMSIS	Vertebral disc compression, shear	6, 8 at head with backrest	Vertical responses at: head, T1, Pelvis
	Kim *et al.* (2005)	6	S	Normal	Other models (71.32)	Optimisation: Genetic Algorithm	Head (Z, pitch), APMS.	4.8, 5.35, 8.34	APMS, STHT-Z,
	Yoshimura & Nakai (2005)	8	S	Erect	Other models (-NA-)	Optimisation: Genetic Algorithm	L1, L5, relative lumbar displacement (Z)	4.3, 6.8, 13.9	Lumbar responses
	Teng *et al.* (2006)	15	S	Erect	Hybrid III crash test dummy (75.92)	-NA-	STHT (Z), Lumbar segment (X, Z, Pitch)	≈ 4	Lumbar responses (Panjabi *et al.*, 1986)
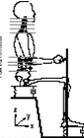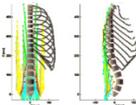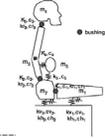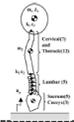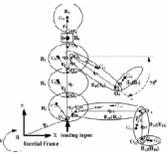
Luo and Goldsmith (1991) proposed a multi-body head-spine model incorporating inter-vertebral discs and non-linear muscle force elements for shock-load simulation typical in automotive crash. The vertebral units of the lumbar and cervical spine were represented by visco-elastic parameters whose values were obtained from the cadaver data (Panjabi *et al.*, 1976; Markolf, 1970), but scaled in accordance with the reported disc cross-section area at different levels of the spine (Yamada, 1970). Further enhancements were made to this model by Fritz (1998) by incorporating non-linear force elements for the cervical and leg musculature (Fritz, 2000) and employed for the derivation of WBV biodynamic responses. The model has also been exploited to obtain estimates of vibration transmission to different segments under sitting and standing postures, frequency-dependent muscular activity (Fritz, 2000; Fritz, 2005) and for definition of a health risk frequency-weighting method based on the derived joint forces (Fritz *et al.*, 2005). This multi-body approach, with the requisite number of body segments and joints, is sufficient and far more efficient in providing reasonable results on human responses to vibration than an overly complex finite element model. It must, however, be noted that other than a comparison with the seat APMS, and STHT response reported in the international standard (ISO 5982, 2001), a thorough validation of this model's biodynamic responses and muscle behaviour is lacking.

Attempts at developing more sophisticated multi-body models with detailed representations of the entire spine with muscle forces have met with limited success. One such formulation by de Craeker (2003) exhibited poor predictions of transmitted vibration to the head compared to a simplified mechanical-equivalent model of the spine, in the seated posture. Furthermore, a hybrid approach integrating a finite element representation of the body surface (skin tissue) and a multi-body model of the entire

skeletal spine was employed by Verver *et al.* (2003) to predict dynamic axial and shear forces at all the spinal units. While the resonant frequency of the model compared well with experimental results, acceleration transmissibility magnitude "through-the-body" was overestimated. A simplified approach has, thus, been adopted in some other studies by modelling only the essential body segments that are thought to undergo relatively higher motion under WBV.

Kim *et al.* (2005) showed that a multi-body model structure including the head, torso with a lumped visceral mass at the abdomen, along with pelvic and thigh segments could efficiently represent multiple biodynamic functions. With five lumbar segments positioned in accordance with the postural conditions of the subjects tested in the vibration experiments, the 10-DOF model developed by Yoshimura *et al.* (2005) was employed to study relative displacements among the lumbar vertebrae. While relative motion in the sagittal-plane were high among these vertebrae around the primary resonance near 6 Hz, the L5-sacrum joint showed greater magnitude at higher frequencies (around 14 Hz) suggestive of separate vibration modes in the lower torso in this frequency range.

6.2.4 Summary of modelling methodologies

It is essential to incorporate sufficient numbers of individual body segments and multi-dimensional joint definitions in a multi-body biodynamic formulation so as to ensure that the model is capable of reproducing the bi-dimensional pitch-plane movements of the upper body exposed to vertical seat vibration (Hinz *et al.*, 1988). However, there is a dearth of information on the visco-elastic properties of tissues due to difficulties in the corresponding biological measurements. Additionally, there is a lack of sufficient measured biodynamic datasets for localised body segments which are essential

for the verification of multi-dimensional MBD models. A more pragmatic approach may thus be the development of biodynamic models that have the required DOF's, while maintaining an anthropometric representation of the human body, along with the capabilities to predict vibration transmission to the most affected segments of the human body (*e.g.*, lumbar or cervical spine). This would prove to be computationally less demanding, and may provide the possibility of validation with a smaller set of critical biodynamic datasets. Such a anthropometric biodynamic human model, sufficiently verified, may then be employed for a variety of applications including: (a) the extraction of vibratory modes under WBV; (b) the study of distribution of vibration energy in the body as a measure in predicting potential health risks; and (c) the simulation of the vehicular vibration with the human operator.

Based on the classifications presented earlier in this section, models with lumped properties, including mechanical-equivalent models and multi-body dynamic formulations cannot be used directly to predict detailed responses such as vibration-induced stresses, strains and the energy absorption within the biological tissue. For such applications, the finite element approach is more suitable to develop the whole-body model or part of the human system in concern. However, as mentioned earlier the complexity of the human body makes it extremely difficult to reliably identify the mechanical properties of biological tissues, which is very essential for FE definitions. Additionally, the finite element model is a relatively expensive and time consuming affair that is also demanding on computational needs. On the other hand, an anthropometric multi-body model offers reasonably good efficiency, and sufficient complexity and versatility to represent the biodynamic responses of the human body measured at different body locations. Moreover, the availability of comprehensive anthropometric

datasets makes it possible to build versatile MBD models with relative ease. The mutli-body dynamic approach is thus chosen in this research dissertation for the development of the anthropometric biodynamic model of the 50th percentile seated male human body on the basis of the target data sets described in chapter 5.

6.3   Formulation of the biodynamic model

In this study, an anthropometric multi-body dynamic (MBD) human model was formulated to depict the sagittal-plane vibration characteristics of a 50th percentile male human body seated in an erect-back posture without a back support, with the hands placed on the lap and exposed to vertical excitations from a rigid seat. This posture is equivalent to the L-NB conditions used in the measurements, as described in chapters 3, 4 and 5. Since this posture is commonly employed in majority of the reported experimental biodynamic studies, the chosen L-NB configuration would facilitate in comparisons of the responses of the developed model with the reported biodynamic measurements.

The MBD model was developed using the MSC-ADAMS (2007) software platform, while the model structure was formulated so as to derive biodynamic responses considered in the experiments. For this purpose, the model structure included rigid bodies representing the head, thoracic, lumbar, sacro-pelvic and thigh segments of the body in order to obtain the apparent mass and vibration transmissibility responses to vertical vibration.

Figure 6-1(a) illustrates the structure of the model with comprising a total of 14 body inertial segments coupled using different types of joints. The body is composed of five separate mass elements representing the head, neck, upper torso (thorax), middle torso (lumbar region) and lower torso (sacro-pelvic unit). This model configuration was based on the Hybrid III human mannequin (Amirouche and Ider, 1988) widely used for

simulating automotive crash scenarios. An additional lumped-mass element representing the abdominal viscera was included in the lumbar region of the model to account for a secondary resonance peak frequently observed in the driving-point apparent mass measurements in the range of 8-12 Hz.

Owing to the supposedly insignificant effects of the hands and legs on the measured driving-point responses, a number of analytical models have neglected these elements by incorporating their mass within the segments of the torso (Table 6-3). While the contribution of the inertias of these segments may be insignificant to the biodynamic responses in the L-NB posture, the effect of constraints provided by these segments in other postures involving the back and hands supports may not be negligible. As an example, the differences in vertical vibration transmitted to the head due to hands placed on the lap and holding a steering wheel was found to vary significantly, especially in the presence of a back support (Wang *et al.*, 2006a). The model structure proposed in this research dissertation is envisioned for applications including the study of postural aspects and coupled human-seat environments in the future, where the inclusion of its extremities may become necessary. Two segments for the arms and legs, each, are thus included for each side of the human body. On either side, the arms and legs are modelled with an upper and lower segment lending eight rigid bodies in the formulation with a total of 19 degrees-of-freedom (DOF).
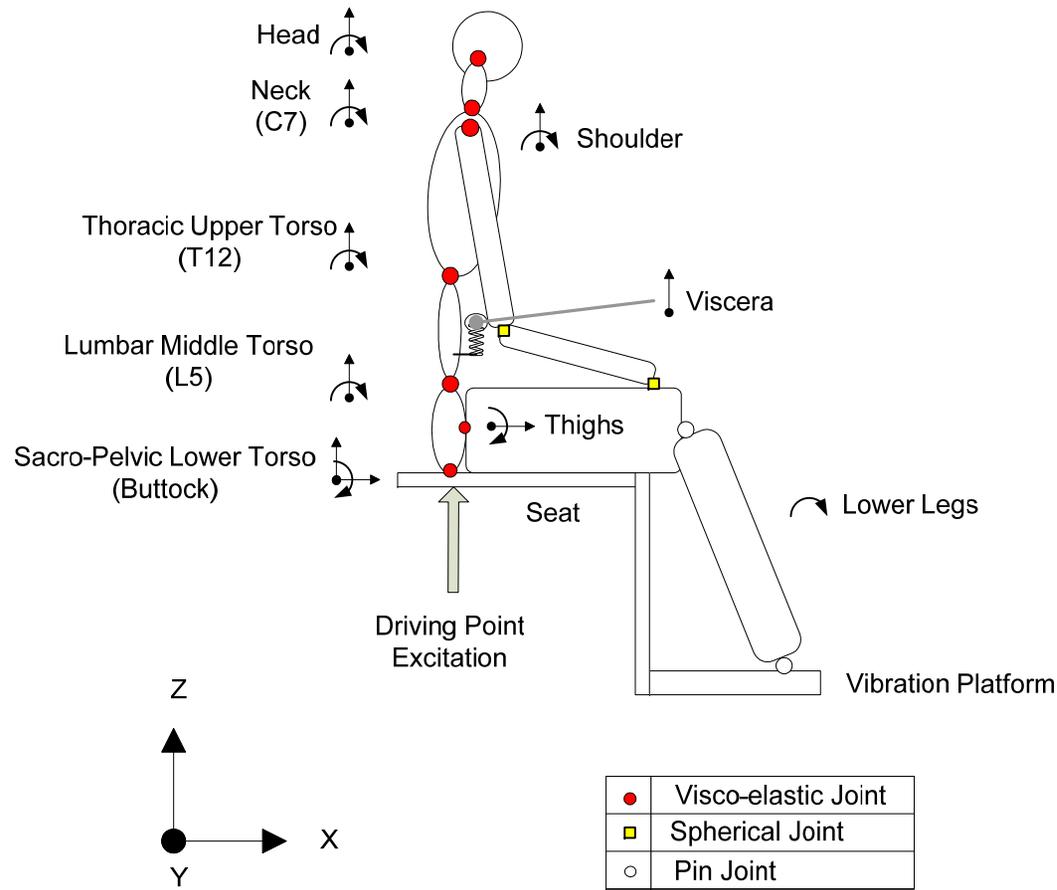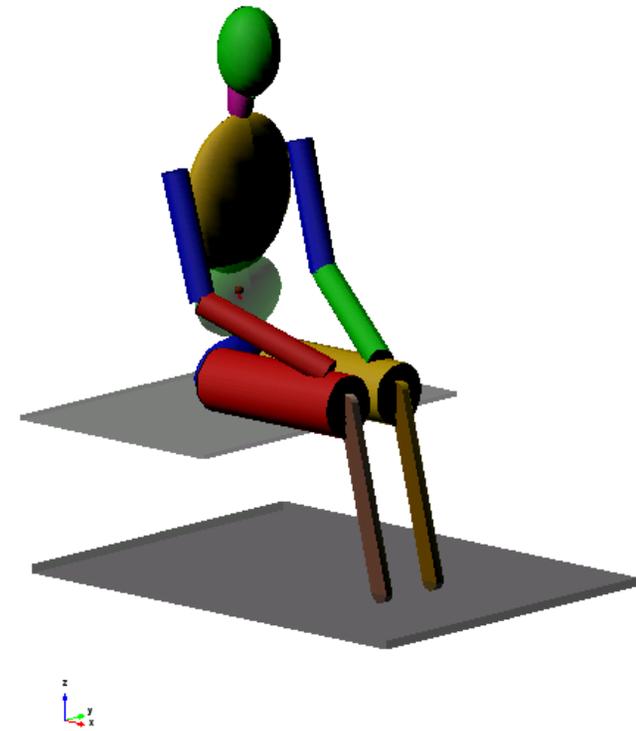
Figure 6-1 (a): Illustration of the seated human multi-body dynamic model showing its segmental degrees-of-freedom at the mid-sagittal plane; (b) Snapshot from MSC-ADAMS platform showing the human model seated without a back support.

214

6.3.1 Joint definitions

Simplistic formulations of the model were initially attempted to gain an understanding of the definitions for appropriate joint properties for the model. In this process, varieties of joint-types were employed for different segments of the model so as to balance the need for sufficient DOF's and improved computational efficiency. The formulations defined only by force constraints through visco-elastic joints connecting the major upper body segments, including the torso elements and thighs, resulted in an unstable solution. The model was thus reformulated with kinematic constraints for each of its joints.

With the exception of the connections at the elbows, knees and feet, all the other joints in the model are composed of kinematic constraints 'wrapped-around' with force-elements. These joint definitions are formulated with the goal of achieving stable solutions to find the sagittal-plane motion in translation and pitch rotations of the segments of the model. Figure 6-1 (a) illustrates the biodynamic model indicating the main joint types employed to represent the human body's sagittal-plane motion when exposed to vertical seat vibration. In addition, Table 6-3 summarises the location of these joints in the model's basicentric coordinates, which are taken from the GEBOD (Cheng *et al.* (1994) for the 50$^{\text{th}}$ percentile adult male population.

While the pair of hip joints permits relative fore-aft translation between the thighs and lower torso, the buttock joint allows for relative vertical, fore-aft and pitch movements between the seat and lower torso segments. The joints at the head, C7, shoulder, T12, L5 and the wrists are defined for movements among the corresponding segments only in axial translation and pitch rotation. 'Bushing' force elements that possess linear stiffness and damping characteristics in both translation and rotation in all

the three axes, are employed in each of these joints along with kinematic constraints. Biodynamic measurements have revealed insignificant movements in lateral translation (basi-centric Y axis) and yaw rotation (about Z-axis) of the seated body when subjected to single axis vertical excitations, most probably due to relatively symmetric inertial properties about the sagittal plane (*e.g.*, DeLeva, 1996). The seated human model's complexity may, hence, be reduced in order to facilitate the solution process. The joint movements are thus constrained to the sagittal plane, by letting the stiffness properties of each bushing element to be extremely high (in the order of 10^{10} N/m) in the lateral translation (Y-axis), and rotations about the X- and Z-axes. In addition, the relative fore-aft translation (X-axis) of the joints at the head, C7, T12, L5, shoulders and wrists are also limited by letting the corresponding stiffness to similarly high values. However, the buttock joint was permitted to have fore-aft translation relative to the seat, so as to allow the pitch rotation of the pelvis, widely hypothesised to occur under vertical WBV (Zimmermann and Cook, 1997).

In the model, the visceral mass is connected to the lumbar segment by a Kelvin element with a translational constraint so as to permit motion along the Z-axis of the lumbar torso, as illustrated in Fig. 6.1(a). This ensures that dynamic forces due of the visceral mass are aligned to the aforementioned axis representing the spatially-constrained movement of the abdominal tissue within the lumbar torso. Additionally, due to this alignment, geometric changes of the lumbar torso due to postural variations are automatically reflected in the visceral element.

Table 6-3: Anthropometric and inertial properties of the body segments and joint coordinates (Cheng *et al.*, 1994)

Body Segment	Mass	Pitch Mass Moment of Inertia	Location (m)†		
	(kg)	(kg.m^2)	X	Y	Z
Head	5.038	0.031	0.024	0	0.644
Neck	1.293	0.003	0.025	0	0.507
Upper Torso	17.343	0.136	0.012	0	0.275
Mid Torso	1.996	0.033	0.003	0	0.074
Viscera	7.986	-	0.003	0	0.094
Lower Torso	8.570	0.038	0.008	0	-0.048
Thigh (each) (Y is ±)	5.13	0.106	0.207	± 0.060	-0.081
Lower Leg (each) (Y is ±)	10^{-6}	10^{-6}	0.455	± 0.080	-0.256
Upper Arm (each) (Y is ±)	1.991	0.014	0.037	± 0.193	0.253
Lower arm (each) (Y is ±)	1.994	0.010	0.213	± 0.137	0.044
Joint Name	I body	J body			
Head	Head	Neck	0.008	0	0.591
C7	Neck	Upper Torso	-0.001	0	0.473
Shoulder (Y is ±)	Upper Torso	Upper Arm	0.000	0.193	0.377
T12	Upper Torso	Mid Torso	-0.014	0	0.163
L5	**Mid Torso**	**Lower Torso**	**0**	**0**	**0**
Buttock	Lower Torso	Seat	0	0	-0.167
Viscera	Viscera	Mid Torso	0.003	0	0.094
Hip (Y is ±)	Lower Torso	Thigh	0.016	0.080	-0.097
Knee (Y is ±)	Thigh	Lower Leg	0.405	0.080	-0.081
Ankle (Y is ±)	Lower Leg	Vibration Platform	0.505	0.080	-0.488
Elbow (Y is ±)	Upper Arm	Lower Arm	0.076	0.193	0.112
Wrist (Y is ±)	Lower Arm	Thigh	0.350	0.080	-0.023

† Coordinates are defined with respect to the L5 joint

The wrist and elbow connections are modelled by spherical joints to allow for the arm's spatial motion due to lateral differences in the location of the shoulder and knee joints (note the difference in Y-axis coordinates between the shoulder and wrist in Table 6-3). Bushing force-elements are employed for the wrist and shoulder joints so as to stabilise the movement of the segments of the hands. Further, these formulations also allow for the extendibility of the model in the future for study of different hands positions where the stabilising muscular activity may significantly affect the vibration transmissibility through the body (Wang *et al.*, 2006a). Pin joints (hinges) have been employed to represent the knee and foot–base (ankle) constraints since these are not expected to play a significant role in determining the dynamic response of the model when exposed to vertical vibration (Fairley and Griffin, 1989). It should be noted that while the muscles act as effectors and controllers in actual human movement, the properties of the muscles are partially represented in the model by the passive visco-elastic elements at the joints.

6.3.2 Method of solution

The biodynamic model of the seated body exposed to vertical vibration is constructed using the multi-body dynamic code MSC-ADAMS (2007), so as to provide the possibility to extend the reach of this research work to the industrial environment where this software package is well-established for human biomechanics as well as for product design. The differential equations of motion for the model are expressed in the generalised form:

$$\{q\} = [M]\{\ddot{X}\} + [C]\{\dot{X}\} + [K]\{X\} \qquad (6.1)$$

Where $[M]$, $[C]$ and $[K]$ are the (nxn) mass, stiffness and damping matrices, $\{X\}$ is the $(nx1)$ vector of generalised coordinates considered at the centre of mass of the body segments, and $\{q\}$ is the forcing vector, which is a function of the seat motion. n is the number for DOF of the model, which is in this case 19. The equations are solved using the GStiff integrator in MSC-ADAMS. Initial values for the model's joint visco-elastic parameters and inertial properties (Table 6-3) have been derived from the reported anthropometric studies and measured biomechanical tissue properties (Tables 6-1 and 6-2). The model subjected to static settling tests showed stable response properties with the chosen model parameters. Although the selected values showed considerable response discrepancies between the model's biodynamic results and the measured responses presented in chapter 4, they serve in establishing approximate ranges for the visco-elastic coefficients.

The model is analysed under vertical sinusoidal displacement excitation at the seat platform swept in the 0.5 to 15 Hz frequency range, while the displacement amplitude corresponding to each excitation frequency was selected to achieve a flat 1 m/s^2 RMS acceleration spectrum to simulate the conditions of the experiment (Chapter 3). The equations of motion are linearised and solved in the frequency domain with the assumption of small joint motions, about an operating point established by a static analysis.

6.4   Model parameters

The inertial parameters of the body segments are taken from the reported anthropometric data, while the visco-elastic properties of various joints are identified through minimisation of errors between the model responses and the measured data.

A number of studies have reported the mass and moments of inertia of various body segments obtained from human cadavers or indirectly from anthropometric measurements on human subjects (*e.g.*, DeLeva, 1996) across different continents. There is a noticeable degree of variations in anthropometric properties of different population. However, taking into account a number of such datasets, a computer programme, Generator of Body Data–GEBOD, has been developed by Cheng *et al.* (1994) to provide the anthropometric properties of the human body or an anthropomorphic dummy, with user inputs in terms of gender, age, body mass and height. The geometric and inertial parameters of the body segments for the multi-body model developed in this dissertation research were conveniently identified using the GEBOD programme for an average body mass of 75.57 kg, standing height of 1.75 m and 30.27 years age, which represents the population chosen for the experimental study (Table 3-1) and approximately the 50th percentile male population.

Table 6-3 summarises the parameter values provided by the GEBOD database including each body segment's mass, its mass moments of inertia about the pitch axis, the coordinates of the centre of mass for each segment and the location of the joints connecting the segments. The thoracic region of the torso understandably shows the greatest segment mass (17.34 kg) due to the heavy skeletal structures of the rib cage, sternum and the longest portion of the spine with 12 vertebral elements. The skeletal part of the mid torso (lumbar region), on the other hand, is composed only of the lumbar vertebra, while the majority of the inertia is derived from the organs and tissue housed in the abdominal cavity (the viscera), which alone accounts for about 10 kg in the 50th percentile male population. Hence, the total lumbar segment mass has been partitioned in this model between the visceral mass (80%) and the lumbar skeletal structures (20%)

based on the reported mass properties of the lumbar vertebrae. The lower torso, weighing 8.57 kg, comprises of heavy spinal structures, including the sacrum and pelvis, which take up the static and dynamic loads of the upper body. Since the inertia of the lower leg (knee to foot) is known to have negligible effects on the biodynamic functions measured under vertical vibration on a rigid seat (Fairley and Griffin, 1989), an insignificant mass of 1 mg each was assumed for the two lower leg segments so as to eliminate singularity in the solution due to a zero value in the major diagonal of the mass matrix. Furthermore, the mass due to the thigh segments was adjusted to obtain the total model mass equal to the mean measured body mass supported by the seat, which is in the order of 74% of the total body mass (Fairley and Griffin, 1989). This model mass value of 55.45 kg also compared quite well with the mean measured APMS magnitude at the low frequency of 0.5 Hz (54.72 kg, Fig. 5-2a).

6.4.1 Identification of visco-elastic joint parameters

Figure 6-1 (a) illustrates the model structure including the joint's inherent DOFs. The challenging task of identifying appropriate visco-elastic parameter values for joints in biodynamic models is a widely reported issue in many analytical WBV studies (*e.g.*, Kim *et al.*, 2005). Due to the large number of assumptions made in order to simplify the structure of multi-body biodynamic human models, it is not possible to directly utilise the mechanical properties measured from the human cadaver spines. Most studies thus employ some form of a parameter-search approach to identify the unknown values in the formulation. It is common to employ an optimisation-based technique that minimises the error between the chosen biodynamic response(s) of the model and the corresponding measurements so as to identify the model's unknown parameter values. This is an acceptable methodology given the limited availability of reliable visco-elastic properties

of biological tissue and the large variability found in the mechanical properties of the spinal substructures reported by different studies (*e.g.*, Panjabi *et al.*, 1976; Markolf, 1970).

The complexity of the minimisation problem in such studies, however, depends on the number and types of target biodynamic functions. The vast majority of the reported studies consider the measured vertical apparent mass as the target function (*e.g.*, Boileau *et al.*, 1997), while a few have taken STHT as the target function (*e.g.*, Cho and Yoon, 2001). It has been shown that the apparent mass function yields rapid convergence of the minimisation problem, while the APMS alone may not describe the contributions of low inertia upper body segments to the total response (*e.g.*, Wang, 2006).

In this study, the parameter identification is undertaken by considering multiple biodynamic response functions, namely the apparent mass, and vibration transmitted to various body segments along the X- and Z- axis. These target functions have been described in chapter 5. While the consideration of multiple target functions yields more complex minimisation problem, the resulting solutions could be more unique compared to the models based on a single target function.

The minimisation task involves identification of a total of 32 parameters that are denoted in Table 6-4. In the table, the variables beginning with 'K_' and 'C_' represent, respectively, the stiffness and damping characteristics in vertical (axial) translation defined at majority of the joints, 'Kx_' and 'Cx_' denote the visco-elastic properties in the fore-aft translational axis at the buttock interface and pelvic-thigh joints. Similarly, the variables 'Kr_' and 'Cr_' are used to apply force constraints for pitch rotations at the upper body joints. The vector of unknown model parameters β is thus defined using the stiffness and damping variables as:

$$\{\beta\} = \{\beta_K \quad \beta_C \quad \beta_{Kr} \quad \beta_{Cr}\} \tag{6.2}$$

Where the individual component vectors, $\{\beta_K\}$, $\{\beta_C\}$, $\{\beta_{Kr}\}$ and $\{\beta_{Cr}\}$, indicated as the "Variable Vector" in Table 6-4, may be defined by the variables in each column of the table, respectively. Hence,

$$\{\beta_K\} = [\quad K\_head \quad K\_C7 \quad K\_shoulder \quad \dots \quad Kx\_butt \,]$$

$$\{\beta_C\} = [\quad C\_head \quad C\_C7 \quad C\_shoulder \quad \dots \quad Cx\_butt \,]$$

$$\{\beta_{Kr}\} = [\quad Kr\_head \quad Kr\_C7 \quad Kr\_shoulder \quad \dots \quad Kr\_wrist \,]$$

$$\{\beta_{Cr}\} = [\quad Cr\_head \quad Cr\_C7 \quad Cr\_shoulder \quad \dots \quad Cr\_wrist \,] \tag{6.3}$$

The target biodynamic response functions measured for the sitting human subjects, namely the apparent mass magnitude (APMS) at the seat and backrest interfaces, and the body segment acceleration transmissibility in the vertical and fore-aft axes, described in chapter 5, are employed for identification of model parameters and validation of analytical biodynamic model. The target datasets, in conjunction with the model responses are used to formulate a response-based error function whose value may be minimised by searching for optimal values for the parameter vector $\{\beta\}$.

Initially, ranges of values for the stiffness and damping parameters were obtained from the available analytical studies (Tables 6-1 and 6-2) and the biomechanical properties of the spine (*e.g.*, Keller *et al.*, 2002; Panjabi *et al.*, 1976), which were used to gain an understanding of the range of the visco-elastic parameters. These were then- used to define limit constraints determining the upper and lower limits (bounds) for the visco-elastic parameters of the model, such that:

$$\{\beta_{min}\} \leq \{\beta\} \leq \{\beta_{max}\} \qquad (6.4)$$

where,

$$\beta_{max} = \{\beta_{Kmax} \quad \beta_{Cmax} \quad \beta_{Krmax} \quad \beta_{Crmax}\}$$

$$\beta_{min} = \{\beta_{Kmin} \quad \beta_{Cmin} \quad \beta_{Krmin} \quad \beta_{Crmin}\}$$

Where, suffixes *max* and *min* denote the limits for the parameter values defined.

Table 6-4: Variables representing the joint visco-elastic parameters of the biodynamic seated human model

Joint	Translational		Rotational	
	Stiffness (N/m)	Damping (Ns/m)	Stiffness (Nm/rad)	Damping (Nms/rad)
	Vertical (axial)		**Pitch**	
Head	K_head	C_head	Kr_head	Cr_head
C7	K_C7	C_C7	Kr_C7	Cr_C7
Shoulder	K_shoulder	C_shoulder	Kr_shoulder	Cr_shoulder
T12	K_T12	C_T12	Kr_T12	Cr_T12
L5	K_L5	C_L5	Kr_L5	Cr_L5
Buttock	K_butt	C_butt	Kr_butt	Cr_butt
Viscera	K_viscera	C_viscera	-	-
Wrist	-	-	Kr_wrist	Cr_wrist
	Fore-Aft			
Hip	Kx_thigh	Cx_thigh	-	-
Buttock	Kx_butt	Cx_butt	-	-
Variable Vector	β_K	β_C	β_{Kr}	β_{Cr}

6.4.2 Definition of biodynamic response error-functions

The scalar error (E_K) of a particular biodynamic dataset (K) can be expressed as a function of the afore-mentioned visco-elastic parameter vector (β), as the sum of the squared error between the measured and corresponding model responses at each discrete frequency, such that:

$$E_K(\beta) = \sum_{f=0.5}^{20} \left(K_T(f) - K_S(f)\right)^2 \tag{6.5}$$

where, subscripts S and T denote the model response and target of the biodynamic response function K, respectively, corresponding to a discrete frequency f.

The MBD model has been developed to represent a human subject sitting on a rigid seat with hands placed on the lap and no back support, while subject to vertical WBV. In keeping with this configuration, the target datasets derived from the human subjects sitting in the L-NB posture (Chapter 5) were selected to define the target and thereby the error functions. Since most of the measured biodynamic responses depict a monotonic behaviour beyond 15 Hz, the error minimisation problem is formulated within the frequency range of 0.5 to 15 Hz. Additionally, the number of sampling points for the target datasets within this frequency range are reduced from 232 to 58 by adopting a frequency resolution of 0.25 Hz (measured resolution: 0.0625 Hz).

The minimisation problem is formulated by considering multiple error functions (E_K) of different biodynamic responses, which include the magnitudes of seat apparent mass and the vertical and fore-aft vibration transmissibility responses measured at different locations (Head, C7, T5, T12, L3 and L5).

It should be noted that the vast majority of the studies have considered only seat APMS for identifying the model parameters (Boileau *et al.*, 1997). Such models thus yield acceptable prediction of APMS response, while considerable errors could be found in other biodynamic responses of the model (Wang, 2006). Furthermore, the resulting model parameters cannot be considered unique solutions of the minimisation problem. It has been suggested that consideration of simultaneously measured multiple biodynamic response functions could help enhance uniqueness of the solutions and prediction ability of the model. The measured biodynamic responses suggest considerable variations in their relative magnitudes. From Fig. 5.2, it can be seen that the magnitude value of the vertical APMS ranges from 15 to 110 kg, while the magnitudes of the transmissibility functions occur within a lower range of 0.1 to 3, in the concerned frequency range. This disparity in the relative magnitudes could bias the parameter search process towards the APMS magnitude error compared to the segmental transmissibility errors. Consequently, the APMS magnitude error function was normalised with respect to the mean sitting APMS value at a low frequency of 0.5 Hz, which resulted in magnitudes comparable to those of the segmental transmissibility magnitudes.

A few studies on the development of mechanical equivalent models have exhibited better matching of apparent mass response with the use of phase error minimisation only (Wei and Griffin, 1998). In addition, the phase could play a significant role in determining the damping properties of the joints in the multi-body model. The phase error functions for the vertical axes responses, APMS and segmental transmissibility, were thus incorporated in the optimisation problem. Due to the excessive fluctuations in the measured fore-aft vibration transmissibility phase, error functions in phase were defined for the vertical APMS and vertical body segment transmissibility

responses. Considering the relatively larger values of the phase response in relation to transmissibility and normalised APMS magnitudes, a weighting was imposed on the phase error functions to ensure their comparable contribution to the composite error function. As an example, the normalised seat apparent mass ($nAPMS$) error function was formulated as:

$$E_{nAPMS}(\beta) = W_M.E_{nAPMS_M}(\beta) + W_P.E_{nAPMS_P}(\beta) \qquad (6.6)$$

where, W_M and W_P are the scalar weightings imposed on the magnitude and phase, respectively, and E_{nAPMS_M} and E_{nAPMS_P} are the errors in the normalised magnitude and phase, respectively. Similarly, the weighted error functions in vertical (Z) and fore-aft (X) acceleration transmissibility for a segment i may be defined in terms of the parameter vector β as:

$$E_{Z_i}(\beta) = W_M.E_{Z_{i_M}}(\beta) + W_P.E_{Z_{i_P}}(\beta) \qquad (6.7)$$

$$E_{X_i}(\beta) = V_M.E_{X_{i_M}}(\beta) \qquad (6.8)$$

Where $E_{Z_{i_M}}$ and $E_{Z_{i_P}}$ are the error in vertical transmissibility magnitude and phase, respectively. V_M is the weighting imposed on the fore-aft response magnitude error, $E_{X_{i_M}}$, and i represents the measured body location, such that: $i = \{Head, C7, T5, T12, L3, L5\}$. The error in a particular body segment response (E_i) may thus be expressed as a sum of the errors in the fore-aft and vertical axes, such that:

$$E_i(\beta) = E_{X_i}(\beta) + E_{Z_i}(\beta) \qquad (6.9)$$

Furthermore, global weighting factors were defined separately for the normalised APMS and body segment vibration transmissibility responses as W_{nAPMS} and W_i, respectively, where i denotes the aforementioned measurement location on the body. The corresponding global weighting variables for the body segments' vibration

transmissibility may be expressed such that: $W_i = \{W_{Head}, W_{C7}, W_{T5}, W_{T12}, W_{L3}, W_{L5}\}$. The composite error function is finally formulated as the summation of the weighted errors in different responses, as:

$$E(\beta) = W_{nAPMS}.E_{nAPMS}(\beta) + \sum_{i=\text{Head}}^{\text{L5}} W_i.E_i(\beta) \qquad (6.10)$$

The global weighs permit for the adjustment of sensitivity of the optimisation process to any chosen response error. As an example, a composite error function in apparent mass and the transmissibility to C7 may be defined by setting the other global weights to zero, *i.e.*:

$$E(\beta) = W_{nAPMS}.E_{nAPMS}(\beta) + W_{C7}.E_{C7}(\beta) \qquad (6.11)$$

for $\qquad\qquad W_{Head} = W_{T5} = W_{T12} = W_{L3} = W_{L5} = 0$

This arrangement allows the above minimisation problem to be solved to identify model parameters, in this example, on the basis of APMS and C7 response errors alone, thus providing the flexibility to define error functions from almost any combination of segmental responses.

6.4.3 Optimisation using Genetic Algorithm

The error minimisation problem, Eqn. (6.10), was solved using the Genetic Algorithm (GA) Toolbox in MATLAB to identify the model parameters on the basis of a total of 20 simultaneously measured biodynamic response functions. These include 13 target functions in APMS and vertical and fore-aft segment transmissibility magnitudes and vertical transmissibility phase. The search process involved simultaneous solutions of the multi-body model in MSC ADAMS and the optimisation problem in MATLAB. The process involved a number of time-consuming trial runs in order to determine a set of GA parameters that could produce an effective and efficient run. The significant parameters

arrived at after these operations are enlisted here. However, it should be understood that these may not necessarily be the most appropriate parameters for a GA problem involving any multi-body biodynamic model.

Population

Population Type   : Double Vector

Size   : 100

Creation function   : Uniform

Initial Range   : Lower and Upper Bounds (β_{min}, β_{max})

Constraints

Bounds   : Lower and Upper Bounds (β_{min}, β_{max})

Fitness Scaling   : Rank

Selection   : Tournament (Haupt and Haupt, 1998)

Size   : 4

Reproduction

Elite Count   : 2

Cross-over fraction   : 0.7

Mutation   : Adaptive Feasible

Cross-over   : Scattered

Migration   : Forward

Fraction   : 0.2

Interval   : 20 (Generations)

Stopping Criteria

Function tolerance   : 10^{-3}

6.5   Model Parameters and Results

The vast majority of the lumped parameter models, with only a few exceptions, have been derived on the basis of APMS alone (*e.g.*, Fairley and Griffin, 1989; Wei and Griffin, 1998). While the APMS response describes the dynamic body-seat interactions at the driving-point alone, the seat to head vertical acceleration transmissibility (STHT) being a "through-the-body" function may account for the vibration modes of the upper body. It has been found in a few studies that consideration of the STHT error function, as opposed to driving-point measure alone, yields better prediction of both the measures (*e.g.*, Wang, 2006; Pranesh *et al.*, 2008). While parameters obtained through APMS error minimisation alone may be sufficient for simple lumped parameter formulations, anthropometric bio-models with multiple DOF's may necessitate the use of error functions based on motion responses of body segments.

The biodynamic responses obtained with subjects sitting erect in the L-NB posture (hands in lap with no back support) under 1 m/s^2 RMS acceleration excitation were considered as the target functions in the composite error minimisation problem. This section discusses the results obtained through minimisation of the error function considering different target functions. Combinations of the measured target dataset were employed in order to identify the error function which could provide model results representative of the human body's vibration responses. Figures 6-2 to 6-12 illustrate the pertinent biodynamic responses obtained from the resulting biodynamic model along with the corresponding measured target datasets for different error functions. Each figure includes comparisons of model and measured responses in terms of the normalised seat APMS magnitude and phase, vertical (Z) acceleration transmissibility magnitude and

230

phase at the head, C7, T5, T12, L3 and L5, and the fore-aft (X) response magnitude at the same segments. The list of error functions employed are summarised in Table 6-5.

Table 6-5: Error functions employed for model parameter identification.

Label	Error Function
EF-1	APMS
EF-2	STHT(Z)
EF-3	APMS + STHT(Z)
EF-4	C7(Z)
EF-5	T5(Z)
EF-6	L3(Z)
EF-7	STHT(X) + STHT(Z)
EF-8	C7(X) + C7(Z)
EF-9	STHT(X) + STHT(Z) + C7(X)
EF-10	STHT(X) + STHT(Z) + APMS
EF-11	STHT(X) + STHT(Z) + C7(X) + APMS

Figures 6-2 and 6-3 illustrate the responses from the model derived by minimising the APMS and vertical STHT (EF-1 and EF-2 in Table 6-5), respectively. As expected, consideration of the APMS error function (EF-1) alone results in very good agreements in driving-point APMS magnitude and phase responses, as seen in Fig. 6.2. This method also yields acceptable degree of agreement in vertical STHT (Head Z) and L5 responses magnitude only up to 6Hz, while the primary resonant frequencies observed in all the

231

vertical responses agree well with those observed in the measured responses. The comparisons show large errors in most of the segment transmissibility responses. The magnitude of errors is significantly higher in the fore-aft transmissibility responses. The model responses generally show a significant secondary peak in the 7-8 Hz frequency range. While this secondary model is also evidenced in a number of measured responses, particularly the phase, the magnitude of error is quite high. The results thus suggest that a model identified on the basis of driving-point responses, the approach employed in majority of the reported models, could yield good prediction of the APMS response alone, with significant errors in the vibration transmissibility responses.

Figure 6-3, in a similar manner, presents comparisons of responses of the model derived through minimisation of the vertical STHT error function alone (EF-2 in Table 6-5) with the measured response. The comparisons show very good agreement between the measured and model STHT response along the vertical axis. A comparison of Figs. 6-2 and 6-3 suggests that the model derived from the vertical STHT target function would yield very good prediction of vertical STHT in the entire frequency range, while the model yields greater deviations in its APMS magnitude and phase response. The model also yields improved estimations of vibration transmissibility of the segments. The results show better agreements of the C7, T5, T12 and L3 vertical transmissibility responses of the model with the mean measured data. Furthermore, the large errors in the vicinity of the secondary peak that was observed in response of the model based on APMS alone (Fig. 6-2) are greatly suppressed by considering vertical STHT response for model verification. The model, however, yields very poor predictions of the fore-aft acceleration transmissibility responses, as observed in the model based on APMS data alone (Fig. 6-2). It is thus concluded that a model based on vertical STHT data would be unsatisfactory for

accurate prediction of APMS and segmental transmissibility responses, particularly along the fore-aft axis.

A target function using the sum of errors of the two aforementioned responses (EF-3: APMS + STHT Z) was subsequently employed to identify the model parameters. Figure 6-4 illustrates the results obtained from the model together with the mean measured responses. The results are comparable to those of the model based on the vertical STHT alone (Fig. 6-3). This may be caused by greater contribution of the transmissibility error in the composite error function, and consideration of alternate weightings may help enhance the model prediction abilities.

While the solutions of the aforementioned three error functions (EF1 based on APMS; EF2 based on vertical STHT; and EF3 based on both the APMS and vertical STHT) resulted in acceptable agreements in some of the vertical responses, all of them converged to highly unsatisfactory behaviour in the horizontal axis. It is evident that any combination of the seat APMS and vertical STHT may not be sufficient to identify model parameters relating to the sagittal-plane motion of the seated human model. The model prediction abilities could be enhanced considering an error function comprising responses measured at other body locations so as to better match its segmental biodynamics, particularly in the fore-aft axis. The measured segmental responses were thus employed to formulate a more complex minimisation function to seek a better method for identifying an effective model for characterising the seated body's vibration characteristics.

The addition of these response functions in the minimisation problem, however, resulted in a far more complex composite function. The solution of such a composite error minimisation problem was thus extensively demanding on computing resources.

233

The model identification process was thus performed in two sequential stages. In the first stage, the vertical segmental vibration transmissibility datasets were incorporated in the composite error function. Both the vertical and fore-aft segmental transmissibility target datasets were employed in the final stage. Although many solutions were obtained by considering different segment transmissibility target data and weightings, the result obtained only from selected combinations are presented and discussed in this section.

The responses of the models identified by minimising the errors in vertical responses of C7, T5 and L3, respectively, are compared with mean measured responses in Figs. 6-5 to 6-7. While the responses of the three derived models consistently revealed better agreements with the respective mean measured responses in the vertical axis, considerable discrepancies could be observed in the vertical L5, STHT and APMS responses apart from the fore-aft axis responses. The minimisation of each of these error functions resulted in better agreements in vertical transmissibility of C7, T5, T12 and L3, while greater errors in STHT, APMS and L5 vertical transmissibility are evident. In addition, the model based on T5 data alone resulted in a more pronounced secondary magnitude peak around 8 Hz in the head, neck and thoracic segment response (Fig. 6-6). Interestingly, however, all the models showed an acceptable match in the vertical responses at the other segments, especially around the primary resonance frequency. Among the three target functions considered, the model based on vertical C7 data alone provided the best agreements with the mean measured vertical transmissibility at the neck, thoracic and L3. The errors in the L5 response and the fore-aft responses, however, are quite significant, irrespective of the target dataset considered.

It is thus deduced that vertical response target functions alone may not be sufficient to represent the two-dimensional sagittal-plane motion of the human body.

234

Alternate composite error functions were thus subsequently formulated to explore fore-aft transmissibility responses for refining the model parameters. A review of the measured fore-aft transmissibility responses suggests more significant motions at the segments above the mid-thoracic (T5) region. The addition of fore-aft responses of segments near and below T5 to the composite error function is thus not expected to yield better convergence. The solutions obtained by considering fore-aft responses alone also revealed significantly large deviations between the mean measured and the model responses. This may be attributed to the exclusion of the fore-aft transmissibility phase data from the error functions. Furthermore, the error functions comprising any combination of thoracic and lumbar segmental targets datasets resulted in comparable model responses.

Figures 6-8 and 6-9 illustrate responses of the models identified considering error functions comprising combinations of vertical and horizontal target responses at the head (EF-7) and C7 (EF-8), respectively. Minimisation of an error function in vertical and fore-aft STHT response resulted in excellent agreement in fore-aft head response, as seen in Fig. 6-8. However, the model's APMS and vertical transmissibility response peaks occur at a relatively lower frequency compared to the primary resonant frequency observed from the mean measured data. The model transmissibility phase responses in the Z-axis also deviate considerably from the corresponding measured responses. The bandwidth of the vertical magnitudes is generally larger than the measured targets, leading to considerable deviations below 10 Hz. A lower frequency peak around 2 Hz is also observed in all the fore-aft responses suggestive of shear in the seat-buttock joint. The vibration response of the model at C7 and thoracic segments along the fore-aft direction also differ significantly from the mean measured responses, as seen in Fig. 6-8.

235

A model derived on the basis of measured response of C7 along the X- and Z-axes (EF-8), on the other hand, yields excellent agreement in C7 responses along both the axes, as seen in Fig. 6-9. The model, however, yields significant error in the fore-aft head vibration response, while it provides relatively lower errors in the vertical segment vibration transmissibility at all locations, with the exception of L5. Furthermore, the magnitude of fore-aft head acceleration response of the model is significantly smaller than the mean measured magnitude. This is suggestive of out-of-phase localised pitch motion in this region. Additionally, the fore-aft motion at the T12, predicted by the model, is significantly lower than the mean measured responses. This could be due to the presence of a node about which the upper body segments pitch. The two models derived based on the error functions in STHT and C7 responses along the X- and Z-axes (EF-7 and EF-8) show dissimilar characteristics in terms of magnitudes and phase of the segmental responses, suggestive of differences in their modal behaviour. Considering the complex pitch motion of the head and neck, the models were subsequently identified considering target functions in (i) vertical and fore-aft STHT and fore-aft motion at C7, EF-9; (ii) vertical and fore-aft STHT together with APMS, EF-10; and (iii) vertical and fore-aft STHT, APMS and fore-aft motion at C7, EF-11.

Figures 6-10 to 6-12 illustrate comparisons of the resulting biodynamic model responses with the mean measured response, respectively. Table 6-6 also summarises the joint parameters obtained for the three models. All the three models revealed somewhat similar results in the vertical and fore-aft axes. The results are generally acceptable given that all the error functions provide satisfactory response matching simultaneously with the driving-point measurement, and segmental motion characteristics in two dimensions. However, a compromise may be needed in prudently selecting the appropriate error

function that efficiently represents the human body under vertical WBV. From the results in Figs. 6-10 to 6-12, it is evident that the inclusion of the APMS in the error function increases the bandwidth of the magnitude of vertical responses around primary resonance, while providing no significant differences in view of segmental responses of the model. The models optimised using EF-10, tends to display considerably deviations in vertical segmental responses from the measured targets below 10 Hz. In addition, this model could overestimate the absorption of vibratory power due to its excessive bandwidth around the primary vertical peak.

The model derived by optimising the error function as a combination of the measured vertical STHT and fore-aft head and C7 motion, appears to provide an optimal solution that satisfactorily follows the primary resonance peak in APMS and segmental transmissibility. The phase response of the vertical transmissibility of most of the body locations also seems to be better reflected in this model suggestive of better estimations for damping parameters. However, the formulation seems to over-estimate the peak vertical magnitude at the body segments, while also slightly reducing the fore-aft response magnitude at the neck. However, this may be acceptable considering the scatter in the measured data. The visco-elastic joint parameters obtained by optimising a target function defined as the sum of the model error in vertical and fore-aft seat-to-head acceleration transmissibilities, and the fore-aft response at the neck joint (C7) may be considered sufficient for the prediction of segmental human biodynamics under vertical vibration, for the postural and excitation considered in this research dissertation. The model's results and possible applications are explored in the subsequent sections.
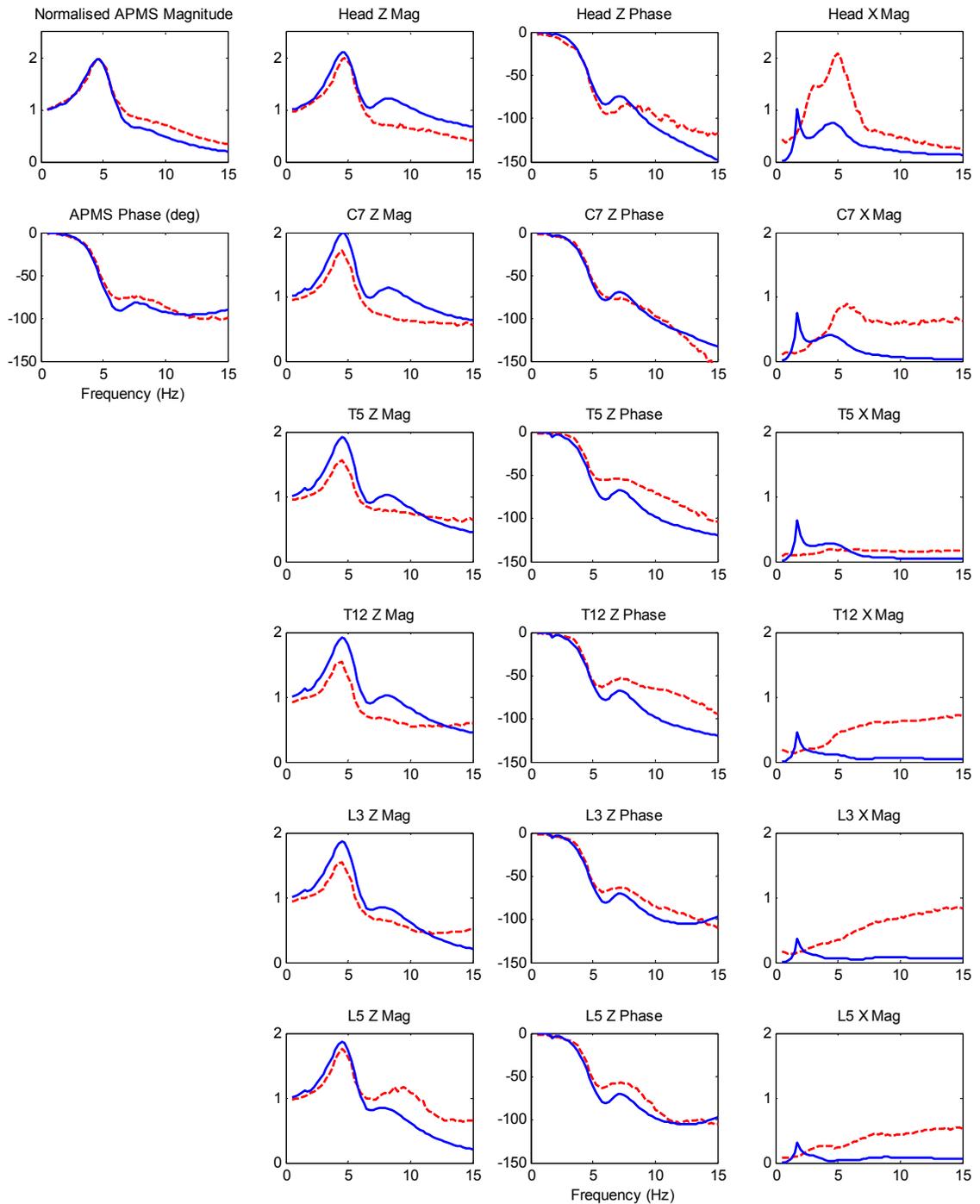
Figure 6-2: Comparison of response of the model derived upon consideration of apparent mass target function alone (EF-1) with mean measured responses (– model; - - measured).
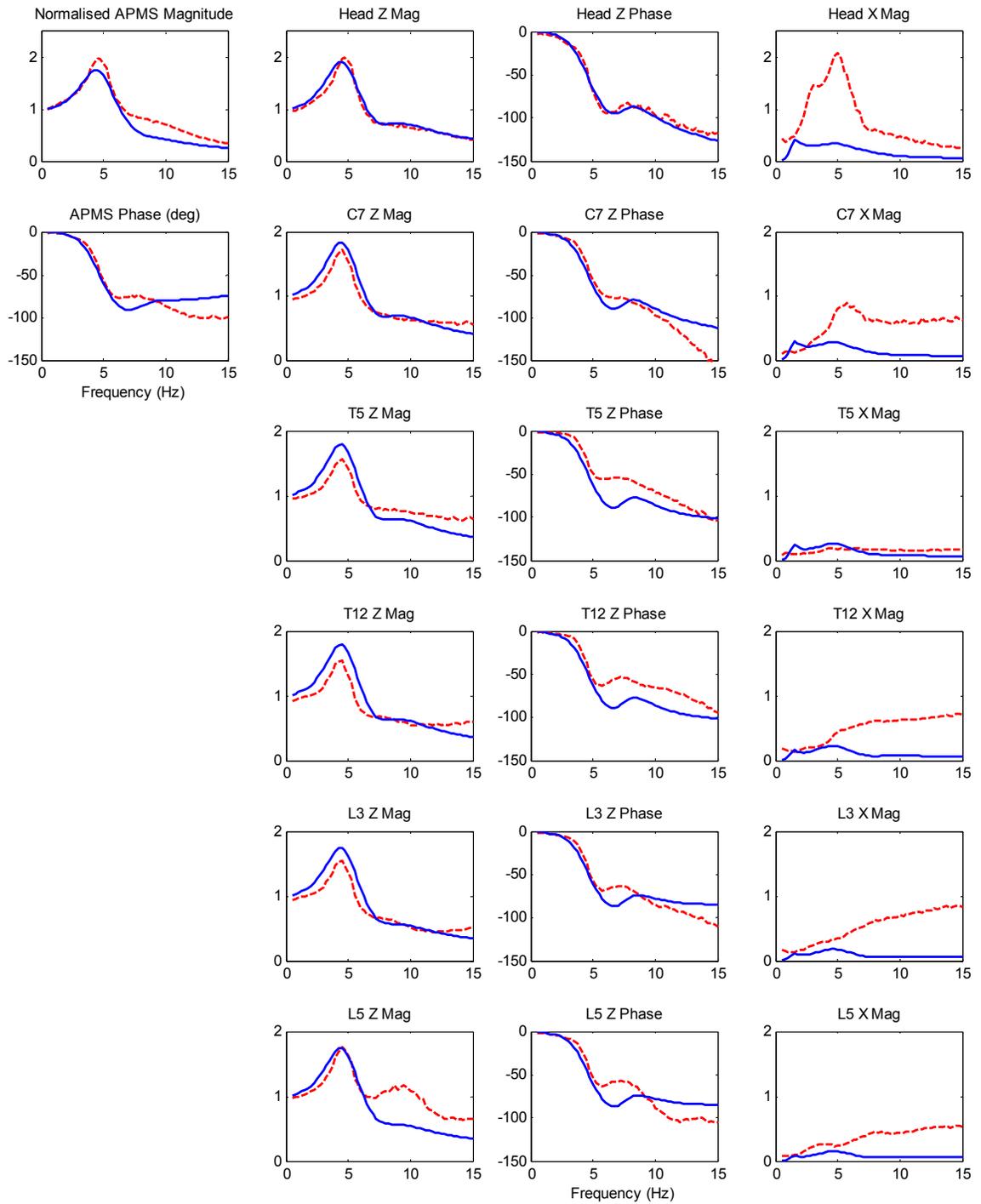
Figure 6-3: Comparison of response of the model derived upon consideration of vertical seat to head transmissibility target function alone (EF-2) with mean measured responses (– model; - - measured).

239
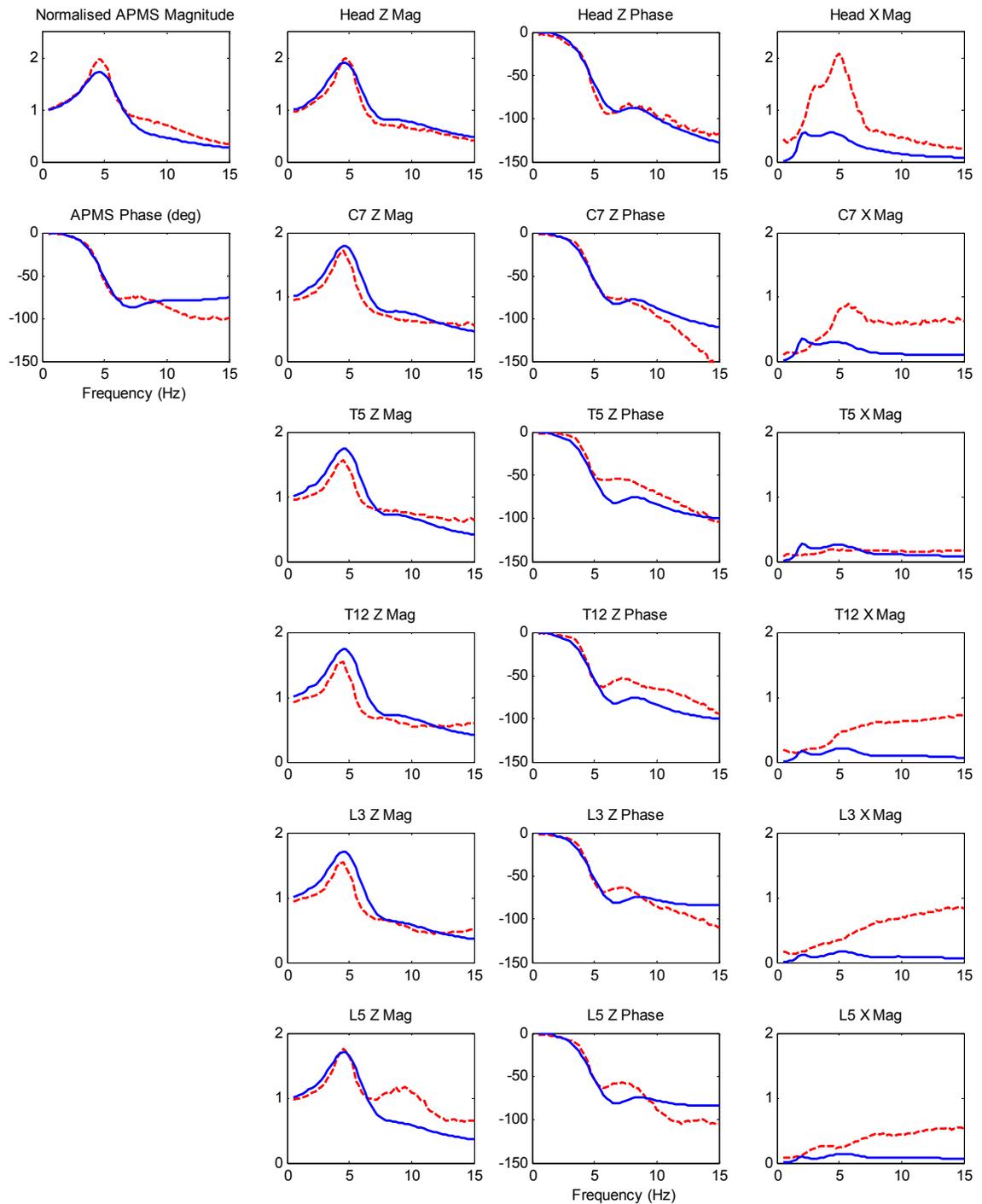
Figure 6-4: Comparison of response of the model derived upon consideration of combination of apparent mass and vertical seat to head transmissibility as target function (EF-3) with mean measured responses (– model; - - measured).
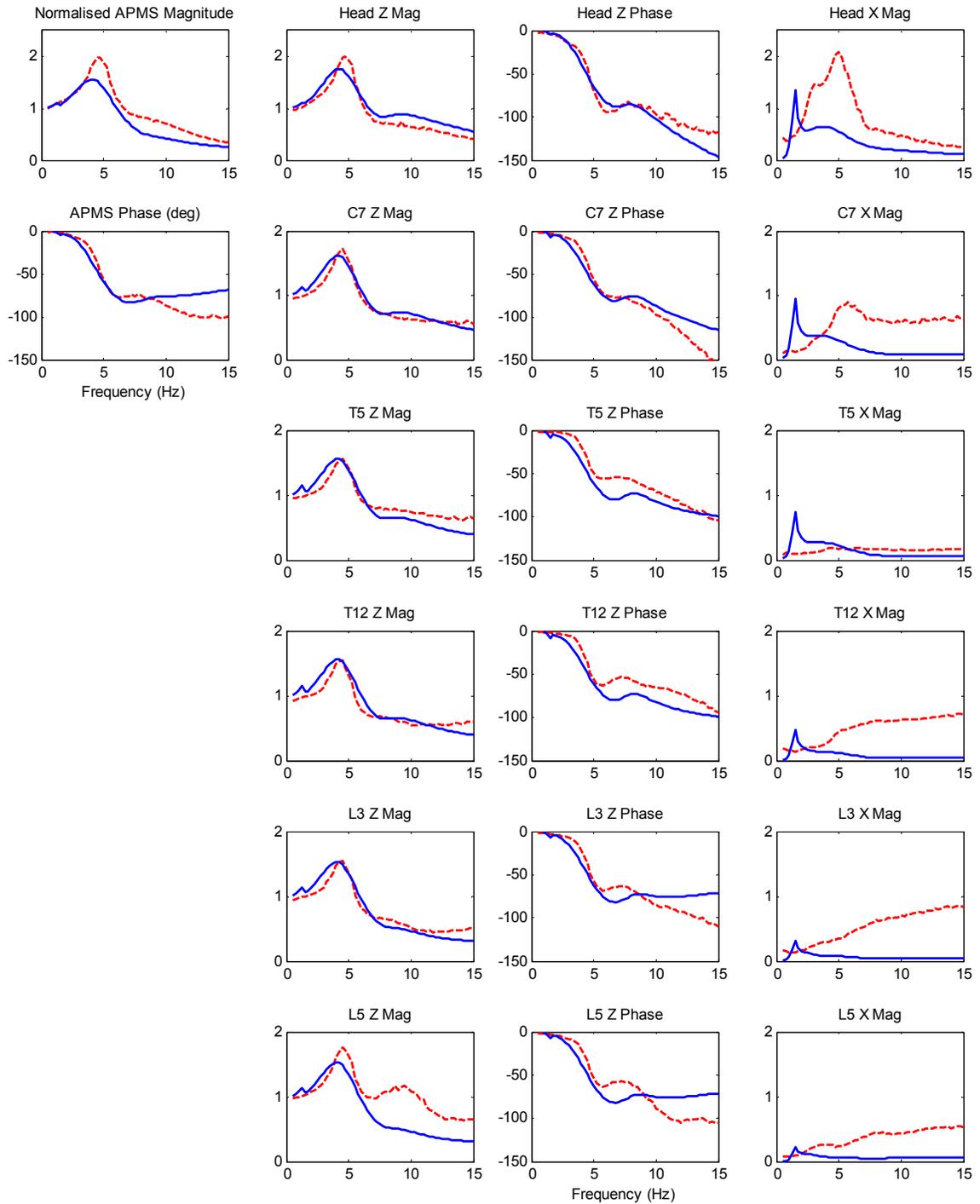
Figure 6-5: Comparison of response of the model derived upon consideration of vertical C7 transmissibility alone as target function (EF-4) with mean measured responses (– model; - - measured).
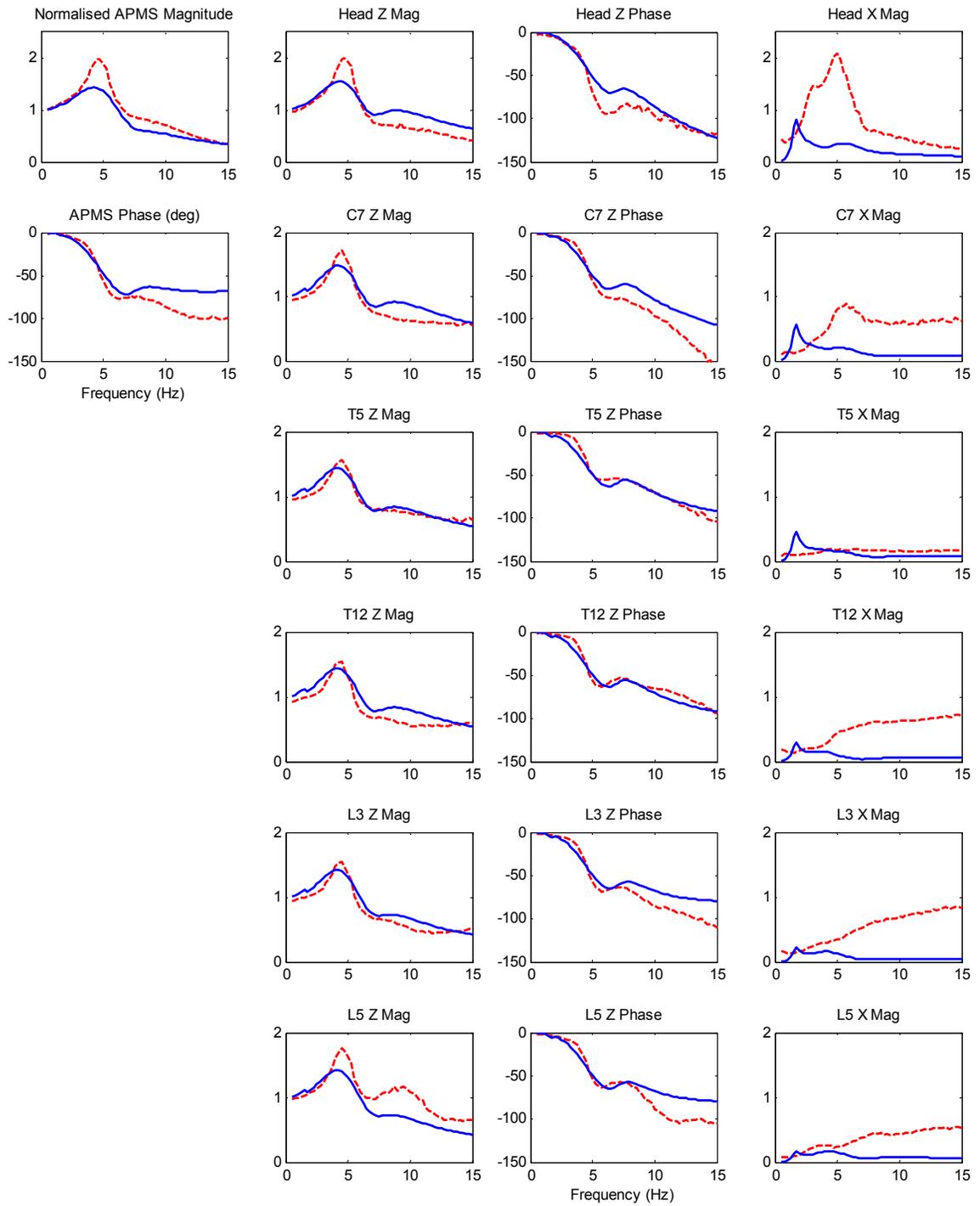
Figure 6-6: Comparison of response of the model derived upon consideration of vertical T5 transmissibility alone as target function (EF-5) with mean measured responses (– model; - - measured).
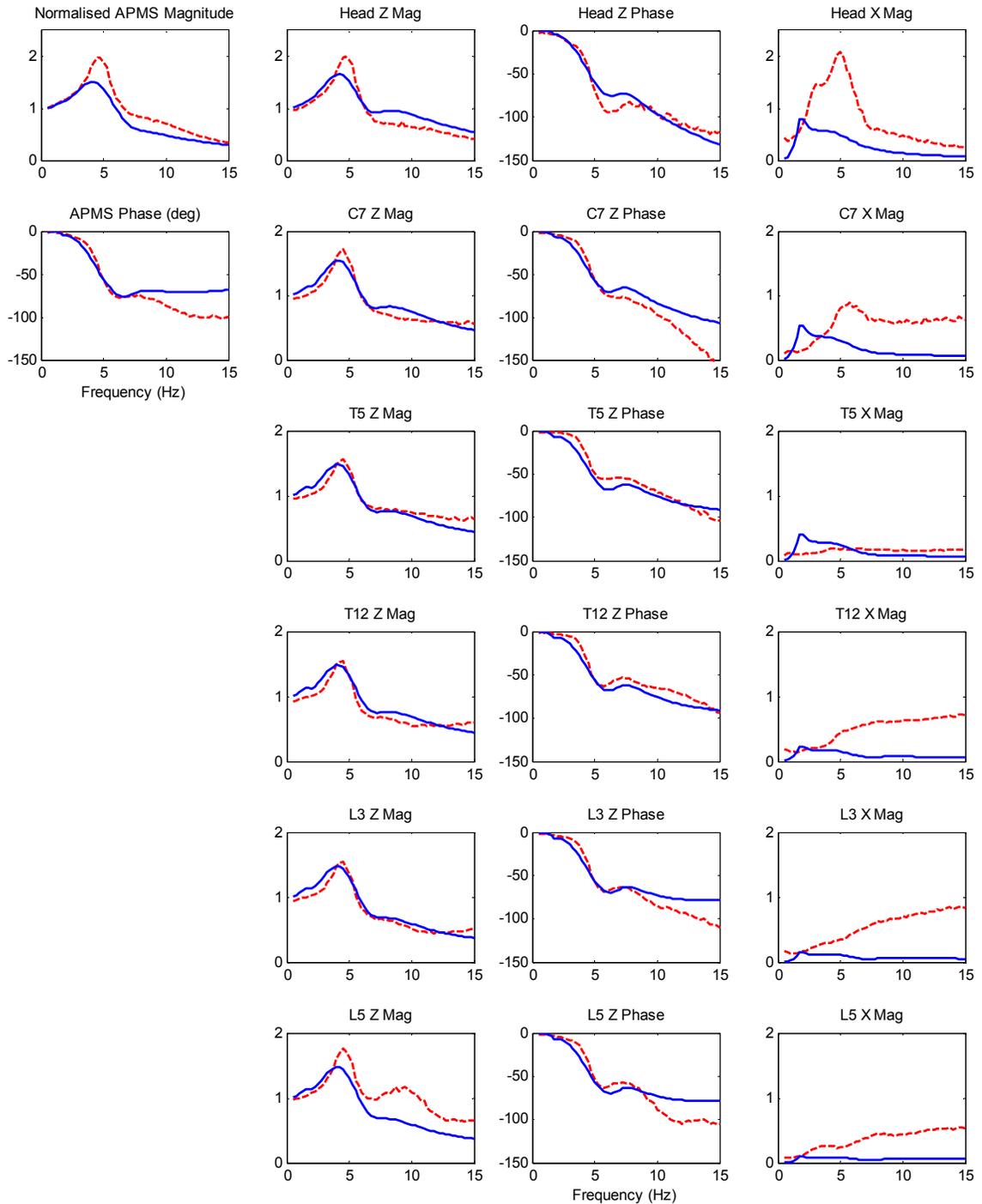
Figure 6-7: Comparison of response of the model derived upon consideration of vertical
L3 transmissibility alone as target function (EF-6) with mean measured responses
(– model; - - measured).

243
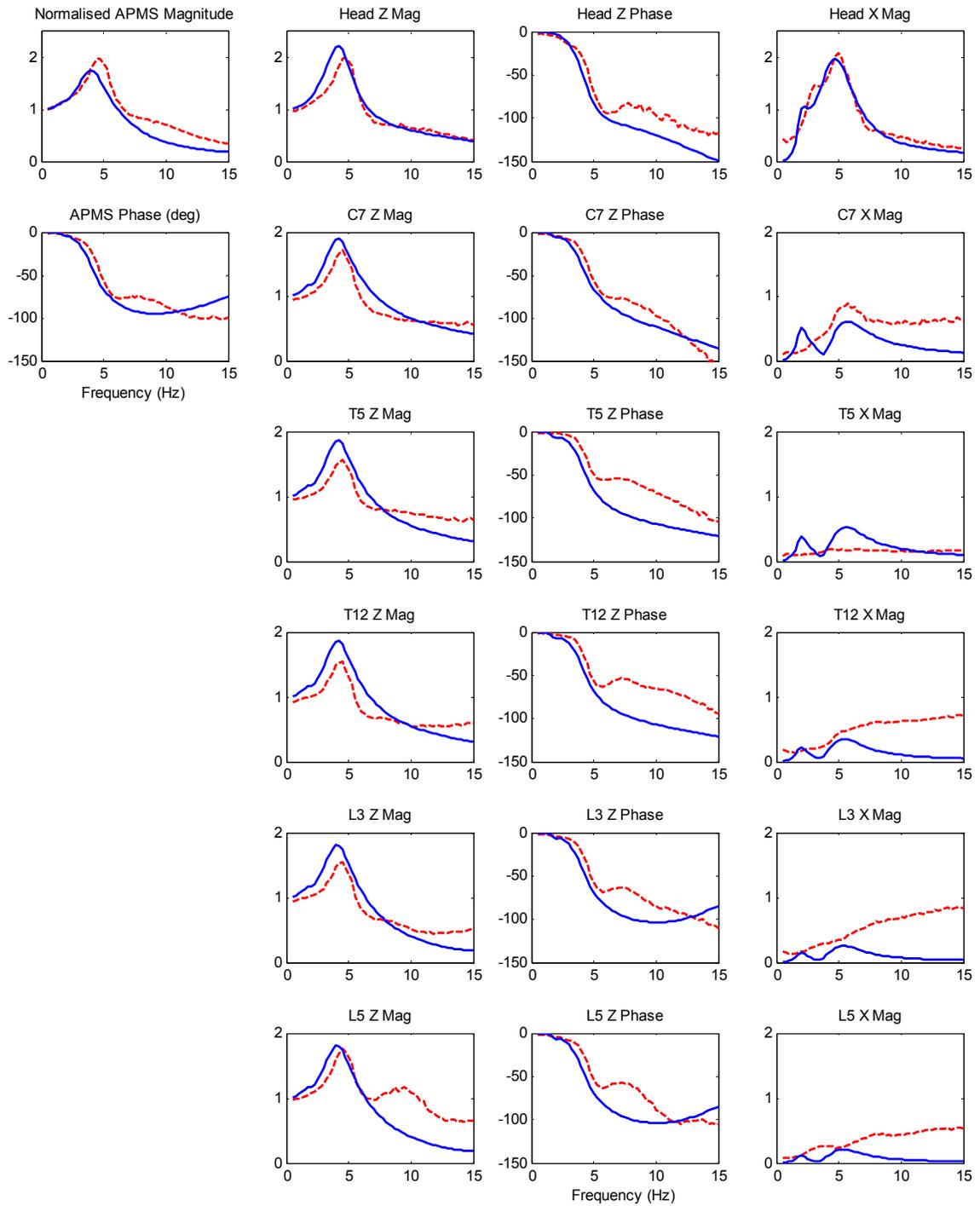
Figure 6-8: Comparison of response of the model derived upon consideration of combination of vertical and fore-aft transmissibility at head as target function (EF-7) with mean measured responses (– model; - - measured).
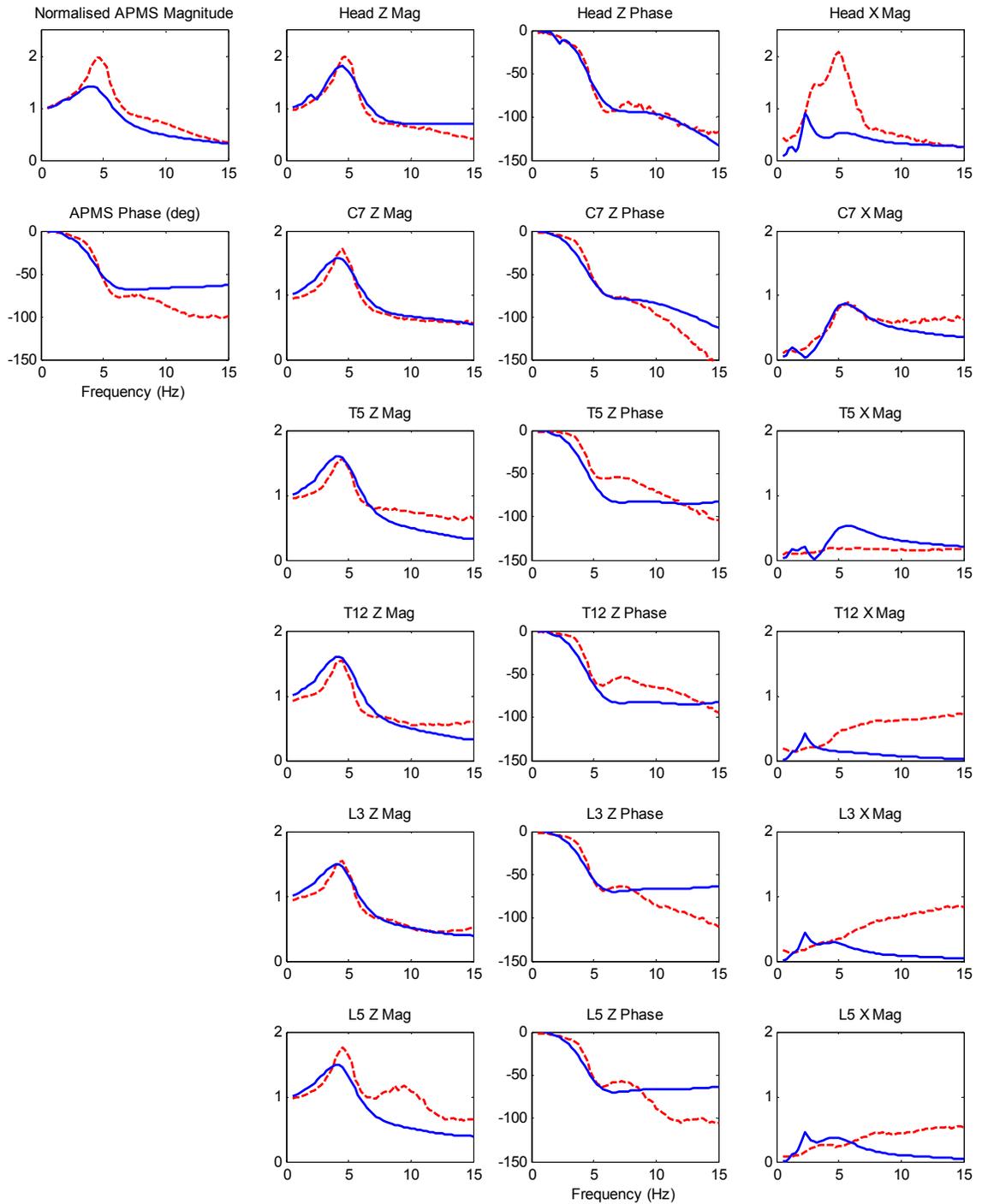
Figure 6-9: Comparison of response of the model derived upon consideration of combination of vertical and fore-aft transmissibility at C7 as target function (EF-8) with mean measured responses (– model; - - measured).
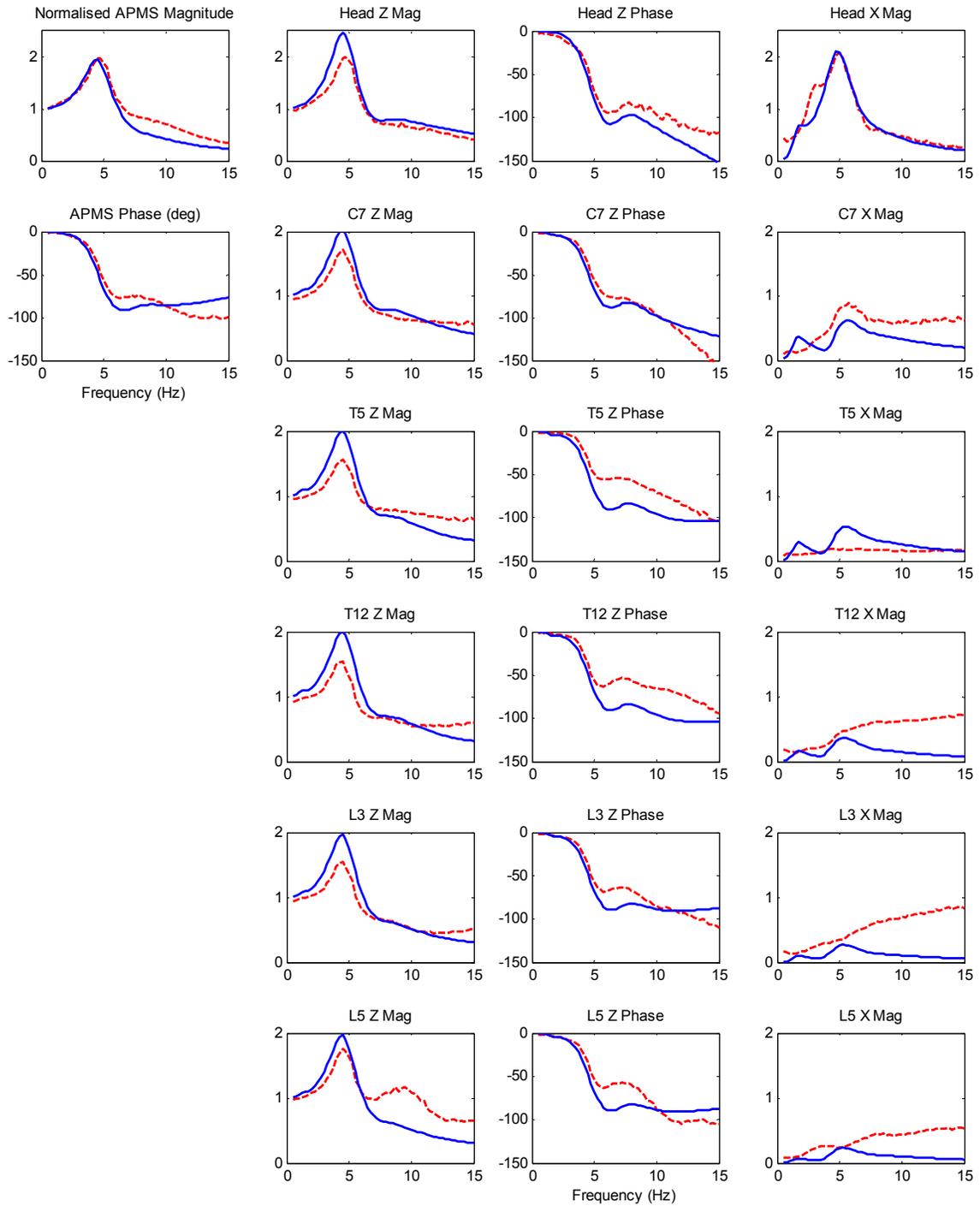
Figure 6-10: Comparison of response of the model derived upon consideration of combination of vertical and fore-aft transmissibility at head, and fore-aft transmissibility at C7 as target function (EF-9) with mean measured responses
(– model; - - measured).
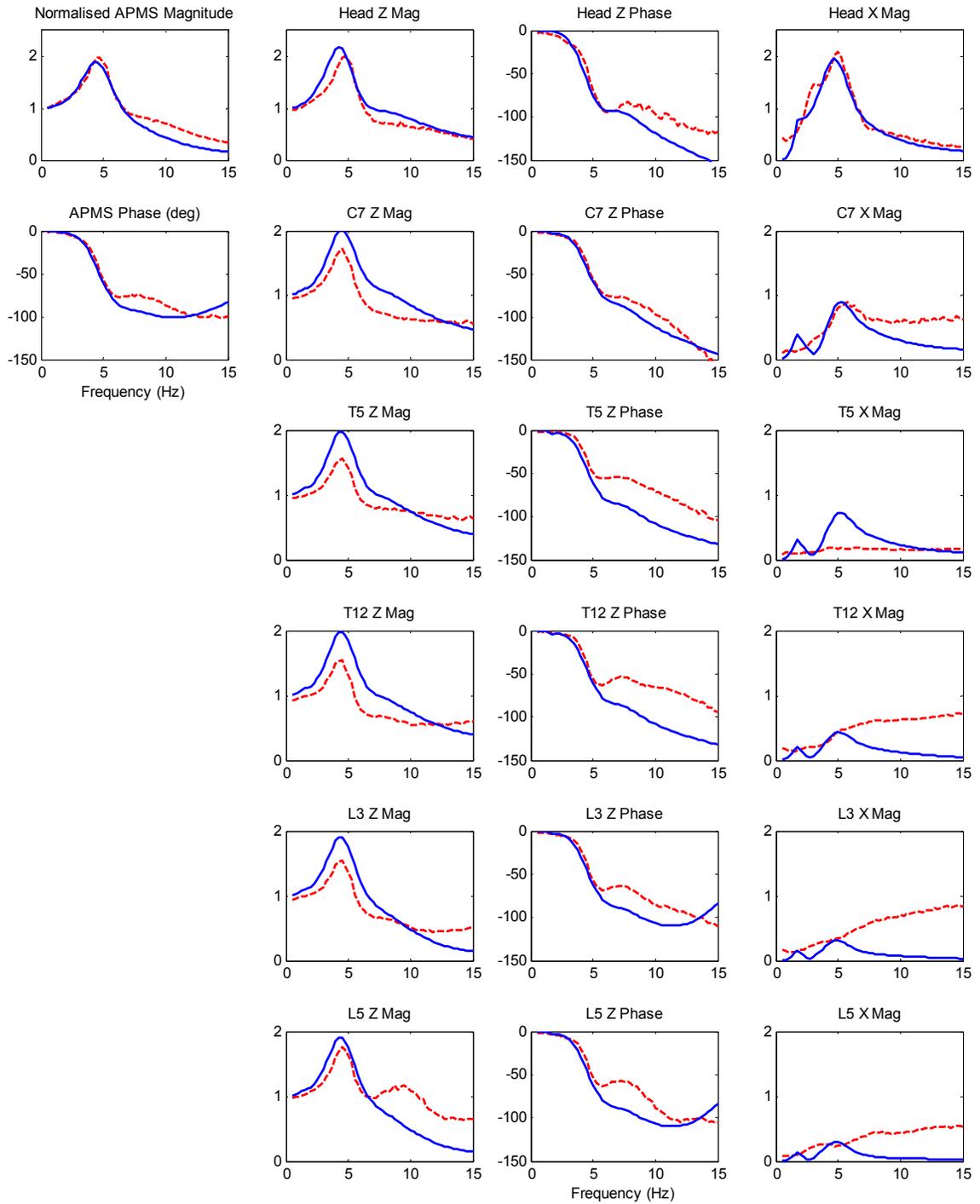
Figure 6-11: Comparison of response of the model derived upon consideration of combination of apparent mass, and vertical and fore-aft transmissibility at head as target function (EF-10) with mean measured responses (– model; - - measured).
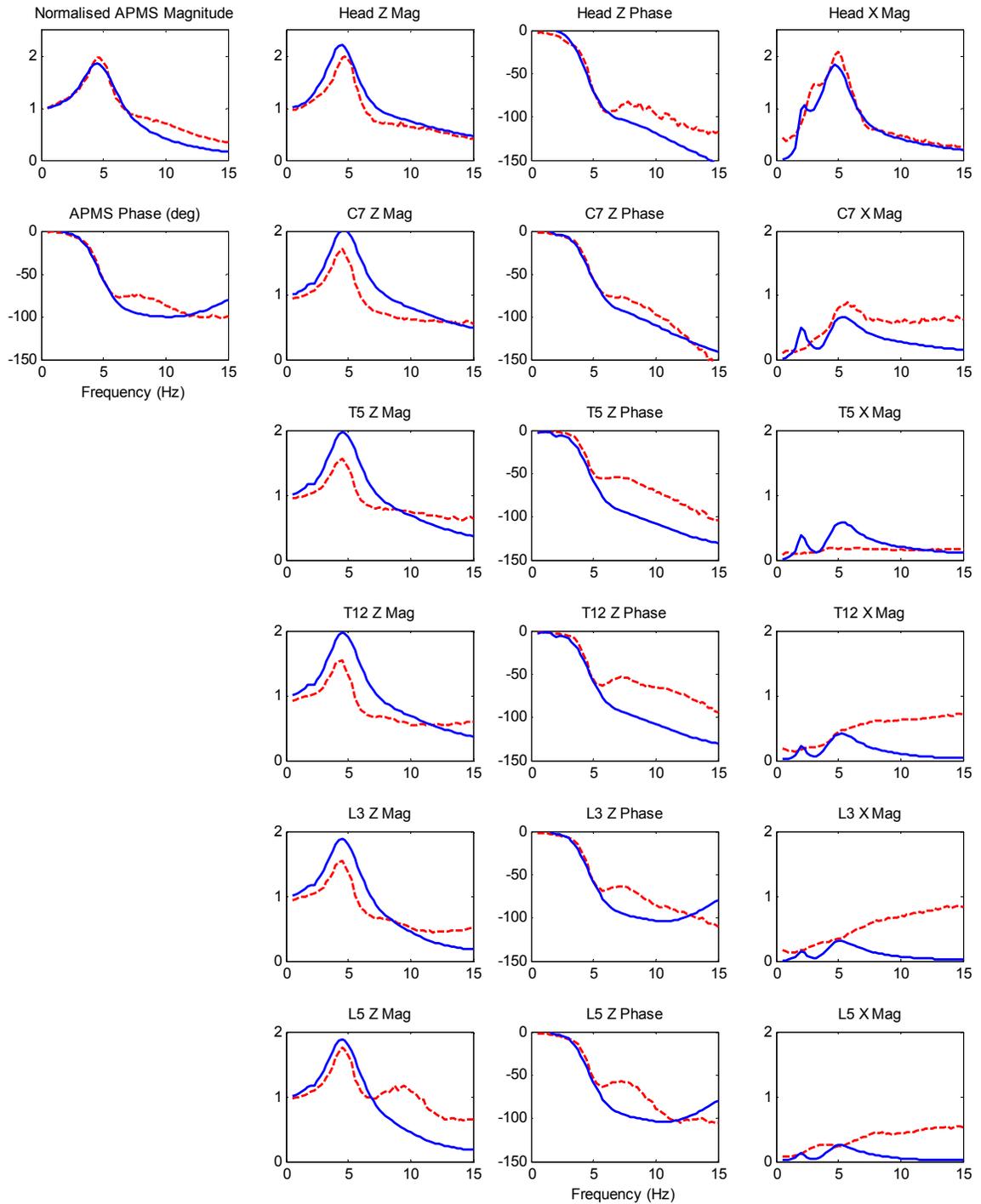
Figure 6-12: Comparison of response of the model derived upon consideration of combination of apparent mass, vertical and fore-aft transmissibility at head, and fore-aft transmissibility at C7 as target function (EF-11) with mean measured responses (– model; - - measured).

Table 6-6: Visco-elastic joint properties of the models obtained through minimisation of error function in following responses: vertical and fore-aft STHT and fore-aft C7 (EF-9); vertical and fore-aft STHT and APMS (EF-10); and vertical and fore-aft STHT, fore-aft C7 and APMS (EF-11).

Translational Stiffness (N/m)	Objective Function			Translational Damping (Ns/m)	Objective Function		
	EF-9	EF-10	EF-11		EF-9	EF-10	EF-11
K_head	55474	91492	90306	C_head	1861	1978	1733
K_C7	190591	184857	192047	C_C7	1931	1784	788
K_shoulder	183493	167258	190743	C_shoulder	140	296	376
K_T12	216549	176045	158764	C_T12	1922	1044	1446
K_L5	298534	160491	161261	C_L5	1975	1693	1425
K_viscera	18451	14661	18799	C_viscera	159	203	294
K_butt	59517	58157	55971	C_butt	1270	1203	1280
Kx_butt	10609	7324	8288	Cx_butt	1718	769	1833
Rotational Stiffness (Nm/rad)	EF-9	EF-10	EF-11	Rotational Damping (Nms/rad)	EF-9	EF-10	EF-11
Kr_head	367	159	130	Cr_head	14	3	1
Kr_C7	220	96	128	Cr_C7	13	1	2
Kr_T12	604	1543	1285	Cr_T12	8	7	9
Kr_L5	1423	579	1870	Cr_L5	44	24	20
Kr_butt	1575	1945	1924	Cr_butt	13	3	20
Kr_wrist	1678	1973	1971	Cr_wrist	48	2	2

6.6   Modal Properties

The model derived through minimisation of the composite error function comprising errors in vertical and fore-aft STHT and fore-aft C7 transmissibility (EF-9) is considered to yield reasonably good predictions of the biodynamic measures. The properties of this model are further evaluated to enhance knowledge on the fundamental deflection behaviours of the segments. The model is also applied to study the global and distributed vibration power absorption characteristics that could be related to potential injuries due to WBV exposure.

An eigen value problem is formulated and solved to evaluate the resonant frequencies and deflection modes of the seated human body model. The solution revealed the presence of 4 significant modes at frequencies below 15 Hz. The natural frequencies and modal damping ratios of these modes are summarised in Table 6-7 together with the observed deflection modes. The results showed that the first mode occurring at 1.56 Hz describes shear (X-axis translation) of the buttock tissue coupled with thoracic pitch about the lower lumbar joint (L5). Two subsequent modes, seen around 5 Hz, in the vicinity of the primary resonance region comprised whole body motion. Mode 2 at 4.76 Hz was due to the vertical movement of the body on the seat caused by deformation of the buttock tissue, coupled with vertical motion of the abdominal viscera. This mode also revealed relative vertical translation between the lumbar (mid-torso) and pelvic (lower-torso) segments connected at the L5 joint, and pitch of the head and neck units about the C1 and C7, respectively. The third mode at 5.71 Hz involved considerable shear at the seat-body interface coupled with rotation of the lower torso (pelvis) segment. This resulted in slight pitch of the upper body segments, also coupled with axial motion of the abdominal viscera. A dominant pitch motion of the head-neck complex about the C7 was

also evident. The fourth mode near 8 Hz showed vertical motion of the abdominal viscera, coupled with relative vertical movements between the head and neck. Along with this, head and neck pitch was distinctly observable. The fifth and high frequency mode observed at 17.21 Hz comprised of the stretch of both the head and neck joints, at C1 and C7.

Table 6-7: Modal properties of the seated human model derived from the eigen analysis.

Mode	Natural Frequency (Hz)	Damping Ratio
1	1.56	0.27
2	4.76	0.24
3	5.71	0.33
4	7.95	0.29
5	17.21	0.41

6.6.1 Discussions on mode shapes

A few published studies on seated body modelling have reported selected modal properties of the body. Table 6-8 compares the reported deflection modes grouped under different ranges. The reported deflection modes are reviewed and discussed in relation with those observed in this study. Using a finite-element model of the seated body, Pankoke *et al.* (1998) reported a spine bending mode near 2.75 Hz, while Kim et al. (2005) found a "spine, visceral and head fore-aft" mode at 2.71 Hz through analysis of a multi-body dynamic model. The modal experiments performed by Kitazaki and Griffin (1998) revealed two modes with coupled head-neck and pelvis fore-aft motions opposed-to and in-phase with each other at 2.2 and 3.4 Hz, respectively.

251

Table 6-8: Modal characteristics of the vibrating human body from selected studies under vertical WBV compared with the developed human model.

Frequency Range (Hz)	Mode
0.1 – 1	Spinal Bending (0.59) ‡ Torso fore-aft (0.35) # Torso vertical (0.51) # Torso pitch (0.96) # Whole Body (WB) pitch about pelvis (0.28) $
1 – 2	Pelvis and upper body pitch (1.1) † Horizontal head and pelvis – in phase (1.49) $ **Buttock shear, torso pitch – in phase (1.56) ₹**
2 – 3	Torso pitch (2.18) £ Spine, head and viscera horizontal (2.71) # Spinal Bending (2.75) ‡ Horizontal head/ neck and pelvis – out of phase (2.81) $
3 – 4	Thigh and pelvis horizontal (3.41) #
4 – 5	Thigh and pelvis pitch (4.12) # WB Vertical (4.68) ‡ **Buttock vertical, visceral vertical, lower lumbar stretch, head-neck pitch (4.76)₹** Head and torso pitch (4.8) # WB vertical (4.86) £
5 – 6	WB vertical, buttock shear with viscera vertical – in phase (5.06) $ WB and viscera vertical (5.35) # WB mode: Pelvis pitch, viscera and thighs vertical (5.66) † **Buttock shear, visceral vertical, upper body pitch, head-neck pitch (5.71) ₹** Spine bending, horizontal pelvis and buttock shear (5.77) $
6 – 8	Thigh and pelvis horizontal (6.39) # Visceral vertical, slight pelvis pitch (7.51) $ Spinal Bending (7.78) ‡ **Visceral vertical, buttock vertical, head-neck pitch (7.95) ₹**
8 – 10	Thigh pitch (8.04) # Spine and head pitch (8.34) # Viscera vertical, pelvis and upper body pitch (8.34) † Pelvic pitch, slight visceral vertical (8.96) $
10 – 15	Shoulder movement (11.42) ‡ Pelvis and upper body pitch, legs vertical (12.3) † Viscera vertical (14.34) ‡
> 15	Local abdominal viscera horizontal (15.39) ‡ Head pitch (16.67) £ **Head and neck vertical stretch (17.21) ₹** WB Vertical (18.38) ‡

£ Amirouche, # Kim, $ Kitazaki, † Matsumoto, ‡ Pankoke, ₹ This study

The model in the present study showed lumbar spine bending about the lower lumbar joint in-phase with buttock shear at 1.56 Hz. The secondary peak in the fore-aft head transmissibility at frequencies below 4 Hz (Fig. 6-10) may be associated with this mode. The primary vertical vibration mode, widely reported to occur in the 4 to 6 Hz range, has been generally associated with whole body vertical vibration due to buttock compression and shear. Experiments by Kitazaki and Griffin (1998) also showed visceral movement at the primary resonance mode around 5 Hz. The same study also showed an additional mode with lumbar and lower thoracic spine bending and head vertical motion at 5.6 Hz (Kitazaki and Griffin, 1998). The model developed in this study shows a whole-body vertical mode at 4.76 Hz due to relative vertical movements at the seat-buttock interface, coupled with a stretch of the lower L5 joint, as portrayed by many of the reported studies (see Table 6-8). The other mode around 5.7 Hz seen in the model, however, is reported at lower frequencies by some previous studies. The visceral mode reported between 8 to 14 Hz range in the published literature (Kim *et al.*, 2005; Kitazaki and Griffin, 1998; Pankoke *et al.*, 1998) is clearly observed in the developed human model at 7.95 Hz. While uncoupled head pitch modes have been observed in some analytical derivations (Amirouche and Ider, 1988) around 16 Hz, the human model in this present study shows the head and neck pitch coupled in the lower frequency modes. However, the model also shows relative translational motion among the head and neck segments around 17 Hz. Additionally, some of the higher frequency motions reported by some studies (see Table 6-8), are not observed in the model developed in this study.

With wide variability in the reported vibration modes, which are mostly attributed to complex movements of the human body, the effects of torso-muscular activity and the presence of highly non-linear damping (Kitazaki and Griffin, 1998), it may be difficult to

understand the modal behaviour of the human body through simple linearised models. Although the model proposed in this study shows satisfactory agreement with reported studies in view of the significant deflection modes, additional modelling efforts and laboratory measurements are vital for improving the reliability of the model.

6.7   Vibration power absorption analysis

It has been hypothesised that the vibration power absorbed by the tissues and muscles relates to potential injuries of WBV exposure. The absorbed power relates to force or stress developed and the velocity of the strain rate. It can thus describe the mechanical stimulus associated with WBV exposure.

The power absorbed by the human body exposed to WBV, measured from the cross-correlation of the force and velocity at the driving-point has thus been commonly considered as an indirect measure of the potential injury risk for the body (VIN, 2001a). However, no relationship has yet been established conclusively with observed injuries and the absorbed power. This may in-part be attributed to the fact that the absorbed power is solely based on the measured driving-point biodynamic response since the reported studies have invariably focus on the total power absorption derived from the measured driving-point impedance or the APMS. Additionally, while the injuries reported under exposure to WBV in the actual work environment have primarily shown occurrences in the spinal structures (Bovenzi and Hulshof, 1998), the measured driving-point absorbed power may not be completely representative of these body sub-segments. Furthermore, currently there are no techniques to quantify the effect of vibration on the spine based on any measurement methodology. Hence, it is essential to study the effect of vibration on the segments of the human body through analytical techniques so as to be able to find methods to relate the measured segmental responses to observed trends from

epidemiological studies. The proposed biodynamic model is further employed for the derivation of power absorbed by the human body.

As mentioned earlier, the multi-body human model developed in this research dissertation is mostly formulated with kinematic constraints 'wrapped-around' with force-elements, so as to achieve sagittal-plane motions both in translation and pitch rotation. Most of these force-elements are composed of two spring-damper elements to account for the translational and rotational visco-elastic properties of the spine. The damping force in translation (F) and damping moment pitch rotation (τ) at a particular joint (i) may be represented as a function of the respective relative velocities ($\dot{\delta}_\iota$ and $\dot{\varphi}_\iota$) across the corresponding damping elements, such that:

$$F_i = C_i \dot{\delta}_\iota \tag{6.12}$$

$$\tau_i = Cr_i \dot{\varphi}_\iota \tag{6.13}$$

Where, C_i and Cr_i are the damping coefficients of the joint i in translation and rotation, respectively, as illustrated in Fig. 6-13. $\dot{\delta}_\iota$ and $\dot{\varphi}_\iota$ are the relative velocities in translation and rotation, respectively, given by:

$$\dot{\delta}_\iota = \dot{x}_i - \dot{x}_{i-1} \tag{6.14}$$

$$\dot{\varphi}_\iota = \dot{\theta}_i - \dot{\theta}_{i-1} \tag{6.15}$$

Where, $\dot{x}$ and $\dot{\theta}$ are the variables representing, respectively, translational and rotational velocities of the bodies coupled through joint i. The power dissipated across the joint may thus be expressed as the translational and rotational components, P_{Fi} and $P_{\tau i}$, respectively, such that:

$$P_{Fi} = C_i \dot{\delta}_\iota^2 \tag{6.16}$$

$$P_{\tau i} = Cr_i \dot{\varphi}_\iota^2 \tag{6.17}$$

In the above formulation, $\dot{\delta}_i^{\,2}$ and $\dot{\varphi}_i^{\,2}$ represent the mean squared relative velocities across a joint i.
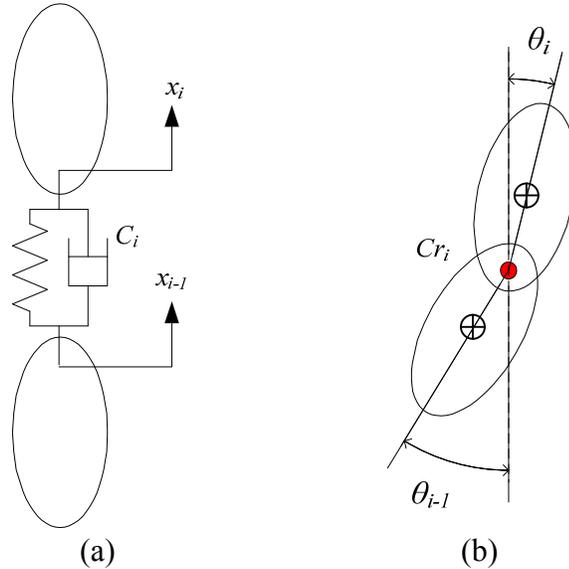
Figure 6-13: Visco-elastic joints formulated between connecting segments in the human body model composed of: (a) vertical; and (b) rotational components.

Under random excitation, relative velocity responses of the joints could be evaluated from the relative velocity transfer functions, such that:

$$S_{\dot{\delta}i}(j\omega) = |H_{\delta i}(j\omega)|^2 S_{\dot{X}_0}(j\omega) \tag{6.18}$$

$$S_{\dot{\varphi}i}(j\omega) = |H_{\varphi i}(j\omega)|^2 S_{\dot{X}_0}(j\omega) \tag{6.19}$$

Where $S_{\dot{\delta}i}(j\omega)$ and $S_{\dot{\varphi}i}(j\omega)$ are the power spectral densities (PSD) of the translational and rotational velocities across joint i, respectively. $S_{\dot{X}_0}(j\omega)$ is the PSD of the excitation velocity at the body-seat interface, which is related to PSD of the input acceleration, $S_{\ddot{X}_0}(j\omega)$:

$$S_{\dot{X}_0}(j\omega) = \frac{S_{\ddot{X}_0}(j\omega)}{\omega^2} \tag{6.20}$$

Functions $H_{\delta i}(j\omega)$ and $H_{\varphi i}(j\omega)$ in Eqns. 6.18 and 6.19, respectively, are the complex relative displacement transfer functions that are related to the displacement transfer functions of bodies connecting the joint;

$$H_{\delta i}(j\omega) = H_{xi}(j\omega) - H_{x\,i-1}(j\omega) \tag{6.21}$$

$$H_{\varphi i}(j\omega) = H_{\theta i}(j\omega) - H_{\theta\,i-1}(j\omega) \tag{6.22}$$

Where $H_{xi}(j\omega)$ and $H_{\theta i}(j\omega)$ are the complex displacement transfer functions of body i in translation and rotation, respectively. For displacement excitation, $X_0(j\omega)$, at the body-seat interface, the displacement transfer functions are derived from:

$$H_x(j\omega) = \frac{X(j\omega)}{X_0(j\omega)} \tag{6.23}$$

$$H_\theta(j\omega) = \frac{\theta(j\omega)}{X_0(j\omega)} \tag{6.24}$$

The equations of motion of the model are solved to determine the relative velocity responses. The spectral density of the power absorbed in translation and pitch of the model can be directly related to PSD's of the velocities, respectively, as:

$$P_{Fi}(\omega) = C_i S_{\delta i}(j\omega) \tag{6.25}$$

$$P_{\tau i}(\omega) = Cr_i S_{\varphi i}(j\omega) \tag{6.26}$$

The spectral density of power (P_i) at joint i is the sum of those associated with translation and rotation:

$$P_i(\omega) = P_{Fi}(\omega) + P_{\tau i}(\omega) \tag{6.27}$$

The overall absorbed power density, P_T, of the multi-body human model is then computed by summing up the power at each joint such that:

$$P_T(\omega) = \sum_{i=1}^{n} P_i(\omega) \qquad (6.28)$$

Where, n represents the total number of damping elements in the model. The global power $\bar{P}$ of the model can be subsequently evaluated through integration of the power density over the frequency range of intent, such that:

$$\bar{P} = \int_0^\omega P_T(\omega)d\omega \qquad (6.29)$$

6.7.1 Distributed and total power absorbed

The total power density of the seated body exposed to vertical WBV was measured in the laboratory from the cross-spectrum of the biodynamic force measured at the driving-point and the driving-point velocity. Figure 6-14 illustrates the power absorbed at the body-seat interface measured from the 12 male subjects in the experiments under broad band random vibration of magnitude 1 m/s^2 RMS. The power was derived from the cross-spectrum of the vertical velocity and the force measured at the seat pan. It should be said at the outset that the absorbed power quantity is very sensitive to the excitation velocity spectrum and would be valid only for the selected broad band excitation. Furthermore, the measured data reveals considerable variation, which is mostly attributed to the high resolution of the FFT filtering process (0.0625 Hz) employed in the data analysis (see chapter 3).
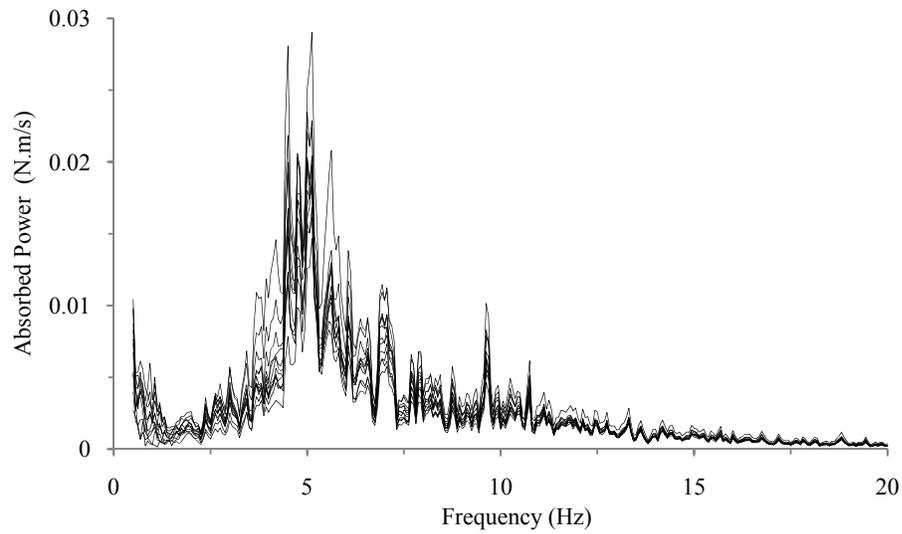
Figure 6-14: Absorbed power measured at the seat for 12 subjects seated erect with no back rest and hands on lap (L-NB), exposed to 1 m/s^2 random vertical seat vibration.
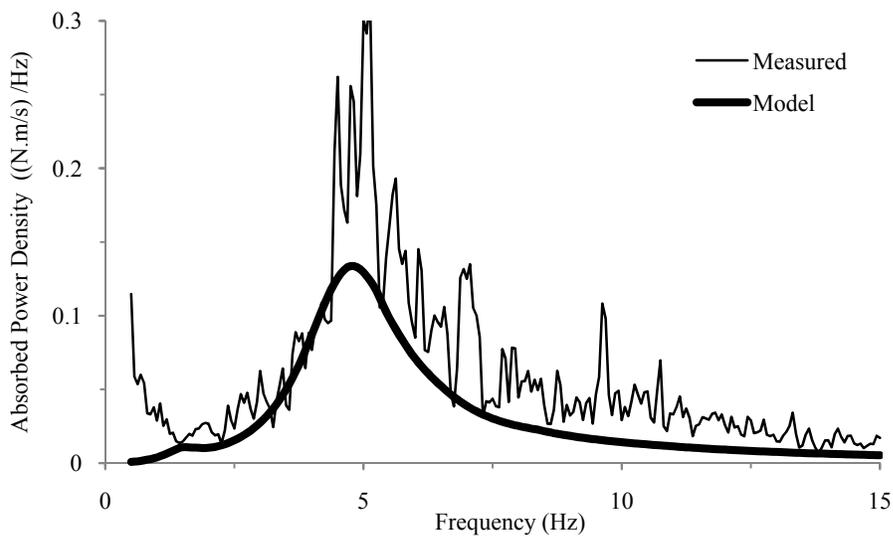
Figure 6-15: Comparison of overall absorbed power density predicted by the model with the mean of the measured results of 12 subjects seated in the L-NB posture, under exposure to 1 m/s^2 random vertical seat excitation.

The measured absorbed power exhibits a distinct peak in the region of primary resonance (5 Hz) for all the subjects, which is identical to the trends in the reported studies (Mansfield, 2005). The scatter in the 12-subject data seems to be greater around this resonance region, as evidenced in the measured biodynamic responses presented earlier in chapters 4 and 5. However, slightly higher peak power values were observed in this study when compared to those reported by Wang *et al.* (2006), which may be due to the aforementioned higher frequency resolution of 0.0625 Hz, while Wang *et al.* (2006) employed a resolution of 0.125 Hz. Subsequently, the average of the measured absorbed power was extracted from the 12-subject data in order to compare with the corresponding quantity derived using the multi-body human model. For this purpose, the mean measured data was expressed in terms of the absorbed power density.

The multi-body dynamic model of the seated body for the L-NB posture was subsequently analysed to derive the spectral density of power under 1 m/s^2 RMS acceleration excitation using Eqns. (6.12) to (6.29). The resulting total power density of the model is compared with the mean measured power density in Fig. 6.15. Although the model shows lower peak power at the primary resonant frequency, it should be noted that the measured power in itself is slightly over-estimated due to the issue of higher measurement resolution in this study. However, the peak power magnitude of the model is in the same order as that reported by Wang *et al.* (2006). It may thus be safely concluded that while the power extracted in this experimental research study show differences in magnitude when compared to previously reported studies, due to variations in the measurement variables, the model seems to be in concurrence with the values reported in earlier studies. Furthermore, the model response exhibits a trend that is close

to that in the mean measured data, while the differences in the magnitude are relatively small. This further demonstrates the validity of the model.

The model responses are thus considered acceptable for further investigations. The spectral density of the absorbed power density is further analysed to derive the absorbed power in third-octave bands with centre frequency below 15 Hz, as seen in Fig. 6-16. This methodology allows for a better appreciation of the quantity of power in the frequency bands. In the same vein, the power dissipated at individual joints of the model is presented for further discussions in the one-third octave frequency bands.
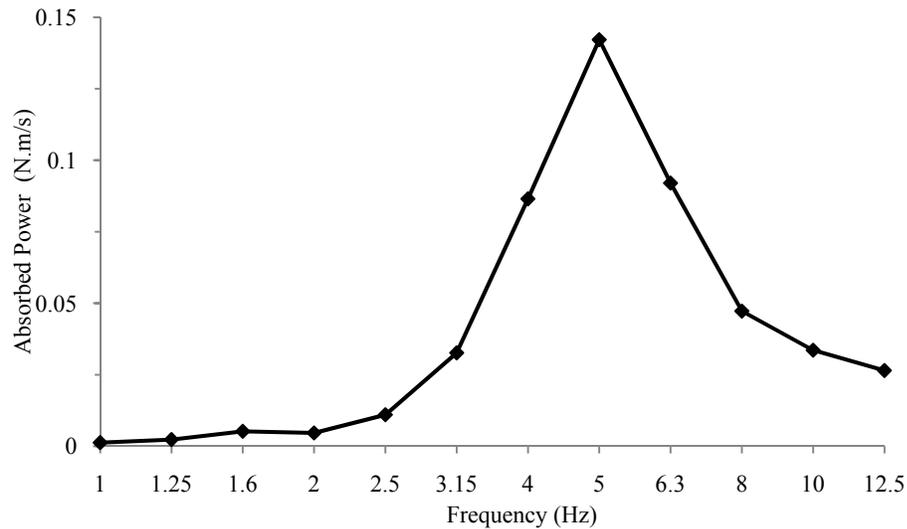
Figure 6-16: Overall power absorbed as predicted by the model represented in terms of one third octave band.

The reported studies here invariably focused on total power measured or evaluated at the driving point. Such a measure, however, does not yield knowledge on the distribution of power dissipated in different joints and bodies. A few recent studies on human hand-arm models have suggested that a study of the distributed power could yield sufficient insight toward injury potentials of the hand-transmitted vibration (VIN, 2001a).

The multi-body model of the seated body, derived in this study, could be applied to assess the power dissipated in individual joints, as seen in Eqns. (6.12) to (6.29), in addition to localised deformations / motions of the joints.

Tables 6-9 and 6-10 summarise the power dissipated, respectively, in translation, P_{Fi}, and rotation, $P_{\tau i}$, within different joints or damping elements of the seated body model subjected to broad band random vertical vibration of 1 m/s^2 RMS acceleration. In addition, Figs. 6-17 and 6-18 illustrate these quantities for better understanding and relative evaluations. From the tables and the figures, it is evident that the order of magnitude of power dissipated in translation (0.46 N.m/s) is much greater than that in rotation (0.02 N.m/s). Additionally, with a few exceptions, most of the joints show insignificant power dissipation at centre frequencies below 3.15 Hz. The total power absorbed by the model, summarised at the right-most column of the tables, also seems to agree with the above observation. The major power dissipation occurs in the 4–6.3 Hz frequency bands in both translation and rotation followed by the 8 Hz band. However, while subsequent power absorption occurs at greater frequencies in translation, rotational power dissipation shifts to lower frequencies. A relatively significant portion of rotational power absorption is also observed in the 1.6 Hz band at the L5 joint (Table 6-10). It is also interesting to note that while the major proportion of the translational power in the joints seems to be dissipated beyond 4 Hz, the rotational component is not insignificant at lower frequencies.
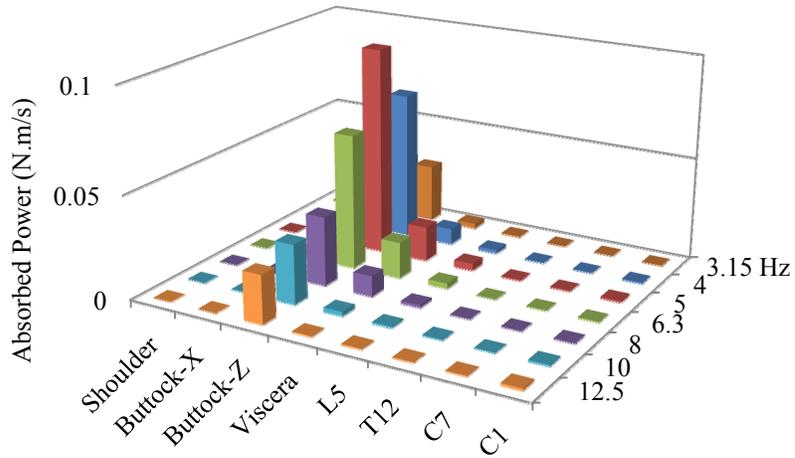
Figure 6-17: Power absorbed by the translational viscous joint elements of the model.
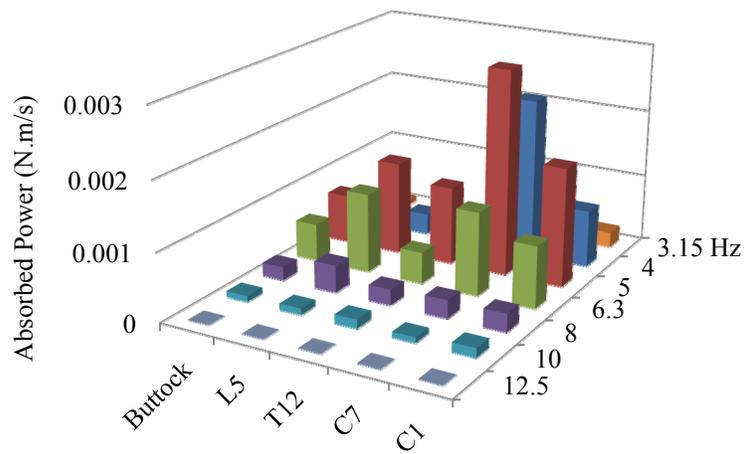
Figure 6-18: Power absorbed by the rotational viscous joint elements of the model.

Table 6-9: Power dissipated in the translational viscous damping elements in the multi-body dynamic model.

Octave Centre Frequency (Hz)	Power Absorbed in Translation (N.m/s)								
	C1	C7	T12	L5	Viscera	Buttock-Z	Buttock-X	Shoulder	**Total**
1	0	0	0	0	0	0.0006	0.0002	0	**0.0009**
1.25	0	0	0.0001	0.0001	0	0.0010	0.0004	0	**0.0015**
1.6	0	0	0.0001	0.0001	0.0001	0.0023	0.0008	0	**0.0035**
2	0	0	0.0001	0	0.0002	0.0030	0.0004	0	**0.0037**
2.5	0.0001	0	0.0001	0.0001	0.0007	0.0092	0.0002	0	**0.0102**
3.15	0.0001	0.0001	0.0001	0.0005	0.0023	0.0282	0.0002	0	**0.0314**
4	0.0004	0.0002	0.0002	0.0016	0.0077	0.0714	0.0009	0.0001	**0.0824**
5	0.0007	0.0003	0.0004	0.0033	0.0168	0.1094	0.0030	0.0001	**0.1339**
6.3	0.0004	0.0002	0.0001	0.0025	0.0175	0.0651	0.0020	0.0001	**0.0877**
8	0.0004	0.0002	0.0002	0.0012	0.0099	0.0334	0.0006	0	**0.0459**
10	0.0007	0.0002	0.0003	0.0007	0.0021	0.0287	0.0003	0	**0.0329**
12.5	0.0010	0.0003	0.0003	0.0005	0.0005	0.0234	0	0	**0.0260**
Total (N.m/s)	**0.0037**	**0.0015**	**0.0019**	**0.0106**	**0.0577**	**0.3756**	**0.0088**	**0.0003**	**0.46**

Table 6-10: Power dissipated in the rotational viscous damping elements in the multi-body dynamic model.

Octave Centre Frequency (Hz)	Power Absorbed in Rotation (N.m/s)					
	C1	C7	T12	L5	Buttock	**Total**
1	0	0	0	0.0004	0	**0.0004**
1.25	0	0	0	0.0007	0.0001	**0.0008**
1.6	0	0	0	0.0015	0.0002	**0.0017**
2	0	0.0001	0	0.0006	0.0001	**0.0009**
2.5	0.0001	0.0002	0	0.0003	0.0001	**0.0007**
3.15	0.0002	0.0008	0.0001	0.0001	0.0001	**0.0013**
4	0.0008	0.0023	0.0004	0.0003	0.0002	**0.0041**
5	0.0017	0.0034	0.0011	0.0014	0.0007	**0.0083**
6.3	0.0009	0.0012	0.0005	0.0012	0.0006	**0.0043**
8	0.0003	0.0003	0.0002	0.0004	0.0002	**0.0014**
10	0.0001	0.0001	0.0001	0.0001	0.0001	**0.0005**
12.5	0	0	0	0	0	**0**
Total (N.m/s)	**0.0042**	**0.0083**	**0.0025**	**0.0069**	**0.0024**	**0.02**

Tables 6-9 and 6-10 also show the total power absorbed at each joint so as to provide an understanding of the proportion of power distributed among the segments of the human body. As expected, vertical translation of the buttock joint at the body-seat interface shows maximum energy dissipation followed by vertical translations at the abdominal viscera and the L5 joint. Further, from Table 6-10 it is evident that maximum rotational energy is dissipated at the C7 joint, followed by the L5 joint in rotation, although these values are lower compared than their translational counterparts. The head-neck complex together accounts for more than 50% of the power absorbed due to pitch rotations.

In conclusion, a large proportion of the vibratory power, as suggested by the multi-body human model, seems to be absorbed at the body-seat interface, primarily by the largely fleshy buttock tissue. However, significant energy dissipation also occurs at the abdominal viscera and the lower lumbar joint (L5). Additionally, the lumbar joint in the model is the only joint that shows relatively high energy dissipation in translation and rotation. This is suggestive of an elevated risk for tissue damage and injury in the lumbar region, commonly cited in many epidemiological studies (*e.g.*, Bovenzi and Hulshof, 1998). Similarly, some field studies have also reported injury and pain in the neck region of operators of mobile machinery (Hoy *et al.*, 2005) that could be associated with the increased energy dissipation observed in the head-neck unit. Although it is not the scope to this thesis dissertation, the model developed herein may be employed to study such relationships.

6.8   Summary

This chapter focused on the development of an anthropometric multi-body biodynamic (MBD) human model for the frequency-domain simulation of biodynamic responses of a 50th percentile male seated on a rigid seat and exposed to vertical WBV. An extensive survey of the reported analytical studies suggested that the MBD technique would be desirable for the development of a sufficiently-, but not overly-, simplified biodynamic model incorporating anthropometric inertial and joint properties. The sagittal-plane multi-segment human model was formulated on the basis of different biodynamic response functions identified from measurements (Chapters 3, 4 and 5), including the global and segmental responses.

Visco-elastic parameters of the model were identified through minimisation of different error functions in different combinations of the measured biodynamic responses using the Genetic Algorithm approach. It was found that model parameters derived through minimisation of an error function as a combination of the measured vertical STHT and fore-aft head and C7 motions provides an optimal solution that satisfactorily follows the primary resonance peak in both the APMS response and the segmental transmissibility. Eigen analysis of the derived human model revealed the presence of 4 significant modes at frequencies below 15 Hz. Two modes were observed in the vicinity of 5 Hz, the primary resonant frequency, suggesting coupled body-segment motions. These modes related primarily to the vertical movement of the whole body and the rotation of the pelvic segment, respectively.

The model, when applied for predicting the vibratory power absorbed by the human body, shows good response matching with the measured total power at the human-seat interface. Hence, the power absorbed across each of its joints was further

investigated to study the distribution of dissipative energy in the body. Results reveal that a large portion of the power is absorbed at the body-seat interface, primarily by the buttock tissue. However, significant energy dissipation also occurs at the abdominal viscera and the lower lumbar joint (L5). Interestingly, the L5 connection is the only joint that shows relatively high energy dissipation both in translation and pitch rotation. The model and the methodology derived in this research study may be further employed to study relationships between segmental power absorption and incidences of tissue damage and pain reported in epidemiological field studies.

7. Conclusions and Recommendations for Future Work

7.1 Major Contributions of the Dissertation Research

This dissertation research is mainly concerned with the study of transmission of vertical whole-body vibration (WBV) through the upper body of seated human beings, the distribution of vibration absorbed power, and the development of a multi-body biodynamic model of the seated human body. The dissertation research involved: (i) simultaneous non-invasive measurement of driving-point biodynamic responses (APMS) and vibration transmission to selected segments of the body, primarily through the spine, under selected test conditions representative of vehicular vibration environments; (ii) characterisation of the seated human's vibration behaviour in terms of the segmental vibration transmission responses; (iii) analyses of primary contributory factors including the back and hands support conditions, and the excitation magnitude; (iv) analyses of relationships between body segment transmissibility and the driving-point APMS responses; (v) identification of target datasets in terms of the measured segmental vibration transmission functions and APMS for bio-model development; (vi) development and validation of an anthropometric multi-body dynamic (MBD) bio-model to simulate the sagittal-plane vibration responses of the 50th percentile seated human body exposed to vertical seat excitations; and (vii) application of the model for estimating distribution of vibration power absorption that may help identify body segments susceptible to WBV injuries. The major highlights and contributions of this research study are summarised below:

i.) The biodynamic responses of the seated body exposed to vertical WBV were measured simultaneously in terms of the driving-point apparent mass (APMS) and

269

segmental vibration transmissibility. The effects of back support condition, hands position and excitation magnitude on the body-segment vibration transmissibility characteristics in the vertical and fore-aft biodynamic axes have been systematically studied through statistical analyses (ANOVA).

ii.) The study has proposed a methodology for measurement of segmental vibration with a back support, which has not yet been attempted. The interplay of the various experimental factors related to sitting posture and WBV magnitude on the driving point APMS and the vibration transmissibility at different body segments was thoroughly studied using single- and multi-factor ANOVA so as to identify the most significant influencing factors.

iii.) The nature and magnitudes of errors associated with non-invasive data acquisition of vibration parameters at different body locations were systematically investigated and documented. Subsequently, appropriate experimental and/or analytical counter-measures were incorporated, particularly for the skin effects, sensor misalignments and seat inertia effect. The visco-elastic properties of the skin tissues near different measurement locations were identified and a mathematical method was employed to correct for the skin effect in the measured vibration transmissibility.

iv.) The results from the ANOVA are used to illustrate the need for identifying sitting posture- and anthropometry-specific biodynamic target functions for the development of effective vibration bio-models for applications in seating dynamics, absorbed power distribution and identification of potential injuries and intervention. This is amongst the most significant contributions of this research dissertation.

v.) A 19 degree-of-freedom (DOF) anthropometric multi-body biodynamic model of a seated 50th percentile human body was developed to simulate the sagittal-plane vibration behaviour of the body exposed to vertical WBV without a back support. The inertial and geometric parameters of the body segments were identified using appropriate databases in the literature and the average total body mass of the subjects employed in the experimental study.

vi.) The visco-elastic parameters of the model were identified using parameter-search operations using Genetic Algorithm, based on the response error of the model with the target datasets extracted from the experimental measurements. It is shown that model identification based on the widely-employed APMS data alone is inadequate for the study of upper body vibration modes and thus the distributed vibration energy.

vii.) The effectiveness of the model developed in the study is demonstrated by comparing the model responses in terms of not only the driving-point measure (as most widely reported) but also the vertical and fore-aft vibration transmissibility, and the total absorbed power.

viii.) A methodology for the prediction of the distribution of dissipative power in the viscous elements of the multi-body model is proposed using the model developed in this study, which cannot be measured using the non-invasive techniques. The power absorbed within a joint could serve as an important basis to derive the localised stresses and strains related to WBV exposure. This aspect is also considered amongst the most significant contributions of the dissertation research.

7.2   Major Conclusions

The following major conclusions are drawn from the methods explored and the results obtained in the course in the dissertation research:

a)   The study of the vibration transmitted to different segments of the seated human body, especially through the spine, plays a significant role in enhancing our understanding of health risks associated with whole-body vibration exposure of the seated body. The body-segment vibration responses reported in a few studies, however, exhibit wide variabilities that are mostly caused by differences in measurement and data analysis methods, experimental conditions and subject anthropometry employed in these studies.

b)   The measurement of vibration transmission to different segments of the human body using non-invasive methods is prone to a variety of errors, namely skin effects and the sensor misalignment, which require appropriate experimental and analytical correction methodologies. The damped free responses of the miniature skin-mounted trunk accelerometers could be effectively applied to account for the skin effects. The results revealed that natural frequencies and damping ratios of the tissues at the considered vertebral locations occur in the 15-20 Hz and 0.51-0.62 ranges, respectively.

c)   The misalignment of the trunk accelerometers from the basicentric axes also induces considerable errors at the C7, T5 and L5 vertebrae, with the sensor at C7 showing the maximum orientation error of about 35˚.

d)   The body-segment vibration transmissibility responses of the twelve subjects considered in this study depict most significant dependence on the support conditions, particularly the back support condition ($p<0.05$). The interactions of

272

the upper body with the backrest caused a large scatter in the fore-aft responses, especially at the thoracic and lumbar locations, which was attributed to variations in the upper-body backrest support across the subjects.

e)   The hands-support condition generally revealed a relatively smaller effect on most of the vertical transmissibility responses. However, hands holding the steering wheel showed greater effects on response magnitudes at C7 and L5. Furthermore, hands holding the steering wheel resulted in relatively lower dispersions in all the responses, probably due to the additional stabilising constraint provided by the steering wheel.

f)   Interactions of the back support resulted in greater attenuation of vibration in the vertical axis to all the body locations, while increasing the fore-aft transmissibility at C7 and T5, suggestive of a probable difference in the modes of vibration between the no back and back supported postures.

g)   An increase in vibration magnitude generally caused a decrease in the resonant frequencies observed from the vertical transmitted vibration data. A similar "softening" effect in the fore-aft responses, however, was seen only at the head and C7.

h)   In order of importance for the understanding of body movements under vertical vibration and model developments, it is shown that the effects of the back support condition assume prime significance followed by the excitation magnitude and the hands position.

i)   The body mass is of prime importance when the target response involves the driving-point measure, namely, the mechanical impedance or apparent mass. In addition to the body mass, the sitting height of subjects showed relatively greater

effects on the vibration transmitted to the body segments. While the peak vertical response magnitude to the thoracic (T5 and T12) and cervical (C7) locations showed insignificant change due to the subjects' sitting height, the head and C7 fore-aft motions displayed relatively higher dependence.

j) It is concluded that separate sets of segmental biodynamic functions need to be identified for different postural conditions and body mass so as to represent the unique contribution of the specific independent parameters when formulating biodynamic models.

k) The review of the reported analytical studies suggests that mechanical-equivalent lumped parameter models are not suitable for the study of multi-dimensional movement of the seated human body exposed to WBV, which was clearly observed in the study. The global and localised vibration responses of the seated body, as a minimum, need to be described by a sagittal plane model.

l) Visco-elastic parameters of a 19 degree-of-freedom (DOF) multi-body biodynamic human model, identified through minimisation of the composite error function comprising vertical head vibration, and fore-aft head and C7 motions data, resulted in acceptable agreements in both the APMS and segmental transmissibility responses.

m) Eigen analysis of the seated human model revealed the presence of 4 significant body modes including the torso pitch mode at 1.56 Hz, the buttock compression mode at 4.76 Hz, pelvic rotation at 5.71 Hz and a visceral mode at 7.95 Hz.

n) The total vibration power absorbed into the model agreed reasonably well with the measured total power.

o)   The model developed in the study was applied to study the distribution of dissipative power within different segment joints considered in the model. The results revealed that a large portion of the power was absorbed at the body-seat interface, primarily by the buttock tissue. However, significant energy dissipation also occurred at the abdominal viscera and the lower lumbar joint (L5). The distributed power absorption characteristics could be interpreted in relation to the potential injury risks due to WBV exposure.

7.3   Recommendations for future work

Low back pain is an obvious issue in the work place involving human interactions with vibration machinery, although a conclusive relationship among the two parameters is yet to be established. The research work performed in this dissertation is considered significant in enhancing the much needed biodynamic target datasets, which may be employed for the development and validation of complex anthropometric biomodels of the seated body exposed to vertical WBV. These datasets were extracted from measurements of force-motion and motion-motion variables simultaneously at the driving-point and at selected segments of the human body under vertical vibration and postures. Further work is, however, required so as to gain a better understanding of the nature of the problem of low back pain and its influence factors through experimental and analytical means. Some of the possibilities for further research immediately following this dissertation and further on are suggested below:

Experiments

- **Subject pool**: This research involved 12 male subjects chosen specifically to represent the behaviour of the segments of the 50th percentile human body. It

275

would be beneficial to extract body segment responses from a larger population so as to identify any effects due to anthropometry and gender.

- **Cushion interface**: The study of body segment vibration would be more representative of actual work conditions if performed with subjects seated on cushion seats used in mobile machinery. Although this may present difficulties in measurement of the driving-point force, the acquisition of body segment vibration transmissibility is very similar to the methodologies employed in this research work.

- **Posture**: The present study suggests a significant influence of the back rest on the vibration transmitted to the body segments. A thorough investigation of the segmental responses under different back rest positions and inclination angles is recommended.

- **Excitation axes:** The current research concentrated on the sagittal-plane biodynamic response of the seated human body to vertical seat vibration. The study of human responses to horizontal-plane vibration input and multi-axes WBV input would be very useful in assessing the human body's responses in the actual work environment. This is highly recommended that body segment vibration responses be measured under horizontal-plane vibration and multi-axis excitations in order to establish the corresponding target response datasets.

Analytical work

- **Coupled human-cushion model**: The human model developed in this research study has been developed with a rigid seat. It is highly recommended that the human model be employed with a cushion interface formulation so as to make it effective for coupled seat-human studies.

276

- **Coupled human-vehicle model**: The integration of the present multi-body dynamic (MBD) human model as is with a vehicle model, preferably an MBD formulation, is highly recommended for the study of the coupled vehicle-human system. Such a coupled model would also be attractive to manufacturers of mobile machinery.

- **Power-based parameter search**: The current model is capable of depicting the total power absorbed in the human body as well as the power absorbed across each joint. It may thus be beneficial to include the joint dissipative power in the parameter-search optimisation process for future applications of the model.

- **Model structure refinement**: The developed human model comprises three lumped inertial entities, *viz.*, thoracic, lumbar and pelvic segments, to represent the torso of the seated human body. It is recommended that the model be further refined to represent individual vertebral segments in the critical segments, especially the neck and lumbar regions, and the parameter-search operation rerun with the target functions employed in this research study to ensure the necessity for such refinements.

- **Model joint refinement**: The parameters of the current model have been identified under vertical WBV. It is highly recommended that the model be adapted for application to forced vibration in other axes and possibly even for a multi-axis input. This work requires refinements to the joint formulations including the (i) addition of degrees of freedom at the appropriate joints; and (ii) additional codes in MSC ADAMS and MATLAB in order to perform the parameter identification for these joint variables.

References

Amirouche F, Ider S. (1988) Simulation and analysis of a biodynamic human model subjected to low accelerations–a correlation study. J Sound and Vibn. 123, 281-292.

Andersson G, Örtengren, R. (1974) Lumbar disc pressure and myoelectric back muscle activity during sitting: II. Studies on an office chair. Scandinavian J Rehab. Med. 3, 115-121.

Andreoni G, Santambrogio G, Rabuffetti M, Pedotti A. (2002) Method for the analysis of posture and interface pressure of car drivers. Applied Ergonomics 33, 511-522.

Basmajian J, Blumenstein R. (1980) Electrode placement in EMG biofeedback. Williams & Wilkins, Baltimore, USA.

Bazrgari B, Shirazi-Adl A, Kasra M. (2008) Seated whole body vibrations with high-magnitude accelerations-relative roles of inertia and muscle forces. J Biomechanics, 41, 2639-2646.

Belytschko T, Privitzer E. (1978) Refinement and validation of a three-dimensional head-spine model. Aerospace Med. Research Lab. Wright-Patterson Air force Base, Ohio. Report No. AMRL-TR-78-7.

BHMS (Boeing Human Modeling System): http://www.boeing.com/assocproducts/hms/

Berkson M. (1977) Mechanical properties of the human lumbar spine flexibilities, intra-discal pressures, posterior element influences, Proc Inst Med Chic 31, 138–143.

Blüthner R, Seidel H, Hinz B. (1995) Can reflex mechanism explain the timing of back muscles during sinusoidal whole-body vibration and transients? UK Conf. HRV, Southampton, UK.

Blüthner R, Seidel H, Hinz B. (2001) Examination of the myoelectric activity of back muscles during random vibration–methodical approach and first results. Clinical Biomechanics 16 Suppl.(1), S25-S30.

Boileau P-É, Rakheja S. (1998) Whole-body vertical biodynamic response characteristics of the seated vehicle driver: Measurement and model development. Intl J Indus Ergonomics, 22, 449-472.

Boileau P-É, Rakheja S, Wu X. (2002) A body mass dependent mechanical impedance model for applications in vibration seat testing. J. Sound and Vibn. 253, 243-264.

Boileau P-É, Rakheja S, Yang X, Stiharu I. (1997) Comparison of biodynamic response characteristics of various human body models as applied to seated vehicle drivers. Noise and Vibn. Worldwide 28, 7-15.

Boileau P-É, Wu X, Rakheja S. (1998) Definition of a range of idealized values to characterise seated body biodynamic response under vertical vibration. J. Sound and Vibn. 215, 841-862.

Bongers P.M., Boshuizen H.C., Hulshof C.T.J., Koemeester A.P. (1988) Back disorders in crane operators exposed to whole-body vibration, Intl. Arch. Occupational Environ. Health, 60, 129-137.

Bonney R., Corlett E. (2003) Vibration and spinal lengthening in simulated vehicle driving. Applied Ergonomics 34, 195-200.

Bovenzi M, Betta A. (1994) Low back disorders in agricultural tractor drivers exposed to WBV and postural stress. Applied Ergonomics, 25 (4), 231-241.

Bovenzi M, Hulshof C. (1998) An updated review of epidemiologic studies on the relationship between exposure to whole-body vibration and low back pain. J. Sound and Vibn. 215 (4), 595-611.

Bovenzi M, Pinto I, Stacchini N. (2002) Low back pain in port machinery operators. J. Sound Vibn. 253 (1) 3-20.

Bovenzi M, Zadani A. (1992) Self-reported back symptoms in urban bus drivers exposed to whole body vibration. Spine, 17, 1048-59.

Brinckmann P, Biggemann M, Hilweg D. (1989) Prediction of the compressive strength of human lumbar vertebrae. Clinical Biomechanics 4 Suppl.(2), S1-S2.

Buck B, Wölfel H. (1996) A dynamic model for human WBV with detailed representation of the lumbar spine. In: Proc. of the 10th conference of the European Society of Biomechanics, Leuven, 338.

Buck B. (1997) Modell für das Schwingungsverhalten des sitzenden Menschen mit detaillierter Abbildung der Wirbelsäule und Muskulatur im Lendenbereich. Dissertation. TH Darmstadt. Darmstadt: Shaker Verlag.

Cappozzo A. (1981) Analysis of the linear displacement of the head and trunk during walking at different speeds. J. Biomechanics, 14 (6), 411-425.

Cats-Baril W.L, Frymoyer J.W. (1991) The Economics of Spinal Disorders. In: Frymoyer J.W. et al., eds. The Adult Spine. Raven Press. New York, USA.

Chaffin D, Andersson G, Martin B. (1991) Occupational biomechanics. 3rd Edition. John Wiley and Sons, Inc. Toronto, Canada.

Cheng H, Obergefell L, Rizer A. (1994) Generator of Body Data (GEBOD) manual. Wright-Patterson Air force Base, Ohio. Report No. AL/CF-TR-1994-0051.

Cho Y, Yoon Y-S. (2001) Biomechanical model of human on seat with backrest for evaluating ride quality. Intl J Indus Ergonomics, 27, 331-345.

Christ W, Dupuis H. (1966) Uber die beanspruchung der wirbesaule unter dem einfluss sinusformiger und stochastischer schwingungen. Intl. W. Angew. Physiol. 22, 258-278.

Coermann R. (1962) The mechanical impedance of the human body in sitting and standing position at low frequencies. Human Factors 4, 227-253.

Cullmann A, Wölfel H. (2001) Design of an active vibration dummy of sitting man. Clinical Biomechanics 16(Suppl. 1), S64-S72.

de Craecker W. (2003) Whole-body vibration comfort analysis based upon spine modelling, 38th UK Conf. HRV, Southampton, UK.

de Oliveira C, Simpson D, Nadal J. (2001) Lumbar back muscle activity of helicopter pilots and whole-body vibration. J Biomechanics, 34, 1309-1315.

DIN 45676 (1992) Mechanical impedances at the driving point and transfer functions of the human body. Deutsches Institut für Normung e.V.

Dobson B. (1987) A straight-line technique for extracting modal properties from frequency response data. Mech. Systems and Signal Proc. 1, 29-40.

Dolan P, Adams M. (2001) Recent advances in lumbar spinal mechanics and their significance for modelling. Clinical Biomechanics 16 Suppl.(1), S8-S16.

Donati P, Bonthoux C. (1983) Biodynamic response of the human body in the sitting position when subjected to vertical vibration. J. Sound and Vibn. 90, 423-442.

Dong R, Rakheja S, Smutz W, Schopper A, Welcome D, Wu J (2002) Effectiveness of a new methods (TEAT) to assess vibration transmissibility of gloves. Intl J Indus Ergonomics, 30, 33-48.

Drerup B, Granitzka M, Assheuer J, Zerlett G. (1999) Assessment of disc injury in subjects exposed to long-term whole-body vibrations. Euro J Spine. 8, 458-467.

El-Khatib A, Guillon F, Domont A. (1998) Vertical vibration transmission through the lumbar spine of the seated subject–first results. J Sound Vibn. 215, 763-773.

El-Khatib A, Guillon F. (2001) Lumbar intradiscal pressure and whole-body vibrations–first results. Clinical Biomechanics 16 Suppl.(1), S127-S134.

ERL human body models: http://www.erlllc.com/erl/human_body_models.php

Fairley T, Griffin M. (1989) The apparent mass of the seated human body: vertical vibration. J. Biomechanics 22, 81-94.

Fritz M. (1998) Three-dimensional biomechanical model for simulating the response of the human body to vibration stress, IEEE Med. Bio. Engg. and Computation, 36, 686-692.

Fritz M. (2000) Simulating the response of a standing operator to vibration stress by means of a biomechanical model, J Biomechanics, 33, 795-802.

Fritz M. (2005) Dynamic properties of the biomechanical model of the human body – influence of posture and direction of vibration stress, J Low Freq Noise, Vibn and Active Control, 24, 233-249.

Fritz M, Fischer S, Brode P. (2005) Vibration-induced low back disorders-comparison of the vibration evaluation according to ISO 2631 with force-related evaluation. Appl. Ergonomics, 36, 481-488.

Gardner-Morse M, Stokes I. (2004) Structural behaviour of human lumbar spine motion segments. J Biomechanics, 37, 205-212.

Gray H. (1918) Anatomy of the Human Body. 20th Ed. Lea & Febiger, Philadelphia, USA.

Griffin M. (1990) Handbook of human vibration. Elsevier Academic Press, London, UK.

Griffin M. (2001) The validation of biodynamic models. Clinical Biomechanics, 16 (Suppl. 1), S81-S92.

Griffin M, Whitham E. (1978) Individual variability and its effect on subjective and biodynamic response to whole-body vibration. J Sound and Vibn. 58, 239-250.

Hagena F, Piehler J, Wirth C, Hofman G, Zwingers T. (1986) The dynamic response of the human spine to sinusoidal Gz vibration. *In vivo* experiments. Neuro-orthopaedics, 2, 29-33.

Härtel T, Hermsdorf H. (2006) Biomechanical modelling and simulation of human body by means of DYNAMICUS. Institute of Mechatronics, Chemnitz University of Technology, Chemnitz, Germany. J Biomechanics, 39 Suppl. 1, Abstracts of teh 5th World Congress on Biomechanics, S549.

Haupt R, Haupt S. (1998) Practical Genetic Algorithm, Wiley Interscience, Hoboken, New Jersey, USA.

Hinz B, Blüthner R, Menzel G, Seidel H. (1994) Estimation of disc compression during transient whole-body vibration. Clinical Biomechanics, 9, 263-272.

Hinz B, Rützel S, Blüthner R, Menzel G, Wölfel H, Seidel H. (2006) Apparent mass of seated man – First determination with a soft seat and dynamic seat pressure distributions. J Sound and Vibn. 298, 704-724.

Hinz B, Seidel H. (1987) The nonlinearity of the human body's dynamic response during sinusoidal whole body vibration. Indus Health, 25, 169-181.

Hinz B, Seidel H, Bräuer D, Menzel G, Blüthner R, Erdmann U. (1988a) Examination of spinal column vibrations: a non-invasive approach. Euro J Appl. Physiology, 57, 707-713.

Hinz B, Seidel H, Bräuer R, Menzel G, Blüthner R, Erdmann U (1988b) Bidimensional accelerations of lumbar vertebrae and estimation of internal spinal load during sinusoidal vertical whole-body vibration: a pilot study. Clinical Biomechanics, 3, 241-248.

Hinz B, Seidel H, Menzel G, Blüthner R. (2002) Effects related to random whole-body vibration and posture on a suspended seat with and without backrest. J Sound and Vibn. 253, 265-282.

Hoy J, Mubarak N, Nelson S, Sweerts de Landas M, Magnusson M, Okunribido O, Pope M. (2005) Whole-body vibration and posture as risk factors for low back pain among forklift truck drivers. J Sound and Vibn. 284 (3-5), 933-946.

ISO 5982 (2001) Mechanical vibration and shock–Range of idealized values to characterize seated-body biodynamic response under vertical vibration.

ISO 2631-1 (1997) Mechanical vibration and shock–Part 1: Mechanical vibration and shock – Evaluation of human exposure to whole-body vibration. General requirements.

ISO 2631-5 (2004) Mechanical vibration and shock–Part 5: Method for evaluation of vibration containing multiple shocks.

Jödicke R. (2001) Dynamic simulation with RAMSIS by linking the ergonomic model with the biomechanical human model DYNAMICUS. Proc. of the RAMSIS User Conference, 2001.

Judic J, Cooper J, Truchot P, Effenterre P, Duchamp R. (1993) More objective tools for the integration of postural comfort in automotive seat design. SAE No. 930113.

Karwowski W, Gaweda A, Marras W, Davis K, Zurada J, Rodrick D. (2006) A fuzzy relational rule network modeling of electromyographical activity of trunk muscles in manual lifting based on trunk angles, moments, pelvic tilt and rotation angles. Intl. J Indus Ergonomics 36, 847-859.

Keller T, Colloca C, Beliveau J-G. (2002) Force-deformation response of the lumbar spine: a sagittal plane model of posteroanterior manipulation and mobilisation. Clinical Biomechanics, 17, 185-196.

Kim T, Kim Y, Yoon Y. (2005) Development of biomechanical model of the human body in a sitting posture with vibration transmissibility in the vertical direction, Intl. J. Indus Ergonomics, 35, 817-829.

Kim S, White S, Bajaj A, Davies P. (2003) Simplified models for the vibration of mannequins in car seats, J Sound Vibn. 264, 49-90.

Kim W, Voloshin A, Johnson S. (1994) Modelling of heel strike transients during running. Human Movement Science, 13, 221-244.

Kitazaki S, Griffin M. (1995) A data correction method for surface measurement of vibration on the human body. J Biomechanics, 28, 885-890.

Kitazaki S, Griffin M. (1997) A modal analysis of whole-body vertical vibration, using a finite element model of the human body. J Sound Vibn. 200, 83-103.

Kitazaki S, Griffin M. (1998) Resonance behaviour of the seated human body and effects of posture. J Biomechanics, 31, 143-149.

Kjellberg A, Wikström B, Landström U. (1994) Injuries and other adverse effects of occupational exposure to whole-body vibration. A review for criteria documentation. Arb Hälsa 41.

Kumar S, Mital A. (1996) Electromyography in ergonomics Taylor and Francis Ltd. London.

Lafortune M, Henning E, Valiant G. (1995) Tibial shock measured with bone and skin mounted transducers. J Biomechanics, 28, 989-993.

Lange W, Coermann R. (1965) Relativbewegungen benachbarter wirbel unter schwingungsbelastrung. Intl. W. Angew. Physiol. 1, 326-334.

Lee K. (2006) CAD systems for human-centered design. Computer-aided design and applications, 3, 615-628.

Lemerle P, Boulanger P. (2006) Lower limb contribution to the dynamic response of the seated man. J Sound Vibn. 294, 1004-1015.

Lewis C. (2005) Variability in measurements of seat transmissibility with an active anthropodynamic dummy and with human subjects, 40th UK Group Meeting on Human Response to Vibration.

Liang C-F, Chiang C-F. (2006) A study of biodynamic models of seated human subjects exposed to vertical vibration, Intl J Indus Ergonomics. 36, 869-890.

Liang C-F, Chiang C-F, Nguyen T-G. (2007) Biodynamic responses of seated pregnant subjects exposed to vertical vibrations in driving conditions. Vehicle System Dynamics, 45, 1017-1049.

LifeMOD: http://www.lifemodeler.com

Lings S, Leboeuf-Yde C. (2000) Whole-body vibration and low back pain: a systematic critical review of the epidemiological literature 1992-1999, Intl. Arch. Occupational Env. Health, 73, 290-297.

Liu W, Nigg B. (2000) A mechanical model to determine the influence of masses and mass distribution on the impact force during running. J Biomechanics, 33, 219-224.

Liu X, Shi J, Li G. (1998) Biodynamic response and injury estimation of ship personnel to ship shock motion induced by underwater explosion. Proc. of 69th Shock and Vibration Symp., St. Paul., Vol. 18, 1-18.

Lundström R, Holmlund P. (1998) Absorption of energy during whole-body vibration exposure. J Sound and Vibn. 215 (4), 789-799.

Luo Z, Goldsmith W. (1991) Reaction of a human head/ neck/ torso system to shock, J Biomechanics, 24, 499-510.

Luoma K, Riihimäki H, Raininko R, Luukkonen R, Lamminen A, Viikari-Juntura E. (1998) Lumbar disc degeneration in relation to occupation. Scandinavian J Work Environment Health, 24, 358-366.

Magnusson M, Hansson T, Pope M. (1994) The effect of seat back inclination on spine height changes. Applied Ergonomics, 25, 294-298.

Magnusson M, Pope M. (1998) A review of the biomechanics and epidemiology of working postures (it isn't always vibration which is to blame!) J Sound and Vibn. 215 (4), 965-976.

Magnusson M, Pope M, Rostedt M, Hansson T. (1993) Effect of backrest inclination on the transmission of vertical vibrations through the lumbar spine. Clinical Biomechanics, 8, 5-12.

Mansfield N. (2005) Impedance methods (Apparent mass, driving point mechanical impedance and absorbed power) for assessment of the biomechanical response of the seated person to whole-body vibration. Indus Health, 43, 378-389.

Mansfield N, Griffin M. (1996) Vehicle seat dynamics measured with an anthropodynamic dummy and human subjects, Proc. of the Inter-Noise'96, Vol. 4, 1725-1730.

Mansfield N, Griffin M. (2000) Non-linearities in apparent mass and transmissibility during exposure to whole-body vertical vibration. J Biomechanics, 33, 933-941.

Mansfield N, Griffin M. (2002) Effects of posture and vibration magnitude on apparent mass and pelvis rotation during exposure to whole-body vertical vibration. J Sound and Vibn. 253, 93-107.

Mansfield N, Maeda S. (2005) Comparison of the apparent mass of the seated human measured using random and sinusoidal vibration. Indus Health, 43, 233-240.

Mansfield N, Maeda S. (2007) The apparent mass of the seated human exposed to single-axis and multi-axis whole-body vibration. J Biomechanics, 40, 2543-2551.

Markolf K. (1970) Stiffness and damping characteristics of the thoracic lumbar spine. Proc. Wshop. Bioengg. on approaches to problems of the spine. National Institute of Health, Bathesda, MA. 87-142.

Matsumoto Y, Griffin M. (1998) Movement of the upper body of seated subjects to vertical whole body vibration at the principal resonance frequency. J Sound and Vibn. 215 (4), 743-762.

Matsumoto Y, Griffin M. (2001) Modelling the dynamic mechanisms associated with the principal resonance of the seated body. Clinical Biomechanics, 16 Suppl.(1), S31-S44.

Matsumoto Y, Griffin M. (2002) Non-linear characteristics in the dynamic responses of seated subjects exposed to vertical whole-body vibration. J Biomechanical Engg. 124, 527-532.

McGuan S. (2001) Human modeling–from bubbleman to skeletons. Proc of the SAE Digital Human Modeling Conference, Arlington, VA, USA.

Mertens H. (1978) Nonlinear behaviour of sitting humans under increasing gravity. Aviation Space and Environmental Medicine, 49, 287-298.

Morrison J, Robinson D, Roddan G, Nicol J, Butler B. (1995) Analysis of skin transfer function in response to mechanical shocks. Proc. UK Informal Group Meeting on Human Response to Vibration, Silsoe.

Muksian R, Nash C. (1974) A model for the response of seated humans to sinusoidal displacements of the seat. J Biomechanics, 7, 209-215.

Natarajan R, Ke J, Andersson G. (1994) A model to study the disc degeneration process. Spine, 19, 259-265.

Nawayseh N, Griffin M. (2004) Tri-axial forces at the seat and backrest during whole-body vertical vibration. J Sound and Vibn. 277, 309-326.

Nawayseh N, Griffin M. (2005) Tri-axial forces at the seat and backrest during whole-body fore-aft vibration. J Sound and Vibn. 281, 921-942.

Nélisse H, Patra S, Rakheja S, Boutin J, Boileau P-É. (2008) Assessments of two dynamic manikins for laboratory testing of seats under whole-body vibration Intl J Indus Ergonomics, 38, 457-470.

Nicholson L, Maher C, Adams R, Phan-Thien N. (2001) Stiffness properties of the human lumbar spine: A lumped parameter model. Clinical Biomechanics, 16, 285-292.

Nigg B, Anton M. (1994) Energy aspects for elastic and viscous shoe soles and playing surfaces. Medicine and Science in Sports and Exercise, 27, 92-97.

Paddan G, Griffin M. (1988) The transmission of translational seat vibration to the head – I. Vertical seat vibration. J Biomechanics, 21, 191-197.

Paddan G, Griffin M. (1998) A review of the transmission of translational seat vibration to the head. J Sound and Vibn. 215, 863-882.

Pain & Disability: http://www.painanddisability.com

Palmer K, Coggon D, Pannett B, Griffin M. (1998) The development of a self-administered questionnaire to assess exposures to hand-transmitted and WBV and their health effects. J Sound Vibn. 215 (4), 653-686.

Pang J, Qatu M, Rao D, Sheng G. (2005) Nonlinear seat cushion and human body model. Intl J Vehicle Noise and Vibn. 1(3/4), 194-206.

Panjabi M, Brand R, White III A. (1976) Three-dimensional flexibility and stiffness properties of the human thoracic spine. J Biomechanics, 9, 185-192.

Panjabi M, Anderson G, Jorneus L, Hult E, Mattson L. (1986) *In vivo* measurement of spinal column vibrations. J Bone Joint Surgery, 68-A (5), 695-702.

Pankoke S, Buck B, Wölfel H. (1998) Dynamic FE model of sitting man adjustable to body height, body mass and posture used for calculating internal forces in the lumbar vertebral disks. J Sound and Vibn. 215, 827-839.

Pankoke S, Hofmann J, Wölfel H. (2001) Determination of vibration-related spinal loads by numerical simulation, Clinical Biomechanics, 16 Suppl. 1, S45-S56.

Patra S, Rakheja S, Nelisse H, Boileau P-É, Boutin J. (2008) Determination of reference values of apparent mass responses of seated occupants of different body masses under vertical vibration with and without a back support. Intl J Indus Ergonomics, 38, 483-498.

Pope M. (1996) Epidemiological and aetiological aspects of low back pain in vibration environments – an update. Clinical Biomechanics, 11 (2), 61-73.

Pope M, Broman H, Hansson T (1989) The dynamic response of subject seated on various cushions. Ergonomics 32, 1155-1166.

Pope M, Kaigle A, Magnusson M, Broman H, Hansson T (1991) Intervertebral motion during vibration. Proc. of Inst. of Mechanical Engr.-Part H 205, 39-44.

Pope M, Magnusson M, Broman N, Hasson T. (1998) The dynamic response of human subjects while seated in car seats. Iowa Othrop. J. 18, 124-131.

Pope M, Svensson M, Broman H, Anderson G. (1986) Mounting of the transducers in measurement of segmental motion of the spine. J. Biomechanics 19, 675-677.

Pope M, Wilder D, Magnusson M. (1998) Possible mechanisms of low back pain due to whole-body vibration. J. Sound and Vibn. 215, 687-697.

Pope M, Goh K, Magnusson M. (2002) Spine Ergonomics. Annual Review Biomedical Engg. 4, 49-68.

Pranesh A, Rakheja S, DeMont R. (2010) Influence of support conditions on vertical whole-body vibration of the seated human body. Indus. Health 48, 682-697.

Quandieu P, Pellieux L. (1982) Study *in situ et in vivo* of the acceleration of lumbar vertebrae of a primate exposed to vibration in the Z-Axis. J. Biomechanics 15, 985-1006.

Rakheja S, Stiharu I, Boileau P-É. (2002) Seated occupant apparent mass characteristics under automotive postures and vertical vibration, J. Sound and Vibn. 253, 57-75.

Rakheja S, Stiharu I, Zhang H, Boileau P-É (2006) Seated occupant interactions with seat backrest and pan, and biodynamic responses under vertical vibration J. Sound and Vibn. 298 (3), 651-671.

Rakheja S, Mandapuram S, Dong R. (2008) Energy absorption of seated occupants exposed to horizontal vibration and role of back support condition. Indus. Health 46, 550-566.

RAMSIS (*Rechnergestütztes* Anthropologisch-Mathematisches System zur Insassen-Simulation): http://www.human-solutions.com/automotive/index_en.php

Reed M, Schneider L. (1996) Lumbar support in auto seats: conclusions from study of preferred driving posture. SAE No. 960478.

Rehn B, Bergdahl A, Ahlgren C, From C, Jarvholm B, Lundstrom R, Nillson T, Sundelin G. (2002) Musculoskeletal symptoms among drivers of all-terrain vehicles. J. Sound Vibn. 253 (1), 21-29.

Rohlmann A, Bauer L, Zander T, Bergmann G, Wilke H-J. (2006) Determination of trunk muscle forces for flexion and extension by using a validated finite element model of the lumbar spine and measured in vivo data. J Biomechanics 39, 981-989.

Safework: http://www.safework.com/

Sandover J. (1998) The fatigue approach to vibration and health: is it a practical and viable way of predicting the effects on people? J. Sound Vibn. 215, 699-721.

Sandover J, Dupuis H (1987) A reanalysis of spinal motion during vibration. Ergonomics 30 (6), 975-985.

Schultz A. (1979) Mechanical properties of human lumbar spine motion segments–part I: responses in flexion, extension, lateral bending and torsion. J Biomechanical Engineering 101, 46-52.

Schwarze S, Notbohm G, Dupuis H, Hartung E. (2002) Dose-response relationships between whole-body vibration and lumbar disk disease – a field study on 388 drivers of different vehicles. J. Sound Vibn. 253 (1), 3-20.

Seidel H. (2005) On the relationship between whole-body vibration exposure and spine health risk. Indus. Health, 43, 361-377.

Seidel H, Blüthner R, Hinz B. (1986) Effects of sinusoidal whole-body vibration on the lumbar spine: the stress-strain relationship. Int. Arch. Occup. Environ. Health 57, 207-223.

Seidel H, Blüthner R, Hinz B. (2001) Application of finite-element models to predict forces acting on the lumbar spine during whole-body vibration, Clinical Biomechanics, 16 Suppl. 1, S57-63.

Seidel H, Blüthner R, Hinz B, Schust M. (1997) Stresses in the lumbar spine due to whole-body vibration containing shocks. Experimental interdisciplinary study-anthropometry, biodynamics, biomechanical model, psychophysics and electromyography (Final Report). Schriftenreihe der Bundesanstalt fur Arbeitsschutz und Arbeitsmeidizin Dortmund/ Berlin, Forschung Fb 777, 197, Wirtschaftsverlag NW, Bremerhaven.

Seidel H, Blüthner R, Hinz B, Schust M (1998) On the health risk of the lumbar spine due to whole-body vibration – theoretical approach, experimental data and evaluation of whole-body vibration. J. Sound Vibn. 215, 723-741.

Seidel H, Griffin M. (2001) Modelling the response of the spinal system to whole-body vibration and repeated shock. Clinical Biomechanics 16 Suppl.(1), S3-S7.

Seidel H., Heide R. (1986) Long term effects of whole-body vibration: A critical survey of literature, Intl. Arch. Occupational Environ. Health, 58, 1-26.

Shirazi-Adl A. (1991) Finite element evaluation of contact loads on facets of an L2-L3 lumbar segment in complex loads. Spine 16, 533-541.

Shirazi-Adl A. (1992) Finite-element simulation of changes in the fluid content of human lumbar discs: mechanical and clinical implications. Spine 17, 206-212.

Shirazi-Adl A, Ahmed A, Shrivastava S. (1986) A finite element study of a lumbar motion segment subjected to pure sagittal plane moments. J Biomechanics 19, 331-350.

Slonim A. (1985) Comparative biodynamic response of two primate species to the same vibrational environment. Aviation and Space Environ. Medicine 56, 945-955.

Snyder W, Cook M. (1975) Report on the task group on reference mass. Intl. Commission on Radiological Protection Publicn. 23. Pergamon Press, Oxford, UK.

Stein G, and Múča P. (2003) Theoretical investigation of a linear planar model of a passenger car with seated people. Proc. of Instn. Mech. Engrs., J of Automobile Engineering, 217, 257-268.

Tchernychouk V, Rakheja S, Stiharu I, Boileau P-É. (2000) Study of occupant-seat models for vibration comfort analysis of automotive seats, Transactions of SAE, J. of Passenger Vehicles–Mechanical Systems, 109(6), 2308-2313.

Technomatix Jack: http://www.plm.automation.siemens.com/en_us/products/tecnomatix/

Teng T-L, Chang F-A, Peng C-P. (2006) Analysis of human body response to vibration using multi-body dynamics method. Proc. Inst Mech Engr. Part K: J. Multi-body Dynamics 220, 191-202.

TNO Automotive (2001) Manual: MADYMO human body models, Delft, The Netherlands.

Toward M. (2001) Effect of backrest interaction on seat cushion transmissibility, Proc. of the 36th UK Group Meeting on Human Response to Vibration, Farnborough, UK, 12-14 September, 106-115.

van Deursen L.L, van Deursen D.L, Snijders C.J, Wilke H.J. (2005) Relationship between everyday activities and spinal shrinkage. Clinical Biomechanics 20, 547-550.

van der Meulen P, Seidl A. (2007) RAMSIS – The leading CAD tool for ergonomic analysis of vehicles. Proc of the First Intl Conf on Digital Human Modeling, Beijing, China.

VDI 2057 (1987) Beurteilung der Einwirkung mechanischer Schwingungen auf den Menschen. Duesseldorf: Verein Deutscher Ingenieure.

VIN: Vibration Injury Network (2001a) Review of methods for evaluating human exposure to whole-body vibration. Appendix W4A to final report: BMH4-CT98-3291.

Verver M. (2004) Numerical tools for comfort analyses of automotive seats. PhD Thesis. Eindhoven University, The Netherlands.

Verver M, van Hoof J, Oomens C, van de Wouw N, Wismans J. (2003) Estimation of spinal loading in vertical vibrations by numerical simulation, Clinical Biomechanics, 18, 800-811.

Vose M.D. (1999) The simple genetic algorithm: foundations and theory, MIT Press, Cambridge, Massachusetts, USA.

Wan Y, Schimmels J. (1995) A simple model that captures the essential dynamics of a seated human exposed to whole body vibration. Advances in Bioengineering, ASME, BED 31, 333-334.

Wang W. (2006) A study of force-motion and vibration transmission properties of seated body under vertical vibration and effects of sitting posture. PhD Thesis, Concordia University, Montréal, Canada.

Wang W, Rakheja S, Boileau P-É (2004) Effects of sitting postures on biodynamic response of seated occupants under vertical vibration. Intl. J Indus. Ergonomics 34, 289-306.

Wang W, Rakheja S, Boileau P-É (2006a) Effects of back support condition on seat to head transmissibilities of seated occupants under vertical vibration. J. Low Freq. Noise and Vibn. 25 (4), 239-259.

Wang W, Rakheja S, Boileau P-É (2006b) The role of seat geometry and posture on the mechanical energy absorption characteristics of seated occupants under vertical vibration. Intl. J Indus. Ergonomics 36, 171-184.

Wang W, Rakheja S, Boileau P-É. (2008) Relationship between measured apparent mass and seat-to-head transmissibility responses of seated occupants exposed to vertical vibration. Journal of Sound and Vibration, 314(5), 907-922.

Wei L, Griffin M. (1998) Mathematical models for the apparent mass of the seated human body exposed to vertical vibration. J Sound Vibn. 212, 855-874.

White III A. (1969) Analysis of the mechanics of the thoracic spine in man. An experimental study of autopsy specimens. Acta Orthopaedica in Scandinavica Suppl. 127.

Whitham E, Griffin M. (1978) The effects of vibration frequency and direction on the location of areas of discomfort caused by whole-body vibration. Applied Ergonomics 9, 231-239.

Wikström B, Kjellberg A, Landstöm U. (1994) Health effects of long-term occupational exposure to whole-body vibration: A review. Intl. J Indus. Ergonomics 14, 273-292.

Wilder D, Pope M. (1996) Epidemiological and aetiological aspects of low back pain in vibration environments–an update. Clinical Biomechanics 11, 61-73.

Wisman J. (1983) Comparison of mass distribution of the Part 572 dummy. Ohio State University, Columbus, Ohio, USA.

Wu X. (1998) Study of driver-seat interactions and enhancement of vehicular ride vibration environment. PhD Thesis, Concordia University, Montréal, Canada.

Yamada H. (1970) Strength of biological materials (edited by Evans F.) Williams and Wilkins Baltimore, USA.

Yang K, King A. (1984) Mechanism of facet load transmission as a hypothesis for low-back pain. Spine 9, 557-565.

Yoshimura T, Nakai K, Tamaoki G. (2005) Multi-body dynamics modelling of seated human body under exposed to whole-body vibration. Indus. Health, 43, 441-447.

Zagorski J, Jakubowski R, Solecki L, Sadlo A, Kasperek W. (1976) Studies on the transmission of vibrations in human organism exposed to low frequency whole body vibration. Acta Physiologica Polonica, 27, 347-354.

Zhang H. (2005) Biodynamic response and body interactions with the seat pan and the backrest under vertical vibration. Master Thesis. Dept. of Mechanical Engg. Concordia University, Montréal, Canada.

Zimmermann C, Cook T (1997) Effects of vibration frequency and postural changes on human responses to seated whole-body vibration exposure. Int. Arch. Occup. Environ. Health 69, 165-179.

Zurada J, Karwowski W, Marras W. (1997) A neural network-based system for classification of industrial jobs with respect to risk of low back disorders due to workplace design. Applied Ergonomics, 28, 49-58.

Appendix

Table A-1: Target datasets of mean magnitude of 12 male subjects: apparent mass and segmental transmissibility, with the corresponding standard deviations, for the hands in lap, back supported **(L-B)** posture, under exposure to 1 m/s^2 vertical vibration.

(a) Fore-aft (X-) axis

L-B	Cross-axis APMS		Head		C7		T5		T12		L3		L5	
Frequency (Hz)	Mean	SD	Mean	SD	Mean	SD	Mean	SD	Mean	SD	Mean	SD	Mean	SD
0.50	6.68	2.93	0.44	0.15	0.05	0.02	0.04	0.04	0.03	0.01	0.02	0.01	0.02	0.01
0.63	7.20	4.44	0.33	0.13	0.07	0.02	0.04	0.04	0.03	0.01	0.02	0.01	0.02	0.01
0.81	6.14	1.44	0.38	0.07	0.07	0.03	0.04	0.03	0.03	0.01	0.02	0.00	0.02	0.01
1.00	6.48	1.64	0.39	0.08	0.09	0.03	0.04	0.03	0.03	0.01	0.02	0.01	0.03	0.01
1.25	6.63	1.46	0.51	0.08	0.10	0.04	0.04	0.04	0.03	0.01	0.03	0.01	0.03	0.01
1.63	7.62	1.38	0.68	0.14	0.15	0.04	0.07	0.05	0.03	0.01	0.04	0.01	0.04	0.01
2.00	8.71	2.56	0.82	0.25	0.19	0.05	0.10	0.06	0.04	0.02	0.04	0.02	0.04	0.01
2.50	9.64	2.92	1.02	0.24	0.26	0.08	0.14	0.07	0.05	0.02	0.07	0.03	0.07	0.02
3.13	10.37	3.70	1.33	0.25	0.44	0.20	0.23	0.18	0.07	0.04	0.10	0.05	0.09	0.04
4.00	17.51	7.93	1.63	0.29	0.74	0.27	0.50	0.16	0.12	0.09	0.12	0.05	0.12	0.07
5.00	34.10	10.30	1.72	0.55	1.03	0.38	0.79	0.12	0.43	0.23	0.38	0.15	0.30	0.18
6.31	26.30	9.52	0.92	0.39	0.95	0.31	0.59	0.28	0.56	0.34	0.56	0.21	0.46	0.19
8.00	15.31	5.33	0.44	0.20	0.81	0.23	0.36	0.21	0.51	0.31	0.56	0.19	0.48	0.18
10.00	9.66	2.55	0.40	0.24	0.79	0.30	0.24	0.15	0.52	0.27	0.59	0.21	0.40	0.28
12.50	6.85	1.89	0.32	0.17	0.85	0.28	0.26	0.14	0.57	0.27	0.67	0.24	0.49	0.25
16.00	4.08	1.42	0.30	0.15	0.74	0.31	0.27	0.15	0.65	0.28	0.76	0.25	0.52	0.25
20.00	2.22	1.19	0.24	0.14	0.47	0.23	0.32	0.17	0.65	0.31	0.74	0.27	0.51	0.22

(b) Vertical (Z-) axis

L-B	Seat APMS		Head		C7		T5		T12		L3		L5	
Frequency (Hz)	Mean	SD	Mean	SD	Mean	SD	Mean	SD	Mean	SD	Mean	SD	Mean	SD
0.50	54.32	8.31	0.97	0.02	0.95	0.01	0.95	0.01	0.03	0.01	0.96	0.01	0.02	0.01
0.63	55.07	8.08	0.98	0.02	0.95	0.01	0.95	0.01	0.03	0.01	0.97	0.01	0.02	0.01
0.81	55.69	8.07	0.98	0.02	0.96	0.01	0.96	0.01	0.03	0.01	0.97	0.01	0.02	0.01
1.00	56.50	8.25	1.00	0.01	0.97	0.01	0.96	0.01	0.03	0.01	0.98	0.01	0.03	0.01
1.25	57.53	8.31	1.02	0.02	0.98	0.01	0.97	0.01	0.03	0.01	0.98	0.02	0.03	0.01
1.63	59.41	8.47	1.06	0.02	1.01	0.02	0.98	0.01	0.03	0.01	1.00	0.02	0.04	0.01
2.00	61.86	8.82	1.09	0.04	1.04	0.02	0.99	0.02	0.04	0.02	1.02	0.04	0.04	0.01
2.50	66.15	9.37	1.17	0.06	1.09	0.03	1.01	0.03	0.05	0.02	1.04	0.06	0.07	0.02
3.13	72.77	9.87	1.31	0.09	1.20	0.06	1.05	0.06	0.07	0.04	1.10	0.10	0.09	0.04
4.00	87.05	11.72	1.58	0.14	1.46	0.14	1.10	0.12	0.12	0.09	1.23	0.21	0.12	0.07
5.00	100.74	20.11	1.61	0.24	1.64	0.20	1.04	0.14	0.43	0.23	1.31	0.26	0.30	0.18
6.31	69.26	14.85	0.92	0.22	1.21	0.20	0.95	0.08	0.56	0.34	1.08	0.15	0.46	0.19
8.00	55.97	13.58	0.98	0.16	1.04	0.19	0.97	0.05	0.51	0.31	1.08	0.17	0.48	0.18
10.00	45.69	7.18	1.02	0.16	1.01	0.18	0.99	0.06	0.52	0.27	0.97	0.17	0.40	0.28
12.50	30.72	4.00	0.85	0.17	0.91	0.21	0.97	0.06	0.57	0.27	0.83	0.14	0.49	0.25
16.00	18.58	2.75	0.64	0.14	0.63	0.18	1.00	0.09	0.65	0.28	0.82	0.18	0.52	0.25
20.00	14.49	2.56	0.48	0.10	0.45	0.16	1.00	0.07	0.65	0.31	0.92	0.22	0.51	0.22

Table A-2: Target datasets of mean magnitude of 12 male subjects: apparent mass and segmental transmissibility, with the corresponding standard deviations, for the hands in lap, back unsupported **(L-NB)** posture, exposed to 1 m/s^2 vertical vibration.

(a) Fore-aft (X-) axis

L-NB	Head		C7		T5		T12		L3		L5	
Frequency (Hz)	Mean	SD	Mean	SD	Mean	SD	Mean	SD	Mean	SD	Mean	SD
0.50	0.44	0.12	0.09	0.03	0.08	0.03	0.19	0.10	0.17	0.07	0.08	0.05
0.63	0.37	0.13	0.15	0.05	0.13	0.03	0.18	0.09	0.14	0.05	0.08	0.04
0.81	0.43	0.10	0.13	0.05	0.11	0.04	0.16	0.10	0.14	0.06	0.08	0.03
1.00	0.38	0.06	0.13	0.04	0.11	0.04	0.16	0.09	0.14	0.05	0.07	0.03
1.25	0.45	0.07	0.13	0.04	0.10	0.05	0.15	0.10	0.14	0.05	0.09	0.03
1.63	0.53	0.09	0.12	0.04	0.09	0.05	0.15	0.09	0.14	0.04	0.10	0.03
2.00	0.70	0.13	0.14	0.04	0.10	0.04	0.17	0.08	0.16	0.03	0.12	0.05
2.50	1.09	0.17	0.19	0.06	0.10	0.03	0.20	0.09	0.20	0.05	0.17	0.06
3.13	1.53	0.24	0.34	0.09	0.12	0.04	0.21	0.11	0.26	0.08	0.25	0.07
4.00	1.56	0.31	0.44	0.15	0.16	0.09	0.26	0.12	0.30	0.11	0.26	0.08
5.00	2.08	0.57	0.80	0.23	0.17	0.09	0.44	0.14	0.34	0.12	0.24	0.12
6.31	1.04	0.39	0.78	0.28	0.18	0.09	0.52	0.11	0.47	0.11	0.32	0.16
8.00	0.61	0.33	0.63	0.23	0.18	0.05	0.62	0.08	0.63	0.10	0.46	0.13
10.00	0.49	0.27	0.57	0.26	0.16	0.07	0.63	0.09	0.70	0.09	0.44	0.17
12.50	0.32	0.18	0.63	0.24	0.16	0.07	0.67	0.09	0.78	0.08	0.51	0.19
16.00	0.25	0.14	0.56	0.27	0.18	0.06	0.70	0.08	0.82	0.06	0.51	0.16
20.00	0.17	0.09	0.36	0.24	0.22	0.06	0.73	0.08	0.86	0.06	0.53	0.10

(b) Vertical (Z-) axis

L-NB	Seat APMS		Head		C7		T5		T12		L3		L5	
Frequency (Hz)	Mean	SD	Mean	SD	Mean	SD	Mean	SD	Mean	SD	Mean	SD	Mean	SD
0.50	54.72	7.68	0.97	0.03	0.95	0.01	0.96	0.01	0.93	0.02	0.94	0.02	0.97	0.01
0.63	55.80	8.06	0.99	0.02	0.95	0.01	0.95	0.01	0.93	0.02	0.95	0.01	0.98	0.01
0.81	57.64	8.86	0.99	0.02	0.96	0.01	0.96	0.01	0.95	0.01	0.96	0.01	0.99	0.01
1.00	58.20	8.69	1.01	0.02	0.97	0.01	0.97	0.01	0.96	0.01	0.97	0.01	1.00	0.01
1.25	59.51	9.27	1.03	0.02	0.98	0.02	0.98	0.01	0.97	0.01	0.98	0.01	1.01	0.01
1.63	61.92	9.74	1.07	0.01	1.01	0.02	1.00	0.01	0.99	0.01	1.00	0.02	1.04	0.01
2.00	64.36	9.90	1.13	0.03	1.05	0.02	1.02	0.02	1.01	0.02	1.02	0.02	1.07	0.02
2.50	68.95	10.38	1.22	0.04	1.12	0.04	1.07	0.04	1.05	0.03	1.07	0.04	1.14	0.03
3.13	75.99	11.75	1.35	0.08	1.25	0.06	1.18	0.08	1.16	0.06	1.16	0.08	1.25	0.06
4.00	96.80	17.55	1.70	0.13	1.59	0.15	1.47	0.17	1.48	0.13	1.46	0.17	1.59	0.14
5.00	103.62	19.72	1.94	0.28	1.54	0.20	1.42	0.15	1.32	0.17	1.37	0.17	1.64	0.25
6.31	58.50	13.04	0.93	0.27	0.85	0.22	0.86	0.09	0.72	0.10	0.74	0.10	1.00	0.25
8.00	46.37	9.75	0.72	0.19	0.71	0.08	0.79	0.08	0.67	0.06	0.65	0.08	1.09	0.46
10.00	38.52	7.51	0.64	0.16	0.63	0.14	0.74	0.14	0.55	0.07	0.50	0.06	1.08	0.32
12.50	26.67	3.78	0.53	0.15	0.58	0.16	0.67	0.15	0.55	0.07	0.46	0.09	0.69	0.28
16.00	17.27	2.93	0.40	0.12	0.54	0.11	0.61	0.10	0.60	0.08	0.54	0.15	0.63	0.12
20.00	13.66	2.49	0.33	0.11	0.45	0.14	0.66	0.18	0.73	0.23	0.74	0.30	0.53	0.33

Table A-3: Target datasets of mean magnitude of 12 male subjects: apparent mass and segmental transmissibility, with the corresponding standard deviations, for the hands on steering wheel, back supported **(SW-B)** posture, exposed to 1 m/s^2 vertical vibration.

(a) Fore-aft (X-) axis

SW-B	Cross-axis APMS		Head		C7		T5		T12		L3		L5	
Frequency (Hz)	Mean	SD	Mean	SD	Mean	SD	Mean	SD	Mean	SD	Mean	SD	Mean	SD
0.50	6.05	2.38	0.49	0.21	0.05	0.02	0.04	0.04	0.03	0.01	0.02	0.02	0.02	0.02
0.63	6.13	2.18	0.36	0.11	0.06	0.03	0.05	0.04	0.03	0.01	0.03	0.01	0.02	0.01
0.81	5.49	1.47	0.38	0.07	0.08	0.03	0.05	0.03	0.03	0.01	0.03	0.01	0.02	0.01
1.00	5.29	1.84	0.37	0.08	0.08	0.04	0.06	0.03	0.03	0.01	0.03	0.01	0.03	0.01
1.25	5.22	1.20	0.50	0.09	0.10	0.04	0.07	0.03	0.03	0.01	0.03	0.01	0.03	0.01
1.63	6.15	1.95	0.65	0.11	0.13	0.04	0.09	0.03	0.03	0.01	0.04	0.01	0.04	0.01
2.00	6.99	2.63	0.82	0.22	0.17	0.05	0.12	0.04	0.04	0.01	0.05	0.01	0.04	0.01
2.50	7.76	3.46	1.03	0.27	0.25	0.05	0.16	0.05	0.05	0.02	0.07	0.02	0.06	0.02
3.13	9.12	3.59	1.27	0.26	0.43	0.10	0.28	0.10	0.08	0.04	0.09	0.04	0.09	0.04
4.00	15.48	5.50	1.53	0.40	0.81	0.21	0.52	0.15	0.13	0.09	0.11	0.04	0.12	0.05
5.00	31.97	8.95	1.59	0.65	1.27	0.27	0.80	0.17	0.47	0.27	0.37	0.15	0.33	0.12
6.31	27.44	9.54	0.73	0.35	1.05	0.18	0.59	0.26	0.64	0.30	0.60	0.17	0.53	0.23
8.00	15.93	5.36	0.44	0.15	0.79	0.15	0.35	0.28	0.61	0.30	0.63	0.16	0.54	0.20
10.00	9.96	2.92	0.43	0.20	0.70	0.24	0.23	0.22	0.61	0.28	0.63	0.15	0.43	0.29
12.50	6.67	1.80	0.31	0.13	0.72	0.15	0.23	0.20	0.61	0.26	0.69	0.15	0.47	0.27
16.00	4.14	1.25	0.28	0.13	0.60	0.25	0.22	0.21	0.69	0.28	0.77	0.18	0.50	0.24
20.00	1.82	0.85	0.21	0.09	0.47	0.22	0.26	0.16	0.66	0.31	0.76	0.19	0.51	0.23

(b) Vertical (Z-) axis

SW-B	Seat APMS		Head		C7		T5		T12		L3		L5	
Frequency (Hz)	Mean	SD	Mean	SD	Mean	SD	Mean	SD	Mean	SD	Mean	SD	Mean	SD
0.50	52.31	7.61	0.96	0.02	0.95	0.01	0.95	0.01	0.95	0.00	0.96	0.01	0.97	0.00
0.63	53.32	7.97	0.98	0.02	0.95	0.01	0.95	0.01	0.95	0.00	0.97	0.01	0.97	0.00
0.81	53.89	7.86	0.99	0.02	0.96	0.01	0.96	0.01	0.96	0.01	0.97	0.01	0.98	0.00
1.00	54.78	7.96	1.00	0.02	0.97	0.01	0.96	0.01	0.96	0.01	0.98	0.01	0.99	0.01
1.25	55.75	8.06	1.02	0.02	0.98	0.01	0.97	0.01	0.96	0.01	0.98	0.01	1.00	0.01
1.63	57.49	8.16	1.05	0.02	1.00	0.01	0.98	0.01	0.97	0.01	0.99	0.02	1.02	0.01
2.00	59.92	8.50	1.10	0.03	1.04	0.02	0.99	0.02	0.98	0.02	1.01	0.03	1.04	0.02
2.50	63.66	8.94	1.18	0.06	1.09	0.03	1.01	0.03	1.00	0.04	1.04	0.06	1.08	0.03
3.13	69.73	9.36	1.30	0.08	1.18	0.05	1.03	0.04	1.03	0.07	1.10	0.10	1.14	0.05
4.00	82.05	10.85	1.53	0.14	1.42	0.09	1.05	0.09	1.11	0.15	1.22	0.20	1.28	0.13
5.00	93.43	17.87	1.59	0.19	1.65	0.17	1.00	0.12	1.12	0.16	1.28	0.29	1.48	0.28
6.31	73.59	15.70	1.07	0.18	1.36	0.24	0.97	0.07	1.01	0.08	1.10	0.20	1.33	0.23
8.00	61.86	15.69	1.14	0.10	1.08	0.18	0.95	0.05	0.97	0.03	1.09	0.22	1.39	0.51
10.00	46.59	8.17	1.05	0.20	0.94	0.19	0.94	0.06	0.89	0.10	0.88	0.21	1.25	0.55
12.50	28.91	4.18	0.82	0.19	0.81	0.19	0.93	0.07	0.88	0.13	0.76	0.17	0.79	0.27
16.00	17.53	3.03	0.62	0.15	0.64	0.21	0.95	0.10	0.91	0.12	0.81	0.15	0.62	0.22
20.00	13.94	2.42	0.50	0.10	0.51	0.31	0.97	0.09	0.94	0.13	0.88	0.22	0.52	0.23

Table A-4: Target datasets of mean magnitude of 12 male subjects: apparent mass and segmental transmissibility, with the corresponding standard deviations, for the hands on steering wheel, back un-supported **(SW-NB)** posture, exposed to 1 m/s^2 vertical vibration.

(a) Fore-aft (X-) axis

SW-NB	Head		C7		T5		T12		L3		L5	
Frequency (Hz)	Mean	SD	Mean	SD	Mean	SD	Mean	SD	Mean	SD	Mean	SD
0.50	0.46	0.18	0.10	0.05	0.06	0.03	0.12	0.06	0.10	0.05	0.06	0.02
0.63	0.38	0.09	0.15	0.05	0.08	0.03	0.12	0.07	0.10	0.05	0.07	0.03
0.81	0.37	0.13	0.14	0.06	0.08	0.04	0.11	0.08	0.09	0.05	0.07	0.01
1.00	0.41	0.11	0.17	0.05	0.10	0.05	0.11	0.07	0.09	0.05	0.06	0.03
1.25	0.46	0.11	0.14	0.05	0.09	0.04	0.09	0.06	0.08	0.05	0.07	0.02
1.63	0.45	0.09	0.12	0.04	0.08	0.04	0.08	0.07	0.10	0.03	0.08	0.02
2.00	0.57	0.10	0.12	0.05	0.08	0.04	0.11	0.05	0.12	0.03	0.10	0.03
2.50	0.87	0.13	0.16	0.06	0.09	0.04	0.15	0.06	0.16	0.04	0.15	0.04
3.13	1.30	0.27	0.23	0.09	0.10	0.03	0.20	0.06	0.22	0.06	0.21	0.06
4.00	1.51	0.30	0.33	0.12	0.17	0.05	0.23	0.07	0.24	0.09	0.22	0.08
5.00	2.03	0.58	0.63	0.16	0.27	0.09	0.48	0.14	0.38	0.12	0.22	0.07
6.31	0.99	0.45	0.53	0.18	0.29	0.07	0.59	0.12	0.53	0.11	0.36	0.12
8.00	0.62	0.40	0.38	0.14	0.26	0.05	0.66	0.08	0.66	0.11	0.45	0.11
10.00	0.51	0.30	0.39	0.19	0.22	0.05	0.64	0.08	0.70	0.10	0.34	0.13
12.50	0.36	0.24	0.47	0.18	0.16	0.07	0.65	0.07	0.76	0.09	0.41	0.15
16.00	0.25	0.15	0.48	0.30	0.17	0.09	0.68	0.06	0.81	0.07	0.42	0.15
20.00	0.18	0.12	0.35	0.32	0.21	0.08	0.74	0.08	0.85	0.08	0.51	0.08

(b) Vertical (Z-) axis

SW-NB	Seat APMS		Head		C7		T5		T12		L3		L5	
Frequency (Hz)	Mean	SD	Mean	SD	Mean	SD	Mean	SD	Mean	SD	Mean	SD	Mean	SD
0.50	52.92	8.09	0.97	0.02	0.95	0.00	0.96	0.00	0.94	0.01	0.96	0.01	0.97	0.01
0.63	53.53	8.43	0.98	0.02	0.95	0.01	0.96	0.01	0.94	0.01	0.96	0.01	0.98	0.01
0.81	54.87	8.46	0.99	0.02	0.96	0.01	0.97	0.01	0.96	0.01	0.97	0.01	0.99	0.01
1.00	55.68	8.47	1.01	0.02	0.97	0.01	0.97	0.01	0.97	0.02	0.98	0.01	1.00	0.01
1.25	57.24	8.82	1.02	0.02	0.99	0.01	0.99	0.01	0.99	0.01	1.00	0.02	1.03	0.01
1.63	59.58	9.08	1.06	0.02	1.02	0.01	1.01	0.02	1.01	0.01	1.03	0.02	1.06	0.02
2.00	62.28	9.49	1.12	0.03	1.06	0.02	1.04	0.03	1.04	0.02	1.06	0.03	1.10	0.02
2.50	66.47	9.98	1.22	0.04	1.12	0.03	1.09	0.04	1.09	0.02	1.11	0.04	1.17	0.03
3.13	72.43	10.60	1.33	0.07	1.23	0.06	1.20	0.08	1.19	0.05	1.20	0.08	1.29	0.07
4.00	91.36	15.84	1.69	0.16	1.56	0.16	1.50	0.19	1.48	0.12	1.51	0.19	1.64	0.17
5.00	103.02	18.46	1.95	0.24	1.60	0.20	1.48	0.18	1.44	0.17	1.45	0.19	1.69	0.21
6.31	61.48	13.73	1.01	0.21	0.95	0.22	0.90	0.11	0.76	0.10	0.75	0.14	1.09	0.16
8.00	49.65	10.48	0.82	0.17	0.75	0.14	0.75	0.11	0.68	0.09	0.65	0.07	1.27	0.34
10.00	38.98	7.10	0.62	0.13	0.67	0.17	0.67	0.12	0.54	0.07	0.50	0.06	1.24	0.28
12.50	26.20	3.71	0.53	0.14	0.62	0.16	0.59	0.15	0.54	0.11	0.43	0.08	0.79	0.26
16.00	16.60	3.01	0.40	0.11	0.60	0.13	0.55	0.12	0.60	0.12	0.51	0.13	0.62	0.13
20.00	13.17	2.69	0.35	0.12	0.58	0.14	0.61	0.19	0.73	0.24	0.71	0.30	0.50	0.30